An *in vivo* functional selection strategy to identify novel genes sustaining cardiac function

PhD Thesis in Molecular Biology

Supervisor: Professor Mauro Giacca

Giulia Ruozi

Scuola Normale Superiore
Academic Year 2012-2013

"Niente di grande è stato fatto al mondo
senza il contributo della passione"

Georg Hegel

TABLE OF CONTENTS

SYNOPSIS **1**

1. INTRODUCTION **6**

1.1. CARDIOVASCULAR PATHOLOGY 6

1.1.1 Atherosclerosis as a risk factor 8

1.1.2 Ischemic Heart Disease 10

1.1.3 Congestive Heart Failure 14

1.1.3.1 Compensatory and pathological hypertrophy 18

1.1.4 Peripheral Artery Disease 21

1.1.5 Conventional treatments for cardiovascular disorders 22

1.1.5.1 Acute Myocardial Infarction 22

1.1.5.2 Long-term management of cardiovascular disease and heart failure 23

1.2. BIOLOGICAL THERAPEUTICS AS NEW TREATMENTS FOR CARDIOVASCULAR DISEASE 27

1.2.1 Recombinant protein administration 28

1.2.2 Cell Therapy 32

1.2.3 Gene therapy approaches for cardiovascular disorders 38

1.2.3.1 Targeting the heart: gene delivery strategies 38

1.2.3.2 Cardiac gene targets 41

1.2.3.3 Clinical trials for therapeutic cardiovascular gene therapy 49

1.3. ADENO-ASSOCIATED VIRAL VECTORS (AAVs) 54

1.3.1 Molecular biology of Adeno-Associated Virus 54

1.3.1.1 Genome organization and structure of virions.....54
1.3.1.2 AAV life cycle.....58
1.3.1.3 AAV infection.....59
1.3.2 Recombinant AAV vectors.....65
1.3.2.1 rAAV vector production and purification.....67
1.3.2.2 Properties of AAV-based vectors.....68
1.3.2.3 rAAV vector optimization.....69

1.4. GHRELIN: A GROWTH HORMONE (GH)-RELEASING PEPTIDE WITH PROMISING BENEFICIAL EFFECTS ON THE MYOCARDIUM.....75
1.4.1 The discovery of ghrelin.....75
1.4.2 Ghrelin gene structure and derived-peptides.....77
1.4.3 Ghrelin receptors.....80
1.4.3.1 Type 1a GHS Receptor (GHS-R1a).....80
1.4.3.2 Non-type 1a GHS Receptors.....84
1.4.4 Ghrelin physiology.....86
1.4.5 Ghrelin effects on the cardiovascular system.....92

1.5. INSULIN-LIKE PEPTIDE 6: A NOVEL MEMBER OF THE RELAXIN FAMILY.....97
1.5.1 The relaxin family peptides and their receptors.....97
1.5.2 Biological functions of relaxins.....100
1.5.2.1 Effects on reproductive organs.....101
1.5.2.2 Effects on other organ systems.....102
1.5.2.3 Effects on the cardiovascular system.....103
1.5.3 Insulin-like peptide 6 (INSL6).....104
1.5.3.1 Identification and characterization of INSL6.....104
1.5.3.2 Functions of INSL6.....106

2. AIM OF THE STUDY..... 108

3. MATERIALS AND METHODS..... 109

3.1. MOLECULAR BIOLOGY PROTOCOLS 109

3.1.1 Generation of the plasmids collection 109

3.1.2 PCR amplification of the pooled viral genomes..... 110

3.1.3 Production and purification of rAAV vectors 111

3.1.4 DNA and RNA extraction and Reverse Transcription (RT) 112

3.1.5 Quantification of nucleic acids by Real-Time PCR 112

3.2. CELLULAR BIOLOGY PROTOCOLS..... 115

3.2.1 Culture of neonatal rat cardiomyocytes 115

3.2.2 Cell viability assay 117

3.3. *IN VIVO* EXPERIMENTAL PROTOCOLS 117

3.3.1 AAV vectors i*n vivo* administration 117

3.3.2 Animal model of hind limb ischemia 118

3.3.3 Animal model of isoproterenol-induced cardiac fibrosis..... 118

3.3.4 Animal model of myocardial infarction (MI) 119

3.3.5 Echocardiography analysis 119

3.3.6 Histology 120

3.3.7 TUNEL assay for apoptotic cells detection 120

3.3.8 Enzyme Immunoassay (EIA) analysis..... 121

3.4. STATISTICAL ANALYSIS 121

4. RESULTS 122

4.1. DEVELOPMENT OF AN *IN VIVO* FUNCTIONAL SELECTION STRATEGY: MATHEMATICAL CONSIDERATIONS..... 124

4.1.1 Mathematical model: variables and formula 125
4.1.2 Selection under ideal conditions 127
4.1.3 Effect of multiplicity of infection (MOI) 127
4.1.4 Influence of the coselection of other cells due to transgene bystander effect 129
4.1.5 Effect of poor efficiency of selection 132
4.1.6 Performing iterative cycles of selection 133

4.2. GENERATION OF AN ARRAYED LIBRARY OF AAV VECTORS EXPRESSING SECRETED FACTORS 137
4.2.1 The mouse secretome cDNA arrayed library 137
4.2.2 Generation of a collection of AAV vectors expressing 100 secreted factors 141
4.2.3 Recombinant AAV vector pooled production 143

4.3. VALIDATION OF THE AAV VECTOR POOLS COMPOSITION 145
4.3.1 Generation of pools of AAV vectors homogeneous for transgenes size is essential to guarantee the faithful maintenance of AAV vectors genomes during pooled production 145
4.3.2 The complexity of a pool does not influence viral packaging efficiency 150
4.3.3 AAV vectors genomes ratios are maintained after *in vivo* transduction and persist in the transduced tissue 152
4.3.4 The levels of transgene expression *in vivo* reflect the original complexity of the AAV pools 155
4.3.5 Generation of the AAV vector pools for the *in vivo* functional selection 157

4.4. *IN VIVO* FUNCTIONAL SELECTION OF NOVEL SECRETED MOLECULES CONFERRING SKELETAL MUSCLE AND CARDIAC PROTECTION..... 159
4.4.1 *In vivo* functional selection in a model of hind limb ischemia 160
4.4.2 *In vivo* functional selection in a model of cardiac damage induced by isoproterenol treatment 165

4.5. CHARACTERIZATION OF THE THERAPEUTIC EFFECTS OF THE *IN VIVO* SELECTED CANDIDATE GENE GHRELIN..... 171
4.5.1 AAV9-Ghrelin prevents isoproterenol- and doxorubicin-induced cell death in neonatal rat cardiomyocytes..... 171
4.5.2 Long-lasting ghrelin expression in mouse heart preserves cardiac function after myocardial infarction (MI) 173
4.5.3 Maintenance of myocardial thickening and reduction of infarct size in AAV9-Ghrelin transduced mice 176
4.5.4 Marked decrease of myocardial apoptosis and inflammatory infiltrate after ghrelin transduction in infarcted mice 179
4.5.5 Ghrelin overexpression counteracts the induction of genes involved in pathological LV remodeling after myocardial infarction 183

4.6. CHARACTERIZATION OF THERAPEUTIC EFFECTS OF THE *IN VIVO* SELECTED GENE INSULIN-LIKE PEPTIDE 6 (INSL6): PRELIMINARY RESULTS..... 185
4.6.1 AAV9-mediated INSL6 expression in mouse heart preserves cardiac function and reduces infarct size after myocardial infarction 185
4.6.2 INSL6 expression in infarcted hearts induces a marked decrease of myocardial apoptosis 187

5. DISCUSSION..... 190

5.1. DEVELOPMENT OF AN INNOVATIVE STRATEGY FOR THE *IN VIVO* FUNCTIONAL SELECTION OF AAV VECTORS EXPRESSING THERAPEUTIC GENES 190

5.1.1 Theoretical confirmation of the feasibility of the AAV-mediated *in vivo* functional selection 192

5.1.2 Recombinant AAV vectors can be generated in pools 194

5.1.3 Definition of critical requirements influencing packaging, *in vivo* transduction and expression of pooled AAV genomes 194

5.2. THE SECRETED FACTORS GHRELIN AND INSL6 RESULTED ENRICHED AFTER *IN VIVO* FUNCTIONAL SELECTION IN TWO MODELS OF ISCHEMIC DAMAGE 200

5.2.1 Ghrelin as a protective gene selected after skeletal muscle damage 200

5.2.2 Implementation of the selection strategy in a model of isoproterenol-induced cardiac damage identified INSL6 as a candidate protective gene 201

5.3. AAV9-MEDIATED GHRELIN EXPRESSION IN THE MOUSE HEART IMPROVES CARDIAC FUNCTION AFTER INFARCTION..... 203

5.3.1 AAV9-Ghrelin prevents neonatal rat cardiomyocytes cell death *in vitro* 203

5.3.2 Cardiac gene transfer of ghrelin exerts beneficial effects after myocardial infarction in mice 204

5.4. CARDIAC GENE TRANSFER OF INSL6 EXERTS BENEFICIAL EFFECTS AFTER MYOCARDIAL INFARCTION IN MICE..... 206

6. BIBLIOGRAPHY 208

7. APPENDIX..... 248

SYNOPSIS

Despite the several advances in cardiovascular therapies, cardiac diseases still remain the leading cause of morbidity and mortality in developed countries. Current therapies essentially aim at either counteracting symptoms or slowing pathological progression, whereas no treatment able to stop or revert these diseases is available. The development of novel therapeutic strategies thus appears of pivotal importance. In this context, a number of studies conducted over the last several years have indicated various growth factors and microRNAs that are able to protect the myocardium against ischemia or sustain the failing heart. None of these molecules, however, have progressed towards clinical experimentation and which factor might turn out into a clinically effective biotherapeutics still remains largely unclear.

In this scenario, this Thesis explores the possibility to exploit viral vectors based on the Adeno-Associated Virus (AAV) as tools to directly select for factors exerting beneficial effects in ischemic tissues *in vivo*, without a priori knowledge of the actual function of the investigated molecules.

Following the birth of genetic engineering, the screening of genetic libraries has provided a powerful means for the rapid identification of genes and peptides possessing desired characteristics. Library screening has generated important biological information, but all the approaches attempted so far, based on biochemical assays or cell culture systems, have suffered a major limitation, in that they cannot predict the *in vivo* relevance of the selected molecules.

In contrast, the currently availability of AAV vectors, which can be produced at very high titres, infect post-mitotic cells very efficiently, and persist in these cells for prolonged periods of time in the absence of

significant transgene silencing, now allows development of a radically new strategy to directly select for potentially therapeutic genes directly *in vivo*. An outline of the novel, *in vivo* Functional Selection (**FunSel**) strategy, is shown in **Figure 1** below.

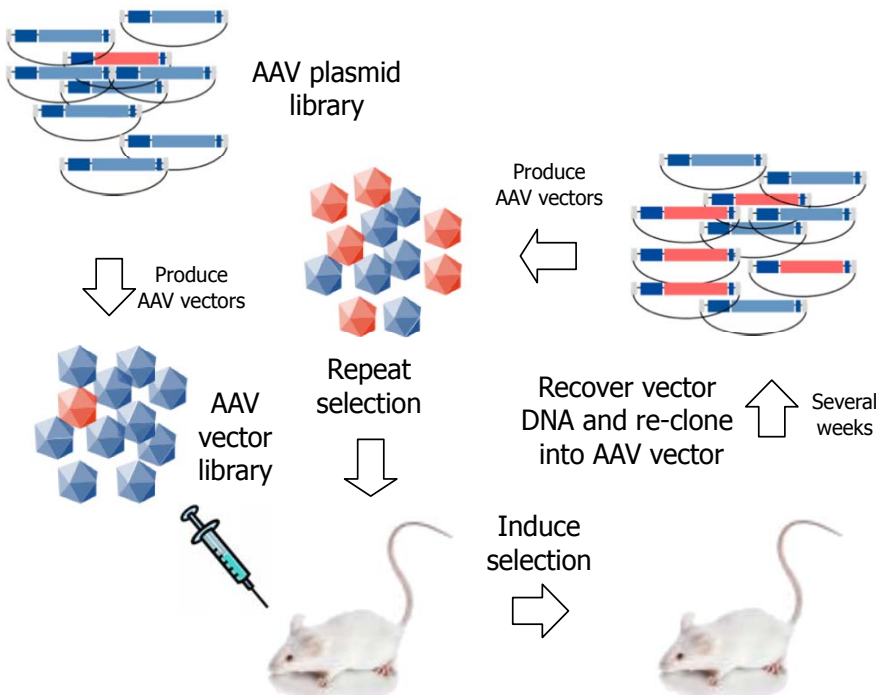

Figure 1 *In vivo* AAV-based Functional Selection (FunSel) strategy
The construction of the AAV plasmid library entails individual cloning of genes coding for secreted proteins into an AAV-backbone plasmid and production of the corresponding pools of recombinant AAV vectors with different serotype specificity according to the applications. The pools are directly delivered *in vivo* and different types of ischemic damage are induced to trigger the selection of protective candidates. Several weeks after the onset of degeneration vector genomes still present in surviving tissues, in principle enriched for protective genes, are recovered by PCR and recloned into the AAV-backbone plasmid to create a new pool of AAVs, which is re-submitted to further cycles of *in vivo* selection, up to the definition of a few candidate therapeutic genes (red vectors code for a putative beneficial factor).

A pool of AAVs, corresponding to a collection of vectors each one coding for a different growth factor, hormone or cytokine, are used to transduce a given tissue *in vivo* (e.g. the skeletal muscle or the heart); each vector infects an individual cell. After delivery, an insult is inferred to the transduced tissue, e.g. by inducing acute ischemia; this will trigger selection for factors exerting e protective effect against the damage. At a few weeks after the onset of tissue damage and degeneration, the animals are sacrificed in order to recover, by PCR, the viral transgenes still present in the surviving tissues, in principle enriched for genes promoting either tissue viability or regeneration. Then, the obtained PCR inserts are re-cloned into an AAV-backbone plasmid to create a new pool of AAVs, which are re-submitted to further cycles of selection, up to the definition of one or more candidate therapeutic genes.

This Thesis provides a proof-of-principle verification of the feasibility of the FunSel approach and describes two novel factors (ghrelin and INSL6), identified by *in vivo* selection, that are effective in protecting the myocardium after infarction *in vivo*.

The Thesis initially reports a series of mathematical considerations that supports the theoretical feasibility of **FunSel** using AAV vectors. By taking into account all the variables possibly involved in AAV transduction and in the function of a possible therapeutic factor, the multiplicity of vectors and the complexity of the vector pools are ideally defined.
Then, the Thesis experimentally validates the feasibility of generating pooled AAV vectors for *in vivo* skeletal muscle and heart transduction. Using a set of 100 different AAV2 vectors, coding for various secreted proteins, including several hormones and growth factors, the Thesis demonstrate that it is possible to generate vector pools that faithfully

maintain the representation of each individual vector, transduce a target tissue at equal efficiency and are comparably expressed over time.

After this extensive, preliminary validation analysis, **FunSel** was applied to different *in vivo* models of tissue degeneration. In particular, we set up models of hind limb ischemia and myocardial isoproterenol-induced damage, in order to trigger the functional selection of pools of AAV vectors, previously delivered to the target tissues. At different time points after the onset of degeneration, viral genomes present in surviving tissues were recovered, re-cloned to obtain new vector preparations and re-submitted to additional cycles of selection, up to the definition of a few candidate therapeutic genes.

By three round of selection in the model of muscle ischemic damage, **FunSel** generated a marked enrichment for surviving myocytes transduced with AAV9-Ghrelin, a neuro-hormone involved in endocrine metabolism. Whereas, a single cycle of selection in the model of cardiac toxic damage was sufficient to appreciate a clear enrichment for AAV vectors coding for the Insulin-like peptide 6 (INSL6), a poorly described member of the insulin gene family.

Finally, the cardioprotective potential of ghrelin and INSL6 was further characterized by a series of morphological and functional assays in a model of myocardial infarction. The persistent AAV9-mediated expression of these genes in the heart preserved cardiac function and reduced infarct size, as assessed by echocardiography and morphometric analysis. Interestingly we observed that, in animals treated with AAV9-Ghrelin or AAV9-INSL6, the marked improvement in cardiac contractility was paralleled by a decreased number of apoptotic cells at early time points after infarction. Moreover, ghrelin counteracted the induction of markers of cardiac damage, like miR21 and MMP-2, and prevented the deregulated expression of markers of pathological left ventricle remodeling such as β-MHC, BNP and others.

Taken together, the results presented in this Thesis support the feasibility of the AAV-based, *in vivo* **FunSel** approach for the identification of factors exerting a beneficial function against myocardial ischemia.
This study encourages further extension of **FunSel** for the analysis of the whole collection of secreted factors encoded by the murine genome.

1. INTRODUCTION

1.1 CARDIOVASCULAR PATHOLOGY

Cardiovascular diseases (CVDs) include a broad range of pathologies that affect the heart and the circulatory system. The two most prevalent forms of CVD are coronary heart disease (CHD) and stroke. Despite remarkable progress in terms of early diagnosis and prevention, CVDs remain the most common, serious, chronic, life-threatening illnesses in Western countries, causing more deaths, disability and economic costs than all other disorders. As estimated by the World Health Organization Report 2011, about 17.3 million people have died from CVDs in 2008, representing 30% of all global deaths (www.who.int/mediacentre/factsheets/fs317) (**Figure 1.1**). Of these deaths, 7.3 million were due to coronary heart disease and 6.2 million to stroke. It is estimated that, by 2030, almost 23.6 million people will die from CVDs, a number which will possibly increase because of a dramatic rise in the prevalence of certain risk factors – including obesity, overweight and diabetes. In particular, in Europe, every year 4.3 million people die from cardiovascular diseases (www.ehnheart.org/cvd-statistics), of which more than 1.8 million before the age of 75. CVDs are responsible for 54% of all deaths in women across Europe and of 43% of deaths in men, killing more people than all cancers together.

Cardiac pathologies are not only a cause of mortality, but also of morbidity and therefore they have a deep impact on the society also from an economical point of view. CVDs cost to the EU € 192 billion every year, of which approximately 57% is due to health care, 21% to loss of productivity and 22% to informal care of people with CVDs www.ehnheart.org/cvd-statistics.

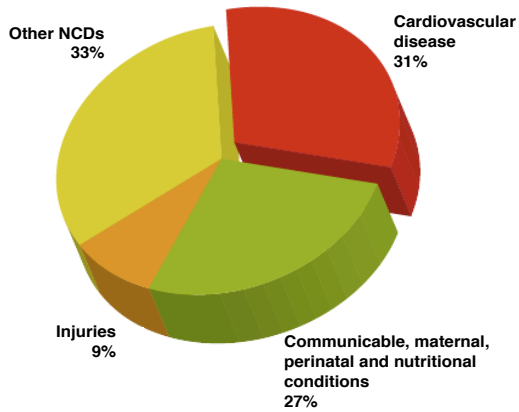

Figure 1.1 Distribution of major causes of death including CVDs
Cardiovascular diseases represent ~30% of the total cause of global death. Other Noncommunicable diseases (NCDs) include cancer, respiratory diseases, diabetes etc. (*Global Atlas on cardiovascular disease prevention and control, WHO 2011*).

Tobacco smoking, physical inactivity, unhealthy diet and the harmful use of alcohol are the main behavioural risk factors of CVDs. Long-term exposure to behavioural risk factors results in raised blood pressure (hypertension), raised blood sugar (diabetes), raised and abnormal blood lipids (dyslipidaemia) and obesity (Roger et al., 2011).

Currently available medical and surgical therapies - including angioplasty, thrombolysis and bypass surgery - have profoundly modified the natural history of CVD and its immediate prognosis, however their applications suffer important limitations in a broad number of patients and their efficacy is often inadequate in the long term. Moreover, many pharmaceutical treatments such as beta-blockers, ACE inhibitors and others improve the patients' conditions, but actually only counteract symptoms or slow down pathology progression, whereas no treatment able to stop or revert the disease is currently available.

1.1.1 Atherosclerosis as risk factor

One of the main underlying pathological processes that lead to myocardial infarction and stroke is atherosclerosis. This is an inflammatory process affecting medium- and large-size blood vessels throughout the cardiovascular system, which usually starts during childhood with damage in the innermost layer of the artery and worsens with ageing.

The initial step of atherosclerosis occurs when LDL particles leave the blood and enter the arterial intima, where, if LDL levels are increased, they accumulate (Insull, 2009). LDLs are afterwards modified by enzymes and oxidized into pro-inflammatory molecules, which provoke reaction of the innate inflammatory system within the intima. Endothelial cells become activated and secrete adhesion molecules, and the smooth muscle cells secrete chemokines and chemoattractants (like IL-1 and TNF-α), which draw monocytes and lymphocyte into the arterial wall (Ait-Oufella et al., 2011). Upon entry, monocytes transform into macrophages, take up lipids as multiple small inclusions, and become foam cells. This in-principle protective function may be overwhelmed and turned into a detrimental disease-causing pathway when the foam cells die and leave the lipid behind as a soft, destabilizing, and rather inert necrotic (atheromatous) core within the plaque (Falk, 2006). The increasing accumulation of lipids and the proliferation of smooth muscle cells stimulated by many growth factors secreted by macrophages, such as PDGF, FGF and others, determine the enlargement of the necrotic plaque, which is progressively covered by a fibrous cap consisting of smooth muscle cells and collagen.

Although advanced atherosclerotic lesions can lead to ischemic symptoms as a result of progressive narrowing of the vessel lumen, acute cardiovascular events that result in myocardial infarction and stroke are generally thought to result from plaque rupture and thrombosis.

Vulnerable plaques generally have thin fibrous caps and increased numbers

of inflammatory cells (Lusis, 2000). Plaque rupture exposes plaque lipids and tissue factor to blood components, initiating the coagulation cascade, platelet adherence, and thrombosis (Glass and Witztum, 2001). Rupture frequently occurs at the lesion edges, which are rich in foam cells, suggesting that factors contributing to inflammation may also influence thrombosis (**Figure 1.2**).

Many ruptures of thin caps are clinically silent; they heal by forming fibrous tissue and collagen fibers but may rupture again with thrombus formation. These cyclic changes of rupture, thrombosis, and healing may recur as many as 4 times at a single site in the arterial wall, resulting in multiple layers of healed tissue. Calcification and neovascularization, common features of advanced lesions, may also influence the stability of atherosclerotic lesions. Intimal calcification is an active process in which pericyte-like cells secrete a matrix scaffold, which subsequently becomes calcified. Moreover, the growth of small vessels from the media may favour the invasion by inflammatory cells. Angiogenesis occurs in association with remodellng and protease activation in surrounding tissues, suggesting that neovascularization could contribute to plaque instability and rupture. The clots generated by thrombosis can cause coronary occlusions that are responsible of myocardial infarction. Should they move into the circulation, they may reach downstream arteries causing thromboembolism. In this last case, the most frequent consequence is brain stroke.

Atherosclerosis risk is influenced by different non-modifiable factors, such as age, gender and inherited genetic disposition, as well as by a series of factors that can be modulate by life style (physical inactivity, tobacco smoking, overweight and unhealthy diet) or pharmacological therapy (hypertension, hypercholestrolemia and diabetes).

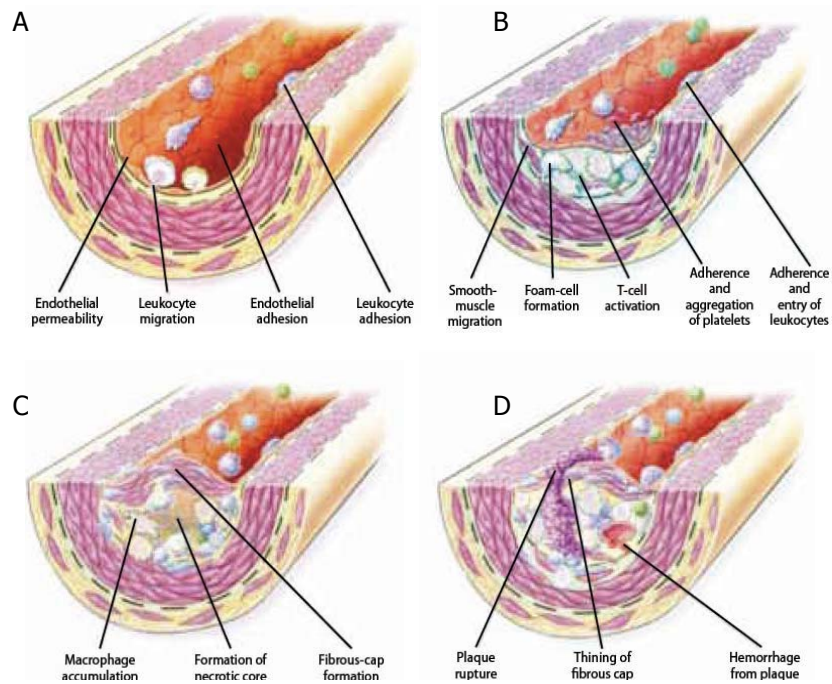

Figure 1.2 Atherosclerotic plaque evolution
A. Endothelial dysfunction: Leukocyte adhesion and migration into the intima **B.** Fatty streak formation: platelet aggregation, foam-cell formation and smooth muscle migration **C.** Fibrous cap and necrotic core formation **D.** Plaque rupture *(Ross, 1999).*

1.1.2 Ischemic Heart Disease

Myocardial ischemia originates from an imbalance between myocardial blood supply and oxygen demand. It has a variety of consequences depending on the severity of the reduction in coronary blood flow, the duration of the ischemic insult, the area of myocardium supplied by the occluded artery and the presence of collateral vessels from other adjacent vascular beds in that portion of the heart (Senter and Francis, 2009) (**Figure 1.3**).

Some episodes of myocardial ischemia are painful, causing angina pectoris, while others are completely silent. The most frequent mechanism leading to angina is an increased oxygen demand in conditions of stress or physical activity; this can be relieved simply by resting or by sublingual nitroglycerin treatment. In contrast, plaque disruption, platelet plugging, and coronary thrombosis are responsible for an acute coronary syndrome, which can determine unstable angina or, more often, myocardial infarction (MI).

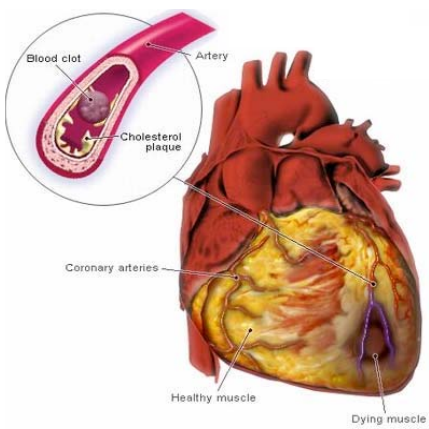

Figure 1.3 Myocardial Infarction (MI) caused by coronary artery stenosis
Myocardial infarction (MI) results from the interruption of blood supply to a portion of the heart and consequent death of the correspondent myocytes. This is most commonly caused by a coronary artery occlusion generated by blood clots derived from atherosclerotic plaque disruption.

The patients suffering of an acute coronary syndrome can be divided into one of two main groups by electrocardiography (ECG) analysis: 1) patients with myocardial infarction with ST-segment elevation (STEMI); the elevated ST segment indicates that a relatively large amount of heart muscle damage is occurring because the coronary artery is totally occluded; 2) patients with unstable angina or non-ST-segment elevation MI (UA/NSTEMI). A common problem when a patient has an acute coronary syndrome without ST-segment elevation is discriminating whether a heart attack is occurring or it is an unstable angina event. An important tool to distinguish between these two possibilities is the measurement of the levels of some cardiac enzymes, markers of myocardial necrosis, such as troponin

T or I, myoglobin and creatine kinase or creatine kinase-MB, the levels of which are all increased after MI (Thygesen et al., 2007).

The very early phase of myocardial ischemia is reversible. During this phase, one of the prominent metabolic changes is potassium loss, which may be related to the early increase in anaerobic glycolysis. Reversibly injured myocytes are edematous and swollen from the osmotic overload and the cell size is increased with cardiomyocytes hypertrophy and decrease in the glycogen content. The myocyte fibers are relaxed and thinned, I-bands are prominent secondary to non-contracting ischemic myocytes. The nuclei show mild condensation of chromatin at the nucleoplasm and the cell membrane (sarcolemma) is intact and no breaks can be identified. The mitochondria are swollen, with loss of normal dense mitochondrial granules and incomplete clearing of the mitochondrial matrix, but without amorphous or granular densities.

When the coronary blood flow is restored after a brief interruption, the reversible abnormalities of the myocytes progressively disappear but, if the blood flow is not restored within approximately 1 hour from the occlusion of the coronary artery, myocardial necrosis starts to occur. Several biochemical and functional alterations occur during the progression to necrotic cell death. These include loss of mitochondrial ATP production, compensatory increase in anaerobic glycolysis with the deleterious accumulation of H^+ ions and lactate, resulting in intracellular acidosis and impairment in fatty acid metabolism (Lopaschuk et al., 2010). Functionally, these changes are followed by a rapid loss of contractile function of the affected region and by electrical abnormalities that may result in severe arrhythmias. Moreover, the cytosolic and mitochondria calcium levels increase and lead to activation of proteases, disruption of myocytes ultrastructure, cell swelling, and, eventually, to the physical disruption of the sarcolemma membrane and cell death.

The oxygen reduction also leads to an increase in reactive oxygen species (ROS) production by the mitochondrial electron transport chain. These also contribute to lipid peroxidation, damage to the cellular cytoskeleton, loss of sarcolemmal integrity, and, finally, to cell death.

Morphologically, a myocardial infarction usually starts in the subendocardium and proceeds towards the subepicardium. Cell death starts rapidly after occlusion in the subendocardium and is generally completed within 3-6 hours. By histological analysis, it is possible to notice an acute inflammation, induced by myocytes nuclear lysis and release of cell content, which occurs in subsequent phases during ischemic necrosis. In 12-72 hours, a prominent neutrophil infiltration in the infarct border zone is observed, followed by the invasion of the infarcted tissue; by day 5-7, macrophages and fibroblasts begin to appear in the infarct border area. After 1 week, neutrophils decline, granulation tissue progressively replaces necrotic tissue and neocapillary invasion and both lymphocytic and plasma cell infiltrations are evident. Lymphocytes may be seen as early as 2-3 days, but they are not prominent in any stage of infarct evolution, while eosinophils are present in the inflammatory infiltrate in only 24% of infarcts. By the second week, fibroblasts are mainly present; they actively produce and deposit collagen, forming a fibrotic infarct scar. Healing is usually completed in 4 weeks, but may also require 8 weeks or more, depending on the extent of necrosis.

Recently, multiple evidence indicated that cardiomyocyte death following ischemia also involves other types of cell death, such as apoptosis and autophagy. These conditions are thought to lead at later stages to necrosis. Apoptosis is energy dependent and characterized by absence of inflammation. Microscopically apoptotic cells show nuclear chromatin condensation and formation of small dense bodies; no cell membrane disruption is present and the cells undergo budding as apoptotic bodies,

with cell shrinkage occurring. Lysosomes are intact inside the cells and neither inflammation nor fibrosis is induced, because apoptotic cells are phagocytosed by neighboring cells or macrophages (Takemura and Fujiwara, 2004). Ischemic myocytes also can undergo autophagy. This degradation process of endogenous proteins and organelles by the lysosomes is activated in conditions of energy deprivation and allows the recycling of proteins or organelles (Yan et al., 2005). Autophagy is also observed in conditions of cell death and its mechanisms are very different from those of necrosis or apoptosis, because the recycling of proteins by autophagy might rather be a survival mechanism to generate energy and new peptides. For these reasons, autophagy may be a long-term survival mechanism sustaining the viability of chronically ischemic myocardium.

The primary cardiac response to myocardial infarction (MI) is cardiomyocyte hypertrophy, which initiates a genetic program culminating in apoptotic myocyte loss, progressive collagen replacement, and enlargement of the left ventricle because cardiomyocytes are not able to actively regenerate after injury. Usually this process, termed cardiac remodeling, leads the ischemic heart to a pathological condition known as heart failure, which results in the progressive decline of ventricular performance.

1.1.3 Congestive Heart Failure

Heart failure is a complex syndrome that arises from inherited or acquired abnormalities of cardiac structure or function, which impair the ability of the heart to pump blood.

The prevalence of congestive heart failure (CHF) in developed countries is 1-2% of the adult population, and approximately 6-10% in the elderly. In the US, congestive HF is responsible for more than 30,000 deaths and 700,000 hospitalizations annually (Blinderman et al., 2008). With an aging

population, increasing rates of obesity and diabetes, and the availability of interventions that prolong survival following cardiac damage, the incidence of heart failure will rise over the coming decades. The costs associated with an increasing number of patients and specialized treatments are contributing significantly to the economic burden caused by this pathology.

Common causes of HF include disorders that chronically increase cardiac workload, such as loss of muscle due to myocardial infarction or pressure overload due to hypertension (**Figure 1.4**). The cardiac response to these conditions entails complex remodeling of cardiomyocytes and the non-myocyte cells, which could initially be adaptive but, eventually, progress to contractile dysfunction, ventricular dilatation, and arrhythmias (Shah and Mann, 2011). This condition is usually called "congestive" heart failure because the heart's inability to pump correctly can cause blood and fluid to back up into the lungs or accumulate in the lower extremities.

Signs and symptoms of heart failure include tachycardia, venous congestion (edema) and low cardiac output (fatigue). HF is generally diagnosed by echocardiography (to evaluate left ventricular function) or electrocardiography (to identify arrhythmias), chest radiography (to diagnose pulmonary edema), angiography (to evaluate the patency of coronary arteries in patients with history of coronary artery disease) and blood and urine tests (to analyze liver function and total blood count).

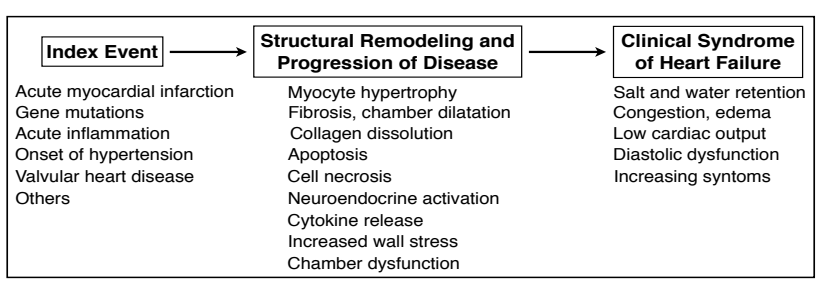

Figure 1.4 Congestive heart failure progression
Initial events, structural remodeling during progression of disease and clinical manifestation of HF *(Francis, 2001)*.

Development and progression of HF could be summarized in three sequential stages (Fedak et al., 2005):

1) *Preserved function:* In the first stage, the myocardium injured or subjected to increased load decrease its pumping capacity, therefore numerous adaptive compensatory mechanisms are activated, in order to preserve a normal cardiac function. Usually, in this phase clinical manifestations are absent. Irrespective of the type, extent, and duration of the initial injury, the majority of patients will anyway progress to the second stage of HF; however, the timing of progression is variable and unpredictable.

2) *Compensated dysfunction:* In the second stage of HF, the continued load, injury, and adaptive compensatory mechanisms act together to progressively deteriorate LV function. Usually the patients in this phase show moderate clinical manifestations that often require treatment. They exhibit myocardial hypertrophy and chamber dilatation and global cardiac function is abnormal. Despite the treatments, the majority of patients inevitably evolve towards the next stage of decompensated dysfunction (Swynghedauw, 1999).

3) *Decompensated dysfunction:* In this phase, the LV structure and size are grossly abnormal and characterized by wall thinning, LV dilatation, and the global cardiac function is severely compromised. This final stage shows high morbidity and mortality and cardiac transplantation is often the only therapeutic solution.

The most common cause of HF is ischemic heart disease, responsible for more than 60% of heart failure events. After the injury, as already mentioned, a series of initially compensatory, but subsequently maladaptive mechanisms, such cardiac remodeling, are activated in order to preserve normal cardiac output. Ventricular remodeling plays a key role in the ventricular dysfunction pathology occurring after an infarct (Zornoff

et al., 2009). Alterations in genome expression resulting in molecular, cellular, and interstitial changes, whose clinical manifestations include modifications in the size, shape, and function of the heart after cardiac damage, are the major determinants of this process (Cohn et al., 2000).

Ventricular remodeling could be divided into an early phase (within 72 hours) and a late phase (beyond 72 hours). The early phase is characterized by the expansion of the infarct zone, which may lead to ventricular rupture or aneurysm formation. Late remodeling involves the left ventricle globally, and is associated with time-dependent dilatation, distortion of ventricular shape, and mural hypertrophy **(Figure 1.5**). The failure to normalize increased wall stresses results in progressive dilatation, recruitment of border zone myocardium into the scar, and deterioration in contractile function (Sutton and Sharpe, 2000).

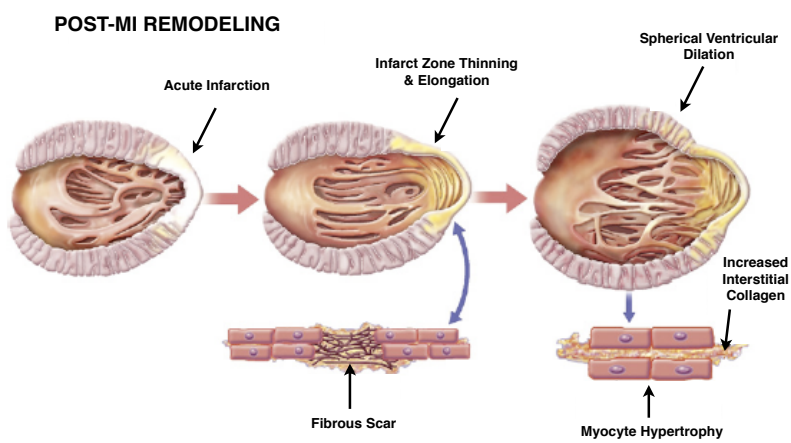

Figure 1.5 Left ventricle post-MI remodeling
The early phase of post-MI LV remodeling is characterized by the formation of a fibrous scar in the infarcted zone, which progressively becomes thinner and start to elongate. On the other hand, the main feature of late remodeling phase is LV dilation, which is driven by myocyte hypertrophy, apoptosis and collagen deposition *(Konstam et al., 2011).*

Additional changes, such as increase in end-systolic and end-diastolic

volumes with decrease in ejection fraction and shortening fraction (Pennock et al., 1997) are frequently observed.

Pathological remodeling is associated with the activation of neuroendocrine, paracrine, and autocrine factors, which are upregulated after myocardial injury and in a context of hemodynamic alterations.

The renin-angiotensin-aldosterone axis, the beta-adrenergic pathway, increased oxidative stress and cell death, changes in calcium transit, release of proinflammatory cytokines and endothelin, energy deficit and collagen accumulation are all contributing factors involved in the onset of ventricular dysfunction (Konstam et al., 2011). Cardiac remodeling can be considered a central target for treatment in patients with congestive HF. Novel therapeutic strategies able to limit it by the modulation of molecular and cellular factors involved in tissue repair could be essential to improve patients' outcome. Therefore, a better understanding of the complex mechanisms underling this process is absolutely required.

1.1.3.1 Compensatory and pathological hypertrophy

Cardiac hypertrophy is the common response of the myocardium to different kinds of stimuli and can be easily defined as an increase in heart mass (Bernardo et al., 2010). Cardiomyocyte hypertrophy is an adaptive mechanism that improves pump function by expanding the volume of contractile myocytes and reduces wall stress by increasing wall thickness. However, when excessive or prolonged, myocyte hypertrophy is maladaptive and it can directly results in congestive heart failure (Fedak et al., 2005).

Physiological cardiac hypertrophy (during normal postnatal growth or in response to exercise or pregnancy) is reversible and is characterized by normal or enhanced cardiac function and by normal cardiac morphology, with proportional growth of cardiomyocyte and vascular network, without

cardiac fibrosis. In contrast, pathological cardiac hypertrophy results from stressing stimuli such as hypertension, which is the most frequent cause of LV hypertrophy, valvular heart disease, myocardial infarction or neuro-hormonal activation. It could also be due familiar hypertrophic cardiomyopathy, a well known hereditary condition with monogenic inheritance. Pathological hypertrophy is typically associated with loss of myocytes and fibrotic replacement, reduction of capillary density, cardiac dysfunction, and increased risk of heart failure and sudden death. In addition to the mentioned structural and functional alterations, during pathological hypertrophy modification of cardiac metabolism also occur. In particular fatty acid oxidation, which is the main metabolic pathway responsible for generating energy, accounting for 60–70% of ATP production, is dramatically reduced and paralleled by an increase in glucose metabolism (Stanley et al., 2005). Many pathways are implicated in cardiomyocyte hypertrophy regulation, acting through a complex network of intracellular signaling cascades (**Figure 1.6**).

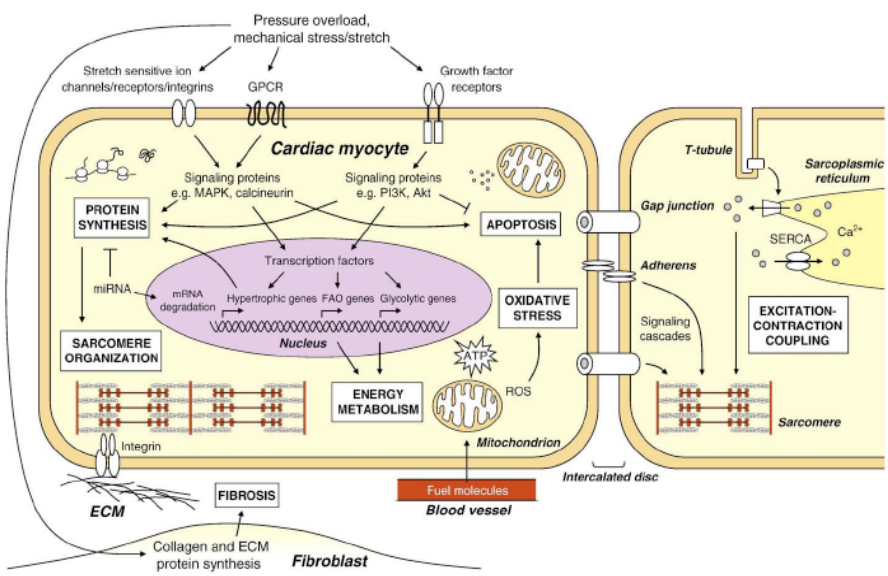

Figure 1.6 Cellular processes leading to the development of cardiac hypertrophy
Growth of cardiac myocytes is dependent on the initiation of several events in response to an increase in functional load, including activation of signaling pathways, changes in gene expression, increases in the rate of protein synthesis, and the organization of contractile proteins into sarcomeric units *(Bernardo et al., 2010)*.

Moreover, it is now well recognized that pathological hypertrophy is associated with alterations in cardiac contractile proteins (a decrease in α- and an increase in β-myosin heavy chain (MHC)), increased expression of fetal genes like atrial natriuretic peptide (ANP), B-type natriuretic peptide (BNP), α-skeletal actin and down-regulation of calcium-handling proteins like sarcoplasmic reticulum Ca^{2+}-ATPase 2a (SERCA2a).

In response to hemodynamic overload, autocrine and paracrine factors including Ang II, endothelin-1, IGF-1, TGF-β and cardiotrophin-1 are released from cardiomyocytes and activate intracellular cascades that trigger Ca^{2+} release and the consequent induction of maladaptive hypertrophic signaling through calcineurin–NFAT activation or calmodulin-dependent kinase (CaMK)–HDAC inactivation. The activation of MAPK signaling pathways is also linked to hypertrophy. This cascade is initiated in cardiomyocytes by GPCRs, receptor tyrosine kinases (IGF-I and FGF receptors), receptor serine/threonine kinases (TGFβ receptors), cardiotrophin-1 and by stress stimuli such as stretch (Heineke and Molkentin, 2006). MAPK cascade ends with phosphorylation and activation of p38, c-Jun, JNKs and ERK that phosphorylate multiple intracellular targets, including many transcription factors that induce the reprogramming of cardiac gene expression.

According to the complexity of the pathological hypertrophic process, it is absolutely required that therapeutic strategies to counteract this disease aim at controlling these maladaptive signaling pathways.

1.1.4 Peripheral Artery Disease

Peripheral artery disease (PAD) is caused by the progressive narrowing of arteries in lower extremities, in particular the iliac, femoral, popliteal and tibial arteries are the most commonly affected. PAD is a relatively common manifestation of atherosclerotic vascular disease, associated with significant morbidity and mortality (Selvin and Erlinger, 2004; Tendera et al., 2011). PAD affects a total of 27 million people in Western Europe and North America, approximately 16% of the total population of these countries, with an age > 55 years. In the United States, a higher prevalence of PAD is observed among African–American and Hispanic populations.

Similar to coronary artery disease and cerebrovascular disease, the risk factors that contribute to the development of PAD are advancing age, hypertension, dysipidemia, diabetes mellitus, smoking and obesity. Additional risk factors associated with PAD include chronic kidney disease, low serum vitamin D levels, and the presence of inflammatory biomarkers such as homocystein, C-reactive protein, β2-microglobulin and cystatin C (Lau et al., 2011).

The clinical presentation of PAD may vary from no symptoms to intermittent claudication, atypical leg pain, rest pain, ischemic ulcers, or gangrene (Olin et al., 2011). However only 10% to 35% of patients with PAD present typical claudication and 1% to 2% progress to critical limb ischemia (CLI), while 50% of all patients with PAD are asymptomatic.

Although therapies to improve symptoms and reduce the complications of PAD are available, detection and treatment rates of this disease are still low (Watson et al., 2006). One explanation for this low rate is the absence or variability of symptoms in patients with the disease, which makes PAD frequently underdiagnosed and thus undertreated. Cardiovascular morbidity and mortality are increased in patients with PAD whether they

are symptomatic or not. Within 1 year from diagnosis, 25% of patients with critical limb ischemia die of cardiovascular disorders and another 25% suffer major limb amputation. Even patients with stable PAD or asymptomatics have a 20% incidence of myocardial infarction or stroke and 15% to 30% of mortality in 5 years (Gandhi et al., 2011).

The treatment of subjects with critical limb ischemia is dependent on the severity of the symptoms and their impact on lifestyle. Patients with a mild to moderate disability are traditionally treated with a regimen of risk-factor modification and exercise, while patients with severe symptoms are usually revascularized by endovascular or surgical approaches, in order to preserve or restore function and limb viability.

1.1.5 Conventional treatments for cardiovascular disorders

1.1.5.1 Acute Myocardial Infarction

The management of patients with an acute myocardial infarction (MI) event includes rapid restoration of blood flow by pharmacological and catheter-based means, block of recurrent ischaemic events through antithrombotic therapies, and treatments aimed at reducing the effects of myocardial necrosis and preventing future events (White and Chew, 2008).

Usually, the immediate treatment for acute MI includes oxygen, aspirin and sublingual nitroglycerin. Nitroglycerin has a vasodilatory effect on the coronary and peripheral vessels; consequently, it leads to a decrease in myocardial wall stress and oxygen demand (Sami and Willerson, 2010). In addition, pharmacological reperfusion with fibrinolysis is the principal treatment for improving survival, frequently associated with percutaneous coronary intervention (PCI), an invasive treatment with cardiac catheterization and angioplasty. The number of patients who need a coronary artery bypass graft (CABG) in the acute phase is instead limited,

but CABG could be indicated after failed PCI (Van de Werf et al., 2008).
As already mentioned, during PCI intervention patients are usually co-treated with anticoagulant/fibrinolytic (heparin) and antiplatelet therapy (aspirin, clopidogrel and GPIIb/IIIa antagonists, able to block the final pathway of platelet aggregation). Other pharmacological therapies for the treatment of acute MI entail the use of β-blockers (Baker et al., 2011). These drugs, which are used both during and after an acute MI, act by competitively blocking the effects of catecholamines on the cardiomyocyte membrane beta-receptors, reducing myocardial contractility, sinus node rate, and AV node conduction velocity. All these effects lead to a decrease in cardiac work and myocardial oxygen demand (Anderson et al., 2007).

1.1.5.2 Long-term management of cardiovascular disease and heart failure

Coronary heart disease is a chronic condition, and patients who have recovered from a MI are at high risk for new events and premature death. From 8 to 10% of post-infarction patients have a recurrent infarction within a year after the first event, and mortality after discharge remains much higher than in the general population. Control of risk factors of cardiovascular diseases has a favourable effect on the incidence of later cardiovascular events. In particular, prevention by controlled lifestyle, physical exercise and the use of drugs to improve cardiac functionality are the most common approaches for this class of pathologies.
The pharmacological interventions for the management of patients affected by ischemic CVD and HF entail the use of different classes of drugs (Jessup and Brozena, 2003) (**Figure 1.7**):

- *Antiplatelet and anticoagulant*: long-term administration of antiplatelet agents like aspirin leads to 25% reduction in the risk of plaque rupture and major vascular events (Antithrombotic Trialists' Collaboration,

2002). The most commonly used agent is aspirin, but also other drugs with similar efficacy but greater cost are available, like the adenosine diphosphate receptor inhibitors clopidogrel, prasugrel and ticlopidine.

- *β-blockers:* several trials and meta-analyses have demonstrated that β-blockers reduce mortality and reinfarction by 20–25% in those patients who have recovered from an infarction (Fonarow, 2005). The primary action of β-blockers as β-adrenergic receptor antagonists is to counteract the harmful effects of endogenous catecholamines like epinephrine, norepinephrine and other stress hormones, exerting an antihypertensive and antiarrhythmic effect. They are used for treating hypertension, angina, myocardial infarction, arrhythmias and heart failure. The first generation of β-blockers (alprenolol, propranolol, etc.) was non-selective, meaning that they blocked both β_1 and β_2 adrenoceptors, while the second generation (atenolol, metopronol, etc.) is now more selective for the β_1 receptor (Frishman and Saunders, 2011). Evidence from all available studies suggests that β-blockers should be used indefinitely in all patients who have recovered from a STEMI and do not have any major contraindication.
- *Angiotensin-converting-enzyme (ACE) inhibitors:* they induce vasodilation and reduce the activity of the renin-angiotensin-aldosterone system by inhibiting the formation of angiotensin II. This vasoconstrictor is formed by the proteolytic action of renin, released by kidney, acting on circulating angiotensinogen to form angiotensin I. Angiotensin I is then converted to angiotensin II by ACE, therefore its inhibition leads to a decrease in blood pressure. Moreover ACE inhibitors block the breakdown of bradykinin, promoting vasodilatation. Another class of drugs that share many common features with ACE inhibitors is the *angiotensin II receptor blockers (ARBs).* Commonly used for patients intolerant to ACE inhibitors, ARBs may offer more complete angiotensin II inhibition by interacting selectively with the receptor site (Barreras and Gurk-Turner, 2003).

Controversy concerns the use of ARBs in patients with chronic heart failure who are already receiving ACE inhibitors; in patients at high risk for vascular events the combination of the two drugs was associated with more adverse events, without an increase in benefit (Yusuf et al., 2008).

- *Aldosterone antagonists*: patients with heart failure produce an excess of adolsterone that can lead to coronary inflammation, cardiac hypertrophy, myocardial fibrosis, ventricular arrhythmias, and necrotic lesions. Aldosterone antagonists act as diuretics; they antagonize the binding of adolsterone to the mineralcorticoid receptor and therefore decrease the reabsorption of sodium and water and the secretion of potassium, reducing edema and cardiac workflow (Nappi and Sieg, 2011).
- *Statins*: this class of drugs blocks the HMG-CoA reductase and, as a consequence, the cholesterol synthesis pathway, therefore they decrease the LDL cholesterol levels. Statins highly reduce the mortality of patients with pre-existing cardiovascular disease acting on cholesterol synthesis, but also modulating inflammatory response, endothelial function and increasing atherosclerotic plaques stability (Shanes et al., 2007).

Beside pharmacological treatments also invasive interventions could be considered as therapeutic options for long-term management of existing vascular diseases. The three most common procedures are the already mentioned *coronary artery bypass graft (CABG)*, *percutaneous coronary intervention (PCI)* and *PCI with stent*. CABG consists in the placement of grafts from the saphenous vein, but recently more often from internal mammary artery, to bypass stenosed coronary arteries. The main indication for CABG is for patients with left main coronary artery stenosis or multiple coronary arteries stenosis with reduced LV function, mainly among diabetics. The main indication for PCI is instead for low-risk patients with single or double vessel disease and poor response to medical treatment. The addition of stents to PCI leads to a decrease in restenosis rate.

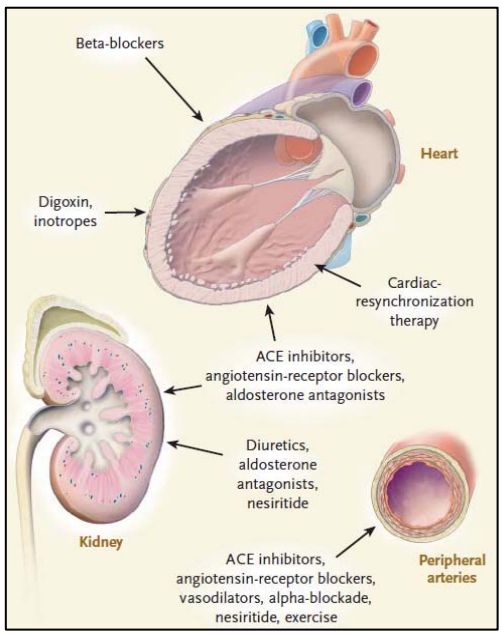

Figure 1.7 Main targets for heart failure treatment
Treatment options for patients with HF target more than one organ system involved in HF pathology *(Jessup and Brozena, 2003).*

Despite the improvements in acute care and the impact of primary and secondary prevention, coronary artery disease remains the leading cause of death worldwide. The improved survival of infarcted patients treated with the common therapies and surgery has moreover led, in the last decades, to a dramatic increase in the number of patient with compromised LV function and suffering from heart failure (Davis et al., 2002; Stewart et al., 2001). Considering the guidelines 2009 of the American Heart Association for treatments of HF (Hunt et al., 2009; Jessup et al., 2009), it is clearly evident that despite the availability of numerous drugs for the management of this pathology long-term prognosis associated with HF remains poor, indicating the need for new therapies. The current recommended treatments have been mainly developed more than 20 years ago thus novel treatments, able to counteract HF symptoms and also to directly impact on cardiomyocyte viability and function, are absolutely required.

1.2 BIOLOGICAL THERAPEUTICS AS NEW TREATMENTS FOR CARDIOVASCULAR DISEASE

Current therapies for cardiovascular pathology essentially aim at either counteracting symptoms or slowing disease progression, whereas no treatment able to stop or revert the disease is available so far. Despite this lack of curative therapies, however notable progresses have been recently achieved in understanding the cellular and molecular mechanisms leading to cardiac disorders. Some of these mechanisms appear common to several forms of degenerative conditions (for example those involved in the regulation of cell apoptosis), whereas others seem to be more specific for a particular disease. It can thus be expected that biological therapeutics, able to interfere with different mechanisms of disease onset and progression, might offer novel, exciting therapeutic opportunities by interacting with both common and specific mechanisms of disease.

Starting with insulin in the 1980s, over 350 biotechnological drugs have now gained clinical approval and over 400 have entered clinical trials (Rader, 2008; Walsh, 2006). These drugs also bear an important value from an economic point of view; in 2007, total recombinant protein-based drug sales were $54.5 billion, and are expected to increase to over $75 billion in 2012 (Pavlou and Reichert, 2004). Typical biological therapeutics that have been successfully introduced into clinical practice include blood coagulation factors (Factor VIII and Factor IX), thrombolytic agents (tissue plasminogen activator), hormones (insulin, glucagon, growth hormone, gonadotropins), vaccines (hepatitis B surface antigen and human papilloma virus L1 capsid antigen), monoclonal antibodies, various growth factors and cytokines and, more recently, nucleic acid–based products.

The delivery of nucleic acids for human therapy includes the use of coding cDNAs, but now is also extended to a variety of novel DNA- or RNA-based

biological therapeutics, including oligonucleotides, short RNA and DNA molecules with catalytic function, short RNAs with regulatory function (siRNA and microRNA), decoy RNA or DNA molecules and aptamers.
Many of the mentioned classes of biological therapeutics have been explored in order to identify novel treatments for cardiovascular disorders and in particular recombinant proteins administration, cell and gene therapy approaches, so far offer the most promising therapeutic perspective in this field. According to the 2011 report from the Pharmaceutical Research and Manufacturers of America (PhRMA) (www.phrma.org) nowadays biopharmaceutical research companies are developing nearly 300 new treatments for cardiovascular diseases and the number is doomed to increase in the future.

1.2.1 Recombinant protein administration

Recent evidence indicates that different cytokines and growth factors have a marked effect on cardiomyocyte viability and contractility in animal models of myocardial infarction and HF. In particular, factors able to stimulate therapeutic angiogenesis and therefore to increase the perfusion of the ischemic region, represent a novel and promising treatment for ischemic heart disease, mainly for patients who are not candidates for current methods of revascularization. Angiogenic growth factors, such as fibroblast growth factor (FGF), vascular endothelial growth factor (VEGF), insulin growth factor (IGF), hepatocyte growth factor (HGF) and others have demonstrated to promote *in vivo* new vessel formation and to exert beneficial effects in ischemic conditions, that are also broader when they are administered in combination (Kano et al., 2005; Lu et al., 2007).

The members of the FGF family bind to various spliced isoforms of the FGF receptors and the activation of these receptors, which are expressed on endothelial cells, smooth muscle cells and myoblasts, induces the

proliferation of these cell types. In particular, FGF-1 and FGF-2 are highly angiogenic and may act synergistically with VEGF (Losordo and Dimmeler, 2004). FGF-1 angiogenic properties have been widely described and it has been shown that its administration induces the development of new vascular structures in the ischemic human heart (Schumacher et al., 1998). Similarly, the administration of FGF-2 in patients with severe CHD was shown to improve myocardial perfusion, enhancing the development of collateral vessels (Laham et al., 2000; Udelson et al., 2000). These suggestions of therapeutic efficacy were tested in a double blind phase II trial, but, awfully, the results from the FGF-2 Initiating Revascularization Support Trial (FIRST) revealed that a single intracoronary infusion of recombinant FGF-2 did not improve exercise tolerance or myocardial perfusion but showed trends toward symptomatic improvement at 90 (but not 180) days, in patients with CAD (Simons et al., 2002).

Hepatocyte growth factor (HGF) is another protein that, among its many functions, exerts also high proangiogenic activity. It acts through the receptor c-met, which is expressed on a variety of cells, including endothelial cells and hematopoietic stem cells (Morishita et al., 1999). In addition HGF is a potent anti-fibrotic factor, which plays an important role in the pathogenesis of fibrotic cardiovascular disease, like cardiomyopathy.

Insulin-like growth factor I (IGF-I) also exhibits attractive therapeutic profile for the treatment of cardiac disorders. This molecule was described as a cardioprotective agent for the first time during the '90s (Buerke et al., 1995), demonstrating that pre-treatment with this growth factor reduced myocardial necrosis, apoptosis, and neutrophils accumulation in a rat model of myocardial ischemia followed by reperfusion. IGF-I is a growth factor very similar to insulin, which is synthesized by various cell types, including cardiomyocytes (Ren, 2002). The IGF-I effects on the cardiovascular system are mainly mediated by an increase in nitric oxide

synthesis after the interaction of IGF-I with its specific receptors on endothelial cells (vascular function and regeneration) and cardiomyocytes (myocardial function and survival) (Conti et al., 2004). Many authors have extensively described the potential cardioprotective role of recombinant human IGF-I; however the temporal window and duration of IGF-I administration were demonstrated to be critical issues in determining the beneficial effects of this molecule. Indeed, persistent expression of IGF-I in a transgenic mouse model initially induced a physiologic hypertrophy, characterized by increased cardiac mass and improved systolic performance; however, later on this hypertrophy progressed to a pathological condition characterized by decreased systolic performance and increased interstitial fibrosis (Delaughter et al., 1999). Recombinant human IGF-I administration actions on cardiovascular system were studied both in health and disease conditions, with particular attention to HF (Donath et al., 1998; Duerr et al., 1995). However, no placebo controlled trial based on recombinant IGF-I administration has so far been conducted, neither in patients with acute atherothrombosis nor in patients with chronic ischemic heart disease.

The proangiogenic factor most extensively studied is VEGF; the mammalian family of the vascular endothelial growth factor includes five structurally related proteins: VEGF-A, VEGF-B, VEGF-C, VEGF-D and placental growth factor (PIGF). The biological effects of this class of molecules are mediated by cell surface tyrosine-kinase receptors (RTKs). In particular, VEGF-A and its splice variants preferentially activate VEGFR-1 and VEGFR-2, VEGF-B only VEGFR-1, whereas VEGF-C and VEGF-D stimulate VEGFR-2 and VEGFR-3, thereby contributing to lymphangiogenesis (Ferrara et al., 2003; Henry et al., 2003; Matsumoto and Claesson-Welsh, 2001). VEGF-A, usually referred to as VEGF *tout court* (Ferrara and Henzel, 1989), was discovered as an essential player in angiogenesis, both in health and disease. The

factor enhances migration, increases permeability and promotes survival of endothelial cells (ECs) (Zachary and Gliki, 2001). VEGF also exerts a variety of pleiotropic effects, which include a cardioprotective effect during acute ischemic conditions (Hausenloy and Yellon, 2009; Luo et al., 1997), by acting on cardiomyocyte survival.

Successful therapeutic angiogenesis has been reported with VEGF protein in numerous preclinical models (Lopez et al., 1998; Pearlman et al., 1995). Initial clinical trials using intracoronary and intravenous recombinant VEGF protein demonstrated safety, tolerability, and encouraging clinical results (Hendel et al., 2000; Henry et al., 2001), leading to the VIVA (Vascular endothelial growth factor in Ischemia for Vascular Angiogenesis) trial (Henry et al., 2003). This trial did not reach some primary endpoints, such as exercise treadmill time or myocardial perfusion improvement (except for the high-dose VEGF group), revealing the main challenges of this therapeutic approach. The most obvious limitation of protein therapy is indeed the demand to maintain therapeutic concentration sufficient to induce the desired angiogenic response for an adequate time in the specific target tissue. More in general, a main obstacle for cardiac therapy based on recombinant proteins is clearly the way by which these are delivered. Oral, intravenous, intrarterial, or intramuscular routes for protein administration are not always as effective as desired, and the therapeutic protein can be metabolized or cleared before it can enter the target tissue.

Gene transfer to the myocardium is nowadays considered the most promising alternative strategy to achieve prolonged local expression of angiogenic proteins in the target tissue. This technology will be described in details in section 1.2.3.

1.2.2 Cell Therapy

Cell therapy could be defined as the transplantation of human or animal cells to replace or repair a damaged tissue. This concept appears certainly appealing in particular for cardiovascular pathologies, for which the possibility to regenerate or repair nonviable myocardium by delivery of stem or progenitor cells from many different sources could open novel, intriguing therapeutic perspectives.

Traditionally, the heart was considered a post-mitotic organ and the possibility to obtain cardiac regeneration has been intensely investigated for more than 150 years (Carvalho and de Carvalho, 2010; Laflamme and Murry, 2011). However, recent evidence raises the possibility that a natural system of myocytes repair exists; around 45% of human cardiomyocytes are exchanged during life span, but of course this percentage is not sufficient to guarantee an adequate repair upon an ischemic insult (Bergmann et al., 2009).

In both preclinical and clinical studies, the potential of various stem cell populations for cardiac repair has been analyzed (**Figure 1.8**):

- *Bone marrow-derived cells (BMCs):* This heterogeneous cell population has been the most studied over the last 15 years in order to define cell therapy strategies for cardiovascular disorders. Initially this approach has been considered as a new opportunity to enhance cardiac performance by the possibility to induce trans-differentiation of the injected cells into cardiomyocytes (Orlic et al., 2001). Starting from this original evidence, several clinical studies, for both chronic ischemic disease and acute myocardial infarction, were initiated (Murry et al., 2005). Most of the trials for chronic myocardial ischemia, confirmed the safety of the procedure and a beneficial effect of the treatment on LV function after long follow up (Perin et al., 2003; Strauer et al., 2010; Tse et al., 2007; van Ramshorst et al., 2009). The vast majority of bone marrow clinical trials

involved patients with acute myocardial infarction. Several of these studies have demonstrated long-term (>3 years) improvement of ventricular performance after stem cell therapy, resulting in an increase in ejection fraction and decreased infarct size (Beitnes et al., 2009; Meyer et al., 2009; Schachinger et al., 2004; Schachinger et al., 2006; Strauer et al., 2002; van der Laan et al., 2008). The increase in cardiac performance, however, turned out to be modest in all these studies. This rather disappointing finding, together with the subsequent demonstration that BMCs actually do not differentiate into cardiomyocytes once injected in the heart (Balsam et al., 2004; Murry et al., 2004) has now markedly lowered the enthusiasm for BMCs transplantation. The modest, beneficial effect these cells exert might be explained by their paracrine secretion of growth factors, especially those stimulating angiogenesis (Du et al., 2008; Kocher et al., 2001; Molina et al., 2009).

Bone marrow includes many different cell populations that possess the ability to proliferate, migrate and differentiate into various mature cell types including the aforementioned haematopoietic stem cells (HSC), but also endothelial progenitor cells (EPC), mesenchymal stem cells (MSC), multipotent adult progenitor cells and "side-population" cells. All these cells have been identified by specific surface markers and individually studied in order to characterize their beneficial potential after transplantation in ischemic hearts. Of these cell populations, a positive effect on cardiac function has been well established in particular for MSCs. Similar to the case of HSCs, the ability of MSCs to transdifferentiate into cardiomyocytes-like cells is also controversial (Shi and Li, 2008; Toma et al., 2002; Wang et al., 2006). Clinical experience of cardiac cell therapy with MSCs is limited to date. The first published clinical trials (Chen et al., 2004; Hare et al., 2009; Yang et al., 2010) reported that these cells are very well tolerated after allogenic transplantation and confirmed the safety of their infusion, with no

deaths reported during follow-up, and no induction of arrhythmias. Because of the promising efficacy data from the above-mentioned trials, the interest towards this therapeutic approach remains high and many clinical trials such as PROMETHEUS (NCT00587990) or POSEIDON (NCT01087996) are currently ongoing both for both MI and HF.

- *Cardiac progenitor cells:* Several investigators have reported the presence of resident populations of cardiac progenitor cells (CPCs) in postnatal hearts, which were identified by the expression of specific surface markers such as c-Kit or Sca-1 (Beltrami et al., 2003; Matsuura et al., 2004; Oh et al., 2003). CPCs expressing c-kit are the most extensively studied of these cells. After isolation from rat and human hearts, c-kit+ cells have been reported to give origin to cardiomyocytes, smooth muscle cells and endothelial cells. Some studied indicated that, when transplanted, these cells induce extensive regeneration of myocardial infarction (Bearzi et al., 2007), whereas others suggest smaller-scale regeneration (Tang et al., 2010). A clinical trial (NCT00474461) based on intracoronary infusion of this cell population is ongoing, but preliminary results of the phase I trial seem very encouraging (Bolli et al., 2011). Another CPCs population currently in clinical trial (NCT00893360) is cardiosphere-forming cells (CSs) (Barile et al., 2007; Messina et al., 2004). These cells grow as clusters, migrate from cultured cardiac tissue fragments and give rise to cardiomyocytes and vascular cells (Chimenti et al., 2010). However, the stemness of these cells has been recently questioned and it has been suggested that they could be mainly cardiac fibroblasts and that spontaneously beating CSs consist of contaminating myocardial tissue fragments (Andersen et al., 2009). So far, the randomized phase I trial confirmed the safety of intracoronary infusion of CSs in infarcted patients and highlighted an increase in viable myocardium after treatment (Makkar et al., 2012).

- *Embryonic stem* cells (ESc): This class of pluripotent cells is able to generate virtually all different cell types and tissues in the organism. Multiple evidence show that ESc can differentiate into cardiomyocytes and improve contractile function upon transplantation into the infarcted myocardium (Kehat et al., 2001). However, the risk of teratoma formation prevents the direct inoculation of these cells *in vivo*, and demands the complete *in vitro* differentiation of these cells into cardiomyocytes before transplantation (Nussbaum et al., 2007). Other problems preventing clinical translation of ESc are their allogenic origin, which can induce a strong immune response in target tissues (Saric et al., 2008), and of course the still opened ethical concerns related to this type of cells.

- *Induced pluripotent stem cells (iPSCs):* The possibility to generate a population of pluripotent stem cells, with plasticity similar to that of ESc, by nuclear reprogramming of somatic cells, has recently opened completely new possibilities for cell therapy (Hochedlinger and Jaenisch, 2006; Yu et al., 2007). This approach could overcome the ethical issues related to the use of embryos to obtain ESc and could also allow to generate patient-specific stem cells, avoiding problems related to immune rejection. Initially iPSCs were generated by retroviral vector delivery of four genes coding for transcription factors regulating "stemness" into skin fibroblasts (Takahashi and Yamanaka, 2006). More recently, many different strategies have been attempted to reduce the number of genes (now Oct4 seems to be the only one necessary for reprogramming) and to avoid the use of viral vectors (Kim et al., 2009; Okita et al., 2008). Some publications have demonstrated the ability of iPSCs to differentiate into functional cardiomyocytes and to exert beneficial properties in models of myocardial infarction (Mauritz et al., 2008; Nelson et al., 2009). Nevertheless, several problems related to the number of cardiomyocytes that can be generated using the iPS technology and to the safety of the approach still need to be

solved before proceeding towards clinical translation for cardiac regeneration.

- *Adipose tissue-derived cells* and *umbilical cord-derived cells* have been also reported to be able to prevent left ventricle dilatation and to enhance cardiac function after MI (Moelker et al., 2007; Planat-Benard et al., 2004). In particular the facilitation of access to fat and its abundance make adipose tissue-derived cells an appealing source for cell based cardiac repair.

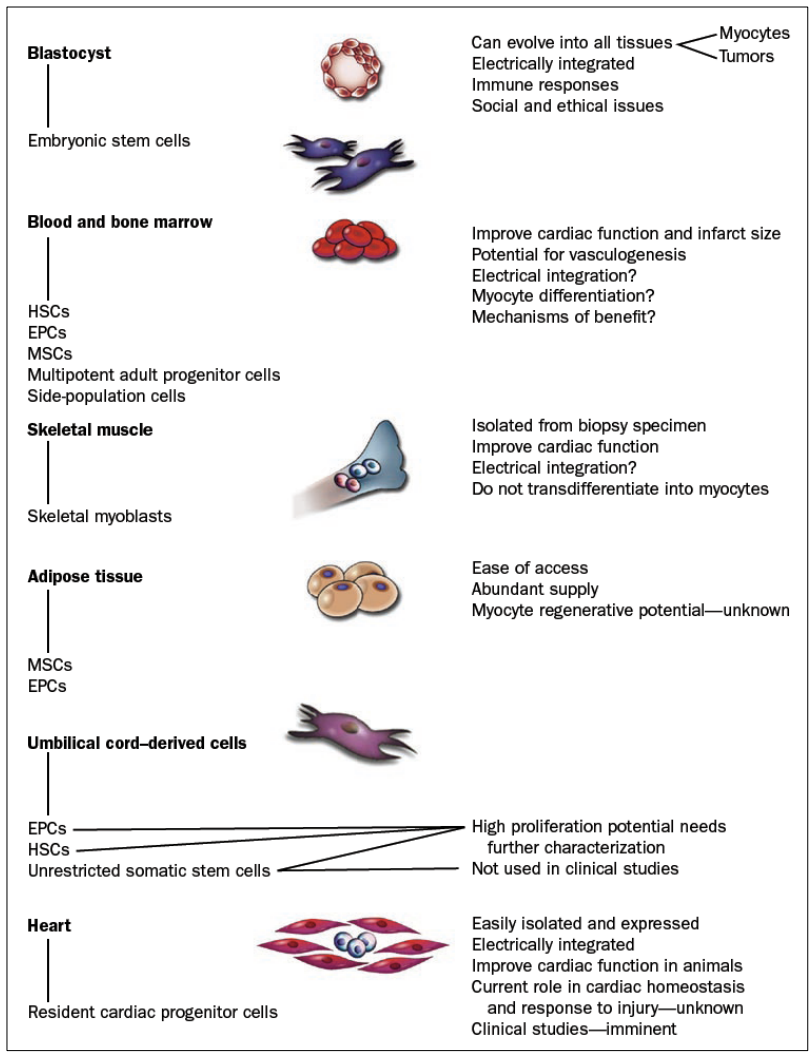

Figure 1.8 Cell therapy: features of different cell types
In the picture the features of many cell types considered as candidates for cell therapy both in preclinical and clinical studies are summarized (*Gersh et al., 2009*).

1.2.3 Gene therapy approaches for cardiovascular disorders

The growing knowledge of the underlying molecular mechanism of myocardial diseases has led to the definition, in the last decades, of novel potential therapeutic targets, such as genes coding for calcium handling proteins, sarcomeric and cytoskeletal proteins, angiogenic or antiapoptotic factors and many other important regulators involved in damaged heart protection or regeneration.

In addition, an essential element for the development of effective gene therapy approaches for cardiovascular disorders is the identification of the best vector and gene delivery system for each pathological condition. In this direction many headway have been achieved in these years, in order to optimize strategies able to guarantee a high efficacy of myocardial gene transfer and a prolonged expression of the therapeutic gene in the target tissue.

1.2.3.1 Targeting the heart: gene delivery strategies

Nowadays a number of vectors and delivery strategies for gene transfer in the myocardium are available. Of course the pathological features of the disease, the timing of intervention and the role of the therapeutic gene, exert an essential role for the definition of the most effective one.

While the choice of the transgenes can be easily modified with increasing knowledge in molecular biology and physiology, obtaining efficient and long-term delivery of the therapeutic genes seems to be the most critical point in clinical gene therapy approaches attempted so far (Muller et al., 2007).

In order to choose the best delivery option for cardiac gene therapy, it is important to consider that a vector has to overcome several physical barriers to reach the target cells and that these barriers can influence its biodistribution, cellular uptake and intracellular trafficking (**Figure 1.9**).

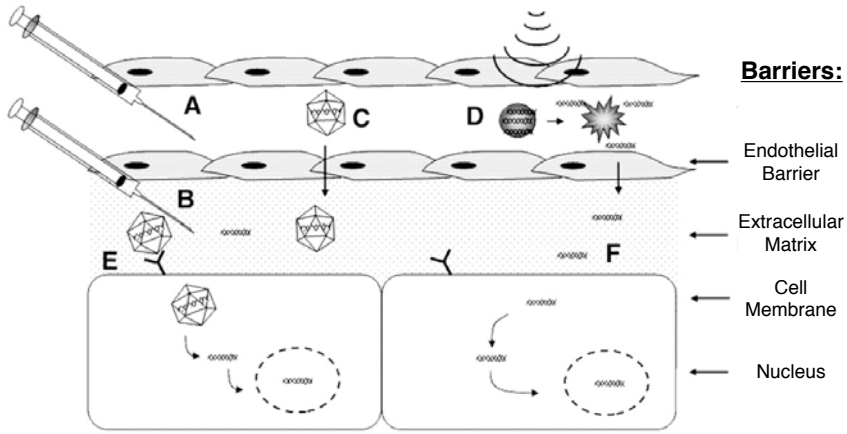

Figure 1.9 Delivery barriers for cardiac gene transfer
Representation of different strategies to pass the cellular barriers and reach the nucleus: a) transvascular approach (intravenous, intraarterial, retroinfusion); b) intramyocardial injection; c) endothelial penetration mediated by viral vector; d) ultrasound mediated vector delivery; e) receptor mediated viral entry; f) DNA penetration of cell membrane by intramyocardial injection, liposome or ultrasound *(Muller et al., 2007).*

In particular, viral vectors need to escape neutralizing antibodies in the bloodstream, because a potential interaction can cause immune activation. Another barrier to cross whether the vectors are not directly injected into the myocardium is the endothelial cell barrier in the capillary wall (Di Pasquale and Chiorini, 2006). Once the vector reaches the interstitial space, it has to take advantage of the naturally occurring endocytosis and intracellular trafficking pathways and release the genetic material into the nucleus.

As previously mentioned, the definition of an optimal gene delivery method, which allows the vector to overcome these barriers, is absolutely essential for successful gene therapy. Several routes have been used to administrate the therapeutic gene to the myocardium (**Figure 1.10**). Intracoronary delivery is usually the preferred way for global myocardial diseases, such as heart failure and cardiomyopathy. However, the barrier

imposed by the coronary endothelium membrane may limit the diffusion of the vectors and the consequent distribution and uptake of the therapeutic transgene; moreover this route of administration could also lead to significant collateral organs gene delivery. In contrast, intramyocardial injection could be a desirable method for gene transfer to specific areas of myocardial disease and this approach has been extensively exploited to deliver angiogenic and cytoprotective genes to ischemic myocardium (Isner, 2002; Schwarz et al., 2000). With this strategy, however, transgene expression is restricted to the area near the site of injection, and multiple injections are often required to treat the damaged tissue and to induce a therapeutic effect. Anyway the direct gene delivery approach was the first one that allowed to establish the efficacy of cardiac gene therapy and it has been successfully used both in experimental models and in Phase I/II clinical trials, demonstrating its therapeutic relevance (Kornowski et al., 2000; Rosengart et al., 1999).

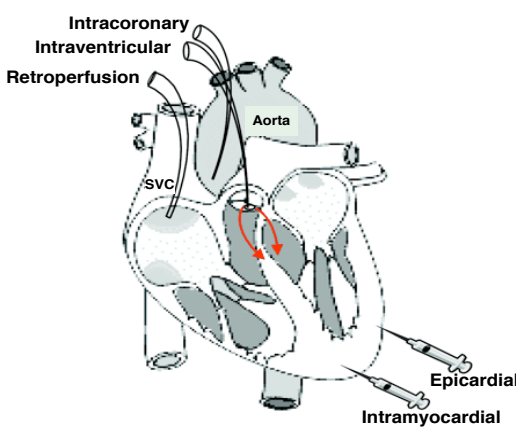

Figure 1.10 Delivery routes of a therapeutic gene to the heart
The five routes most commonly used for the administration of therapeutic genes into the heart include: intramyocardial and epicardial direct injection, intracoronary infusion using catheters, intraventricular delivery or retroperfusion *(Melo et al., 2004).*

In addition, a variety of catheters have been developed both for intracoronary and intramyocardial delivery (Sylven et al., 2002; Vale et al., 2001). As already mentioned, antegrade intracoronary injection is one of

the most direct way to deliver vectors to the myocardium (Kawase et al., 2008), while another strategy less commonly used is the retrograde injection into the coronary sinus or cardiac vein (Raake et al., 2004). Recently, a novel technique that allows a closed recirculation of vector genomes in the cardiac circulation using cardiopulmonary bypass (MCARD) has been developed. This approach efficiently isolated the heart from the systemic circulation *in vivo* and resulted in global cardiac-specific LV gene expression (White et al., 2011). A direct injection of the vector into the myocardium, on the other hand, can be achieved surgically or percutaneously, by direct or catheter-based ventricular delivery or by pericardial delivery (Fromes et al., 1999; Katz et al., 2011; Ly et al., 2007).

1.2.3.2 Cardiac gene targets

As mentioned in the previous paragraph a significant evolution in the understanding of the pathophysiology of cardiovascular disorders has been reached over the past 20 years and several genes have emerged as potential targets for gene therapy approaches. Strategies for rescuing the failing myocardium included the delivery of genes coding for proangiogenic growth factors, in order to promote neovascularization of ischemic myocardium or, in the post-infarction period, the inhibition of genes involved in regulation of ventricular remodeling such as the matrix metalloproteinases (MMPs) that participate in extracellular matrix degradation. In addition, potential strategies for rescuing contractile function include over-expression of the sarcoplasmic reticulum calcium ATPase (SERCA2a), β-adrenergic receptor, and adenylate cyclase. Moreover, many approaches to obtain cardiac protection have been described, such as the overexpression of cytoprotective and pro-surviving genes coding for antiapoptotic proteins or antioxidant enzymes, or the

inhibition of genes expressing pro-inflammatory proteins. These approaches are briefly described below.

Angiogenic gene therapy

Genes coding for factors able to induce therapeutic angiogenesis are certainly the most explored in these years, with numerous clinical trials already completed (Giacca and Zacchigna, 2012; Yla-Herttuala and Alitalo, 2003). Therapeutic blood vessel growth into an ischemic tissue can be achieved by gene transfer, either as single vectors or in combinations, of members of the VEGF family, FGF family, by HGF, IGF-I, PDGF, angiopoietins, hypoxia inducible factor–1α (HIF-1α) and also by several other "less popular" molecules, currently under investigation.

Traditionally, new blood vessel formation in the adult life occurs through capillary sprouting from pre-existing vessels. The process starts with the proliferation and migration of endothelial cells, paralleled by a wide extracellular matrix remodeling. Afterwards, the new capillaries progressively mature by the addition of mural cells (pericytes and smooth muscle cells) allowing proper functionality, and a vascular network formed by arterioles and venules is formed (Risau, 1997).

In physiological conditions, the main regulator of angiogenesis is hypoxia. In situations of low oxygen, the transcription factor HIF-1 (Hypoxia Inducible Factor–1) activates the expression of many genes such as the vascular endothelial growth factor (VEGF) and its receptors, which are essential for the angiogenetic process (Giacca, 2007). Thanks to its prominent role in promoting neovascularization, VEGF has been the most investigated molecule for the promotion of therapeutic angiogenesis. As already mentioned, the VEGF family is composed of five members (VEGF-A, B, C, D and PlGF), with different isoforms arising from alternative splicing (Ferrara, 1999). VEGF-A is surely the best-characterized one; it originates

four main isoforms of 189, 165, 149 and 121 amino acids and among them VEGF-165 is the most potent in promoting new blood vessels formation (Giacca, 2010; Rissanen and Yla-Herttuala, 2007).

In addition to the results obtained by recombinant VEGF administration (described in section 1.2.1), also the *in vivo* overexpression of VEGF by viral vectors has been shown to stimulate excellent angiogenesis, remodeling of the capillary network and consequent perfusion increase, both in ischemic and healthy skeletal muscle and myocardium (Giacca and Zacchigna, 2012). VEGF-165 gene therapy mediated through plasmids or adenoviral vectors in rats induced significant neovascularization and improved fractional shortening after infarction (Hao et al., 2007; Schwarz et al., 2000). In porcine and dog models of MI, VEGF-165 increased myocardial blood flow, improved wall thickening (Jacquier et al., 2007), increased ejection fraction and myocardial viability (Ferrarini et al., 2006) thereby leading significant benefits to cardiac function. Also in models of hind limb ischemia, VEGF-165 delivery as naked DNA or by adenoviral vector gene transfer induced capillaries and arterioles sprouting and augmented development of collateral vessels (Rissanen et al., 2005; Takeshita et al., 1996; Tsurumi et al., 1996).

Another important member of the VEGF family, which is emerging as a major cytoprotective factor, is VEGF-B. This factor selectively binds VEGF receptor (VEGFR)-1, a receptor that does not mediate angiogenesis; therefore it exerts its cardioprotective action upon AAV-mediated gene delivery in infarcted myocardium by limiting apoptotic cell loss and delaying the progression toward heart failure (Pepe et al., 2010; Zentilin et al., 2010).

Beside VEGF, another gene extensively studied for the induction of therapeutic angiogenesis is FGF. The FGF family actually includes 22 related proteins, which affect cellular growth, proliferation and migration

(Itoh and Ornitz, 2011). These factors are potent endothelial cell mitogens and also act as ligands for other cell types including vascular smooth muscle cells and fibroblasts. FGF-1 (aFGF) and FGF-2 (bFGF) are the prototypic members of the family and they were the first that were shown to induce new blood vessel growth both after plasmid mediated transduction (Ishii et al., 2004; Kondoh et al., 2004) or by viral gene transfer (Muhlhauser et al., 1995). Also FGF-4 and FGF-5 showed peculiar angiogenic properties when administered by adenoviral vectors into ischemic skeletal muscle (Giordano et al., 1996; Rissanen et al., 2003).

HGF has been also studied as pro-angiogenic factor. Human HGF gene transfer induced angiogenesis in rats and swine after MI (Aoki et al., 2000; Wang et al., 2006). Additionally, it has been shown that HGF improves remodellng and contractility of the heart (Jin et al., 2004), decreases apoptosis and fibrotic scar formation after injury (Ahmet et al., 2002).

Moreover the role of platelet-derived growth factors (PDGFs), especially PDGF-B, in the recruitment of pericytes to growing vessels makes them attractive candidates for combined use with VEGFs, in order to obtain a better microvascular maturation and collateral growth, resulting in a significant gain in perfusion and muscle function (Kupatt et al., 2010).

Besides endothelial cell sprouting, functional new blood vessel formation also requires other factors that act at later time points to promote vessel maturation. Among these, an essential role is played by the angiopoietins. Angiopoietin-1 and -2 (Ang-1 and Ang-2) form an agonist–antagonist pair of molecules that modulate the maturation of blood vessels via binding to Tie-2 receptor. Ang-1 is anti-inflammatory and acts stabilizing vessels, and counteracting VEGF-induced vascular permeability (Arsic et al., 2003; Thurston et al., 2000). Ang-2 is the natural antagonist of Ang-1; it binds to but not activates the Tie-2 receptor, thereby resulting in the disruption of

angiogenesis in the absence of VEGF (Lobov et al., 2002).

In addition to the genes mentioned above, other candidate therapeutic genes, currently under investigation to induce therapeutic angiogenesis, include HIF-1α (Patel et al., 2005), eNOS (Namba et al., 2003), Del-1 (Zhong et al., 2003), IGF-I and IGF-II (Su et al., 2003), netrins (Wilson et al., 2006), stromal cell derived factor-1α (Hiasa et al., 2004), Sonic hedgehog (Kusano et al., 2005) and various transcription factors like zinc finger transcription factors, which could induce simultaneous expression of many growth factors and cytokines, leading to a more natural angiogenic response (Yamamoto et al., 2010).

Gene therapy to rescue contractile function

Rescue of contractile function is another potential target for cardiac gene therapy. The failing myocardium is characterized by alterations in calcium handling, decreased myofilament sensitivity, excessive catecholamine release, and adrenergic receptor down-regulation and desensitization, leading to a decrease in contractility (Towbin and Bowles, 2002). The genetic manipulation of these therapeutic targets represents a potential strategy for HF treatment.

A hallmark of HF is the presence of alterations in cardiac β-adrenergic signaling, which is mediated by the β_1 (the most abundant) and β_2 adrenergic receptors (β-ARs). These alterations, including receptors down-regulation, up-regulation of β-AR kinase and increased inhibition of G_i protein function, lead to β-ARs desensitization and decreased signaling through their pathway. Overexpression of β-AR was initially tested as a simple way to overcome its downregulation, but transgenic mice overexpressing the human β_1 receptor gene in the heart suffered from severe cardiomyopathy (Engelhardt et al., 2004), although this did not happen in mice overexpressing the murine β_1-AR gene (Noma et al., 2007).

On the contrary, the overexpression of β_2-AR led to an improvement in LV function in different animal models (Maurice et al., 1999; Shah et al., 2000), suggesting a potential benefit of β_2-AR enhancement. The two receptors activate the same pathway (AC-cAMP-PKA pathway), but β_2-AR is coupled to both Gs and Gi and probably this is the reason of the different phenotype caused by their individual overexpression (Hata et al., 2004).
Other possible gene therapy approached are based on the inhibition of G-protein-coupled receptor kinases (GRKs), which regulate the receptor activity and are usually overexpressed in HF (Dzimiri et al., 2004; Penela et al., 2010), or on the activation of cardiac adenylyl cyclase VI activity, often downregulated in failing hearts (Phan et al., 2007). Both strategies have demonstrated their efficacy in a large number of preclinical studies (Rebolledo et al., 2006; Williams et al., 2004).

Ca^{2+} plays a crucial role in contraction and relaxation of the cardiac muscle; therefore gene therapy strategies for normalization of myocardial cytosolic calcium transients also have shown promising results in experimental models of heart failure. Usually, an action potential at the cell membrane induces Ca^{2+}-influx through sarcolemmal L-type calcium channel and this triggers further Ca^{2+} release from the sarcoplasmic reticulum (SR) to the cytosol via the major SR Ca^{2+}-release channel ryanodine receptor (RyR2). Ca^{2+} then binds troponin C on the myofilament, triggering the contraction process, while muscle relaxation occurs when Ca^{2+} detaches from the troponin complex and is either taken up into the SR by sarcoplasmic/endoplasmic reticulum Ca^{2+} ATPase (SERCA2a) (responsible for 75% of Ca^{2+} removal in humans) or removed by the sarcolemmal Na2 /Ca^{2+} exchanger (NCX) (Bers, 2008).
A decrease in SERCA2a activity has been observed in HF, therefore different gene therapy approaches has been developed, aimed at overexpressing this gene and rescuing cardiac function. Intracoronary

delivery of Adv-SERCA2a in a rat model of HF showed improvement in LV function and survival rate 28 days after treatment (del Monte et al., 2001). Similar results were obtained by AAV1-SERCA2a administration through epicardial coronary artery infusion in pigs with mitral valve impairment (Kawase et al., 2008). Starting from these results, a clinical trial based on AAV1-SERCA2a gene delivery to the myocardium of patients with HF was initiated, which will be described in section 1.2.3.3 (Hajjar et al., 2008; Jaski et al., 2009).

Another interesting gene therapy target is phospholamban (PLN), a protein implicated in regulation of SERCA2a activity. When unphosphorylated, PLN inhibits SERCA2a, while PLN phosphorylation relieves its inhibitory effect and results in increased SERCA2a activity with improved Ca^{2+} handling. In order to act on PLN in experimental HF models, PLN inhibitory or dominant-negative molecules have been developed. In the first case, a mutant form of PLN with a mutation at serine-16 (S16E), the site of PKA action, generated and used to promote SERCA2a activity. AAV-mediated overexpression of PLN-S16E prevented post-MI cardiac dysfunction in both hamsters and rats models of HF (Hoshijima et al., 2002; Iwanaga et al., 2004) and intracoronary administration of an AdV-PLN-S16E in a sheep model of cardiomyopathy led to a clear improvement in cardiac activity (Kaye et al., 2007). Moreover, an RNAi therapeutic approach based on rAAV9-shPLB intravenous administration was tested in a rat model of HF, showing a restoration of LV function (Suckau et al., 2009).

Other critical players in this process are the protein phosphatase 1 (PP1), a serine/threonine phosphatase that dephosphorylates PLN in the heart and its inhibitor phosphatase inhibitor protein 1 (I-1). The inhibition of PP1 and the activation of I-1 have been shown to enhance cardiac function in different preclinical models of HF (Pathak et al., 2007; Pathak et al., 2005).

Gene therapy for myocardial protection

Oxidative injury plays a critical role in several cardiovascular diseases including myocardial infarction, myocardial ischemia/reperfusion (MI/R) injury, atherosclerosis, hypertension, cardiomyopathies and HF (Abrescia and Golino, 2005; Levonen et al., 2008). Reoxygenation of the ischemic myocardium increases the formation of reactive oxygen species (ROS), which cause lipid peroxidation, protein oxidation and affect Ca^{2+} handling proteins, such as RYR2 and SERCA2a. Gene therapy aimed at increasing antioxidant activity or inducing the expression of cytoprotective genes has therefore been devised as a promising strategy against I/R injury. This novel concept of preventive gene therapy may potentiate the native protective response of the myocardium, rendering it resistant to future ischemic insults and thereby minimizing the need for acute intervention (Wu et al., 2009).

In this perspective, viral vector-mediated overexpression of most antioxidant enzymes, such as superoxide dismutase (SOD), glutathione peroxidase (Gpx), catalase or hemeoxygenase-1 (HO-1) has been tested in different animal models of myocardial I/R injury. Extracellular superoxide dismutase (Ec SOD) overexpression in rats and rabbits infarcted hearts was shown to improve LV ventricular function, decrease infarct size and prolong survival (Agrawal et al., 2004; Li et al., 2001). Similar results were obtained by AAV-mediated HO-1 transduction in a model of rat myocardial infarction (Liu et al., 2007; Melo et al., 2002). Significant protection from ROS-induced injury was also achieved by overexpression of other antioxidant enzymes such as Cu/Zn SOD (Woo et al., 1998), catalase, and glutathione peroxidase (Shiomi et al., 2004).

Additional strategies to obtain myocardial protection from ischemic damage have been devised targeting genes involved in cell death pathways. For example, in a model of rabbit acute ischemia/reperfusion, overexpression

of the anti-apoptotic protein Bcl-2 reduced the rate of cardiomyocyte apoptosis and preserved heart function (Chatterjee et al., 2002).

Another gene therapy target is the heat shock proteins family (HSPs); adenoviral-mediated HSP-70 gene delivery to the rabbit heart before MI decreased infarct size (Okubo et al., 2001), and similar results were obtained by gene transfer of HSP-20 in rat myocardium, 4 days before an acute I/R injury (Zhu et al., 2005). Cardiac protective properties of numerous genes have been described over time in various preclinical models, among these, are the pro-survival genes Akt (Cittadini et al., 2006), kallikrein (Agata et al., 2002), cardiotrophin-1 (Ruixing et al., 2007) TGFβ-1 (Dandapat et al., 2008), leukemia inhibitory factor (Berry et al., 2004) and others.

A potential strategy for protection from I/R injury may also entail the inhibition of proinflammatory genes activated by damage. A decoy oligonucleotide inhibiting the action of NF-κB has been shown to reduce MI size in rats (Morishita et al., 1997); besides, approaches based on *in vivo* delivery of NF-κB inhibitors (IκBs) were able to obtain comparable beneficial effects on injured myocardium (Squadrito et al., 2003). In addition, TNF-α is a pro-apoptotic cytokine and the delivery of its antagonist, the soluble TNF-α receptor-1 gene, reduced infarct size and improved cardiac function after MI in mice (Sugano et al., 2004).

From the results described above it is possible to conclude that the long-term overexpression of anti-oxidant enzymes and/or cytoprotective genes in the myocardium provides a promising strategy for enhanced protection from cardiac injury. In the future, further understanding of molecular apoptosis and autophagy pathways, could therefore define novel, interesting targets for therapeutic gene therapy approaches aimed at myocardial protection from ischemic insults.

1.2.3.3 Clinical trials for therapeutic cardiovascular gene therapy

Among cardiovascular gene therapy trials, the vast majority was designed to induce therapeutic blood vessel growth using growth factors, mainly VEGF (Atluri and Woo, 2008; Zachary and Morgan, 2011).

As previously reported, after the identification of VEGF and FGF as powerful inducers of angiogenesis, various clinical trials were conducted delivering these factors as recombinant proteins, but despite the brilliant results obtained in preclinical models, the administration of these proteins produced only modest or no result at all in the treated patients. To overcome the limitations associated with this approach several clinical trials based on VEGF or FGF gene transfer, were started in the last 15 years, initially based on naked plasmid DNA delivery. The first pilot trials were based on the administration of plasmid DNA encoding human VEGF165 for treatment of hind limb ischemia (Baumgartner et al., 1998; Isner et al., 1996); these studies reported the resolution of rest pain and an increase in collateral vasculature after treatment. A series of over 20 clinical trials followed, which entailed the injection of naked plasmids encoding VEGF to the myocardium by different routes of administration. In many trials the treated patients exhibited an improvement of clinical status, myocardial perfusion, collateral growth and LV function (Losordo et al., 1998; Sarkar et al., 2001; Vale et al., 2001). Most of these procedures were well tolerated, with few major adverse cardiac events and without complications related to gene expression. However, these results should be interpreted with caution, considering the uncontrolled, open-label design of the trials. Indeed, a double-blinded, placebo-controlled experimentation performed few years later (the Euroinject One trial) failed to show any significant difference between injection of a plasmid encoding VEGF165 and placebo (Gyongyosi et al., 2005; Kastrup et al., 2005). Similarly, the NORTHERN

trial, also involving VEGF-165 plasmid delivery, did not show any improvement in perfusion in patients with angina (Stewart et al., 2009).
Other ongoing clinical trials, also based on naked plasmid DNA gene transfer, take advantage of a plasmid encoding FGF-1. After a phase II, double-blind, randomized, placebo-controlled trial in patients with critical limb ischemia, no improvement in wound healing was observed, however the treatment significantly reduced the risk of amputation and might thus lower mortality rates (Nikol et al., 2008). Finally, two additional trials used naked DNA for gene transfer in patients with PAD; the first was based on the delivery of HGF (Powell et al., 2008), while the second was based on the administration of a plasmid encoding the angiomatrix protein Del-1 (developmentally regulated endothelial locus 1) and both showed not significant clinical efficacy (Rajagopalan et al., 2004).

Despite the relative ease of production of naked plasmid DNA, the clinical success obtained by their direct injection has been generally poor, mainly because of the low efficiency of tissue transfection and transgene expression. Given these limitations, other clinical trials exploited adenoviral vectors to deliver therapeutic genes.
In the REVASC trial, the administration of Ad-VEGF121 via intramyocardial injection in patients with severe angina resulted in increased exercise time and improved anginal symptoms at 26 weeks of follow up (Stewart et al., 2006). The same vector was also tested in the RAVE trial, a phase II study designed to test efficacy and safety of intramuscular delivery of this vector in subjects with PAD. In this study however a single intramuscular administration of Ad-VEGF121 was not associated with improved exercise performance or quality of life, and did not support further experimentation.
Two trials assessed the efficiency of an adenovirus expressing VEGF165 or of a plasmid expressing the same gene delivered in a liposome formulation (VEGF-P/L) injected intra-arterially in patients with PAD and CAD (KAT

trial). Both the adenovirus and liposome formulations were reported to increase the collateral vessels of the treated limbs 3 months after therapy and to enhance myocardial perfusion in the CAD patients 6 months after therapy (Hedman et al., 2003; Makinen et al., 2002).

The angiogenic gene therapy (AGENT) trials have addresses the safety and efficacy of delivery of an adenoviral vector expressing FGF-4 (Ad5FGF4) in patients with stable angina. These trials established that intracoronary administration of this vector was safe, and that a single dose could provide an anti-ischemic effect up to 12 weeks of evaluation (Grines et al., 2002; Grines et al., 2003). These preliminary results led to a phase II/III trials, but unfortunately, the obtained preliminary data clearly indicated that the trial, as designed, would provide insufficient evidence of efficacy, and further recruitment was stopped in 2004 (Henry et al., 2007).

Despite the initial highly positive results, therefore, the overall outcome of the subsequent randomized trials has been much more disappointing. Certainly novel vectors and improved delivery methods are needed before a real clinical success might be reached. The only viral vector system that, at present, appears suitable for gene therapy of cardiovascular disorders is based on AAV. As discussed in chapter 1.3, these vectors display many appealing features for gene transfer to the heart and skeletal muscle and, for this reason, they probably will play a central role in the clinical cardiovascular gene therapy experimentation in the next future.

As already mentioned, most of the ongoing clinical gene therapy trials target the revascularization of the ischemic myocardium, as chronic HF is most commonly caused by myocardial infarction. However, HF can also be due to a variety of causes that cannot be managed by angiogenesis. Taking into account the molecular pathways involved in HF, few other gene candidates, identified and characterized in extensive preclinical studies, are currently being assessed in clinical trials.

Based on a large amount of data in preclinical models, the first phase I clinical trial (CUPID) was recently started in HF patients, through intracoronary infusion of AAV1-SERCA2a. This trial exploited, for the first time, AAV vectors-mediated delivery strategies to express the therapeutic gene in the heart. The results of this study demonstrated a good safety profile and improvements at 12 months of LV functional parameters (Jaski et al., 2009). The safety profile of this phase I study led to the approval of a double-blind placebo-controlled randomized trial of AAV1-SERCA2a. At 6 months, the AAV1-SERCA2a–treated patients demonstrated improvement or stabilization in many functional parameters, demonstrating that SERCA2a is a critical target in the pathogenesis of HF.

Two other clinical trials targeting SERCA2a are currently enrolling patients. The first trial is in patients with advanced HF and who will receive either AAV6-SERCA2a or saline. A second, Phase II double-blind randomized placebo-controlled, parallel study will be performed, with the primary objective to investigate the impact of AAV6-CMV-SERCA2a on cardiac remodeling parameters in patients with severe HF.

In a recent randomized, double-blind phase I/II clinical trial, which is still enrolling patients, the safety and efficacy of adenoviral gene transfer of human adenylyl cyclase type 6 (AC6) will be assessed in patients with congestive HF (trial NCT00787059). An additional trial is then examining the effects of Stromal Cell-derived Factor-1 (SDF-1) intramyocardial injection in patients with ischemic heart disease (trial NCT01082094).

1.3 ADENO-ASSOCIATED VIRAL VECTORS (AAVs)

1.3.1 Molecular biology of Adeno-Associated Virus

The Adeno-Associated Virus (AAV) is a small non-enveloped, single stranded (ss) DNA virus with a diameter of 18–25 nm, belonging to the family Parvoviridae and the genus Dependovirus. The members of this genus, in contrast to those belonging to the other genus (erythroviruses) of the Parvoviridae family, are incapable of autonomous replication and depend on the superinfection of the cells with another virus to complete their replicative cycle, hence the name. The AAV name derives from its original isolation as a contaminant of cell cultures infected with adenovirus (Atchison et al., 1965). In the absence of helper virus (adenovirus, but also herpesvirus), AAV (serotype 2) can establish latency by integrating into chromosome 19q13.4, representing the only mammalian DNA virus capable of site-specific integration (Daya and Berns, 2008).

The members of the Dependovirus genus are very diffuse in nature; twelve human serotypes ad more than 100 AAV variants from nonhuman primates have been discovered to date, and new serotypes are continuously identified (Gao et al., 2005). Although all AAV serotypes share a similar structure, size and genome organisation, each serotype has a specific tissue tropism, essentially determined by the capacity to bind different cell surface receptors. Despite the high seroprevalence of AAV in the human population (approximately 80% of humans are seropositive for AAV2) the virus has not been linked to any human pathology.

1.3.1.1 Genome organization and structure of virions

The AAV has a linear single-strand DNA genome of about 4.7 kb and contains two open reading frames, corresponding to the genes *rep* and *cap,* flanked by 145 nucleotides (nt) long inverted terminal repeats (ITRs).

The *rep* region codes for replication-related proteins while the *cap* region codes for the three structural proteins VP1, VP2, and VP3 that together form the viral capsid (Srivastava et al., 1983). Through the use of two different promoters, (p5 and p19) and the inclusion or not of an exon, the *rep* gene codes for 4 protein isoforms (Rep78, 68, 52 and 40) (**Figure 1.11**). The larger Rep proteins (Rep78 and Rep68) are transcribed from the P5 promoter, whereas Rep52 and Rep40 from the P19 promoter. Rep78 and Rep68 are important regulatory proteins that act in trans in all phases of the AAV life cycle; indeed they regulate AAV gene expression and are required for DNA replication and integration. Rep52 and Rep40 instead are involved in the accumulation of single-stranded viral genomes from double-stranded replicative intermediates, for packaging within AAV capsids (Chejanovsky and Carter, 1989). All four Rep proteins have helicase and ATPase activity and Rep78 and Rep68 possess also strand- and site-specific endonuclease activity and site-specific DNA binding activity.

The structural proteins VP1, VP2 and VP3 are generated from the *cap* gene from a single promoter (p40), but using three different start sites for translation. All the AAV transcripts have the same polyadenylation site, located at the 5' of the genome. VP1, VP2 and VP3 together assemble into the capsid shell, with icosahedral symmetry (T=1), a diameter of 18-25 nm and which is composed by 60 subunits, with a ratio of 1:1:18 for the three proteins (each virion has 3, 3 and 54 VP1, VP2 and VP3 proteins respectively). The capsid includes the viral genome, a single stranded DNA, having either positive or negative polarity; usually, in any AAV preparation, about half of the virions have a DNA with positive polarity and the other half a DNA with negative polarity. Moreover, VP1 protein contains a phospholipase A2 (PLA2) motif that seems to be required between the translocation of the AAV genome into the nuclear compartment and the initiation of viral gene expression (Girod et al., 2002).

Recently, it has been shown that AAV encodes another protein required for capsid formation by means of a nested, alternative ORF of the *cap* gene. This protein, designated assembly-activating protein (AAP), is localized in the host cell nucleolus, where AAV capsid morphogenesis occurs. AAP targets newly synthesized capsid proteins to this organelle; this event appears to be important in the assembly reaction itself (Sonntag et al., 2010).

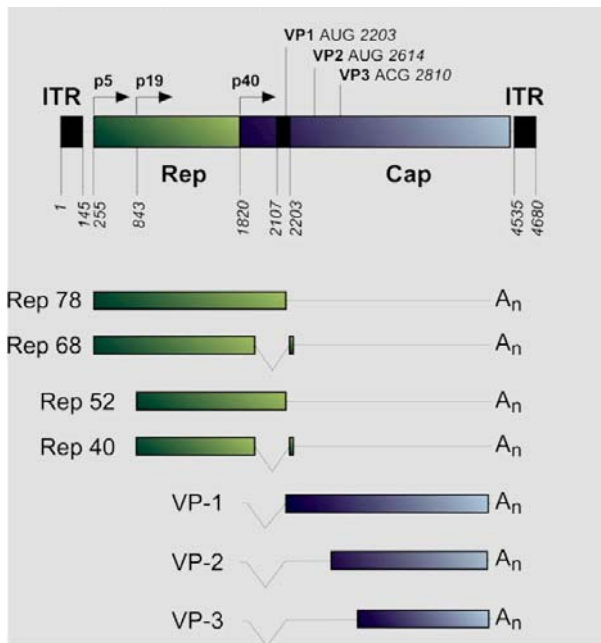

Figure 1.11 Organization of the AAV genome
Rep and *cap* genes flanked by the ITRs. The different Rep and Cap transcripts are produced from their respective promoters (p5, p19 and p40).

As mentioned above, the coding region of the viral genome is flanked by two ~145 nucleotides (nt) long inverted terminal repeats (ITRs), of which first 125 nt constitute a palindrome, which folds upon itself forming a T-shaped hairpin structure, identical at the two viral ends (Bohenzky et al.,

1988). The ITRs provide a free 3' hydroxyl group essential for the initiation of viral DNA replication by a mechanism of self-priming single-strand displacement, involving leading-strand and double-stranded replicative intermediates synthesis (Berns, 1990). The virus does not encode a polymerase and exploits cellular polymerase activities to replicate its DNA (Ni et al., 1998). For viral genome replication and integration, the presence of the Rep68 or Rep78 proteins is also essential. These proteins specifically bind the Rep binding element (RBE), a sequence within the ITR, and cleave in a site- and strand-specific manner at the terminal resolution site (TRS) located 13 nucleotides upstream of the RBE (**Figure 1.12**).

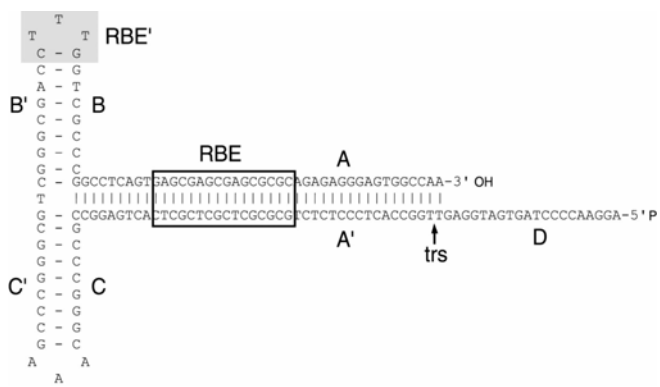

Figure 1.12 AAV2 Inverted Terminal Repeats (ITRs)
AAV2 ITR secondary structure showing the Rep binding element (RBE) and the terminal resolution site (TRS) sequences *(Goncalves, 2005).*

In addition, the ITRs play a key role in viral genome integration into the host genome as well as in the subsequent rescue of viral DNA from the integrated state. A 33 bp sequence spanning the chr19 RBE and the TRS homology element, called AAVS1, is present in human chromosome 19q13.4 and represents the minimal sequence necessary and sufficient for AAV site-specific integration (Kotin et al., 1990; Samulski et al., 1991). The AAVS1 region is located in a centromeric position with respect to the genes

coding for the slow skeletal muscle troponin T (TNNT1) and cardiac troponin I (TNNI3), located 15 and 26 kb apart respectively (Dutheil et al., 2000). Recently novel hotspots near consensus RBE were identified on chromosome 5p13.3 (AAVS2) and on chromosome 3p24.3 (AAVS3), demonstrating that targeted AAV integration is not as strictly specific for AAVS1 as previously assumed (Huser et al., 2010).

The ITRs are the only sequences preserved during AAV vectors generation, while a transcriptional cassette (composed by a promoter, the therapeutic gene and the polyadenylation site) substitutes the *rep* and *cap* genes.

1.3.1.2 AAV life cycle

As described in the previous paragraph, the AAV life cycle strictly depends on the presence or absence of host cell co-infection with a helper virus (**Figure 1.13**). In the presence of helper virus (adenovirus or herpesvirus), a lytic stage ensues and AAV undergoes productive infection characterized by genome replication, viral gene expression, and viral particles production. Adenovirus and herpesvirus provide different genes for helper function, but they both regulate cellular gene expression, providing a permissive intracellular environment for AAV productive infection.

On the other hand, under non-permissive conditions, the AAV genome mainly integrates into the AAVS hot spots regions, where it establishes a latent infection for indefinite periods of time. The viral components that are required for target integration have been identified. These include the already mentioned ITRs and Rep78 and Rep68 proteins, but also a 138-bp sequence, the integration efficiency element (IEE), located within the P5 promoter *in cis* (Feng et al., 2006; Philpott et al., 2002).

When a latently infected cell is super-infected with a helper virus, the AAV gene expression program is re-activated, leading to the AAV Rep-mediated rescue of the provirus DNA from the host genome, followed by replication

and packaging of the viral DNA. The lytic phase of AAV life cycle can also be induced in the absence of a helper virus, though with less efficiency, when the host cell is subjected to DNA damaging agents such as UV or γ-irradiation or exposed to genotoxic compounds (Yalkinoglu et al., 1988).

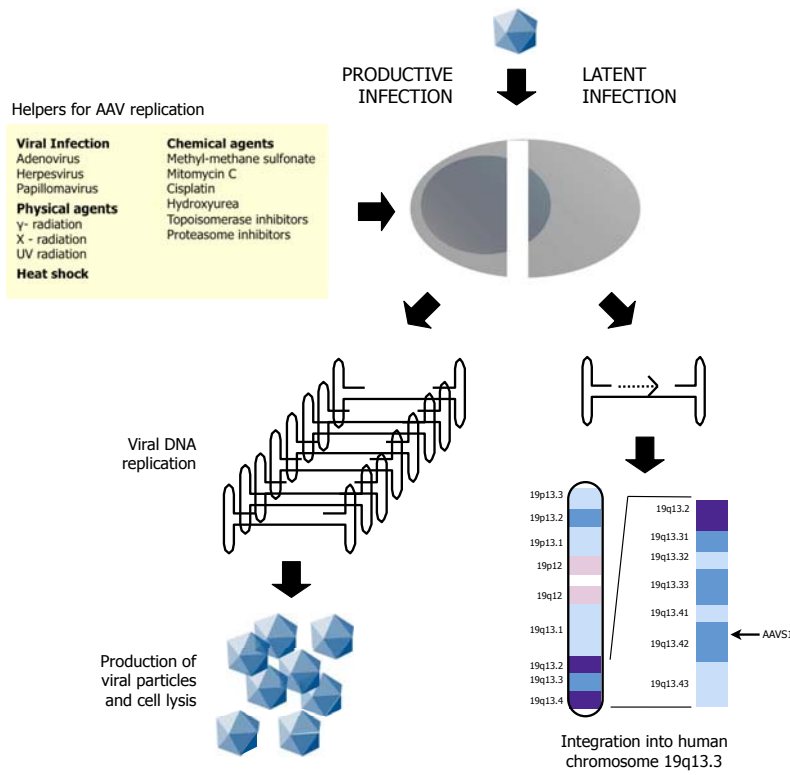

Figure 1.13 AAV life cycle
Permissive conditions allow the AAV replicative cycle, which ends with the release of novel viral particles from the host cell. On the contrary, under non-permissive conditions, the viral DNA undergoes site-specific integration into the AAVS1 region of chromosome 19q13.4 *(adapted from Giacca 2010)*.

1.3.1.3 AAV infection

Viral infection is a process that requires virions to pass through different steps (receptor binding, cell entry, intracellular trafficking, endosomal

release, viral uncoating and nuclear entry) before delivering the genome into the nucleus for replication. A detailed understanding of this process is pivotal to overcome limitations and to optimize the efficiency and safety of viral vectors (**Figure 1.14**).

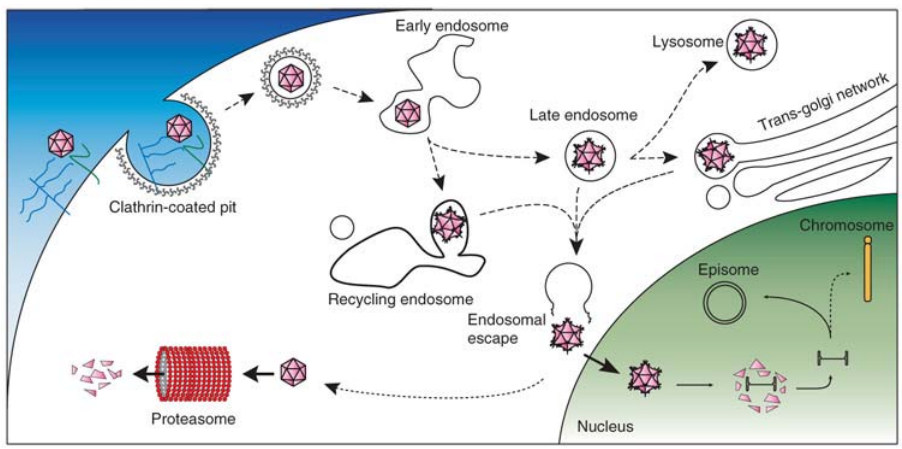

Figure 1.14 AAV intracellular trafficking
AAV infection is a multistep process. After the entry of the virus trough receptor-mediated endocytosis, the trafficking of the viral particles to the nucleus involves different pathways, leading to endosomal release, viral uncoating and nuclear entry (*Schultz and Chamberlain, 2008)*.

Cell membrane attachment. The first step in AAV infection consists in the binding of the virus to specific receptors, which mediates its entry inside the cell. Heparan sulphate proteoglycan (HSPG) has been identified as one of the primary attachment receptors for AAV2 (Summerford and Samulski, 1998), but after virus binding the interaction with a coreceptor seems to be necessary for internalization of the virus. So far at least six coreceptors are known, including $\alpha_v\beta_5$ integrins (Summerford et al., 1999), FGFR-1 (Qing et al., 1999), HGFR (Kashiwakura et al., 2005), $\alpha_v\beta_1$ integrin (Asokan et al., 2006), and 37/67 kDa laminin receptor (Akache et al., 2006). The laminin receptor has been also indicated as the primary attachment receptor for AAV8. HSPG has also been reported to represent

the binding receptor for AAV3, while sialic acid is the primary attachment receptor for AAV4 and AAV5. AAV5 primarily uses N-linked sialic acid for binding and platelet-derived growth factor receptor has been identified as its coreceptor (Di Pasquale et al., 2003; Walters et al., 2001), whereas AAV4 preferentially uses O-linked sialic acid for attachment (Kaludov et al., 2001). AAV1 and AAV6, whose capsid proteins differ in only six amino acids, both uses N-linked sialic acid for binding (Wu et al., 2006), while recently has been shown that N-linked glycans with terminal galactosyl residues represent the primary receptors for AAV9 (Shen et al., 2011).

Endocytosis and intracellular trafficking. After receptor binding, internalization is the next step in the AAV viral entry pathway. AAV2 is internalized through clathrin-coated pits (Bartlett et al., 2000), while AAV5 seems to use both coated pits and caveolae during this process (Bantel-Schaal et al., 2009). In the first case, viral endocytosis is dependent from dynamin, a 100 kDa cytosolic GTPase that regulates the pinching off of clathrin-coated vesicles from the cell membrane (Duan et al., 1999).

The cellular events that mediate AAV trafficking post-entry are not completely characterized. The endocytosis process has been associated with many signaling pathway molecules; because integrins are known AAV coreceptors, their pathways have been extensively analyzed. The activation of the GTP-binding protein Rac1 and its downstream molecule PI3K is essential for intracellular movement of AAV2 to the nucleus via both microfilaments and microtubules (Sanlioglu et al., 2000).

For a successful AAV infection to occur, the viral particles need to escape from these endocytic vesicles. The lowering of the pH inside these compartments during their maturation from early to late endosomes, triggers conformational changes of the viral capsid leading to exposure of previously hidden regions; this process seems to be essential for virus escape and establishment of an active infection (Douar et al., 2001).

As already mentioned, the phospholipase A2 (PLA2) motif at the N-terminal of VP1 has been reported to exert a critical role in this phase, probably inducing pore formation in the endocytic vesicles (Stahnke et al., 2011; Zadori et al., 2001). However, on the basis of studies performed in AAV2, AAV5 and canine parvovirus, at least five potential trafficking pathways have been postulated, involving multiple types of endosomes, lysosomes and the Golgi apparatus (specifically for AAV5), as shown in **Figure 1.14** (Ding et al., 2005).

Nuclear translocation. Once AAV has escaped from the endosomes some of the virions are ubiquitinated and degraded by the proteasome, while others traffic to the nucleus. Experimental studies have shown that inhibition of the proteasome leads to an accumulation of AAV genome into the nucleus, in the case of AAV2 and other different serotypes, such as AAV7 and AAV8. These findings suggest that proteasome-mediated degradation may represent a significant limitation of AAV-mediated transduction in certain cell types (Yan et al., 2004).

For a long time, the process of AAV nuclear translocation has been considered slow and inefficient. In most studies, only a small portion of internalized AAV can be found in the nucleus at short time points post-infection, with a prominent accumulation of viral particles in the perinuclear compartment (Bartlett et al., 2000). However, following the movement of free virus in the cytoplasm and the nucleus by real-time imaging of fluorescent AAV, it was suggested that ATP-dependent molecular motors on tubular networks probably facilitate this traffic that seemed much faster than previously observed (Seisenberger et al., 2001). Relatively little is still known on the processes that control the nuclear translocation of the virus across nuclear pores. Theoretically, the 26-nm diameter capsids of the parvoviruses should be able to pass through the nuclear pore complex (NPC) intact by diffusion (Harbison et al., 2008). However, some evidence

indicates that the viruses might not enter the nucleus through the NPC, despite the NLS- targeting sequences in the N- terminus of VP1 that are exposed during entry. Disruption of the nuclear envelope has been observed indicating a pore-independent mechanism of AAV nuclear entry (Cohen et al., 2006).

Uncoating. Viral uncoating is believed to occur in the nucleus; consistently, several investigators have reported the presence of fluorescent capsids inside cell nuclei (Sanlioglu et al., 2000; Seisenberger et al., 2001). Moreover, nuclear injection of antibody against intact capsids dramatically reduced viral transduction (Sonntag et al., 2006). On the contrary, other studies using GFP labelled viruses concluded that the entry of intact AAV capsids into the nucleus is inefficient and favoured the occurrence of viral uncoating before or during nuclear entry (Lux et al., 2005). A recent study has demonstrated that AAV2 virions enters the nucleus and accumulates in the nucleolus, whereas empty capsids are not able to reach the nucleus. The subsequent mobilization of the virions from the nucleolus permits uncoating and subsequent gene expression or genome degradation (Johnson and Samulski, 2009). Viral uncoating is considered a rate-limiting step of transduction. Recently, it was reported that the rate of viral uncoating is serotype- and cell-specific (Sipo et al., 2007).

Genome processing and viral particles release. After virion uncoating, the free AAV ssDNA genomes must be converted into dsDNA to be transcribed. As mentioned in the previous paragraph, the AAV DNA, during the lytic phase, undergoes second-strand synthesis, using the ITR 3' OH free end as a primer for the host-cell DNA polymerases. This conventional replication scheme requires *de novo* synthesis of the complementary DNA strand, but an alternative mechanism, involving the annealing of complementary strands from two infecting viruses, was also suggested

(Nakai et al., 2000).

It is known that AAV viral particles contain both sense and antisense ss genomes at equivalent numbers. Therefore, when multiple viral genomes transduce the same cell, the two strands could potentially anneal. These two possible mechanisms are not mutually exclusive and their relative contribution to AAV transduction has been investigated through the use of modified ss AAVs that are able to package only one polarity of the vector genome, thus precluding the process of complementary strand annealing (Zhong et al., 2008; Zhou et al., 2008). Single-polarity vectors transduce different cell types with the same efficiently as conventional ss AAV, supporting the hypothesis that second-strand DNA synthesis is a primary pathway in dsDNA conversion.

Once the second strand has been generated, the fate of the input viral genome is still under the control of host cell factors. As mentioned before, under non-permissive conditions, the viral genome enters a latent cycle and integrates into the host cell DNA in a site-specific manner. On the contrary, whether the infection process is productive, at the end of the replication process two viral genomes are generated, with complementary polarity and both of them are packaged inside the virions at equal efficiency. In a few hours, every cell produces $5x10^5$-$1x10^6$ viral particles; the infected cells eventually are lysed and the virions released outside.

It is still largely unclear which are the molecular determinants governing cell permissivity to productive AAV replication. A number of treatments increase the efficiency this process, including co-infection with adenovirus, DNA-damaging agents (ultraviolet, γ-irradiation, X-radiation, alkylating agents, radiomimetic drugs, etc.), agents that inhibit DNA synthesis (hydroxyurea), thereby suggesting that DNA damage repair (DDR) mechanisms may be involved in transduction (Alexander et al., 1994). In particular, proteins of the MRN complex (Mre11, Rad50 and Nbs1) bind the

AAV genome. Indeed, the AAV genome, similar to damaged cellular DNA, is single-stranded and bears imperfectly paired DNA sequences at the level of its terminal hairpins (Cervelli et al., 2008; Zentilin et al., 2001). These proteins block replication of the genome by impeding its conversion to a double-stranded form. Once the cell is treated with chemical or physical agents, the DDR proteins are recruited to other sites of cellular DNA damage, thus permitting the AAV genome to complete its replication.

1.3.2 Recombinant AAV vectors

The characteristics of AAV life cycle, including its defectiveness and ability to persist in infected cells as a latent viral genome, early suggested that this virus could be an excellent tool for *in vivo* gene transfer (Tratschin et al., 1984). In the early 1980s, pioneering work on the successful cloning of AAV established the foundation of recombinant AAV vectors capable of expressing foreign genes in mammalian cells (Coura Rdos and Nardi, 2007).

AAV vectors are usually obtained starting from the AAV2 genome, cloned in a plasmid form, by removing all the viral sequences (*rep* and *cap* ORFs) with the exception of the two 145 bp ITRs (Hermonat and Muzyczka, 1984). Between the ITRs, an expression cassette is cloned containing the therapeutic gene and its regulatory elements (**Figure 1.15**). The ITR sequences of the parental virus are the only required cis elements for viral genome replication and its packaging into viral particles, while the excised structural and non-structural proteins can be provided in trans, by an helper plasmid. In contrast to retroviruses, the replicative cycle of which involves the generation of both RNA and DNA genomic forms and in which the choice of the promoter is thus critical to determine the vector efficiency, AAV replication only involves DNA intermediates. As a consequence, any promoter can be chosen to direct expression of the

therapeutic gene, without interfering with the production of vectors. This includes strong constitutive, inducible or tissue-specific promoters.

The only strict requirement is that the transcriptional cassette cloned between the two ITRs does not exceed 4 - 4.5 kb.

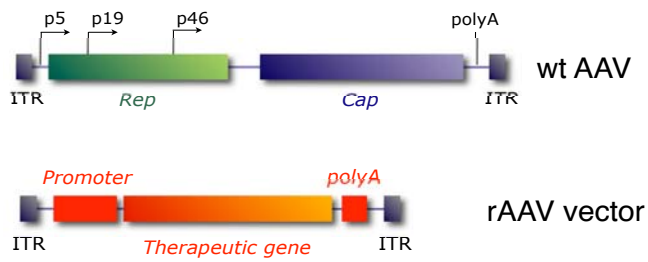

Figure 1.15 Recombinant AAV vectors structure
A rAAV vector is constructed from its wild type counterpart by replacing the *Rep* and *Cap* genes with an expression cassette, containing the therapeutic gene and its regulatory elements.

As already mentioned, site-specific integration of AAV genome is dependent on the Rep proteins. The *rep* gene is removed from the vector DNA genome, therefore the current generation of AAV vectors persists inside non-dividing cells mainly as extrachromosomal DNA; many studies have confirmed the long-term role of the DNA episomes in transgene expression (Nakai et al., 2001; Schnepp et al., 2005). Although rAAV episomes are the main actors in long-term transduction, viral integration could occur as well, but this event is very rare. In this case, given the absence of Rep, the vector genome integrates in a random manner (Miller et al., 2005). Recent studies have demonstrated that AAV vectors exhibit a preference for targeting DNA palindromes of at least 20 bp arm-length, near gene regulatory sequences (Inagaki et al., 2007; Nakai et al., 2005). Given the lack of homology between vector sequences and chromosomal junction points, non-homologous recombination is probably the mechanism responsible for integration (Rutledge and Russell, 1997).

1.3.2.1 rAAV vector production and purification

Traditionally, rAAV production was based on co-transfection of the vector plasmid together with a second plasmid, supplementing the *rep* and *cap* gene functions, into Adenovirus-infected cells (usually HEK293 or Hela cells) (Merten et al., 2005). In this case, the resulting viral preparation was contaminated with adenoviral particles that could easily induce a relevant host immune response. To avoid this problem, adenovirus co-infection was afterwards substituted by the co-transfection of a third helper plasmid providing the adenoviral sequences (E2A, E4, VA), necessary for AAV replication (Xiao et al., 1998). Nowadays, a single packaging/helper plasmid containing both the AAV2 *rep* and *cap* genes and the adenoviral helper genes is the most exploited system for AAV2 vector generation; in this case, the production of vectors involves cell transfection with only two plasmids (Grimm et al., 1998b). For the other serotypes, a separate Cap expressing plasmid is transfected along with the vector and a helper plasmids. Since the transfection method has been often considered unsuitable for large-scale production, many efforts have been attempted in the past in order to overcome the dependency on transient transfection, establishing packaging cell lines stably expressing the *rep* and *cap* genes (Liu et al., 2000). Nonetheless, these efforts have met very limited success so far, mainly due to the cellular toxicity caused by a constitutive Rep protein expression (Saudan et al., 2000). For these reasons, transient transfection still remains the method of choice to obtain AAV vector preparations.

After 48 hours from transfection, the cells start to show a cytopathic effect, due to viral replication, and a large number of virions are present both in the supernatant and in cell lysates. AAV genomes are very resistant to treatment with chemical and physical agents; thus, they can easily be purified by cesium chloride or iodixanol density gradient centrifugation or

chromatography (O'Riordan et al., 2000; Zolotukhin et al., 1999), for large-scale production. The obtained viral preparations are pure and the titers can reach or surpass $1x10^{14}$ viral particles/ml, achieving concentrations higher than those obtained from either VSV-G-pseudotyped retroviral vectors or adenoviral vectors.

A standard AAV production protocol entails utilization of the AAV2 ITRs in conjunction with the AAV2 *rep* and *cap* genes. However, the capsid proteins corresponding to any AAV serotype can recognize the AAV2 ITRs and mediate packaging of the AAV2 genome inside the virions. By this strategy, it is possible to obtain chimeric viral particles simply by using, during production, an expression vector for any desired *cap* gene (Rabinowitz et al., 2002).

1.3.2.2 Properties of AAV-based vectors

This increasing interest on AAV vectors for *in vivo* gene transfer is justified by their characteristic features that distinguish them from others viral vector systems.

Based on a widely diffused, non-pathogenic virus, AAV vectors retain less than 10% of the original viral genome; they maintain only the viral sequence corresponding to the ITRs, which greatly improves their safety for human clinical applications by reducing the risk of recombination with wild-type virus. These vectors do not express any viral protein, therefore they are not immunogenic and do not cause inflammation. As a consequence, therapeutic gene expression usually lasts for years after transduction; this represent a major requirement for many gene therapy approaches and constitutes one of the most distinguishing features of AAV vectors.

AAV vectors transduce particularly well post-mitotic tissues such as brain (neurons), heart (cardiomyocytes), retina (ganglion cells, photoreceptors

and pigment epithelium cells) and skeletal muscle (myofibers). In these tissues they persist in an episomal form, probably as head-to-tail or head-to-head extrachromosomal concatamers, therefore avoiding the problem of insertional mutagenesis typical of retroviral vectors.
Finally, AAV vectors can be generated at high titers and exhibit a high multiplicity of infection, thus allowing the simultaneous expression of different genes from the same cells or tissues. This property could be of great importance in light of the possibility to deliver *in vivo* multiple growth factor coding genes, which represent one of the main point of this Thesis.

1.3.2.3 rAAV vector optimization

Several novel technologies have recently been developed to optimize different properties of AAV vectors, with the aim to improve the therapeutic potential of this class of vectors. In particular, these concern the development of innovative approaches to overcome the limitations imposed by the AAV genome size and the conversion of the genome to a dsDNA format.

AAV vectors with increased genome capacity

The small packaging capacity of AAV vectors is one of their main limitations, since, in some instances, it excludes the possibility to deliver therapeutically important genes or large regulatory elements. Taking advantage of the ability of the AAV genomes to form head-to-tail concatamers in the target cells through intermolecular recombination in the ITRs, a system based on the split of a long transgene between two AAV vectors able to recombine was developed (Yan et al., 2002; Yan et al., 2000). Transcription from the recombined molecules is followed by trans-splicing of the ITR sequences, resulting in a functional gene product (**Figure 1.16**). Although this approach has allowed the delivery of almost double-sized genes (Ghosh et al., 2007; Reich et al., 2003), its efficiency

was lower than using rAAV vectors encoding a full-length transgene. More recently, the strategy to generate these vectors has undergone revision and optimization (Ghosh et al., 2008).

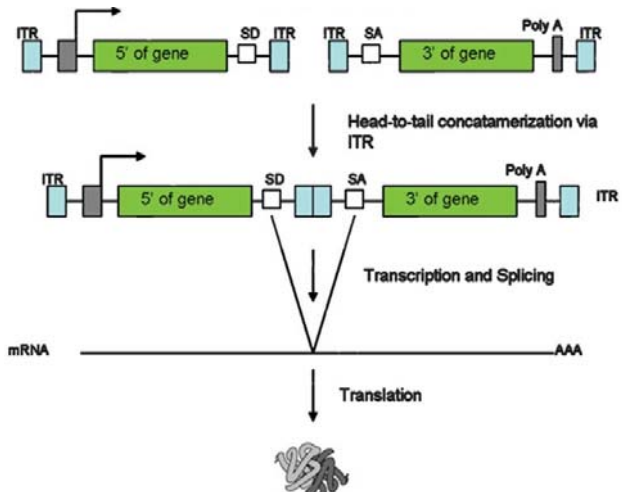

Figure 1.16 Trans-splicing strategy
A large gene is divided into two AAV vectors. One of them contains a promoter, the 5' half of the gene and a splice donor site (SD), while the other a splice acceptor sequence (SA), the 3' portion of the gene and a polyadenylation signal. Both the cassettes are cloned between ITRs sequences. Intermolecular recombination between the two vectors restores the full-length gene and results in the synthesis of the desired protein after the splicing of the ITR sequences from the primary transcript *(Daya and Berns, 2008).*

Enhanced gene expression

AAV is a ssDNA virus, but both wild type AAV genes and rAAV-mediated transgene expression require the conversion of ss to dsDNA before transcription. By mutating one of the ITRs, it is possible to generate vectors that exclusively package self-complementary AAV (scAAV) DNA genomes; these vectors can fold upon themselves, immediately forming transcriptionally competent dsDNA, which results in greater and more rapid *in vivo* transduction (McCarty et al., 2003). The main disadvantage of this approach, however, is the need to limit the transgene size to approximately

half the length of the already small AAV genome (Wu et al., 2007) (**Figure 1.17**).

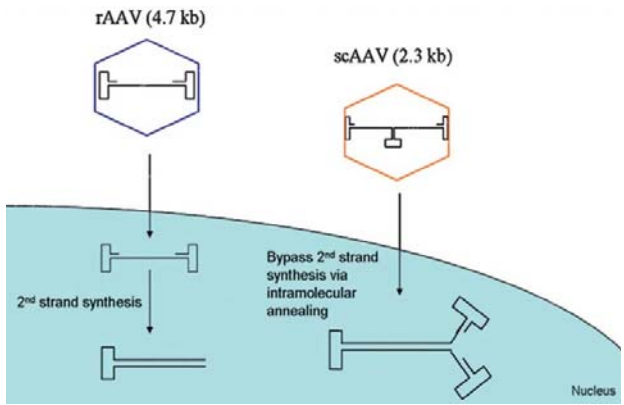

Figure 1.17 Structure of scAAV vectors
Comparison between classical rAAV (on the left) and self-complementary AAV vectors (on the right) *(Daya and Berns, 2008).*

AAV serotypes and molecular engineering of the capsid

Nowadays, at least 12 different serotypes, and over 100 AAV variants, have been isolated from adenovirus stocks and tissues of human, nonhuman primate, and other animal sources. All these viruses share a similar structure, genome size and genetic organization and only differ in the amino acid forming the capsid proteins (Gao et al., 2005). Despite the isolation of such a wide variety of AAV variants, AAV2 still represents the best-characterized AAV serotype; its cellular entry, trafficking and replication have been extensively described and therefore its genome constitutes the starting point for the generation of recombinant AAV vectors. However, AAV-2 vectors are rather inefficient at transducing some tissues such as liver and, in addition, gene transfer might be hampered by neutralizing anti-AAV-2 antibodies, which are highly prevalent in the human population.

In recent years, significant efforts have been made on isolating new AAV serotypes and engineering AAV capsids, in order to increase the efficiency of vectors transduction and also to target non-permissive cells. Since the capsid is an essential vector component for cell infection, starting from the natural serotypes, capsid mutant have been generated by different strategies.

As reported above, the most exploited approach has been the generation of pseudo-typed AAV vectors, combining the AAV2 genome with different capsid serotypes. Each of the currently available serotypes exhibits a specific profile of transduction efficiency and tissue tropism (**Figure 1.18**). Recombinant AAV2 infects a broad number of tissues, such as skeletal muscle, heart, brain and kidney, while rAAV1, rAAV6 and rAAV7 are more specific for the muscle (Blankinship et al., 2004; Louboutin et al., 2005). Retinal epithelium is efficiently transduced by rAAV4 (Weber et al., 2003) and rAAV5 and the latter exhibits strong tropisms also for the lung (Auricchio et al., 2002). Regarding the central nervous system, rAAV serotypes 1, 2, 4, 5, 7, and 8 have been found to be efficient transducers of neurons in different regions of the brain (Burger et al., 2004; Taymans et al., 2007). Recombinant AAV8 and rAAV9 are able to pass through the endothelial blood barrier so, when systemically administered by intraperitoneal or intravenous injection, they transduce a wide number of tissues throughout the body. AAV9 appears to be the most naturally cardiotropic serotype (Bish et al., 2008; Pacak et al., 2006). As mentioned above however, although extremely high levels of cardiac expression are observed after rAAV9 administration, other organs (including liver, skeletal muscle, and pancreas) also display high levels of transduction (Inagaki et al., 2006; Prasad et al., 2011). AAV8 and AAV9 exhibit also the higher level of hepatocyte transduction (Sands, 2011). Serotypes 10 and 11 resemble AAV8 and AAV4, respectively; they both infect muscle, heart, kidney and

lung and AAV10 targets also the liver (Mori et al., 2004). AAV12 targets muscle and nasal epithelium, however, little is still known about its cell tropism and biodistribution *in vivo* (Quinn et al., 2011; Schmidt et al., 2008).

Organ		**Serotype**
Liver		AAV8, AAV9
Skeletal muscle		AAV1, AAV7, AAV6, AAV8, AAV9, AAV2, AAV3
CNS		AAV5, AAV1, AAV4, AAV2
Eye	Retinal epithelium	AAV5, AAV4, AAV1, AAV6
	Fotoreceptors	AAV5
Lung		AAV5, AAV9
Heart		AAV9, AAV8
Pancreas		AAV8
Kidney		AAV2

Figure 1.18 AAV serotype tropism
Each AAV serotype exhibits a specific tropism for different organs and tissues.

In addition to investigations on the naturally occurring serotypes, many efforts are underway to modify AAV capsids for designer tissue tropism or immune system evasion (Kwon and Schaffer, 2008). "Mosaic" AAV vectors, for example, have been generated mixing VP capsid subunits from different serotypes. The advantage of this technique is the ability to combine selective features from different sources that synergistically enhance transgene expression (Hauck et al., 2006; Rabinowitz et al., 2004).
Another exploited approach has been the adsorption of receptor ligands to the AAV capsid surface. For example AAV-specific antibodies able to interact with receptors expressed from non-permissive cells have been used, such as a bispecific $F(ab'\gamma)_2$ antibody with specificity for AAV2 capsid

and the surface receptor $\alpha_{IIb}\beta_3$ expressed by non-permissive megakaryocyte cells (Bartlett et al., 1999). Another study utilized biotinylated viruses able to react with a bispecific fusion protein, composed by avidin and FGF or EGF, in order to target the AAV vectors towards cells expressing FGFR or EGFR (Ponnazhagan et al., 2002). As an alternative to attaching molecules to the capsid surface, another described approach has been the molecular engineering of the capsid by direct modification into the *cap* gene. An example of this technique is the generation of "chimeric" AAV vectors, containing capsid proteins that have been modified by domain- or amino acid-exchange between different serotypes. By exploiting the sequence homology between AAV serotypes to induce recombination, it has been possible to rescue infectious or target phenotypes in mutant virions (Bowles et al., 2003). This approach allows also the insertion of a foreign epitope into the capsid sequence. Of course, the success of this strategy requires a site on the capsid that is tolerant to the insertion, ensuring that assembly and DNA packaging within the mutant remains efficient. Modifications of the *cap* gene have been achieved by insertion of peptide sequences on the basis of known ligand–receptor interactions (Wu et al., 2000), or have selected for peptides in phage-display libraries (Work et al., 2006). Another strategy has been to insert random sequences of amino acids, followed by *in vitro* selection of the best performing capsids (Perabo et al., 2003).

1.4 GHRELIN: A GROWTH HORMONE (GH)-RELEASING PEPTIDE WITH PROMISING BENEFICIAL EFFECTS ON THE MYOCARDIUM

The work described in this Thesis, which was focused on the selection of novel secreted factors able to defend the myocardium from ischemic damage, led to the identification of ghrelin as a powerful cardioprotective factor.

In the last decade, the identification of ghrelin (GHRL) (Kojima et al., 1999), a gastric polypeptide displaying strong growth hormone (GH)-releasing activity by activation of the type 1a GH secretogogue receptor (GHS-R1a) located in the hypothalamus-pituitary axis, has introduced novel perspective in neuroendocrine and metabolic research.

The major active product of the ghrelin gene is a 28-amino acid peptide, which becomes acylated at Ser3 position with an octanoyl group (C8:0). The same gene can also generate other bioactive molecule besides ghrelin, mainly obestatin and des-Gln^{14}-ghrelin, obtained from alternative splicing. In addition, a vast part of ghrelin in the body remains non-acylated (des-acyl ghrelin). Although the receptors for these other peptides have not yet been identified, the biological activity of these molecules suggests the existence of a complex system composed by multiple effectors.

1.4.1 The discovery of ghrelin

It is well established that GH release is stimulated by hypothalamic GH-releasing hormone (GHRH) and inhibited by somatostatin (Anderson et al., 2004). More recently, however, another pathway regulating GH release was identified from studies involving the GH secretagogues (GHSs). Synthetic GHSs are a family of synthetic, peptidyl and non-peptidyl, molecules designed in the late 1970s (Bowers et al., 1980), that act

stimulating GH release, working through a G protein-coupled receptor (GPCR), the GHS-receptor 1a (GHS-R1a) (Korbonits et al., 1999). GHSs are artificial compounds and do not exist naturally. Therefore, it was assumed that an endogenous ligand that binds to GHS-R1a and exerts functions similar to GHSs must exist.

To discover this natural ligand, the orphan receptor (GHS-R1a) was overexpressed in a cell line system and used to identify tissue extracts able to stimulate the receptor as monitored by a second messenger (Ca^{2+}) activation. Several groups unsuccessfully tried to isolate the endogenous GHS-R1a ligand from extracts of brain, pituitary, or hypothalamus, the known sites of GHS-R1a expression. Unexpectedly, however, it was finally identified and purified through four steps of chromatography from the rat stomach in 1999 (Kojima et al., 1999; Kojima et al., 2001). This small peptide was called "ghrelin", from "ghre", the Proto-Indo-European root of the word grow, and "relin" that refers to its GH-releasing activities.

The purified ligand was a peptide of 28 amino acids, mainly synthesized and secreted by X/A-like cells in the stomach (Ariyasu et al., 2001). Later on, ghrelin mRNA was also found in other tissues, such as gut, brain, small intestine, pancreas, heart, lung and others (Gnanapavan et al., 2002). The serine 3 residue of the peptide was *n*-octanoylated and this modification was observed to be essential for its GH-releasing activity. Although they share common functions, there was no structural homology between ghrelin and GHSs, such as GHRP-6 or hexarelin.

The discovery of ghrelin clearly constituted an example of "reverse pharmacology", starting with the synthesis of synthetic analogs, then leading to the isolation of a natural receptor and finally to the discovery of the endogenous ligand for this receptor.

1.4.2 Ghrelin gene structure and derived-peptides

The human ghrelin gene is located on chromosome 3p25-26; it consists of five exons and three introns (the short first exon is only 20 bp long and encodes for part of the 5' untranslated region), and encodes for a transcript of 511 bp, corresponding to a 117 amino acids precursor called pre-proghrelin (**Figure 1.19**). This precursor contains a signal peptide and the pro-ghrelin protein, coding for the two mature peptides ghrelin and obestatin. As it enters the ER, pre-proghrelin is processed to pro-ghrelin by a cleavage, which removes the 23 aa sequence corresponding signal peptide-corresponding sequence. Pro-ghrelin is further processed to ghrelin by the enzyme pro-hormone convertase 1/3, which cleaves after arginine-28 of pro-ghrelin, generating the mature 28 aa peptide (Zhu et al., 2006). Before this last cleavage, a post-translational modification occurs, which consists in the esterification of a fatty acid, usually *n*-octanoic acid, on the third amino acidic residue, which correspond to a serine (Ser3). As already mentioned, only acylated-ghrelin is able to bind the GHS-R1a, therefore this modification is considered essential for ghrelin biological activity. The enzyme responsible for the acylation has been recently discovered and named ghrelin-O-acyltransferase (GOAT) (Yang et al., 2008). GOAT is encoded by the MBOAT4 gene and is highly conserved in vertebrates. The relative tissue distribution of GOAT mRNA matches that of ghrelin and it is highest in stomach, but, recently, low levels of GOAT expression have also been observed in other tissues, including the heart (Lim et al., 2011).

A mechanism of alternative splicing of the ghrelin gene transcript can trigger the production of a minor active isoforms of the molecule called des-Gln^{14}-ghrelin, identical to the main form of the molecule, except for the deletion of glutamine in position 14. Des-Gln^{14}-ghrelin undergoes the same process of acylation as ghrelin (Hosoda et al., 2000).

The presence, in much smaller amounts, of biologically active analogues of

ghrelin with acyl chains of 10 or 11 C has also been reported (Hosoda et al., 2003). These peptides showed lower calcium mobilization activity and GH-release than octanoylated ghrelin.

In addition to Ghrelin, from the pro-ghrelin precursor another small peptide of 23 amino acids named obestatin is also generated (Seim et al., 2011). Obestatin seems to exert opposite effects to ghrelin on food intake, acting on a different G protein-coupled receptor (GPR39) (Zhang et al., 2005). Although this effect remains debated, other biological functions of obestatin have also been described, such as memory improvement, activation of cortical neurons and modulation of sleep (Carlini et al., 2007)

Des-acyl ghrelin, lacking *O-n*-octanoylation at serine 3, is also produced in the stomach and constitutes the major molecular form secreted into the circulation. Plasma des-acyl/acyl ghrelin ratio ranges from 3:1 to 10:1 in different metabolic conditions (Garcia et al., 2005; Yoshimoto et al., 2002). However, des-acyl ghrelin does not bind GHS-R1a, and thus does not exert the same physiological function as ghrelin. While des-acyl ghrelin was originally considered inactive, it is now clear that this peptide exerts a number of autonomous functions, which will be described later. Most likely, these activities are mediated by an additional, not-yet identified, receptor, different from GHS-R1a (Baldanzi et al., 2002).

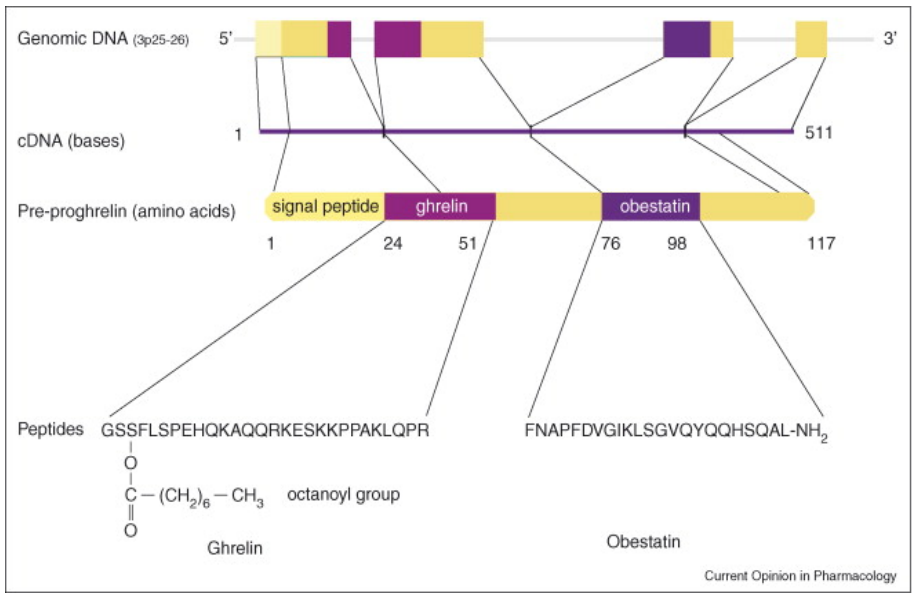

Figure 1.19 Human ghrelin gene
The ghrelin gene is located on chromosome 3, it is composed of five exons and generate a 511 bp mRNA. The pre-proghrelin precursor contains a signal peptide and the proghrelin protein, which gives origin to the two mature peptides: ghrelin (28 aa), *n*-octanoylated in the third serine, and obestatin (23 aa) *(Garcia and Korbonits, 2006*).

Ghrelin is highly conserved in vertebrates (**Figure 1.20**). Rat and human sequences, for example, differ in only two residues, and the 10 amino acids in the N-terminus of the protein, containing the acylated Ser3, are identical among all mammalian ghrelins.

Studies dealing with the minimal sequence needed to activate GHS-R1a showed that the entire sequence is not necessary for ghrelin activity: short N-terminus tetra- or penta-peptides including the first Gly-Ser-Ser(n-octanoyl)-Phe amino acids seem to constitute the "active core", able to activate GHS-R1a (Bednarek et al., 2000). The *n*-octanoyl group of ghrelin is one of the principal structural features determining its potency on GHS-R1a, which requires bulky hydrophobic groups at the side chain of Ser3.

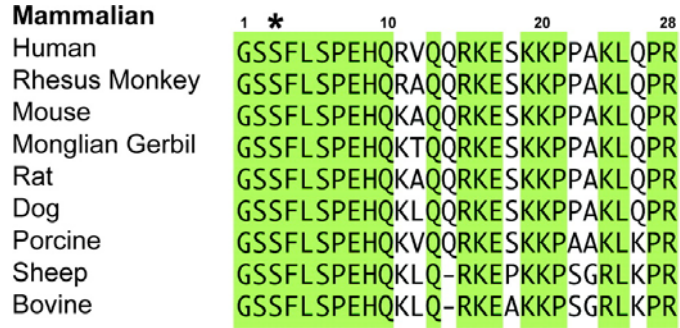

Figure 1.20 Ghrelin sequences comparison among vertebrates
Ghrelin sequence is highly conserved among species and the N-terminus with the acyl-modification in the third serine (marked with as asterisk) is perfectly conserved among all mammalian ghrelins *(Kojima and Kangawa, 2005).*

1.4.3 Ghrelin receptors

Since its discovery and characterization as a GH-releasing and orexigenic factor, acyl ghrelin has been demonstrated to be a pleiotropic molecule, displaying many different functions, which do not necessarily require the presence of the GHS-R1a. An increasing number of reports on the presence of specific binding-sites recognized by both acyl and des-acyl ghrelin (Bedendi et al., 2003) have suggested that GHS-R1a is not the only ghrelin receptor, but most likely one of the ghrelin receptor subtypes.

1.4.3.1 Type 1a GHS Receptor (GHS-R1a)

The ghrelin receptor, or GHS-R, is a typical GPCR with seven transmembrane domains (7-TM). The human GHS-R gene is located on chromosome 3q26.2, and is highly conserved across species (Camina, 2006). This gene is composed of two exons (the first one encodes TM-1 to TM-5 and the second TM-6 and TM-7). Alternative spicing of the pre-mRNA generates two transcripts, designed GHS-R type 1a (GHS-R1a) and GHS-R type 1b (GHS-R1b) (Howard et al., 1996) (**Figure 1.21**).

The human full-length GHS-R1a is a polypeptide of 366 amino acids with 7-TM domains, which exhibits high affinity for GHSs and ghrelin. Molecular modelling and site direct mutagenesis were exploited to identify the ligand-binding pocket of GHS-R1a. Ghrelin and synthetic GHSs share common binding at TM-3, while other contact points in TM sites are specific for different GHSs (Feighner et al., 1998). Recently, it was shown that ligand binding and activation of GHS-R1a by ghrelin requires the ligand to interact with one pocket formed by polar amino acids and one formed by non-polar amino acids present in TM2/TM3 and TM5/TM6, respectively (Pedretti et al., 2006). Acylation at Ser3 of the ghrelin peptide is essential for GHS-R1a activation; however, short peptides composed only by the first four or five residues of ghrelin were found to activate GHS-R1a about as efficiently as full length ghrelin; only the segment Gly-Ser-Ser-(*n*-octanoyl)-Phe appeared to constitute the 'active core' required for receptor binding (Bednarek et al., 2000).

On the other hand, the GHS-R1b transcript is encoded by one exon and gives origin to a truncated peptide of 289 amino acids, only containing 5-TM domains with additional 24 amino acids at the C-terminus. GHS-R1b fails to bind either GHSs or ghrelin and its functional activity has to be clearly determined to date. A recent hypothesis is that it could play a role in modulating other GPCRs, including GHS-R1a, through GPCR homo- and/or hetero-dimerization (Chu et al., 2007). GHS-R1a/1b heterodimerization has been already described; by this interaction, GHS-R1b could attenuate the GHS-R1a-mediated PLC activation. GHS-R1b may act as a dominant-negative regulator of GHS-R1a by reducing the cell surface expression of the receptor and, therefore, reducing its constitutive signaling (Leung et al., 2007).

GHS-R1a is a member of a subfamily of G-protein coupled receptors, whose endogenous ligands are mainly gastrointestinal peptides or neuropeptides.

This family is composed of receptors for neurotensin and neuromedin U (30-35% homology), motilin (52% homology) and other GPCRs, including GPR39 (27-32% homology), which was initially described as the obestatin receptor (Holst et al., 2004). The thyrotropin-releasing hormone receptor also possesses high homology (56%) to GHS-R1a.

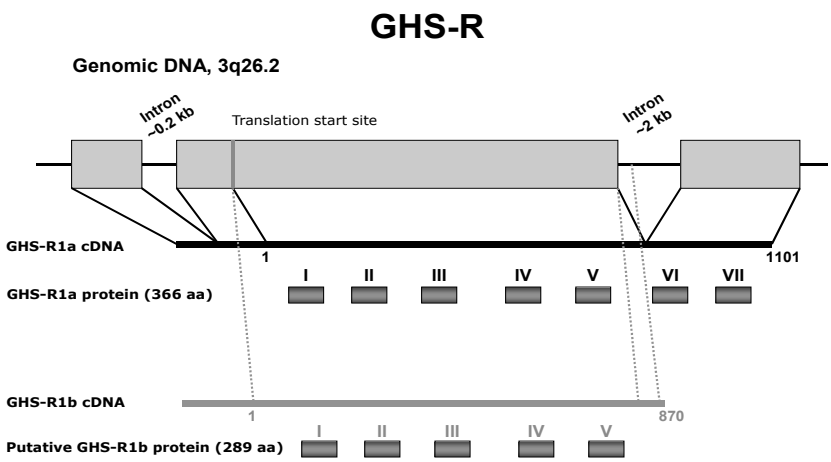

Figure 1.21 Growth Hormone Secretogogue Receptor (GHS-R) gene structure
GHS-R gene and its transcripts GHS-R type 1a and type 1b. Black boxes represent the putative transmembrane domains *(Korbonits et al., 2004).*

GHS-R1a is highly expressed in the hypothalamus and pituitary, consistent with its metabolic functions. However, its expression has also been reported in different areas of the CNS like the hippocampus, substantia nigra, cortex and others, in the vagal nodose ganglion and in multiple peripheral organs, such as stomach, intestine, pancreas, thyroid, gonads, kidney, heart and vasculature, bone and various tumors and cell lines (Gnanapavan et al., 2002).

This broad expression of the receptor is fully in agreement with the rising spectrum of actions of ghrelin. GHS-R1a, as its ligand ghrelin, is highly

conserved among vertebrates, highlighting its important physiological functions.

Signal transduction from the ghrelin receptor

Two endogenous GH-releasing peptides have been identified, ghrelin and GHRH. GHRH acts on GHS-R1a to activate adenylate cyclase and increase intracellular cAMP, which in turn activates protein kinase A. This clearly demonstrates that GHS-R1a is coupled to a Gs subunit. On the other hand, the binding of ghrelin to GHS-R1a activates the protein kinase C (PKC) system and induces an increase in intracellular Ca^{2+} concentration, indicating that the receptor is also coupled to a Gq subunit. In particular, the ghrelin/GHS-R1a interaction induces phospholipase C to hydrolyze phosphatidyl-inositol-4,5-biphosphate, stored in the plasma membrane, to give both diacylglycerol (DAG) and inositol-triphosphate (IP3). IP3 binds to its receptor on the endoplasmic reticulum and induces Ca^{2+} release from intracellular storage, while DAG activates PKC that, through tyrosine phosphorylation, inhibits the potassium channel, causing depolarization and the opening of voltage-dependent L-type Ca^{2+} channels. A possible crosstalk between Gs and Gq might be responsible of the multiple described effects of GHS-R1a. Additionally, different ligands could also induce different conformations of the receptor, favouring coupling to different G proteins and activation of various signaling pathways (Maudsley et al., 2005).

Another important feature to underline is that, besides the activation upon ligand-receptor interaction, GHS-R1a is constitutively highly active, also signaling at approximately 50% of the ghrelin-induced activity in the absence of agonists (Holst et al., 2004). It has been suggested that this high level of constitutive activity may be of physiological importance in its role as a regulator of both GH secretion and appetite control (Holst et al., 2003).

The interaction between GHS-R1a and its ligands results in rapid desensitization, due to the uncoupling of the receptor from heterotrimeric G proteins and to receptor internalization, mediated by clathrin-coated pits, from the cell surface to intracellular compartments. Once the ligand-receptor complex is internalized into vesicles, it is sorted into endosomes where the complex is dissociated and the receptor is then recycled to the membrane (Camina et al., 2004). The recycling of GHS-R1a requires approximately one hour, while surface binding reaches normal levels after 3-6 hours.

1.4.3.2 Non-type 1a GHS Receptors

Even if the formation of heterodimeric receptor complexes may partially account for the GHS-R1a alternative signaling in response to ghrelin, it is likely that other, yet unidentified receptors exist (**Figure 1.22**). Many studies demonstrated that ghrelin is active also in tissues or cell lines not expressing GHS-R1a, giving strength to the hypothesis that GHS-R1a is not the only receptor for this peptide (Filigheddu et al., 2007; Gauna et al., 2006; Thompson et al., 2004). Besides the mentioned GPCR homologues of GHS-R1a and its splicing variant GHS-R1b, many reports have confirmed the existence of alternative receptors binding either acyl and des-acyl ghrelin or specific for the latter. In addition, an unidentified obestatin receptor must also exist.

Since des-acyl ghrelin does not bind GHS-R1a, acylation at Ser3 being essential for receptor activation, the described effects induced by this peptide should be mediated by other receptors. Recently, an increasing number of ghrelin sensitive tissues or cell lines have been shown to be responsive also to des-acyl ghrelin, sometimes with different functional profiles. Both acyl and des-acyl ghrelin are able to prevent cell death of cultured cardiomyocytes and endothelial cells by activation of ERK1/2 and

Akt pathways (Baldanzi et al., 2002) and to improve survival and proliferation of cells of pancreatic islets (Granata et al., 2007). They also induce neurogenesis in rat fetal spinal cord (Sato et al., 2006), increase osteoblasts proliferation (Delhanty et al., 2006), promote adipogenesis (Thompson et al., 2004) and inhibit isoproterenol-induced lipolysis (Muccioli et al., 2004). This evidence clearly demonstrates that at least one receptor exists, different from GHS-R1a or 1b, which is shared by the acylated and non-acylated forms of ghrelin.

Moreover, the existence of receptors able to discriminate between acyl and des-acyl ghrelin derives from the observation that, in some cells, the two peptides exert opposite functions (Gauna et al., 2005). In addition, it was reported that des-acyl ghrelin, when centrally administered, is able to stimulate food intake in GHS-R1a knockout mice, thus revising the concept that GHS-R1a is the only mediator of this function (Toshinai et al., 2006).

Obestatin was initially reported to be the endogenous ligand of the orphan receptor GPR39, which shares homology with GHS-R1a. However, recent reports have challenged this conclusion by showing that, in GRP39 expressing cells, there is neither specific binding of the peptide nor activation of a signal transduction pathway, which is, in contrast, activated by Zn^{2+} (Lauwers et al., 2006).

Finally, there is also evidence for the existence of receptors only specific for the GHSs. Among these, the only one identified so far is CD36, a class B scavenger receptor expressed in many tissues such as vascular endothelium, skeletal and smooth muscle cells, monocytes and macrophages, which is activated by hexarelin and others structurally related GHSs (Demers et al., 2004).

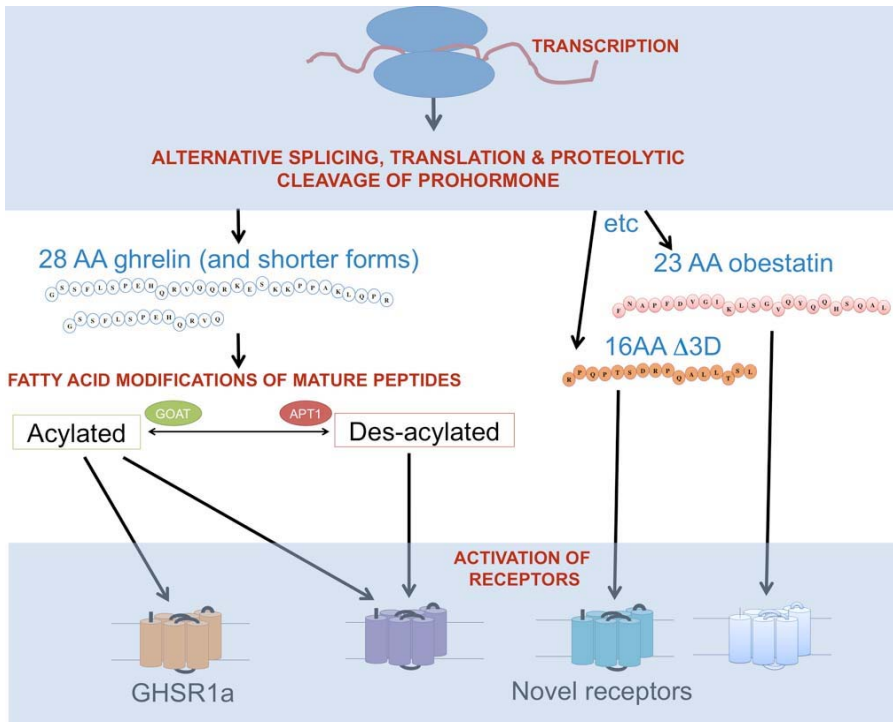

Figure 1.22 Ghrelin peptides and receptors
Acyl-ghrelin binds GHS-R1a, while both acyl and des-acyl ghrelin are believed to also act through a yet unidentified alternative receptor. Moreover, the existence of receptors specific for des-acyl ghrelin has been hypothesized. The receptor for the ghrelin gene-derived peptide obestatin is also still unknown *(Seim et al., 2011).*

1.4.4 Ghrelin physiology

Ghrelin is a pleiotropic hormone, with a wide spectrum of biological actions. Although it was initially discovered as an endogenous GH-releasing peptide, very soon it became clear that it exerts a wide range of different functions, which are briefly summarized in this paragraph.

GH-releasing activity

As already mentioned, acylated-ghrelin stimulates GH release in a dose-dependent and GHS-R1a-mediated manner. Intravenous injection of this

molecule induces potent release of GH both in rats and in humans. Ghrelin stimulates this release from primary pituitary cells, thus acting at pituitary and hypothalamic level; a prominent role of the vagus nerve in mediating this action has been described (Popovic et al., 2003). In addition, high doses of ghrelin in humans also increase the circulating levels of ACTH, prolactin, and cortisol (Takaya et al., 2000).

The GH-releasing function of ghrelin is linked with age; indeed it increases at puberty, remains constant during adulthood and decreases in elderly people (Broglio et al., 2003). It has been hypothesized that the decline of GH secretion during lifespan would reflect age-related decrease in ghrelin levels and/or GHS-R activity/expression levels.

Feeding regulation

A balance of stimulating and inhibiting forces in the hypothalamus regulates feeding. However, the regulatory mechanisms of this process are not only in the central nervous system, but also involve appetite-regulating humoral factors secreted from peripheral tissues. Leptin is a known feeding-inhibitor produced by the adipose tissue, while acyl ghrelin is the only known gastrointestinal peptide able to stimulate appetite and increases meal size, among dozens of factors secreted by the gastrointestinal tract in response to food in the lumen. Fasting induces the elevation of ghrelin in mice and rats, whereas re-feeding restores it (Guo et al., 2008). In humans, pre-prandial increase and post-prandial fall in ghrelin levels (Natalucci et al., 2005) support the idea that ghrelin has a role in meal initiation. When injected into the cerebral ventricles of rats, ghrelin stimulates food intake and in particular enhance fat ingestion, inducing an increase in the fat body mass (Nakazato et al., 2001). A similar effect has been observed also after intravenous or subcutaneous administration of ghrelin.

The role of ghrelin in various eating disorders such as anorexia nervosa

(Otto et al., 2001), obesity and cardiac cachexia (Nagaya et al., 2004), has been analyzed. Ghrelin was found at high concentrations in patients suffering from anorexia nervosa and at low concentrations in obese subjects. These observations suggest that ghrelin plays a substantial role in long-term energy homeostasis. Despite this, ghrelin$^{-/-}$ mice have display growth rate, feeding behaviour and body composition comparable to ghrelin$^{+/+}$ mice, implying that ghrelin is not an essential orexigenic factor or that it function can be compensated for by other mechanisms (Sun et al., 2003).

Ghrelin exerts its feeding-promoting activity on the hypothalamic arcuate nuclei (ARC) in the central nervous system, stimulating the neuropeptide Y (NPY)/agouti-related protein (AgRP) producing neurons and, as a consequence, inducing the release of the corresponding orexigenic peptides (Morton and Schwartz, 2001). Within the ARC, another ghrelin-responsive cell group is the population of neurons identified by the co-expression of POMC (proopiomelanocortin) and CART (cocaine- and amphetamine-regulated transcript), which is often referred to as an anorexigenic population. Ghrelin stimulation of NPY/AgRP neurons also induces the release of the inhibitory neurotransmitter GABA, which acts on the POMC/CART neurons, blocking their anorexigenic activity. The action on these classes of neurons is mediated by GHS-R1a, which is bound by both hypothalamic ghrelin and the peripheral produced peptide that reach the hypothalamus trough the bloodstream or via afferent vagal fibers (Date et al., 2002). Leptin also acts on ARC exerting effects opposite to ghrelin (Nogueiras et al., 2008) (**Figure 1.23**).

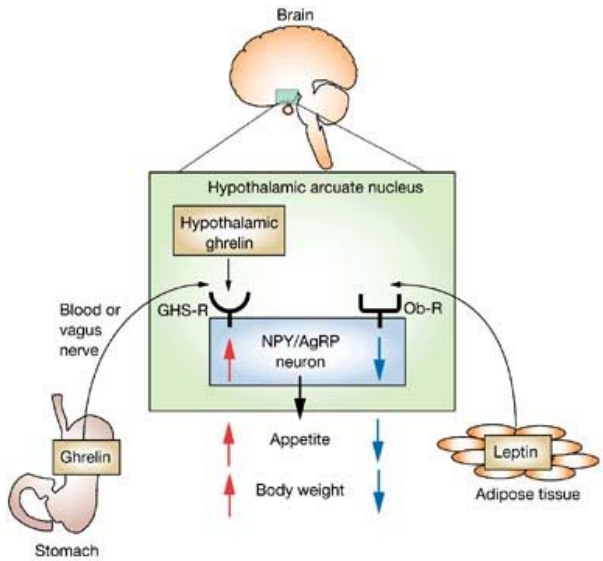

Figure 1.23 Ghrelin and leptin action on the hypothalamus
Both ghrelin and leptin are peripheral hormones with central functions. They act on the hypothalamic arcuate nuclei (ARC) in the central nervous system stimulating orexigenic (ghrelin) or anorexigenic (leptin) effects.

Gastrointestinal effects

Available data suggest that ghrelin affects many aspects of gastrointestinal function; indeed intravenous administration of the peptide increases gastric acid secretion and motility (Masuda et al., 2000). Ghrelin induces motor activity of the gastrointestinal tract both by a central mechanism (mediated by vagus nerve and NPY neurons) and by a peripheral effect similar to motilin. Ghrelin may also stimulate cell proliferation and differentiation of the gastrointestinal epithelium.

Des-acyl ghrelin, on the contrary, does not influence gastric secretion while it inhibits gastric emptying without altering small intestinal transit. This function is probably due to des-acyl ghrelin direct activation of brain receptor CRF-2 by crossing the blood-brain barrier and not by the activation of vagal pathways (Chen et al., 2005).

Glucose metabolism

The first report showing an effect of ghrelin on glucose homeostasis demonstrated that this peptide acutely inhibits insulin secretion in humans after intravenous injection, despite increased glucose levels (Broglio et al., 2001). The same metabolic effects are not induced by synthetic GHS or by des-acyl ghrelin, which seems to exert exactly the opposite effect, increasing insulin concentration. The observation that insulin levels in the blood were suppressed despite the increase in glucose concentration led to the hypothesis that ghrelin could differentially modulate glucose metabolism and insulin secretion. In the first case, ghrelin seems to exert a direct effect on hepatic glucose handling (Gauna et al., 2005), while the influence on insulin production has been more debated; ghrelin may act regulating pancreatic β-cells function by inhibiting glucose-stimulated insulin secretion. In conclusion, despite the controversial data about the direct effect of ghrelin on insulin release, ghrelin modulates circulating glucose levels, increasing insulin resistance and stimulating gluconeogenesis.

Lipid metabolism

Ghrelin has also been implicated on the regulation of lipid metabolism, with effects in the liver, skeletal muscle and adipose tissue. As mentioned above, ghrelin favours lipid accumulation. The observed tendency to increase body fat in ghrelin-treated animals seems to be independent from changes in food intake or weight gain (Tschop et al., 2000). The increase in respiratory quotient following both central and peripheral administration of ghrelin is likely to reflect reduced whole body lipid oxidation.

In fat tissue, both ghrelin and des-acyl ghrelin promote adipogenesis and inhibit lipolysis, and both peptides also modulate lean tissue fat distribution and metabolism. Subcutaneous injection of acyl ghrelin in rats induces tissue-specific changes in mitochondrial and lipid metabolism genes,

favouring triglyceride deposition in liver over skeletal muscle (Barazzoni et al., 2005). These results supported the hypothesis that ghrelin is involved in adaptive changes of lipid distribution and metabolism in the presence of caloric restriction and loss of body fat.

Moreover, both acyl and des-acyl ghrelin inhibited isoproterenol-induced lipolysis in rat adipocytes, therefore confirming the existence of a not yet identified receptor, different from GHS-R1a, specific for both peptides and mediating the ghrelin actions on lipid metabolism (Muccioli et al., 2004).

Bone formation

Ghrelin and its receptor are synthesized in bone cells, such as chondrocytes and osteoblasts. Both acyl and des-acyl ghrelin stimulate osteoblasts proliferation and differentiation, increase osteoblastic markers like osteocalcin and bone alkaline phosphatase, and repress osteoblasts apoptosis via phosphatidylinositol 3-kinase and mitogen-activated protein kinase signaling (Delhanty et al., 2006).

Immunomodulation

Many studies have revealed that ghrelin regulates immune cell proliferation and activation and secretion of pro-inflammatory cytokines. Human monocytes, neutrophils, B and T lymphocytes express ghrelin. In general, the effects of ghrelin are anti-inflammatory and immune-enhancing. For example, it acts through GHS-R1a to specifically inhibit the expression of cytokines such as interleukin 1 and 6, TNF-α, and nuclear-factor kappa B (Dixit et al., 2004) and stimulates proliferation of thymic epithelial cells and T lymphocytes. Ghrelin also suppresses neutrophil and macrophage migration. In contrast, des-acyl ghrelin has no role in immunomodulation.

Cell proliferation

Numerous studies have demonstrated that both acyl and des-acyl ghrelin exert mitogenic and antiapoptotic actions on pancreatic islets, spinal cord,

cortical and brainstem neurons, osteoblasts, endothelium, cardiomyocytes, and adipocytes (Baldanzi et al., 2002; Chung et al., 2008; Granata et al., 2007; Kim et al., 2005; Kui et al., 2009). The observation of several cell-cycle effects induced by either acyl or des-acyl ghrelin has raised the possibility of the involvement of both GHS-R1a and non-GHS-R1a receptor pathways.

Behavioural effects

In addition to the described central and peripheral actions, ghrelin seems to be involved also in behavioural functions, such as sleep-wake regulation, memory improvement and stress adaptation (Steiger et al., 2011).

1.4.5 Ghrelin effects on the cardiovascular system

Widespread expression of ghrelin and GHS-R1a is observed in the cardiovascular system (Gnanapavan et al., 2002). The mRNA encoding GHS-R1a was detected in myocardium and aorta, of course in a much lower amount compared to the pituitary. Furthermore, several groups have confirmed the presence, in the heart, of the previously mentioned putative ghrelin receptor distinct from GHS-R1a, exhibiting the same affinity both for acyl and des-acyl ghrelin (Baldanzi et al., 2002) or a receptor specific for des-acyl ghrelin (Lear et al., 2010). This receptor might be responsible of the opposing metabolic properties exhibited by acyl and des-acyl ghrelin in glucose and fatty acid uptake observed in cardiac cells.

Some of the so far described effects exerted by either acyl or des-acyl ghrelin on the cardiovascular system and mediated by GHS-R1a or by yet unidentified putative alternative receptors, are summarized below.

Vasoactive function

Acyl ghrelin has direct vasodilatatory, endothelium-independent, effects in humans. Intravenous injection of ghrelin peptide into human healthy

volunteers induced a decrease in blood pressure without changing the heart rate (Nagaya et al., 2001a). This effect appeared to occur through an action on the nucleus of the solitary tract (NTS), by which ghrelin suppresses sympathetic activity (Lin et al., 2004). Similarly, des-acyl ghrelin, upon injection into the NTS, reduced arterial pressure and heart rate, suggesting that it also contributes to cardiovascular regulation and that a receptor other than GHSR-1a exists in NTS (Tsubota et al., 2005).
Another possible mechanism that could explain the vasodilatatory effect of ghrelin is its antagonistic action on the vasoconstrictor endothelin-1, observed in isolated mammary arteries (Wiley and Davenport, 2002).

Cardiotropic effects

Several studies have suggested a role of ghrelin as an inotropic regulator; however it was difficult to establish whether the enhancement of cardiac output observed in these conditions is due to a direct effect on cardiac contractility, rather than on vasodilation and reduced after-load, or secondary to increased secretion of GH. Recently, a few studies suggesting inotropic effects reported an improvement of systolic function in the absence of decreased peripheral resistance, thus excluding a vasodilatatory effect (Enomoto et al., 2003). However, experiments to investigate the effect of ghrelin on isolated papillary muscle contractility have demonstrated a reduction of contractile force upon both acyl and des-acyl ghrelin administration. This action was dependent on NO synthesis, on endocardial endothelium integrity and independent from the receptor GHS-R1a, therefore reinforcing the hypothesis of a direct effect of the peptides on cardiac contractility, with a mechanism totally independent from GH release (Soares et al., 2006).

Ghrelin is effective in improving cardiac performance in pathological cardiac conditions, such as chronic HF. Rats with HF treated with acyl ghrelin, showed higher cardiac output and stroke volume compared to placebo-

treated animals; furthermore ghrelin increased posterior wall thickness, inhibited LV enlargement and increased fractional shortening (Nagaya and Kangawa, 2003; Nagaya et al., 2001b).

Similar beneficial effects upon ghrelin administration were also observed in patients with HF. Repeated administration of the peptide improved LV function, exercise capacity, and muscle wasting in these patients (Nagaya et al., 2004). Cardiac cachexia, a catabolic state characterized by weight loss and muscle wasting, occurs frequently in patients with end-stage HF and is a strong risk factor for mortality. Plasmatic ghrelin level is increased in cachectic patients, probably as a compensatory mechanism in response to anabolic- catabolic imbalance.

Protective effects on myocardial ischemia

Recently, it was observed that acyl ghrelin peptide administration for two weeks after rat myocardial infarction (MI) prevents an increase in cardiac sympathetic tone, improves cardiac remodeling, LV function and reduces mortality (Soeki et al., 2008). Interestingly, similar protective effects were observed also after early treatment, when ghrelin was administered <2 hours after the infarct (Schwenke et al., 2008). Although further investigations are needed to establish whether the described beneficial effects of ghrelin also provides long-term benefit for improving cardiac function, taken together, these data suggest the potential usefulness of this peptide as a new cardioprotective hormone early after MI. In addition, ghrelin and GHS-R1a in the myocardium are up regulated during isoproterenol-induced myocardial injury. A protective effect of both acyl ghrelin and des-acyl ghrelin against isoproterenol-induced myocardial injury and fibrosis has been described, which suggests that both the peptides could represent endogenous cardioprotective factors in ischemic heart disease (Li et al., 2006).

Several studies have investigated the potential mechanisms responsible for

the cardiac beneficial functions of ghrelin. Its protective effect against cardiac ischemia could be partially explained by an inhibitory activity of the molecule on cardiomyocytes cell death. A possible direct effect of ghrelin in inhibiting apoptosis has been demonstrated on primary adult and H9c2 cardiomyocytes and endothelial cells *in vitro* (Baldanzi et al., 2002). These effects are regulated via a MAPK- and Akt-dependent pathway. Des-acyl ghrelin is similarly active. Moreover, H9c2 cardiomyocytes do not express the ghrelin receptor, again suggesting that another receptor is involved.

Many reports further confirmed the antiapoptotic effect of ghrelin in different cell types through similar signaling pathways. Recently it was demonstrated that, in mouse cardiomyocyte cell line HL-1, des-acyl ghrelin also recognizes specific binding sites and that both acyl and des-acyl ghrelin exert antiapoptotic activities, despite their opposite metabolic effects. Indeed, acyl ghrelin inhibited insulin-induced glucose uptake and had no effect on fatty acid uptake, whereas des-acyl ghrelin reversed the inhibitory effect on glucose uptake and increased fatty acid uptake and glucose transporter-4 translocation to the cell membrane (Lear et al., 2010).

In a model of doxorubicin induced cardiac damage it was shown that ghrelin not only reduces apoptosis and markers of oxidative stress but also increases anti-oxidative enzyme activity and preserves mitochondrial membrane potential and energy metabolism through the TNF-α/NF-kB pathway (Xu et al., 2008). Accordingly, ghrelin was previously found to counteract cytokine-induced apoptosis and to reduce inflammation. The ability of ghrelin to reduce endoplasmic reticulum stress after I/R injury was confirmed both *in vitro* and *in vivo* (Zhang et al., 2009).

The recently identified ghrelin gene-derived peptide obestatin was also described as a protective molecule against apoptosis in several cell types, including the myocardium (Alloatti et al., 2010). The antiapoptotic effect

appears to be mediated by the PKC, PI3K, and ERK1/2 pathways. Despite these results, to date the physiological role of obestatin is still largely unknown (**Figure 1.24**).

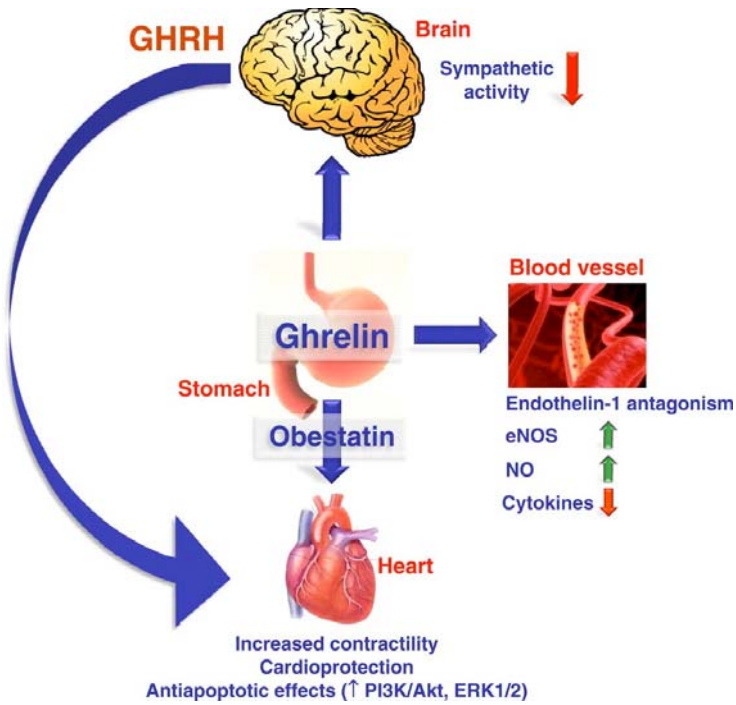

Figure 1.24 Ghrelin action on the cardiovascular system
The interactions between GHRH, ghrelin, and obestatin with the CNS and the cardiovascular system are summarized in the picture *(Granata et al., 2011).*

1.5 INSULIN-LIKE PEPTIDE 6: A NOVEL MEMBER OF THE RELAXIN FAMILY

Another factor that was identified in the course of this Thesis work as a powerful cardioprotective molecule was Insulin-Like Peptide 6 (INSL6), a member of the relaxin family of proteins.

Frederick L. Hisaw discovered relaxin in 1926, when he reported the relaxation of the interpubic ligament of female guinea pigs following injection of serum from pregnant guinea pigs or rabbits. Relaxin was first isolated in 1930 from extracts of porcine ovary, however, the interest towards this molecule increased only in the '80s after peptide purification, which allowed the identification of its amino acidic sequence (Fields and Larkin, 1981). Afterwards, the genes coding for two human molecular forms of relaxin with high sequence homologies (95%), designed H1 and H2 relaxins, were identified (Hudson et al., 1984).

Relaxin was originally described as a pregnancy hormone, produced in the reproductive tract of many mammals during pregnancy and primarily secreted by the corpus luteum, even if the main source of relaxin varies among species. Recent research has revealed that relaxin is also produced by non-reproductive organs and acts through endocrine, paracrine and autocrine mechanisms on a wide range of tissues (Sherwood, 2004).

INSL6 was originally identified in the testis of humans and rats (Lok et al., 2000) and found to be a member of the relaxin family of proteins.

1.5.1 The relaxin family peptides and their receptors

Relaxin belongs to the insulin/relaxin superfamily that includes the insulin family (insulin, IGF-I and IGF-II), that diverged early in vertebrate evolution from the relaxin family, composed by relaxin-1, relaxin-2, relaxin-3 (Bathgate et al., 2002), and the insulin-like (INSL) peptides, INSL3,

INSL4, INSL5 and iNSL6 (Wilkinson et al., 2005) (**Figure 1.25**).

Despite the overall sequence identity of these peptides is low, they are all synthesized as pro-hormones, comprising a signal sequence and a B-C-A domain configuration. Afterwards, the removal of the C chain and the formation of three disulfide bridges between six invariant cysteine residues found on the A and B chains, produces the active protein. The B domain is responsible for the primary interaction with the receptors, whereas the A chain is essential for the maintenance of the correct three-dimensional conformation of the peptides (Bathgate et al., 2006). The amino acid motif Arg-X-X-X-Arg-X-X-Ile, located in the middle of the B chain, is required for relaxin bioactivity and is therefore conserved among species (Bullesbach and Schwabe, 2000)

Relaxin-1 is found only in humans and the great apes and its gene expression is limited to decidua, placenta, endometrium and prostate. Relaxin-2 is the major circulating form of the relaxin in humans, and the relaxin-1 equivalent in non-primates. The major source of relaxin-2 is the corpus luteum of the ovary, from which it is secreted into the bloodstream; however, relaxin-2 is not merely a hormone of pregnancy, but has a number of other roles *in vivo*, such as the regulation of collagen metabolism and the actions on receptors located in the vasculature and in the brain (discussed in the next section). Relaxin-2 is also locally produced and acts as a paracrine/autocrine factor in the endometrium, mammary gland, placenta, prostate and heart. Relaxin-3 shows, on the contrary, brain specific expression and has putative actions as a neuropeptide. It has a role in mediating stress response and appetite regulation (McGowan et al., 2009; Smith et al., 2010). The gene coding for relaxin-3 is highly conserved among species, therefore it is considered the ancestral relaxin gene. INSL3, or relaxin-like factor (RLF), is expressed in testis and ovary and is critical for testis descent, oocyte maturation and male germ cell

survival (Kawamura et al., 2004), while INSL5 is widely found in kidney and colon, as well as in the brain and pituitary. INSL4 and INSL6 are mainly expressed in the placenta and testis, respectively, and their functions are still poorly characterized.

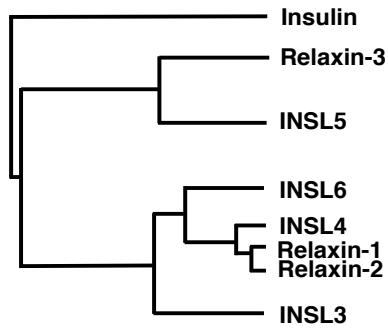

Figure 1.25 Relaxin family evolution
Phylogenetic evolutionary tree of the relaxin-family peptides *(Ivell and Grutzner, 2009).*

Given the structural similarity between relaxin and insulin, the relaxin receptor was thought to be a tyrosine kinase receptor, similar to the insulin one. However, it was finally demonstrated in 2002, that two orphan G protein-coupled receptors, LGR7 and LGR8, are activated by relaxin-2 and INSL3, respectively (Hsu et al., 2002; Kumagai et al., 2002). The leucine-reach-repeat containing GPCR (LGR) family consists of three class of receptors: class A, composed by the luteinizing hormone receptor (LHr), thyroid stimulating hormone receptor (TSHr) and follicle stimulating hormone receptor (FSHr); class B, which includes the orphan receptors LGR4, LGR5 and LGR6 and class C, composed of the relaxin receptors LGR7 and LGR8. These receptors, now termed relaxin family peptide receptor-1 (RXFP1) and RXFP2, have a widespread distribution throughout the body.

The binding of relaxin-2 and INSL3 to their receptors mainly stimulates the G_s-cAMP-PKA-dependent signaling pathway, but there is evidence that

relaxin-2 also causes tyrosine kinase phosphorylation and can also acts through the MAPK pathway in different cell types (Van Der Westhuizen et al., 2007). In addition relaxin-2 can act by increasing the activity of nitric oxide synthase (NOS) (Failli et al., 2002).

Subsequently, other two GPCRs, GPCR135 and GPCR142 (now termed RXFP3 and RXFP4), were identified as the specific receptor for relaxin-3 and INSL5, respectively (Liu et al., 2003; Liu et al., 2005). According to its ligand expression, the relaxin-3 receptor RXFP3 is mainly present in the brain, while RXFP4 is also expressed in numerous peripheral tissues. Although these four receptors are all Type I GPCRs, they are very distantly related and, in particular, RXFP3 and RXFP4 are coupled to cAMP inhibition, exerting opposite functions of RXFP1 and RXFP2.

INSL4 and INSL6 do not interact with any of the RXFP receptors and their native receptors are currently unknown.

1.5.2 Biological functions of relaxins

In the past 30 years it has been established that relaxin is essential for numerous aspects of pregnancy, including the modification of the pelvic girdle in many mammalian species, as show by the initial studies by Hisaw and collaborators. However, it has become evident that relaxin also affects non-pregnant animals, exerting many functions on different tissues, including the male reproductive organ.

A role for relaxin in protecting several organs from the progression of fibrosis was confirmed by studies with relaxin knockout mice, which display a number of changes, including increased lung, renal and ventricular collagen deposition with age (Du et al., 2003; Samuel et al., 2004b) and increased pulmonary and dermal fibrosis (Samuel et al., 2005).

1.5.2.1 Effects on reproductive organs

As already mentioned, relaxin has been traditionally viewed as a hormone of pregnancy and parturition, able to induce lengthening of the interpubic ligament and softening of the birth canal's tissue by induction of collagen remodeling, in order to facilitate the fetus passage. However, in contrast to the elevated relaxin serum levels observed during the third trimester of pregnancy in guinea pigs and other mammals, H2 relaxin functions differently in higher primates and humans, where the highest plasma levels are observed during the first three months of pregnancy (Parry and Vodstrcil, 2007). This finding suggested that, in humans, relaxin might facilitate embryo implantation rather than being involved in maintenance of pregnancy and parturition. Indeed, in both humans and other primates relaxin has been associated with endometrial angiogenesis, thickening and bleeding (Goldsmith et al., 2004). In addition, relaxin is important in the development of mammary nipple and mammary gland of a number of species, including humans (Sherwood, 2004).

Slower progress has been made towards the understanding of the role of endogenous relaxin in males. Relaxin is not a circulating hormone in males, but it is locally expressed by the prostate. In addition, the observation that both relaxin gene knock-out (M1RKO) and relaxin receptor knock-out (LGR7KO) male mice display underdeveloped testis, underdeveloped reproductive tract, and reduced fertility provide evidence that relaxin plays a role in the development of the male reproductive system (Samuel et al., 2003). So far, other relaxin family peptides have been associated to male reproductive organ development; in particular, the expression of INSL5 and INSL6 was described in testis, while INSL3 was reported to be a major player in the process of testicular descent (Kumagai et al., 2002).

1.5.2.2 Effects on other organ systems

Relaxin also exerts important actions on non-reproductive organs both during pregnancy and in non-pregnant females and males, where it is produced by numerous cell types to act in a paracrine or autocrine manner. As mentioned above, relaxin promotes tissue remodeling by increasing collagen turnover during pregnancy but, in addition, it exerts the same function also in other relaxin-expressing tissues, as demonstrated by the observation that relaxin knock out mice develop a progressive fibrosis in many organs, such as heart, lung, kidney and skin, with aging.

The use of the relaxin peptide to limit collagen production was effective in restoring normal functions in numerous models of organ fibrosis (Lekgabe et al., 2005; Mookerjee et al., 2006). It was shown that relaxin acts directly on TGF-β-stimulated human dermal fibroblasts, lung and cardiac fibroblasts (Samuel et al., 2004a) to reduce type I and type III collagen synthesis, and to increase matrix metalloproteinases (MMPs) expression. Moreover, relaxin successfully modifies the extracellular matrix in dermis, lung, liver and kidney (Samuel and Hewitson, 2006; Tang et al., 2009). Interestingly, in all of these experimental conditions, relaxin only affects aberrant collagen deposition, induced by pro-fibrotic stimuli, but has little effect on normal collagen levels.

Another relaxin property that was shown to involve both reproductive and non-reproductive organs is its ability to induce blood vessels dilation. This activity, which determines hypotension, is consequent to the ability of relaxin to dilate not only microvessels such as arterioles, but also capillaries and postcapillary venules in numerous sites throughout the body. Relaxin exerts its vasodilatatory action through the stimulation of nitric oxide (NO) production in the target cells (Failli et al., 2002; McGuane et al., 2011).

1.5.2.3 Effects on the cardiovascular system

It has been demonstrated that relaxin protects the cardiac tissue against myocardial injury caused by ischemia and reperfusion (IR) or myocardial infarction. When relaxin is present during IR, it reduces the areas of damage, ventricular arrhythmias, mortality, neutrophils accumulation, and morphological features of myocardial cell injury in rats (Bani et al., 1998). This effect could be partially ascribed to the mentioned vasodilatatory and anti-fibrotic activities of the peptide (**Figure 1.26**). Moreover, in a rat model of myocardial infarction it was shown that relaxin might influence the perfusion of ischemic sites by inducing VEGF-A and FGF-2, thus augmenting collateral vessel formation (Unemori et al., 2000). Relaxin may also mediate its cardioprotective effects through inhibition of inflammatory cell activation (Masini et al., 2004), or counteracting cell death, oxidative stress and calcium overload (Moore et al., 2007).

The evidence for a local production and release of relaxin by cardiomyocytes suggests that this peptide may act as an autocrine or paracrine physiological regulator of cardiac function. It has been reported that expression of both H1 and H2 relaxin genes is increased in failing cardiac tissue, and that plasma concentrations of relaxin correlates positively with the severity of congestive heart failure (Dschietzig et al., 2001), a finding that is however controversial (Fisher et al., 2003).

A phase II clinical trial (Pre-RELAX-AHF), based on the intravenous administration of recombinant relaxin protein in acute heart failure (AHF) patients, was recently completed. The results of this trial demonstrated that the infusion of relaxin improved prognosis in patients with AHF, without significant safety concerns. A phase III clinical trial (RELAX-AHF-1) is currently ongoing (Ponikowski et al., 2012).

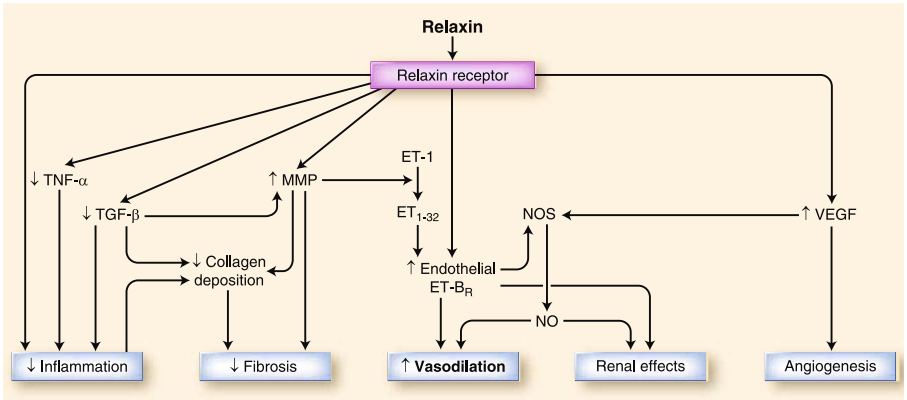

Figure 1.26 Relaxin beneficial effects in heart failure
One of the main properties of relaxin consists in the modulation of vascular tone. In HF condition, relaxin relieves systemic and renal vasoconstriction inducing vasodilation both by NO production and also activating the endothelin B (ET-B) receptor on endothelial cells. In addition, relaxin counteracts inflammation, decreases fibrosis and induces the expression of pro-angiogenic factors, such as VEGF *(Teichman et al., 2010).*

1.5.3 Insulin-like peptide 6 (INSL6)

1.5.3.1 Identification and characterization of INSL6

Insulin-like peptide 6 (INSL6) is a member of the insulin/relaxin superfamily. The factor was identified for the first time in 2000 from an Expressed Sequence Tag (EST) database, searching for proteins containing the insulin family B-chain cysteine motif (Lok et al., 2000). Afterwards, using a probe derived from the EST sequence, a 790 bp rat and a 717 bp human cDNA encoding INSL6 were isolated from testis cDNA libraries. INSL6 exhibits the hallmark of the family, comprising a signal peptide, B- and A- cysteine domain and an intervening C-domain (**Figure 1.27**). The prohormone of human INSL6 has longer C- and A- domains than rat INSL6 and an open reading frame of 213 vs 188 amino acids. Within the B- and A- domains, the two INSL6 exhibit 55% identity.

In humans, INSL6 maps to chromosome 9p24, the same position where the gene coding for INSL4, another family member associated with reproductive tissues, is also located. This region also harbours an autosomal testis-determining factor locus (TDFA). Failure of testis development was associated with rearrangement of the 9p24.1 region, demonstrating that this chromosome portion is important for reproductive function (Ion et al., 1998). In mice, both INSL6 and relaxin map to chromosome 19, which is syntenic to human chromosome 9.

Initially, human INSL6 expression was only detected in the germ cells of the testis (in spermatocytes and spermatidis, but not in either Leyding or Sertoli cells), while, in the rat, INSL6 transcripts were also detected in the prostate. INSL6 mRNA expression was detectable at low levels at embryonic day 14.5 and 17.5, and the level of expression remained low until postnatal day 20, when there was a 40- to 50-fold increase in mRNA abundance with maximum levels attained by day 40 and maintained up to day 90 of age (Lu et al., 2006). Later, the INSL6 mRNA was also detected in other tissues in mice, such as kidney, small bowel, heart, thymus, brain, intestine, uterus, ovary, spleen, lung and liver (Brailoiu et al., 2005; Kasik et al., 2000). However, the level of expression in these tissues was only 1-8% of that observed in the testis. Pro-protein convertase 4 (PC4), a furin-like protease expressed only in testis, is believed to be involved in INSL6 protein maturation from its prohormone precursor. In addition to prohormone processing, INSL6 undergoes other post-translational modifications, such as disulfide bond formation between the B- and A-domains typical of all the peptides of the family, and ubiquitination (Lu et al., 2006).

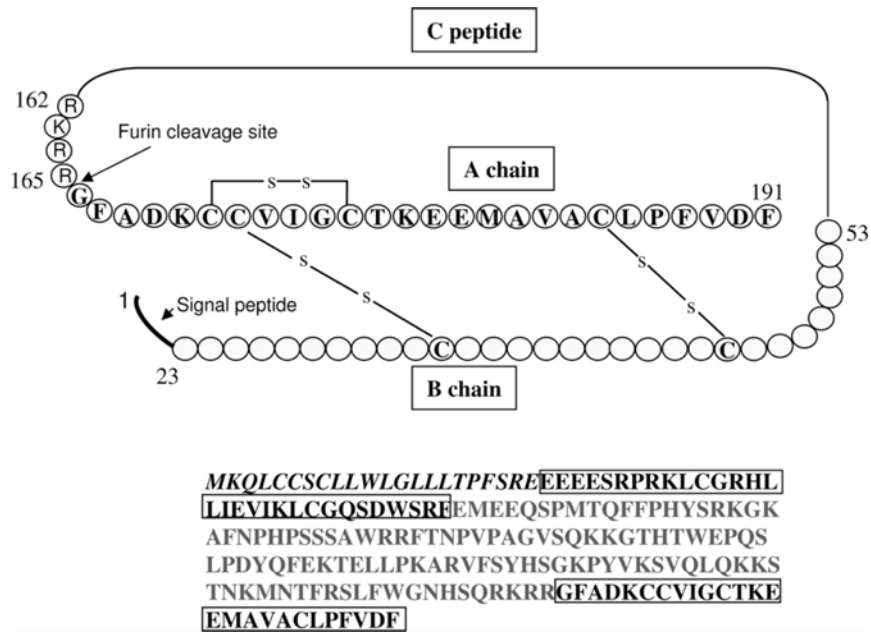

Figure 1.27 Murine INSL6 protein
The signal peptide, the A-, B- and C- domains and the location of disulfide bonds and furin cleavage sites are indicated in the picture (*Lu et al., 2006*).

1.5.3.2 Functions of INSL6

Given the predominant expression on INSL6 in the testis, INSL6-deficient mice have been generated in order to elucidate the role of this molecule in germ cell development (Burnicka-Turek et al., 2009). INSL6 resulted to be not essential for embryogenesis and gonadal differentiation, while it turned out of be required for spermatogenesis. INSL6$^{-/-}$ mice exhibited a clear impairment of this process, which was arrested at the stage of late pachytene spermatocytes because of a failure in completing meiosis. Immature germ cells were released, with a consequent significant decrease in the number of spermatozoa, which also had a reduced motility. Thus, the INSL6 deficiency appeared to lead to an arrest in the development of most germ cells at the end of meiotic prophase; enhanced apoptosis was

demonstrated to cause germ cell depletion after the arresting step.

Recently, INSL6 was reported to have a function in skeletal muscle (Zeng et al., 2010). Exploiting a model of cardiotoxin (CTX) induced injury, Zeng and co-workers showed that INSL6 is a muscle-derived factor that is up regulated by damage; the same effect was also observed after induction of Akt signaling in skeletal muscle-specific, conditional Akt1 transgenic mice. In contrast, the other insulin-like family members did not change their level of expression in these conditions. When expressed in the muscle by an adenoviral vector or in transgenic mice overexpressing the transgene from a muscle-specific promoter, INSL6 was able to activate satellite cells and accelerate the muscle regeneration process after damage, promoting muscle progenitor cell proliferation and survival.

The receptor mediating INSL6 actions both in testis and other tissues has not been identified so far.

2. AIM OF THE STUDY

The overall purpose of this study was the development of an innovative functional selection procedure (**FunSel**), based on the *in vivo* gene transfer and selection of a collection of secreted factors cloned into AAV, aimed at identifying new potential therapeutic molecules providing benefit to degenerative disorders. In particular, this Thesis work was aimed at developing a pilot project to assess the feasibility of **FunSel** and establishing the technology required.

The direct, *in vivo* selection of factors exerting a beneficial effect against tissue degeneration has never been attempted before and, basically, it is now rendered possible by the property of AAV vectors to be produced at high titers, infect tissues at high multiplicity of infection (MOI), persist in the transduced cells for prolonged periods of time and express their transgenes at high efficiency *in vivo*.

The specific objectives of the Thesis work were:

1. To establish a theoretical background supporting the feasibility of the **FunSel** *in vivo* selection approach based on pooled AAV gene transfer;
2. To construct of an arrayed collection of AAV vectors, corresponding to 100 secreted factors, which were arbitrarily chosen among the mouse secretome cDNA collection.
3. To experimentally test **FunSel** using such an AAV collections in a mouse model of hind limb ischemia and a mouse model of isoproterenol-induced myocardial damage, in order to identify secreted molecules protecting against these conditions.
4. To individually verify the capacity of the selected molecules in exerting a cardioprotective effect after myocardial infarction.

3. MATERIALS AND METHODS

3.1 MOLECULAR BIOLOGY PROTOCOLS

3.1.1 Generation of the plasmids collection

The RIKEN Mouse Secretome cDNAs Collection was provided by S. Gustincich (SISSA, Trieste) in collaboration with P. Carninci (RIKEN Institute, Japan) and the FANTOM Consortium.

The cDNAs were obtained from the original cloning plasmids (modified pBluescript SK (+)/modified Bluescript1 and pFlcI) by PCR with specific primers to insert the *Xho I* (CTCGAG) and *Not I* (GCGGCCGC) restriction sites at the 5' and 3' ends of each cDNA. The annealing temperatures of the two sets of primers were respectively 65ºC for the modified pBluescript SK (+) and 66ºC for the pFlcI plasmids.

PRIMER pBluescript FW:

5' - CTG TCC GCT CGA GCC AGT GAA TTG TAA TAC GAT - 3'

PRIMER pB/pF REV (common for both):

5' - ATA AGA ATG CGG CCG CCT AAA GGG AAC AAA AGC - 3'

PRIMER pFlcI FW:

5' - CTG TCC GCT CGA GTA CGA AGT TAT GGA TCA GGC - 3'

The amplified cDNAs were individually sub-cloned into the Multiple Cloning Site of the pZac2.1 AAV-backbone plasmid by the restriction sites *Xh oI* and *Not I.* This vector is specific for AAV vectors generation indeed it contains two Inverted Terminal Repeat sequences (ITRs), a CMV IE promoter, a multiple cloning site (MCS), and an SV40 polyA site (**Fig. 3.1**). PZac2.1 is a small vector, only 4543 bp long, and it allows the cloning of cDNAs longer than 3000 bp without any interference during the viral particles encapsidation process.

3.1.2 PCR amplification of the pooled viral genomes

After the individual cloning of a subset of cDNAs in pZac2.1, homogeneous pools of plasmids were mixed in equimolar amount to obtain the correspondent pools of AAV vectors. Viral genomes, recovered from each pooled AAV preparation, were submitted to a PCR amplification step carried by a pair of primers annealing on the common pZac2.1 vector sequence and spanning the MCS. The sequences of the primers, with annealing temperature of 58°C, are:

PRIMER pZac2.1 FW: 5' - GTG TCC ACT CCC AGT TCA AT - 3'

PRIMER pZac2.1 RV: 5' - GTG GTT TGT CCA AAC TCA TC - 3'

AAV vector genomes recovered from skeletal muscle or heart after each cycle of *in vivo* functional selection, were amplified using these primers and then visualized on a 1% agarose gel, in order to evaluate the obtained pattern of bands corresponding to each genome and to identify eventually enriched viral genomes.

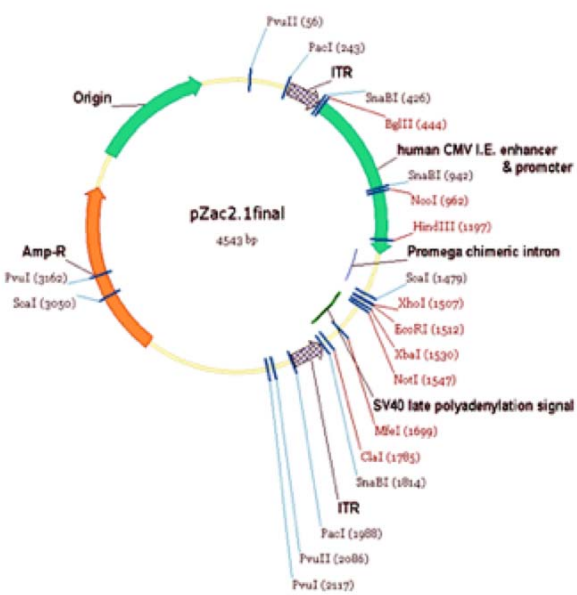

Figure 3.1 Map of the pZac2.1 AAV-backbone plasmid

3.1.3 Production and purification of rAAV vectors

The rAAV vectors used in this study were produced by the AAV Vector Unit at ICGEB Trieste (www.icgeb.org/avu-core-facility). Infectious AAV2 and AAV9 vector particles were generated in HEK 293 cells, cultured in 150-mm-diameter Petri dishes, by co-transfecting each plate with 20 µg of each vector plasmid together with 45µg of the packaging/helper plasmid, pDG (provided by J.A. Kleinschmidt, Heidelberg, Germany), expressing AAV and adenovirus helper functions. Viral stocks were obtained by CsCl gradient centrifugation (Arsic et al., 2003; Zacchigna et al., 2008) and rAAV titers were determined by measuring the copy number of viral genomes in pooled, dialyzed gradient fractions using Real-Time PCR.

The vectors used in this study express the cloned cDNAs under the control of the constitutive CMV immediate early promoter and all the viral stocks had titers between $1x10^{12}$ and $1x10^{13}$ viral genome particles/ml.

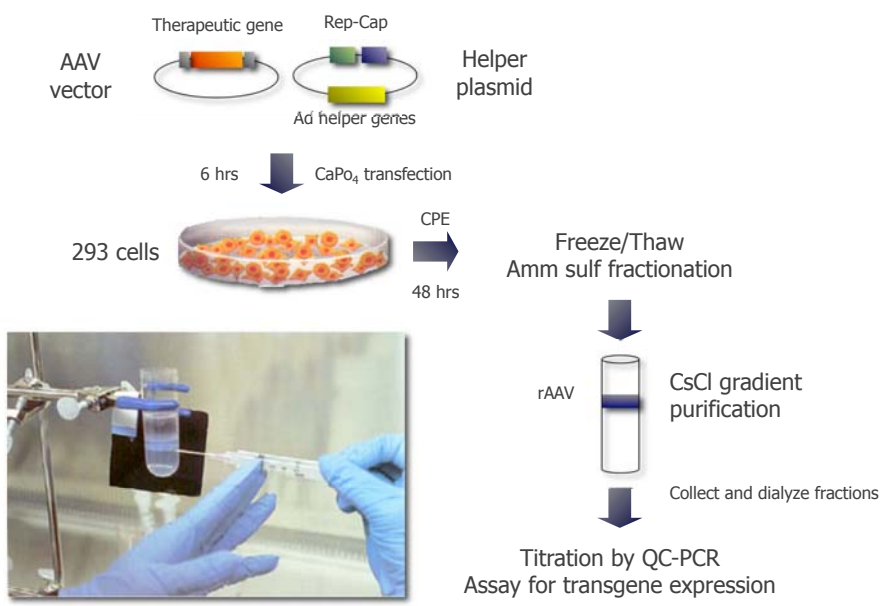

Figure 3.2 Production and purification of rAAV vectors

3.1.4 DNA and RNA extraction and Reverse Transcription (RT)

Total DNA was extracted from skeletal muscle and cardiac tissue using the DNeasy Blood and Tissue kit (Qiagen), according to the suppliers' protocol.
Total RNA from the same tissue samples was extracted using TRIzol reagent (Invitrogen, Carlsbad, CA, USA) according to the manufacturer's instructions, digested by DNAse I and reverse-transcribed using hexameric random primers.

3.1.5 Quantification of nucleic acids by Real-Time PCR

Quantification of gene expression was performed by Real-Time PCR; the cDNA was used as template to analyze the transgene expression levels of candidate factors like ghrelin and iNSL6 in skeletal muscle and heart, as well as α-MHC, β-MHC, SERCA2a, RYR2, ANF, BNP and PGC1α, IL1-β, IL6, TNF-α, miR21 and MMP-2 expression in the LV myocardium. The murine housekeeping gene GAPDH (the U6 promoter for miRNA quantification) was used to normalize the results. All the amplifications were performed on BIORAD (CFX96 real-time system), using predeveloped and custom-designed assays (Applied Biosystems, Foster City, CA, USA) or SYBRGreen (Bio-Rad Laboratories, Hercules, CA, USA).
Q-PCR was used also for the detection of vector specific DNA in muscle ad heart samples with the aim to calculate the ratio between viral particles coding for different factors. The amount of each vector was quantified by SYBRGreen assay and compared with the total viral DNA content respectively in pool of plasmids, viral lysates and muscles transduced with the correspondent pools of vectors. A Taqman probe and primers that specifically recognize CMV promoter, which is common to all the AAV vectors in the study, was used to quantify the total viral genomes.

Below the sequences of primers and probes; the efficiency of each single couple of primers have been tested and normalized.

Primers for viral DNA quantification:

Mouse D11 (Gast):	F: 5′-GTGGACAAGATGCCTCGACT-3′
	R: 5′-TGTTCCAGGTCCTCATTGGT-3′
Mouse E2 (Ghrl):	F: 5′-GCCCAGAGCACCAGAAAG-3′
	R: 5′-TGATCTCCAGCTCCTCCTCT-3′
Mouse C12 (INSL6):	F: 5′-AACCCTCACCCTTCTTCCTC-3′
	R: 5′-GCTCCCAAGTGTGTGTTCCT-3′
Mouse G4 (Ccl7):	F: 5′-CCCAAGAGGAATCTCAAGAGC-3′
	R: 5′-AGCCTCCTCGACCCACTTCT-3′
Mouse F8 (Pomc):	F: 5′-CACTGAACATCTTTGTCCCCA-3′
	R: 5′-CGACTGTAGCAGAATCTCGG-3′
Mouse H2 (Cxcl9):	F: 5′-CCGCTGTTCTTTTCCTCTTG-3′
	R: 5′-GCATCGTGCATTCCTTATCA-3′
Mouse G5 (Vip):	F: 5′-TTCACCAGCGATTACAGCAG-3′
	R: 5′-GTGTCGTTTGATTGGCACAG-3′
Mouse 2E4 (Plgf):	F: 5′-CTGCTGGGAACAACTCAACA-3′
	R: 5′-CCTCATCAGGGTATTCATCCA-3′
Mouse F2 (Afp):	F: 5′-CCAAAGCATTGCACGAAAAT-3′
	R: 5′-CTTCCGGAACAAACTGGGTA-3′
Mouse 1D12 (Tgfbi):	F: 5′-ATCACCAACAACATCCAGCA-3′
	R: 5′-CCAGCACGGTATTGAGTCCT-3′
Mouse 1F6 (Btd):	F: 5′-ATCAGCAGGAGGCGGGACGAG-3′
	R: 5′-AGCGCAGAACAGCCGAGGAA-3′
Mouse 2C12 (Ces2a):	F: 5′-GCCTGACCTCATCTCTGACACTT-3′
	R: 5′-TTACTCTTTGCTCTCAGGCAGTGGA-3′
Mouse 4A3 (Cyp2c55):	F: 5′-AGCTTGATGGCCACTGTAACC-3′

	R: 5′-ACGTGATCGATCTCTGCCTG-3′
Mouse 4C10 (Spon2):	F: 5′-ACTCGCTGGTGTCCTTCGTGGT-3′
	R: 5′-TCGGTCCCTGCATCGTGTG-3′
Mouse 1D3 (C8b):	F: 5′-ACCAAACGCTTCGCCCACACT-3′
	R: 5′-GCAGGCTCTTGACCCTCTGA-3′
Mouse 2C11 (Ces2e):	F: 5′-TGGAGTGGGGTGAGGGATGGG-3′
	R: 5′-CCTCATGGGCATGGGCTG-3′
Mouse 1C9 (Mau2):	F: 5′- GCCTGCTCCCTTGTGCTGCT-3′
	R: 5′- CATGGCGTTCCCACATGC-3′
CMV DNA:	F: 5′-TGGGCGGTAGGCGTGTA -3′
	R: 5′-GATCTGACGGTTCACTAAACGAG-3′

Primers for gene expression:

Mouse IL1-β:	F: 5′-GCTGTGGCAGCTACCTGTGTCTT-3′
	R: 5′-GGGAACGTCACACACCAGCAGGT-3′
Mouse TNF-α:	F: 5′-CCACCACGCTCTTCTGTCTAC-3′
	R: 5′-TTGGGAACTTCTCATCCCTTT-3′
Mouse MMP-2:	F: 5′-GGATGCCGTCGTGGACCTGC-3′
	R: 5′-GCTCAGCAGCCCAGCCAGTC-3′
Mouse miR21:	F: 5′- -3′
	R: 5′- -3′
Mouse β-MHC:	F: 5′-TCCGCAAGGTGCAGCACGAG-3′
	R: 5′-CACGGGCACCCTTGGAGCTG-3′
Mouse α-MHC:	F: 5′-ATGTTAAGGCCAAGGTCGTG-3′
	R: 5′-CACCTGGTCCTCCTTTATGG-3′
Mouse Serca2a:	F: 5′-CGCTACGGTGCCTGGCTCTG-3′
	R: 5′-TGCCCACACAGCCGACGAAA-3′
Mouse RYR2:	F: 5′-AAGGCGAGGATGAGATCCAGTTCCT-3′
	R: 5′-ATCCTTCTGCTGCCAAGCACAGCT-3′

Mouse ANF:	F: 5′-TCCAGCTGCTTCGGGGGTAGG-3′
	R: 5′-CCGCAGCTCCAGGAGGGTGT-3′
Mouse BNP:	F: 5′-GTCCTTCGGTCTCAAGGCAGCAC-3′
	R: 5′-GGGGAAAGAGACCCAGGCAGAGTC-3′
Mouse PGC1α:	F: 5′-CAACCGCAGTCGCAACATGCTCA-3′
	R: 5′-CCCTTGGGGTCATTTGGTGACTCTG-3′

Taqman probes (assay):

Mouse Ghrl:	Mm00445450_m1
Mouse INSL6:	Mm01964671_s1
Mouse IL6:	Mm00446190_m1
CMV:	(FAM)-TGGGAGGTCTATATAAGC-

3.2 CELLULAR BIOLOGY PROTOCOLS

3.2.1 Culture of neonatal rat cardiomyocytes

Isolation

Ventricular myocytes from 1 to 2 days-old Wistar rats were prepared according to a previously detailed protocol, yielding 90% purity (Collesi et al., 2008). The hearts were retrieved, the ventricles isolated from atria and vessels and minced in small pieces with diameter of about 2-3 mm.

The fragments were dissociated in CBFHH (calcium and bicarbonate-free Hanks with Hepes) buffer containing 2 mg/ml of trypsin and 20 μg/ml of DNase II, repeating the digestion in fresh buffer approximately 10 times for 10 minutes each with slow stirring, preceded by 10 times up and down gentle pipetting of tissue pieces. After each cycle the supernatant was collected into a solution containing calf serum (10% v/v) to neutralize the action of trypsin.

At the end of the cycles of digestion the collected cells were centrifuged for

10 minutes at 1,200 rpm and the cellular pellet was resuspended in DME containing 5% bovine calf serum (HyClone).

Cells were preplated for 2 hours into 100-mm dishes, in order to allow the engraftment on the plate of fibroblasts. By this procedure stromal cells were separated from unattached myocytes that were then plated in dishes for primary cells.

Culture and treatments

Neonatal rat ventricular myocytes were plated at low density in DME/4.5g glucose containing 5% bovine calf serum, vitamin B12 (2 mg/ml) and penicillin-streptomycin (100 U/ml) and cultured as described previously (Deng et al., 2000). Cardiomyocytes were plated at a density of 500 cells/mm^2 into multi-well plates (Costar) and incubated at 37°C, 5% CO_2.

For cardiomyocyte transduction using AAV vectors (AAV9-LacZ and AAV9-Ghrl), neonatal rat cardiomyocytes were infected with MOI 10^4 the day after plating and, 12 hours later, the culture medium was changed. After additional 12 hours apoptosis was stimulated treating the cells with 2 different chemical compounds either (-)-Isoproterenol hydrochloride 10µM (Sigma) for 48 hours or Doxorubicin hydrochloride 1µM (Sigma) for 24 hours.

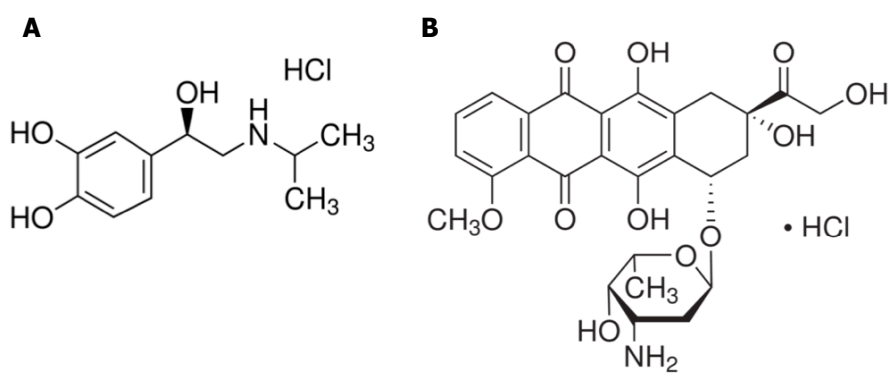

Figure 3.3 Drugs chemical structures

(A) (-)-Isoproterenol hydrochloride **(B)** Doxorubicin hydrochloride

3.2.2 Cell viability assay

To quantify neonatal rat cardiomyocytes viability after pro-apoptotic drugs stimulation we used the LIVE/DEAD Viability/Cytotoxicity Kit (Invitrogen), following manufacturer's instructions. After the staining cells were fixed in 3% PFA and 2% sucrose in PBS and their fluorescence was analyzed by the ImageXpressMICROTM microscope and by the software MetaXpressTM, both from Molecular Devices.

3.3 *IN VIVO* EXPERIMENTAL PROTOCOLS

Animal care and treatment were conducted in conformity with institutional guidelines in compliance with national and international laws and policies (EEC Council Directive 86/ 609, OJL 358, December 12th 1987). CD1 mice, C57/Bl6 mice and Wistar rats were obtained from Harlan and maintained under controlled environmental conditions.

3.3.1 AAV vectors *in vivo* administration

Tibialis anterior muscles of C57/Bl6 mice (1 month old) were transduced by direct injection of 50 µl (titer of 10^{12} vg/ml) of AAV vector preparation (AAV2-Pool25, AAV2-Pool50, AAV2-Pool100, AAV2-E2, AAV2-C12) for AAV genomes *in vivo* maintenance analysis.

For the *in vivo* selection in the hind limb ischemia model 30 µl of pooled AAV2 vectors (AAV2-PoolA+B+C; titer of 10^{12} vg/ml) were bilaterally delivered to tibialis anterior muscles of adult CD1 mice, 5 days before the surgical intervention of unilateral femoral artery ligation.

For the *in vivo* selection in the model of isoproterenol-induced cardiac damage three days old C57/Bl6 mice were injected intraperitoneally (i.p.) with 30 µl of pooled AAV9 vectors (AAV9-PoolA to AAV9-PoolL) preparations (titer of 10^{12} vg/ml).

In the myocardial infarction model 30µl (titer of 10^{12} vg/ml) of recombinant AAV vectors (AAV9-Control, AAV9-Ghrl or AAV9-INSL6) were administered, immediately after LAD coronary artery ligation, in three separate injections into the infarct-bordering zone.

3.3.2 Animal model of hind limb ischemia

Before femoral artery ligation, CD1 mice were anesthetized with an intraperitoneal injection of ketamine (100 mg/kg) and xylazine (10 mg/kg), injected intraperitoneally and placed on a warming pad to maintain core body temperature between 36.8 and 37.8°C.

Unilateral hind limb ischemia was induced, by resecting a 2.5 cm segment of the left femoral artery (Arsic et al., 2004). Animals were sacrificed 15 days later and total DNA was extracted, as previously described, from both ischemic and non-ischemic transduced skeletal muscle for subsequent analysis of the viral genomes content in the tissue.

3.3.3 Animal model of isoproterenol-induced cardiac fibrosis

Three weeks after AAV vector pools administration in neonatal mice, a single high dosage (200 mg/kg) of (-)-Isoproterenol hydrochloride (Sigma) was administered by intraperitoneal injection in C57/Bl6 mice to determine an acute damage, consisting in coagulative myocytolysis and myofibrillar degeneration (Milei et al., 1978). After 15 days mice were sacrificed and the hearts retrieved. Total DNA was extracted, as previously described, from both Iso-treated and untreated transduced hearts for subsequent analysis of the viral genomes content in the tissue.

The proper Isoproterenol concentration for the *in vivo* functional selection was previously set up comparing the cardiac damage induced by three different dosages (100, 200 and 300 mg/kg) of (-)-Isoproterenol hydrochloride.

3.3.4 Animal model of myocardial infarction (MI)

Myocardial infarction was produced in CD1 mice (8-10 weeks old), by permanent left anterior descending (LAD) coronary artery ligation, as described previously (Michael et al., 1999).

Mice were anesthetized with ketamine (100 mg/kg) and xylazine (10 mg/kg), placed on a warming pad to maintain body temperature at 37°C and endotracheally intubated and connected to a rodent ventilator (Model 131, Nemi scientific Inc.). The beating heart was accessed via a left thoracotomy; after removing the pericardium the heart was exposed and the descendent branch of the LAD coronary artery was visualized by a stereomicroscope and ligated with an 8-0 silk suture. Ligation was considered successful when the anterior wall of the LV turned pale.

As already mentioned, immediately after LAD coronary artery ligation 50 µl of recombinant AAV vectors (AAV9-Control, AAV9-Ghrl or AAV9-INSL6) were administered in three separate injections into the myocardium bordering the infarct zone, using a tuberculin syringe (30G) (Roche).

The chest was closed and the mice moved to a prone position and kept on the heating pad until they recovered spontaneous breathing.

3.3.5 Echocardiography analysis

To analyze LV function and dimension, transthoracic two-dimensional echocardiography was performed 2, 7, 30, 60 and 90 days after myocardial infarction, in mice sedated with 5% isoflurane, using the Vevo 770 Ultrasound (Visualsonics), equipped with a 30-MHz linear array transducer.

M-mode tracing were used to measure left ventricular anterior and posterior wall thickness and internal diameter at end-systole and end-diastole, fractional shortening and ejection fraction.

3.3.6 Histology

After echocardiography analysis (either at day 2 after myocardial infarction for apoptosis and inflammatory cells infiltration evaluation or after 3 months, at the end of the LV functional follow up) the animals were sacrificed, hearts were collected and washed in PBS. For histological analysis, tissue samples were snap frozen or fixed in 4% formaldehyde and embedded in paraffin. In both cases they were finally cut in 5μm thick slices for subsequent analysis. Heart's frozen sections recovered at day 2 post-MI were used for TUNEL assay (described in the next paragraph), while paraffin embedded sections were stained with hematoxylin-eosin (H&E) for inflammatory cells infiltration analysis (quantified in 5 random fields per slide at 200x power, using ImageJ software). The samples collected 90 days after the infarct were submitted to Azan's trichrome staining (Bio-Optica), according to manufacturer protocol. Infarct size was measured on the stained sections as the percentage of (endocardial + epicardial circumference of infarct area) / (endocardial + epicardial circumference of LV).

Azan's trichrome staining was used also to evaluate the extent of mice cardiac fibrosis after high dosage (-)-Isoproterenol hydrochloride intraperitoneal injection.

3.3.7 TUNEL assay for apoptotic cells detection

TUNEL (TdT-mediated dUTP nick-end labelling) assay was performed on frozen sections (5μm thick) of LV infarcted hearts, collected 2 days after MI. The sections were fixed with 4% paraformaldehyde and permeabilised with 1% Triton X100 for 30 minutes. After 1 hour in blocking solution (2% BSA in PBS) at 37°C, the primary monoclonal antibody anti-sarcomeric α-actinin (EA-53, Abcam, Cambridge MA, USA) was used and diluted 1:100 in blocking buffer. Alexa Fluor 488 donkey anti-mouse was used as secondary

antibody. Apoptotic cells were visualized by in situ cell death detection kit, TMR red (Roche Diagnostics, Mannheim, Germany), according to manufacturer's instructions. Nuclei were stained with DAPI (H-1200, Vector laboratories, CA).

All images were acquired by a DMLB upright fluorescence microscope (Leica Mycrosystems, Wetzlar, Germany) equipped with charge coupled device camera (CoolSNAP CF, Roper Scientific, Trenton, NJ, USA) using MetaView 4.6 quantitative analysis software (MDS Analytical Technologies, Toronto, Canada). At least 10 high-magnification fields were counted for each experimental condition.

3.3.8 Enzyme Immunoassay (EIA) analysis

The levels of acyl and des-acyl ghrelin peptides in the LV after AAV9-Ghrelin intracardiac injection was assayed by a specific EIA kit from Phoenix Pharmaceuticals (Belmont, CA), according to the protocol provided by the supplier.

3.4 STATISTICAL ANALYSIS

One-way ANOVA and Bonferroni/Dunn's post hoc test were used to compare multiple groups. Pairwise comparison between groups was performed using the Student's t test. $P<0.05$ was considered statistically significant.

4. RESULTS

The overall design of the **FunSel** approach, based on the iterative selection of secreted factors upon *in vivo* gene transfer using AAV vectors, is described and schematically illustrated in the Thesis Synopsis. The specific purpose of the work described in this thesis was to demonstrate the feasibility of **FunSel** in the cardiovascular system using a pool of 100 AAV vectors each one expressing a different secreted factor from the mouse secretome.

The results described in this Thesis can be divided into five main points, representing the essential steps of this project:

1. Development of an in vivo functional selection strategy: mathematical considerations

We wanted to support the feasibility of the *in vivo*, AAV based, **FunSel** functional selection strategy by generating a mathematical model that takes into account the parameters influencing *in vivo* selection of genes after gene transfer. These parameters include variables such as transduction efficiency, multiplicity of *in vivo* infection, effects of the unwanted co-selection of non transduced cells, efficiency of selection the transduced cells, complexity of vectors pools and number of selection cycles. Applying the developed model over a range of possible conditions permitted to identify those that support the feasibility of the iterative selection approach.

2. Generation of an arrayed library of AAV vectors corresponding to secreted genes

We generated a collection of 100 AAV vector plasmids, each one expressing a secreted factor. The construction of this collection of clones entailed the individual cloning of 100 different cDNAs, selected from the

FANTOM Project mouse secretome collection and enriched in growth factors and hormones, into an AAV-backbone plasmid under the control of the constitutive CMV IE promoter.

3. Validation of the AAV vector pool composition

This part of the project was aimed at assessing whether it is possible to simultaneously obtain pools of AAV vectors with variable complexity. We analysed the critical steps in library construction, including vector packaging, *in vivo* transduction, persistence and level of expression. The ultimate purpose of this part of the project was to find the experimental conditions that guarantee a balanced representation of the different viral genomes in each viral vector pool during vector production and after *in vivo* transduction.

4. In vivo functional selection of the AAV vectors collection

Next we wanted to provide a proof-of-principle result that supported the efficacy of **FunSel**. To identify novel potentially therapeutic secreted molecules exerting a protective effect against cardiovascular damage, **FunSel** was applied, using the developed 100 clones, to two models of damage in the mouse. The first one corresponded to hind limb ischemia while the second to isoproterenol-induced myocardial injury. Two novel factors were identified in the tested pool of 100 genes, namely ghrelin in the former case and INSL6 in the latter.

5. Validation of the therapeutic effect of the in vivo selected genes

Ghrelin and INSL6 were individually tested for efficacy after myocardial infarction in the mouse after intracardiac AAV gene transfer. Both factors were proven to exert a marked effect in preserving cardiac function, as concluded by echocardiographic evaluation of cardiac contractility over time. Both factors were shown to exert a marked anti-apoptotic effect.

4.2 DEVELOPMENT OF AN *IN VIVO* FUNCTIONAL SELECTION STRATEGY: MATHEMATICAL CONSIDERATIONS

This section reports a mathematical model that, taking into account the most relevant variables affecting the outcome of *in vivo* functional selection for potentially therapeutic genes, supports the feasibility of the approach. **FunSel** is essentially based on:

i) the production of a pool of AAV vectors of variable complexity;

ii) the transduction of a given tissue *in vivo* with this pool of vectors;

iii) the delivery of a selection stimulus to the tissue, typically the induction of cell damage; cells transduced with a protective gene will preferentially survive over cells transduced with an irrelevant vector or cells that are not transduced.

iv) at a give time from damage, the recovery of vectors from the tissue and the analysis of the representation of each individual vector;

v) the eventual cloning of the recovered vectors to generate a new pool of vectors and the iterative repetition of the selection.

The success of **FunSel** essentially depends on the capacity of an AAV vector pool to transduce a target tissue by delivering several genes simultaneously, on the capacity of one or more of these genes to induce selection against an insult and thus become enriched compared to the others, and on the number of iterations required for the selection to become detectable.

4.1.1 Mathematical model: variables and formula

The ultimate purpose of the AAV selection procedure is the *in vivo* selection of one AAV coding for a desired transgene (**T**) from a pool of several AAVs (**POOL**), each one coding for a different factor. The ratio between T and POOL is defined as **R** (**R=T/POOL**).

The increase of R is an indication of the success of the selection procedure.

At the beginning of the selection experiment: R=T/POOL=1/(number of vectors in the analyzed pool);

At the end of the experiment: R=1/(number of selected vectors).

For example, if a pool of 25 vectors, each one present in equimolar amount to the others, is injected, R=1/25=0.04 at start. Any increase (up to R=1) at the end of the experiment indicates successful selection.

Five variables are considered that are expected to affect the selection experiment:

Variable	Description	Symbol	Range of reasonable values
Transduction efficiency	Measures the fraction of cells transduced	**ET**	>0 to 1 (ET=1 when all cells are transduced)
Multiplicity of infection	Measures how many AAV genomes are present in a single cell nucleus	**MOI**	>0 to 1,000
Co-selection effect	Measures the extension of the selection effect exerted by the transgene on neighboring cells	**COSEL**	0 to 100
Efficiency of selection	Measures how efficient is the selection process, namely the selective advantage offered by the transgene	**ES**	>0 to 1 (ES=1 when all cells not containing the desired transgene are eliminated after selection)
Complexity of vector pool	Measures how many different AAV vectors are used for transduction	**POOL**	>1 to 100

At each cycle of selection, when the number of vectors with the desired transgene is set to 1 (T=1), the total number of AAV vectors after transduction and selection consists of the sum of:

(i) The number of vectors co-infecting the same cell as the desired vector (**MOI**);

(ii) The number of vectors present in the cells close to the selected cell and co-selected with this (**COSEL*ET*MOI**);

(iii) The total number of vectors in the cells containing other transgenes but surviving the selection **((POOL-MOI)-COSEL*ET*MOI)*(1-ES)**.

Thus:

R=1/(i + ii + iii)

Or:

R=1/(MOI + (COSEL*ET*MOI) + ((POOL-MOI)-COSEL*ET*MOI)*(1-ES))

The value of R at the end of each cycle of the selection procedure has to be compared with its value at start, when R=1/POOL.
POOL represents the number of vectors that are initially used for the selection, when all these are equimolarly represented. Thus, 1/POOL is the fraction corresponding to the vector of interest. When subsequent cycles of selection are iteratively applied, at each cycle 1/POOL corresponds to the R-value obtained from the previous cycle of selection.

Note: In the above formula and all throughout the following calculations, it is assumed that the number of different AAVs forming each pool is sufficiently large and the multiplicity of infection is sufficiently low to render the possibility that more than one AAV containing the transgene of interest enters the same cell very unlikely.

4.1.2 Selection under ideal conditions

Under ideal conditions, multiplicity of infection is 1 (a single vector transduces each cell; **MOI=1**), there is no co-selection of cells not expressing the desired, selectable transgene (**COSEL=0**), and no cells other than those containing the transgene are selected (**ES=1)**. Under these conditions, **R=1**. Therefore, a single round of selection is sufficient to completely select the transgene-expressing cells (**Figure 4.2**). Of notice, under these conditions, the efficiency of transduction (ET) is irrelevant as is the complexity of the vector pool (POOL).

ET	Any
MOI	1
COSEL	0
ES	1
POOL	Any
R=1	

Figure 4.2 Ideal conditions of selection
If we are under ideal selection conditions (MOI=1, COSEL=0 and ES=1) in a single round (R=1) we are able to select the cells expressing the candidate transgene.

4.1.3 Effect of multiplicity of infection (MOI)

Since AAV can transduce cells at a high multiplicity of infection, this parameter needs to be taken into account during the selection procedure. If **COSEL=0** (no coselection of cells due to the diffusion of the transgene effect) and **ES=1** (selection affects only the transduced cells), then **R=1/MOI**.

In simple terms, under these conditions, the efficiency of the strategy will be reflected by the number of genomes that are co-selected together with the transgene within the same cell. Additional cycles of selection beyond the first one will not improve selection; similar to above, the complexity of the pool (POOL) and the efficiency of transduction (ET) are irrelevant (**Figure 4.3**).

As noted in the first paragraph, this conclusion holds true if it is assumed that the complexity of the analyzed pool of AAV vectors is sufficiently large and the multiplicity of infection is comparatively low to exclude that more than one AAV containing the transgene enter the same cell.

ET	Any
MOI	>1
COSEL	0
ES	1
POOL	Any
R=1/MOI	

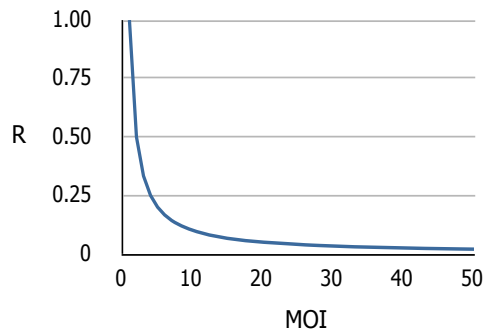

Figure 4.3 Effect of multiplicity of infection (MOI)
If COSEL=0 and ES=1 then R=1/MOI. In this case the efficiency of the strategy is related to the MOI, while ET, POOL are irrelevant. A single cycle of selection is sufficient.

We suppose to transduce cells at an efficiency of 40% (ET=0.4), that 3 vectors enter each cell (MOI=3), that we start with a complexity of the library of 6 vectors (POOL=6), that the efficiency of selection is complete (ES=1) and there is no coselection due to transgene diffusion (COSEL=0). If we analyze 25 cells, 10 cells will be transduced, each one harbouring 3 AAVs (10x3=30 vectors in total). Of these, 30/6=5 will correspond to the selectable transgene. After selection, only the 5 cells containing the transgene will survive; when the total AAV vectors will be recovered and analyzed for the presence of the transgene, there will be 15 total vectors, out of which 5 will correspond to the transgene (T). Thus, R=5/15, which equals 1/3=0.33. This value has to be compared to R=1/MOI=1/6=0.17 at start.

4.1.4 Influence of the coselection of other cells due to transgene bystander effect

Now we consider a case in which the efficiency of selection (ES)=1, and thus only the cells containing T survive the selection, but there is a bystander effect due to the diffusion of the product of T. In this case, the formula becomes:

R=1/(MOI + (COSEL*ET*MOI))

Under these conditions, a certain number of cells will be co-selected together with those containing T. This effect is taken into account by the COSEL parameter, which ranges from 0 (no coselection) to a positive number, which is proportional to the number of cells selected with every cell containing T. The probability that a co-selected cell contains an AAV vector depends on the efficiency of transduction (ET), while the number of AAV vectors contained inside this cells is measured by MOI.

The graphs below (**Figure 4.4**) show the combined influence of the multiplicity of infection (MOI; 1 to 10) and the coselection parameter (COSEL; 0 to 9) variations at three fixed efficiencies of transduction (ET=1, 0.5 and 0.1). In this case R changes independently from the complexity of the vector pool (POOL). As above, performing iterative cycles of selection do not increase R.

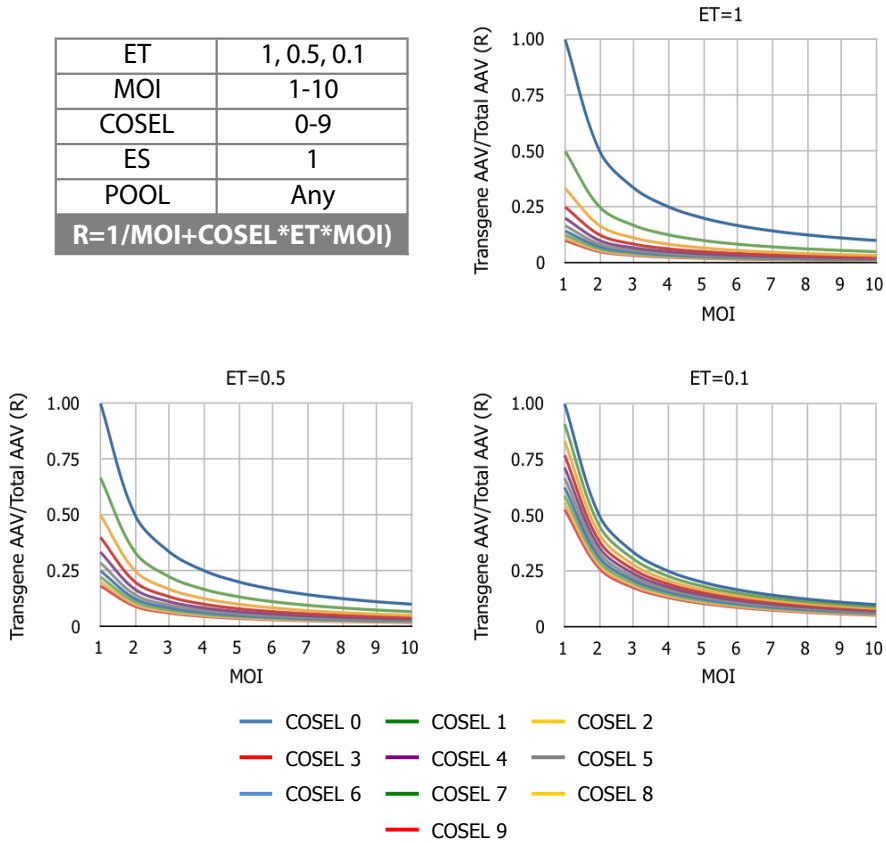

Figure 4.4 Effect of coselection (COSEL)
Combined influence of the multiplicity of infection (MOI; 1 to 10) and the coselection parameter (COSEL; 0 to 9) at three fixed efficiencies of transduction (ET=1, 0.5, and 0.1).

As it can be appreciated, the problem of the coselection due to the transgene bystander effect becomes less and less relevant (the lines corresponding to different COSEL values are closer each other) as the efficiency of transduction decreases (the lower the number of transduced cells, the lower the chance that cells containing an irrelevant transgene neighbour those containing T).

The following graphs (**Figure 4.5**) well illustrate this concept at three fixed MOIs: 1, 3 and 10.

ET	0.1-1
MOI	1, 3, 10
COSEL	0-9
ES	1
POOL	Any
R=1/(MOI+COSEL*ET*MOI))	

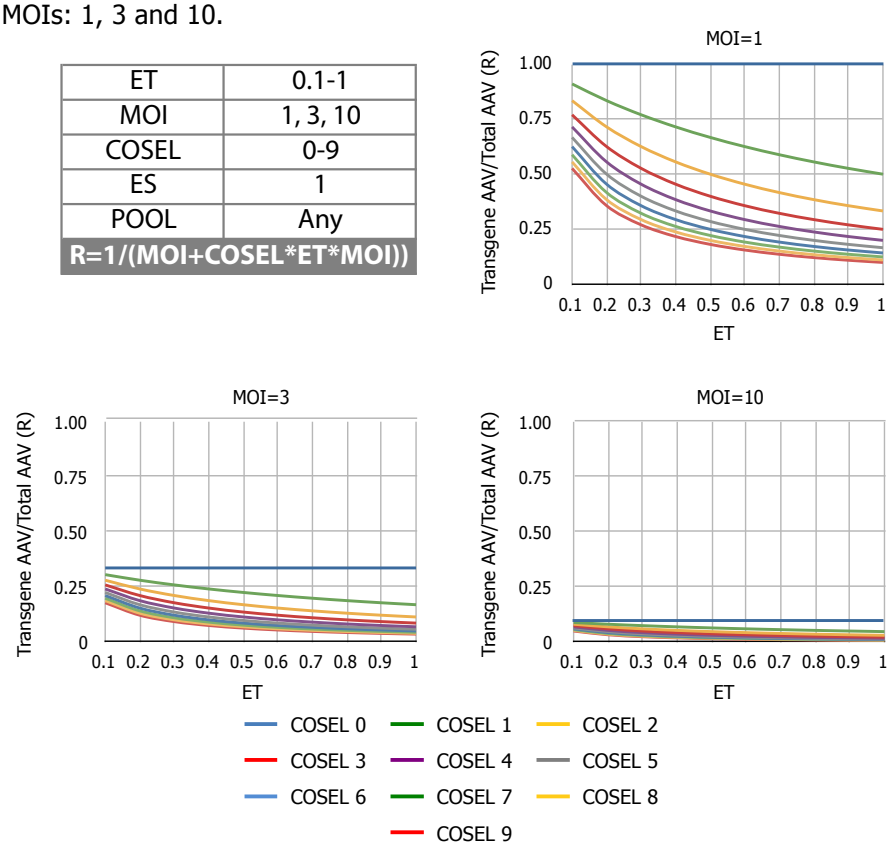

Figure 4.5 Effect of coselection (COSEL)
Combined influence of the coselection parameter (COSEL; 0 to 9) and the efficiencies of transduction (ET; 0.1 to 1) at three fixed multiplicity of infection (MOI=1, 3 and 10).

As in the cases considered above, performing subsequent cycles of selection beyond the first one does not improve T enrichment, since it is assumed that only cells containing the transgene survive the selection itself (ES=1).

For the same reason, complexity of the vector pool (POOL) equally has no influence.

4.1.5 Effect of poor efficiency of selection

In the case the efficiency of selection (ES) is <1 (for example that a certain number of cells survive the selection although not containing the transgene or anyhow not because of a bystander transgene effect), then the equation describing R needs to also take into account the presence of these cells. These can be described as:

((POOL-MOI)-COSEL*ET*MOI)*(1-ES)

In this case, POOL-MOI describes the number of surviving cells while COSEL*ET*MOI the transduced cells anyhow selected because of the transgene bystander effect (taken into account in the previous paragraph). Here, the complexity of the initial pool of vectors becomes important (POOL). If COSEL=0, then the equation measuring R becomes R=1/(MOI+(POOL-MOI)*(1-ES).

Of notice, when no coselection due to transgene bystander effect occurs (COSEL=0), the efficiency of transduction (ET) does not influence the ratio between the selectable transgene and the other AAV inserts.

The graphs below (**Figure 4.6**) describe R according to POOL for different MOIs considering efficiency of selection (ES) of 0.9, 0.6 and 0.3.

As it can be appreciated, the probability of selecting T decreases dramatically concomitant with an increase in the initial vector pool complexity and the decrease in the efficiency of selection.

ET	Any
MOI	1-10
COSEL	0
ES	0.3, 0.6, 0.9
POOL	10-100
R=1/(MOI+(POOL-MOI)(1-ES))	

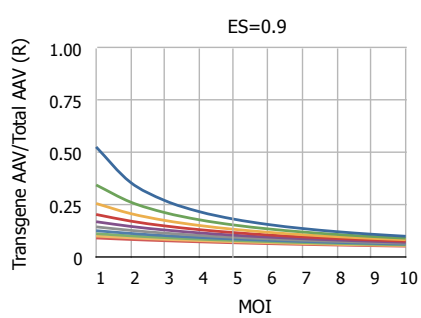

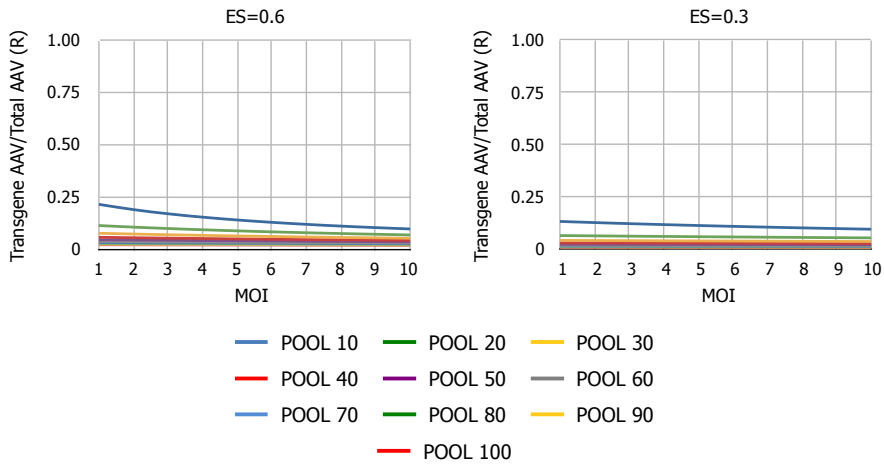

Figure 4.6 Effect of poor efficiency of selection (ES)
Combined influence of the complexity of vector pools (POOL; 10 to 100) and the multiplicity of infection (MOI; 1 to 10) at three, fixed efficiency of selection (ES=0.9, 0.6 and 0.3).

4.1.6 Performing iterative cycles of selection

When the efficiency of selection (ES) is <1, the performance of the process is substantially increased by performing subsequent, iterative cycles of selection, which includes the recovery of all transgenes from the cells or tissues (by PCR) and re-cloning of these inserts into new vector plasmids, followed by production of a new vector pool which is then resubmitted to the selection process. At each of these steps, the complexity of the vector pool (POOL) reflects the number of different vectors recovered from the tissue, in which the ratio between T and all the other transgenes progressively increases.

As discussed above, performing multiple cycles of selection does not improve selection in conditions when there is an effect of the transgene extending to other cells, since, in this case, the ratio between the transgene of interest and the other AAV inserts essentially depends on the

multiplicity of infection and the transduction efficiency. Similar to above, we will therefore only consider cases in which there is no co-selection of cells not containing the transgene (COSEL=0).

We analyzed a case in which we start with 25 different vectors (POOL=25), assume a fixed value for MOI (MOI=3) and consider the influence of the efficiency of selection (ES). The graph below (**Figure 4.7**) reports the effect of performing 1-10 subsequent cycles of selection in these conditions.

ET	Any
MOI	3
COSEL	0
ES	0.1-1
POOL	25
R=1/(MOI+(POOL-MOI)(1-ES))	

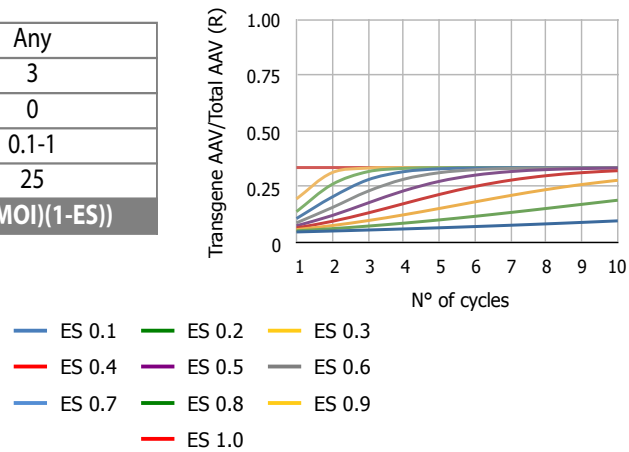

Figure 4.7 Effect of iterative cycles of selection
Combined influence of efficiency of selection (ES; 0.1 to 1) and rounds of selection (number of cycles from 1 to 10), at a fixed multiplicity of infection (MOI=3) and pool complexity (POOL=25).

As it can be appreciated, subsequent cycles of selection progressively improve enrichment of the desired transgene, up to a maximum corresponding to the theoretical value of 1/MOI (1/3=0.33 in the specific considered case, to be compared with R=0.04 before initiating the selection procedure).

We now consider the influence of the POOL size on the selection, again by choosing a fixed value of MOI=3 and an efficiency of selection ES=0.5 (**Figure 4.8**).

ET	Any
MOI	3
COSEL	0
ES	0.5
POOL	10-100
R=1/(MOI+(POOL-MOI)(1-ES))	

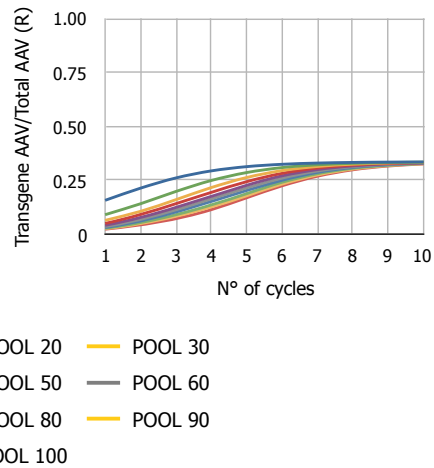

Figure 4.8 Effect of iterative cycles of selection
Combined influence of pool complexity (POOL; 10 to 100) and number of selection cycles (from 1 to 10), at a fixed multiplicity of infection (MOI=3) and efficiency of selection (ES=0.5).

Also in this case, R progressively reaches a plateau corresponding to 1/MOI; this plateau is already reached at cycle 7 when POOL=10 or at cycle 10 when POOL=80. In this respect, however, it is worth noting that, even in the worst scenario (POOL=100), while R=1/100=0.01 before the selection, it becomes R=0.02 at the first cycle and 0.32 at cycle 10, thus rendering the identification of the effective transgene theoretically possible.

To conclude, a realistic (or even slightly unfavourable) scenario, might entail an efficiency of transduction (ET) of 10% of the cells, an average number of 3 vectors per cell (MOI), a bystander co-selection effect of 2 additional cells every cell expressing the selectable transgene (COSEL), an efficiency of selection (ES) of 30% and a pool size (POOL) of 50 different vectors.

As shown in **Figure 4.9** under these conditions it is possible to clearly observe a progressive increase in the enrichment of the desired transgene upon 10 cycles of selection. Indeed, at the tenth cycle of selection, R=0.18, a value that has to be compared with the initial value R=1/50=0.02 before beginning the selection procedure.

ET	0.1
MOI	3
COSEL	2
ES	0.3
POOL	50
R=1/(MOI + (COSEL*ET*MOI) + ((POOL-MOI)-COSEL*ET*MOI)*(1-ES))	

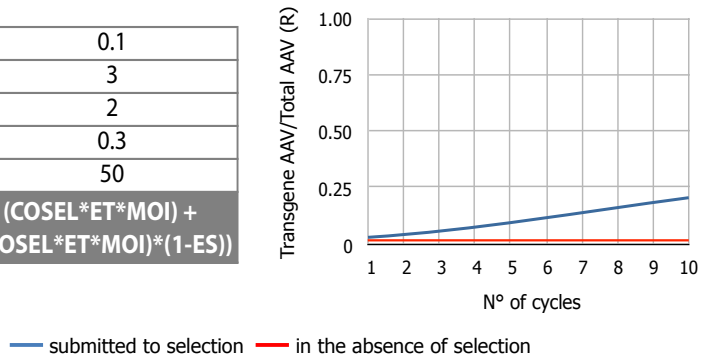

CYCLE	1	2	3	4	5	6	7	8	9	10
R	0.02	0.03	0.04	0.05	0.07	0.09	0.11	0.13	0.16	0.18

Figure 4.9 Transgene enrichment upon iterative cycles of selection
Example of transgene enrichment, taking into account all the variables individually analyzed in the previous paragraphs. Considering the combined influence of ET=0.1, MOI=3, COSEL=2, ES=0.3 and POOL=50 the R-values plotted in the graph and summarized in the table below are generated. Initially, R=0.02 (plotted in red) when iterative cycles of functional selection are performed R increases (plotted in blue).

Taken together, the theoretical considerations illustrated in this Thesis section fully support the feasibility of the **FunSel** iterative functional selection strategy.

4.2 GENERATION OF AN ARRAYED LIBRARY OF AAV VECTORS EXPRESSING SECRETED FACTORS

The ultimate purpose of the **FunSel** project is the creation of an arrayed library of cDNAs corresponding to the mouse secretome, their delivery *in vivo* using AAV vectors and the *in vivo* selection of clones exerting a beneficial effect. This Thesis reports a pilot experiments, demonstrating the feasibility of the **FunSel** approach, using a subset of 100 clones.

4.2.1 The mouse secretome cDNA arrayed library

A first step in the project was the creation of a collection of cDNAs coding for secreted proteins cloned into an AAV-backbone plasmid, followed by the generation of the correspondent collection of AAV vectors.

The arrayed library we generated is composed of clones derived from the mouse secretome, which can be defined as the subset of proteins secreted into the extracellular environment of a cell. In particular, we had access to portions of the RIKEN secretome collection of clones (Grimmond et al., 2003), selected by a computational approach, from the RIKEN mouse genes encyclopedia (Kawai et al., 2001; Okazaki et al., 2002). This is a collection of more than 60,000 fully sequenced cDNA clones, created by the Fantom (Functional Annotation of the mouse) Consortium, led by the RIKEN Institute. During the process of generation of the mouse secretome, these authors identified 2,033 unique soluble proteins that are potentially secreted from the cell, including hundreds of novel proteins of unknown function.

Since the work described in this Thesis was the generation of a collection of recombinant AAV vectors coding for secreted factors, we had to face the restrain posed by the small size of the AAV genome, which limits the length of inserts to <4.0 kb, including the cloned cDNA, a promoter and a

polyadenylation site.

By a careful initial selection of the clones in the database http://fantom3.gsc.riken.jp/, we eventually reduced the number of factors eligible for the individual sub-cloning into the pZac2.1 vector, a specific AAV backbone-plasmid for AAV production, to approximately 1,600 cDNAs.

The main criteria applied for the selection of these cDNAs were:

- cDNA size <3,000 bp;
- Availability of the complete coding sequence;
- Lack of transmembrane domain or intracellular localization signal;
- Presence of a signal peptide (required for entry into the secretory pathway);
- 5' and 3' UTR not truncated.

Abundant and rare transcripts are equally represented in this arrayed collection of clones, and the majority of the cDNAs included in our selection (a total of 1,600 cDNAs representing the 85% of the full collection) are less than 3,000 bp long (**Figure 4.10**).

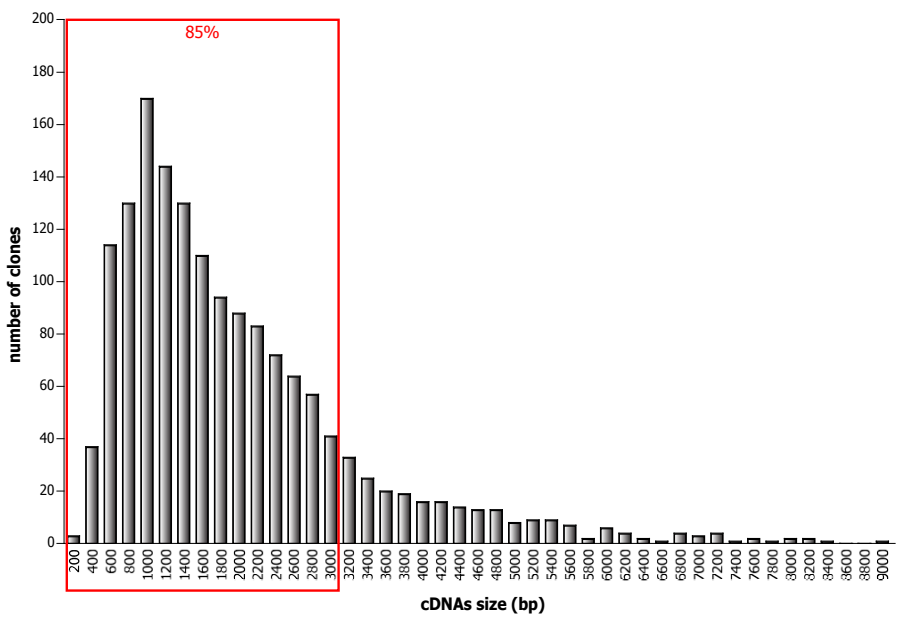

Figure 4.10 cDNAs size distribution
Size distribution of the cDNAs of mouse genes coding for putative secreted proteins. The boxed are shows those selected for possible cloning into AAV vectors.

Among the 1,600 cDNAs eligible for **FunSel**, we arbitrarily choose a first group of 100 cDNAs, for the set-up and proof-of-principle work described in this Thesis. These 100 factors were chosen without any a priori selection for their function.

In **Figure 4.11** is reported a list of the chosen factors which are members of different classes of secreted molecules, namely chemokines, interleukins, hormones, growth factors, secreted enzymes, extracellular matrix proteins, secreted molecules of unknown function and others.

Chemokines and Interleukins	**GENEBANK**	**NCBI RefSeq**
chemokine (C-C motif) ligand 6	Ccl6	NM_009139
chemokine (C-C motif) ligand 7	Ccl7	NM_013654
chemokine (C-C motif) ligand 8	Ccl8	NM_021443
chemokine (C-C motif) ligand 11	Ccl11	NM_011330
chemokine (C-C motif) ligand 12	Ccl12	NM_011331
chemokine (C-X-C motif) ligand 9	Cxcl9	NM_008599
chemokine (C-X-C motif) ligand 13	Cxcl13	NM_018866
chemokine (C motif) ligand 1	Xcl1	NM_008510
interleukin 17A	Il17	NM_010552
interleukin 20	Il20	NM_021380
interleukin 27	Il27	NM_145636
Hormones and Growth Factors		
apelin	Apln	NM_013912
insulin-like 6	Insl6	NM_013754
family with sequence similarity 198, member A	Fam198a	NM_177743
family with sequence similarity 3, member B	Fam3b	NM_020622
follicle stimulating hormone beta	Fshb	NM_008045
gastrin	Gast	NM_010257
growth hormone releasing hormone	Ghrh	NM_010285
ghrelin	Ghrl	NM_021488
gastric inhibitory polypeptide	Gip	NM_008119
neuromedin U	Nmu	NM_019515
natriuretic peptide precursor type C	Nppc	NM_010933
neurotensin	Nts	NM_024435
pro-opiomelanocortin-alpha	Pomc	NM_008895
peptidoglycan recognition protein 1	Pglyrp1	NM_009402

prolactin family 3, subfamily b, member 1	Prl3b1	NM_008865
prolactin family 3, subfamily d, member 1	Prl3d1	NM_008864
prolactin family 5, subfamily a, member 1	Prl5a1	NM_023746
prolactin family 7, subfamily b, member 1	Prl7b1	NM_029355
prolactin family 7, subfamily d, member 1	Prl7d1	NM_011120
prolactin family 8, subfamily a, member 81	Prl8a8	NM_023741
prolactin family8, subfamily a, member 9	Prl8a9	NM_023332
trefoil factor 1	Tff1	NM_009362
trophoblast specific protein beta	Tpbpb	NM_026429
thyrotropin releasing hormone	Trh	NM_009426
vasoactive intestinal polypeptide	Vip	NM_011702
Secreted Enzymes		
arylsulfatase A	Arsa	NM_009713
biotinidase	Btd	NM_025295
carboxylesterase 2A	Ces2a	NM_133960
carboxylesterase 2E	Ces2e	NM_172759
cystatin 9	Cst9	NM_009979
cystatin 11	Cst11	NM_030059
cystatin 12	Cst12	NM_027054
cystatin 13	Cst13	NM_027024
chymotrypsinogen B1	Ctrb1	NM_025583
cathepsin R	Ctsr	NM_020284
glucosidase, beta, acid	Gba	NM_008094
kallikrein 1	Klk1	NM_010639
lysozyme-like 1	Lyzl1	NM_026092
matrix metallopeptidase 1a	Mmp1a	NM_032006
napsin A aspartic peptidase	Napsa	NM_008437
progastricsin (pepsinogen C)	Pgc	NM_025973
phospholipase A2, group IB	Pla2g1b	NM_011107
renin 1	Ren1	NM_031192
Extracellular Matrix Proteins		
amelogenin X chromosome	Amelx	NM_009666
asporin	Aspn	NM_025711
fibromodulin	Fmod	NM_021355
intelectin b	Itlnb	NM_001007552
keratocan	Kera	NM_008438
matrilin 3	Matn3	NM_010770
nephrocan	Nepn	NM_025684
nephronectin	Npnt	NM_033525
spondin 2	Spon2	NM_133903
transforming growth factor, beta induced	Tgfbi	NM_009369
vitronectin	Vtn	NM_011707
Secreted Molecules (Unknown Function)		
RIKEN cDNA D730048I06 gene	D730048I06Rik	NM_026593
RIKEN cDNA 1600029D21 gene	1600029D21Rik	NM_029639
RIKEN cDNA 1700016D06 gene	1700016D06Rik	NM_024271
RIKEN cDNA 1700029I15 gene	1700029I15Rik	NM_183112
RIKEN cDNA 1700040I03 gene	1700040I03Rik	NM_028505
RIKEN cDNA 2010109I03 gene	2010109I03Rik	NM_025929
RIKEN cDNA 2210415F13 gene	2210415F13Rik	NM_001083884
RIKEN cDNA 4930568D16 gene	4930568D16Rik	NM_029463
RIKEN cDNA 4930597L12 gene	4930597L12Rik	
RIKEN cDNA 5430402E10 gene	5430402E10Rik	NM_027768
RIKEN cDNA 5530400C23 gene	5530400C23Rik	NM_027784
Hypothetical protein	Gm10344	
pre-B lymphocyte gene 3	Vpreb3	NM_009514

Others		
proacrosin binding protein	Acrbp	NM_016845
acrosomal vesicle protein 1	Acrv1	NM_007391
alpha fetoprotein	Afp	NM_007423
anterior gradient homolog 3	Agr3	NM_207531
complement component 8, beta polypeptide	C8b	NM_133882
carcinoembryonic antigen-related cell adhesion molecule 13	Ceacam13	NM_027210
CD48 antigen	Cd48	NM_007649
defensin, alpha, 20	Defa20	NM_183268
defensin beta 22	Defb22	NM_001002791
ephrin A1	Efna1	NM_010107
coagulation factor VII	F7	NM_010172
GLI pathogenesis-related 1 like 1	Glipr1l1	NM_027018
lipocalin 9	Lcn9	NM_029959
odorant binding protein Ia	Obp1a	NM_008754
oocyte secreted protein 1	Oosp1	NM_133353
phosphatidylethanolamine binding protein 4	Pebp4	NM_028560
regenerating islet-derived 3 delta	Reg3d	NM_013893
regenerating islet-derived 3 gamma	Reg3g	NM_011260
salivary protein 1	Spt1	NM_009267
seminal vesicle antigen-like 1	Sval1	NM_027832
testis expressed gene 101	Tex101	NM_019981
wingless related MMTV integration site 2b	Wnt2	NM_023653

Figure 4.11 cDNAs selected for FunSel approach set up
Different classes of factors (chemokines, interleukins, hormones, growth factors, secreted enzymes, extracellular matrix proteins, secreted molecules of unknown function and others belonging to different classes), have been chosen among the 1,600 cDNAs eligible for FunSel and included in the group of 100 cDNAs used for the set-up and proof-of-principle validation of the selection strategy.

4.2.2 Generation of a collection of AAV vectors expressing 100 secreted factors

In order to perform several rounds of *in vivo* selection, according to the **FunSel** strategy, each cDNA needs to be cloned into the same vector backbone, exploiting common restriction sites. The cDNAs were therefore obtained from the original RIKEN plasmids (either modified pBluescript SK (+) or pFlcI) by PCR amplification with common primers carrying *Xho I* and *Not I* restriction sites at their 3' extremities, to allow oriented cloning into the Multiple Cloning Site (MCS) of pZac2.1 AAV backbone plasmid. This vector contains two Inverted Terminal Repeat sequences (ITRs), essential

for recombinant vector production, the CMV IE promoter to drive transgene expression and the SV40 polyadenylation site (**Figure 4.12**).

Each plasmid clone was obtained individually by the described approach, and its identity and preservation of correct sequence were verified by direct DNA sequencing. Indeed, in addition to allowing the *in vivo* functional selection of possible therapeutic genes, the availability of individual AAV clones from the library will represent an important tool for any future research based on *in vivo* gene transfer.

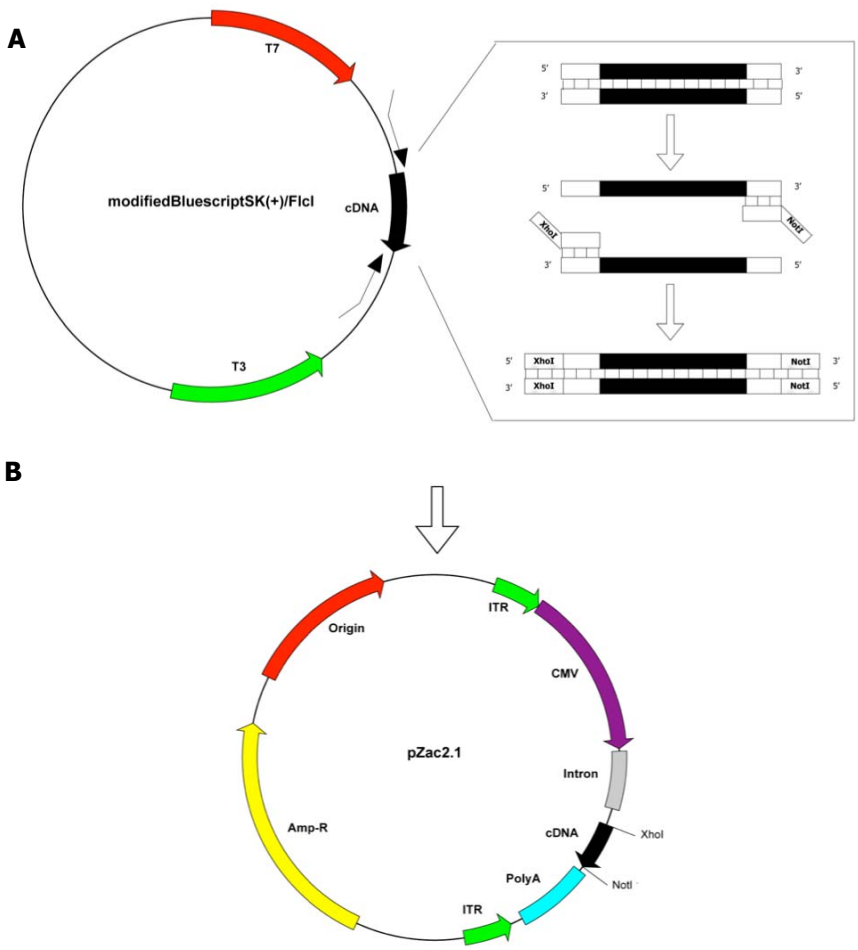

Figure 4.12 Scheme of the sub-cloning in the AAV backbone plasmid pZac2.1
A. The selected cDNAs have been obtained from the original RIKEN cloning vectors modified pBluescript SK (+) or pFlcI by PCR amplification with common primers carrying *XhoI* and *NotI* restriction sites at their 3' extremities.
B. The same restriction sites have been used for a directional cloning of each cDNA into the MCS of pZac2.1 AAV-backbone plasmid, containing the ITRs sequences, necessary for recombinant viral vector production, a CMV IE promoter that drives transgene expression and the SV40 polyA site.

4.2.3 Recombinant AAV vector pooled production

The model of functional selection we developed entails the concomitant *in vivo* expression of several genes obtained from the collection; therefore the first essential goal was to demonstrate the feasibility of viral vectors pooled production. For this purpose, after the individual cloning of the cDNAs collection, we wanted to validate the production of individual viral preparations composed by pools of AAV vectors expressing different genes. A first experiment was performed by selecting 10 different AAV plasmids, having inserts of different length, mixing them each one a 1/10 concentration compared to the amount commonly used for AAV vector production, and transfecting them into HEK 293T cells together with and AAV2 helper plasmid.

After vector production, viral genomes, recovered from each pooled AAV preparation, were submitted to PCR amplification using a single pair of primers annealing to the common pZac2.1 vector sequence and spanning the MCS. As shown in the representative pool of 10 genes in **Figure 4.13,** the competitive amplification of the cDNAs composing the pool allowed the unambiguous identification of each clone in the viral lysate, confirming the feasibility of pooled viral vector production.

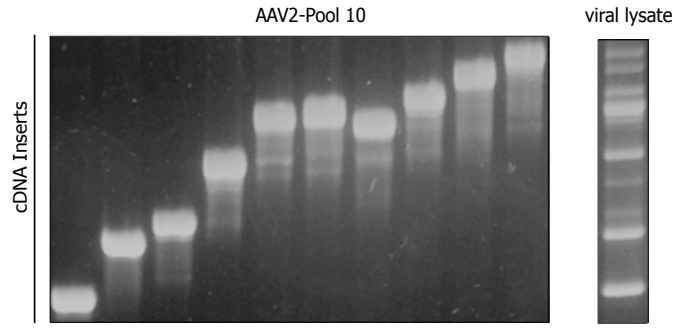

Figure 4.13 Recombinant AAV vectors can be generated in pool
Transgene PCR amplification from single plasmids coding for 10 different factors composing a pool (left panel) and from the total viral lysate recovered after pooled viral vectors production (right panel).

4.3 VALIDATION OF THE AAV VECTOR POOLS COMPOSITION

To guarantee a balanced representation of each viral genome in a pool of vectors, different vector pools were then tested for their packaging potential, ability of *in vivo* transduction, and level of transgene expression. These results gave us important information for a better definition of the advantages and limitations of the **FunSel** strategy.

4.3.1 Generation of pools of AAV vectors homogeneous for transgenes size is essential to guarantee the faithful maintenance of AAV vector genomes during pooled production

Once demonstrated that it is possible to generate AAV vectors in pools, we decided to investigate which are the critical steps that influence the packaging process of the viral particles, in order to take them into account during pooled vector production.

First, we wanted to understand whether differences in cDNA length might affect the DNA packaging process. We constructed an AAV pool composed of 25 cDNAs of different length (**Figure 4.14**), representative of the variety of clone lengths present in the secretome collection (from 459 bp to 2941 bp), and analyzed the packaging efficiency after viral vector production. Equimolar amounts of each plasmid were used to obtain a 25-vector pool, which was transfected into the packaging cells to generate infectious AAV virions (AAV2-Pool25).

Then, we quantified the copy number of 10 genes in both the plasmid preparation and the viral lysate by quantitative Real-Time PCR using insert-specific primer pairs. The 10 analyzed genes were selected in order to be representative, as far as length was concerned, of all clones. The total

number of vector DNA copies in the pool was quantitatively measured by real-time amplification with a Taqman probe using primers specific for the CMV promoter, common to all vectors.

The proportion of each gene in the pool was calculated by the ratio between total viral genomes and the genomes corresponding to each cDNA (expected value: 25) followed by normalization with the number of cDNAs in the pool (expected value after normalization: 1).

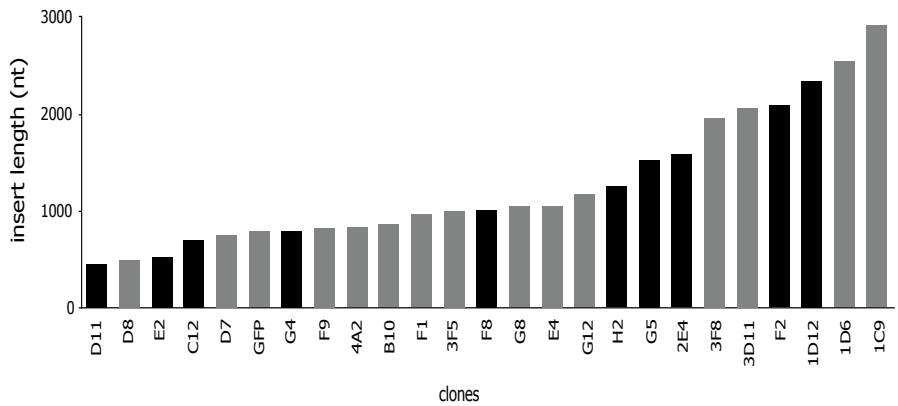

Figure 4.14 Size distribution of 25 AAV plasmids, each one coding for a different secreted protein (indicated by codes), composing the AAV2-Pool25

The insert lengths ranged from 459 bp to 2941 bp. Clones shown in black were subsequently chosen for PCR quantification in the plasmid pool and in the AAV virion preparation.

The results obtained showed that representation of all the investigated constructs in the infectious viral preparations remained substantially similar to that in the input pool of plasmids. There was a trend of reduced packaging correlating with increase insert length (**Figure 4.15A**). Despite this evidence, the ratio between the individual cDNA representation in the plasmid and the vector pools was within a ±2 fold range for 9 out of 10 clones (**Figure 4.15B**). This relatively narrow variation was considered acceptable in the context of pooled AAV production.

The three clones having >1500 bp were packaged at efficiencies of 0.55, 0.68 and 0.46 compared the expected value of 1, confirming the relevance of insert size on packaging efficiency; the only gene that dropped out the ±2 fold interval was 1D12, the longer one (2340 bp).

From these results we can conclude that clones of similar length show comparable packaging efficiency. Therefore, it appears important to generate homogeneous pools, in order to give all the cDNAs an equal chance to be produced into viral particles.

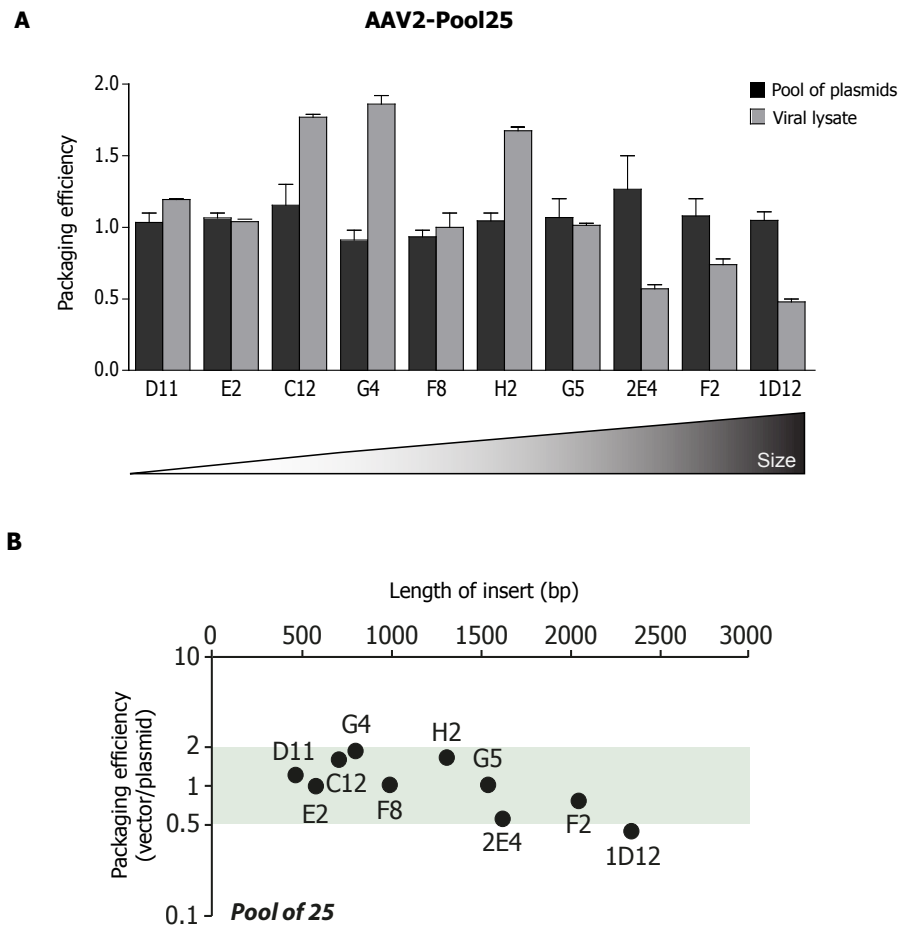

Figure 4.15 Packaging efficiency of 10 genes from the AAV2-Pool25
A. Packaging efficiency of 10 cDNAs of different size from the AAV2-Pool25 was calculated both in the pool of plasmids and in the viral lysate upon viral production. The efficiency is expressed as a ratio between total viral genomes (quantified as CMV promoter copy number) and genomes corresponding to each cDNA, followed by a normalisation on the total number of cDNAs in the pool.
B. Abundance of 10 selected constructs in the vector and plasmid pools (Collaboration), distributed according to size. The green area indicates the ±2 fold

To further explore this issue and exclude that the relatively reduced packaging efficiency observed for clones 2E4, F2 and 1D12 might correlate with intrinsic properties of their genomic sequences, rather than size, these clones were then mixed with other 22 clones of length >1500 bp, and an additional AAV pool of 25 factors with large size genomes was generated (AAV2-Pool25Big) **(Figure 4.16)**.

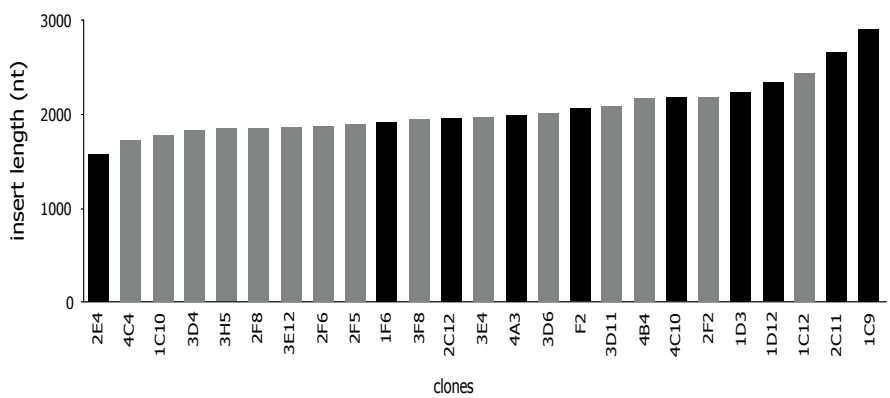

Figure 4.16 Size distribution of 25 AAV plasmids, each one coding for a different secreted proteins (indicated by codes), composing the AAV2-Pool25Big (1500 bp - 3000 bp)
Clones shown in black were subsequently chosen for PCR quantification in the plasmid mix and in the AAV virions preparation.

As in the previous experiment, we designed specific primers for 10 genes of different size present in this pool, including 2E4, F2 and 1D12, and

verified by quantitative PCR their relative amount, before and after AAV production **(Figure 4.17A)**.

In this case, most of the cDNAs were packaged at good efficiency (within ±2-fold range compared to expected). These also included 2E4 and F2, thus supporting the conclusion that the relatively poor packaging efficiency of these clones observed previously was a consequence of their length and not their primary DNA sequence.

On the other hand, also in this pool, genomes of major size exhibited reduced packaging ability. In particular, the three longest clones (1D12, 2C11 and 1C9) dropped out the fixed tolerance range of ±2 fold compared to the expected packaging efficiency value **(Figure 4.17B)**.

From these results we can conclude that, to generate AAV pools for *in vivo* selection, it is essential to organize the clones in groups homogeneous for insert length, in order to guarantee that all factors are packaged into the viral particles at the same efficiency.

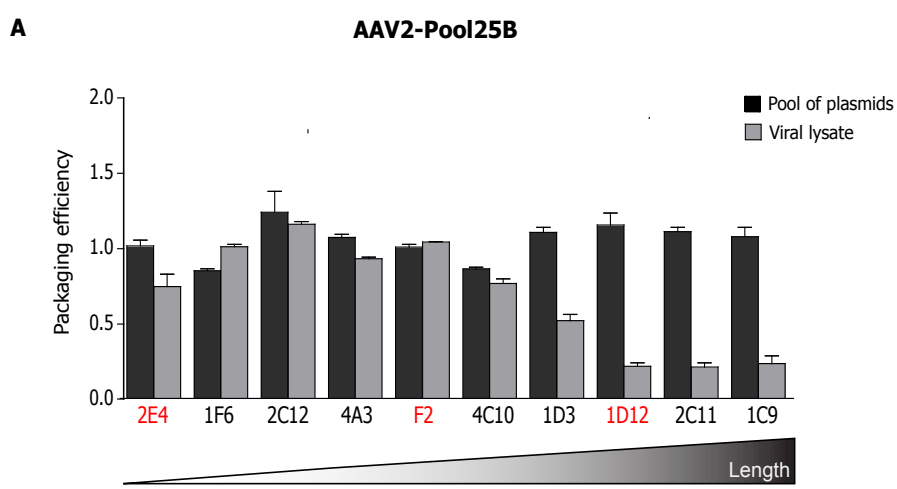

B

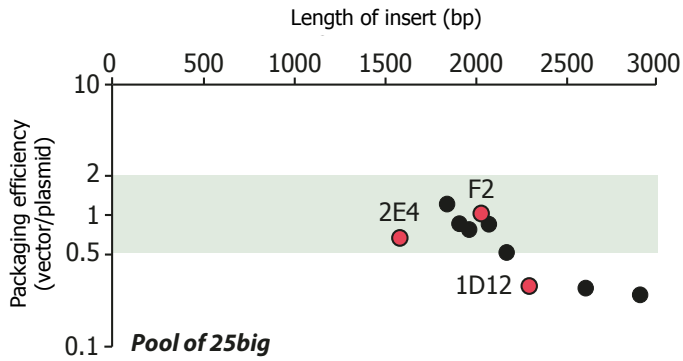

Figure 4.17 Packaging efficiency of 10 genes from the AAV2-Pool25B
A. Packaging efficiency of 10 cDNAs of different size from the AAV2-Pool25B calculated in both the pool of plasmids and the corresponding viral lysate upon viral production. The efficiency is expressed as a ratio between total viral genomes (quantified as CMV promoter copy number) and the genomes corresponding to each cDNA, followed by a normalisation on the total number of cDNAs in the pool. The clones previously analyzed in the AAV2-pool25 are indicated in red.
B. Abundance of 10 selected factors, when mixed in a pool of 25 vectors carrying inserts with size >1500 bp. The ratios between abundance of each construct in the vector and plasmid pools is shown, distributed according to size. The green area shows the ±2-fold interval.

4.3.2 The complexity of a pool does not influence viral packaging efficiency

To investigate whether AAV vector production might be influenced by the number of different, simultaneously packaged constructs, we generated two pools of vectors, composed of equimolarly represented 50 or 100 clones (AAV2-Pool50 and AAV2-Pool100). Both pools included the clones of the previous analyzed AAV2-Pool25, consisting of cDNAs representative of all possible insert lengths; Pool100 included the entire collection of the selected, secreted molecules.

In both AAV2-Pool50 and AAV2-Pool100, quantification of the same 10 genes already analyzed in AAV2-Pool25 revealed that these were all

represented within the ±2-fold range compared to the expected values, again with the exception of clones F2 and 1D12 (**Figure 4.18**). This result indicated that, in order to generate a vector collection in which all vectors are equally represented, the complexity of the collection itself in terms of number of clones is less relevant that the homogeneity of the individual clone lengths.

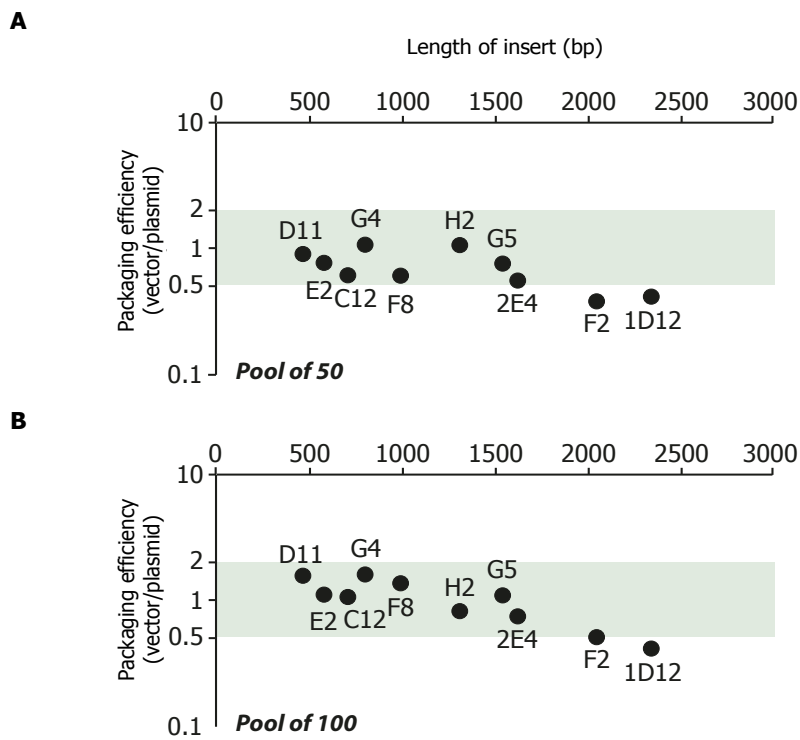

Figure 4.18 Packaging efficiency of 10 genes from the AAV2-Pool50 and AAV2-Pool100
Abundance of the same 10 selected constructs analyzed in the AAV2-Pool25, when included in (**A**) 50- and (**B**) 100-vector pools. Shown are the ratios between abundance in the virus and plasmid preparations, distributed according to size. The green area shows the ±2-fold interval.

When considered collectively, these results are consistent with the conclusion that multiple (at least up to 100) AAV vectors can be packaged simultaneously and that the individual representation of each construct in the vectors pool fairly represents its original amount in the mix of plasmids.
An exception to this rule is represented by constructs carrying inserts >1500-2000 bp, which may be not favoured in competitive packaging.
To be included in complex vector mixtures, these constructs should better be considered in combination with other constructs carrying inserts of comparable size.

4.3.3 AAV vectors genomes ratios are maintained after *in vivo* transduction and persist in the transduced tissue

An additional important question needing investigation was the *in vivo* transduction performance of the AAV pools. Therefore, we investigated whether individual AAV vectors maintained their infectivity when present in complex mixtures.
To address this issue, the original AAV2-Pool25 was injected into the murine skeletal muscle, followed by the quantification of the same previously investigated 10 genes before and after *in vivo* transduction, comparing their relative genome copy number in the viral lysate and in the transduced tissue.
We delivered ~50 µl of a $1x10^{12}$ viral genomes (vg)/ml vector preparation of AAV2-Pool25 in the tibialis anterior (TA) muscle of C57/Bl6 mice (n=4) and sacrificed the animals three days after transduction. Total DNA was extracted from the tissue and then quantitative PCR was performed as already described. In particular, we quantified the copy numbers corresponding to the 10 genes and verified whether each of these genes, as expected, actually represented 1/25 of the total viral genomes rescued from the tissue (**Figure 4.19**).

All vectors were able to efficiently transduce skeletal muscle, since all the viral genomes were detectable in tissue extracts 3 days after vector delivery. The proportion of each vector over the total viral DNA content in the tissue (expressed as CMV copy number) was perfectly comparable with that measured in the viral preparation, before *in vivo* transduction.

From this result we can conclude that pools of AAV vectors are able to efficiently transduce skeletal muscle and that individual vector abundance is maintained *in vivo*, with no evidence of unbalanced representation of the analyzed factors upon pooled *in vivo* delivery.

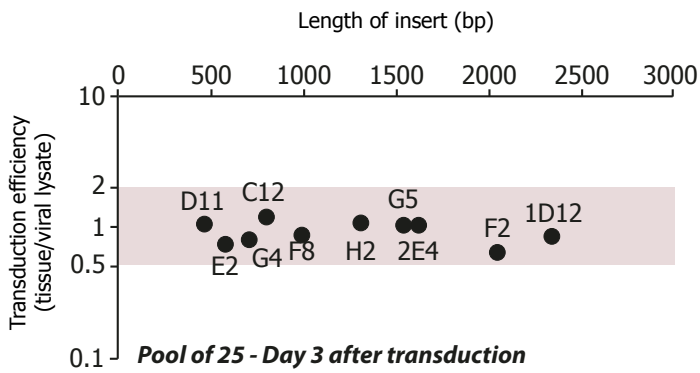

Figure 4.19 *In vivo* transduction efficiency
Analysis of TA muscle transduction efficiency 3 days after AAV2-Pool25 delivery, by quantification of the relative abundance of genomes corresponding to 10 factors in the tissue and in the viral lysate (ratio), distributed in the graph according to size. The pink area shows the ± 2-fold interval.

Subsequently, we analyzed the skeletal muscle vector genome content at a longer time point after transduction, to evaluate persistence and maintenance of pool composition *in vivo.* A second group of C57/Bl6 mice (n=4), was sacrificed 30 days after TA muscle transduction with ~50 µl of a $1x10^{12}$ vg/ml viral preparation of AAV2-Pool25; the individual genome ratios were analyzed as described above **(Figure 4.20)**.

Previous experiments in our laboratory had indicated that the levels of AAV DNA found in the skeletal muscle *in vivo* undergoes a decline of ~1 order of magnitude in the first month after injection, while it remains constant afterwards for prolonged periods of time (Tafuro et al., 2009; Zentilin et al., 2010). Our experiment indicated, as expected, a reduction in the total viral content recovered from the muscle at day 30 after transduction (data not shown). The ratios between different viral genomes were close to the values observed at day 3-post transduction for 8 out of 10 analyzed genes (within the ±2-fold range), with the exception of clones D11 and E2, which appeared significantly enriched after 30 days. From this finding we can speculate that, even in the absence of specific selective pressure, some transgenes are preferentially maintained *in vivo*, possibly because they give an advantage to the transduced cells. In this specific case, clone D11 encodes for gastrin, a gene never associated with specific functions into the skeletal muscle so far, while clone E2 encodes for ghrelin, whose action on myocytes has been previously mentioned.

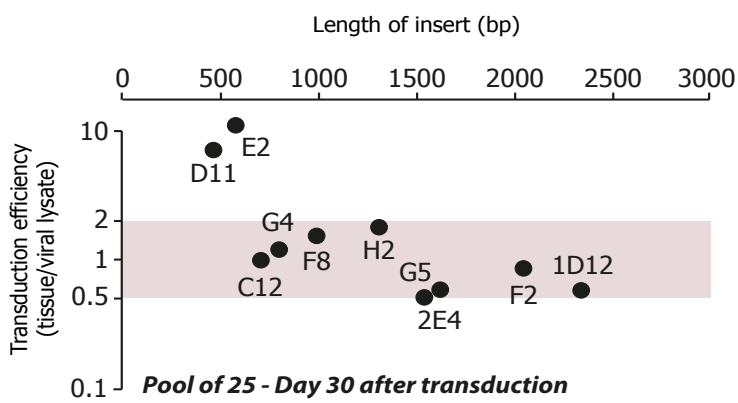

Figure 4.20 *In vivo* viral genomes maintenance 30 days after skeletal muscle transduction
Analysis of viral vectors persistence in the muscle 30 days after *in viv*o transduction, by quantification of the relative amount of genomes corresponding to 10 factors from the AAV2-Pool25 in the tissue and in the viral lysate (ratio), distributed in the graph according to size. The pink area shows the ± 2-fold interval.

4.3.4 The levels of transgene expression *in vivo* reflect the original complexity of the AAV pools

The results reported above indicate that homogeneity of insert size, more than total number of grouped clones, is a key parameter to generate balanced pools of AAV vectors. However, the complexity of these pools still is expected to impact on the levels of expression of each viral transgene.

To assess whether the level of expression of the a given vector is maintained proportionally to its abundance in the pool after *in vivo* delivery, we injected, into the TA muscle of C57/Bl6 mice (n=3 for each experimental condition), the AAV2-Pool25, AAV2-Pool50 and AAV2-Pool100, as well as two additional vectors singularly encoding for two selected factors (E2 and C12, both included in all three pools), plus an empty vector as a control. All animals received the same amount of AAV viral particles ($\sim 1x10^{11}$ vg) and the expression levels of the two transgenes were analyzed, after total RNA extraction, 15 days after transduction.

The level of E2 gene expression was 1595 fold over control when the gene was administered alone (complexity: 1:1), after normalization over the levels of the corresponding endogenous gene. Its levels decreased to 62.5, 36.8 and 13.5 in the AAV2 pools with complexity 1:25, 1:50 and 1:100 respectively (**Figure 4.21A**). These values have to be compared to the expected values of 63.8, 31.9 and 15.9 respectively.

The level of C12 gene expression was 981 fold over control when the gene was administered alone. This value is lower in comparison with E2 because the higher level of expression of the corresponding endogenous gene in the muscle. C12 expression levels decreased to 41.3, 23.2 and 7.0 in the AAV2 pools with complexity 1:25, 1:50 and 1:100 respectively (**Figure 4.21B**). These values have to be compared to the expected values of 39.2, 19.6 and 9.8 respectively. From these results we demonstrated that each plasmid was still transcribed when it was included in a complex pool of AAV

vectors and that there was a reasonable proportionality between the individual cDNA representation in the AAV mixture and its level of expression.

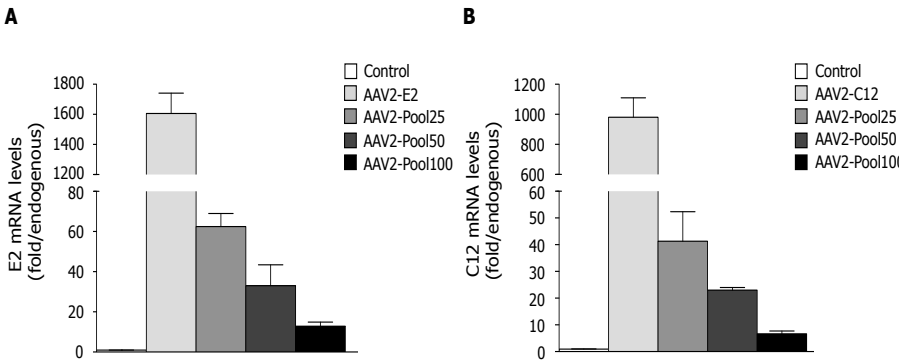

Figure 4.21 Transgenes overexpression *in vivo:* comparison between AAV vectors expressing single factors and AAV-Pools
Quantification of transgene overexpression over endogenous gene (all the samples are also normalized for the housekeeping gene GAPDH) for two factors included in all the AAV-Pools: (**A**) E2 and (**B**) C12. The analysis was performed on transduced muscle 15 days after empty vector (Control), AAV2-E2 or AAV2-C12, AAV2-Pool25, AAV2-Pool50 and AAV2-Pool100 delivery.

4.3.5 Generation of the AAV vector pools for *in vivo* functional selection

Once confirmed the feasibility of pooled AAV production, we started to generate pools of vectors for the *in vivo* functional selection of the collection of secreted factors. Taking into account the important indications gained from the experiment described in the previous paragraphs, we decided to group the 100 cDNAs in pool of 10 clones with similar genome size (**Figure 4.22**).

This decision was prompted by the consideration that the parameter most influential on pooled production and infection was insert size. Therefore, it appeared that the production of vector pools with low complexity would allow most efficient grouping of vectors carrying inserts of comparable length.

The collection is composed by clones containing cDNAs with length ranging from ~300 to ~3000 bp. Therefore, we decided to organize the clones into 10 pools (A-L) composed of clones with no more than 500 bp size difference.

POOL A	
D11	Gastrin (Gst)
D8	Chemokine (C-C motif) ligand 8 (Ccl8)
C3	Growth hormone releasing hormone (Ghrh)
D1	Cystatin 12 (Cst12)
E2	Ghrelin (Ghrl)
E10	Chemokine (C-C motif) ligand 12 (Ccl12)
F6	RIKEN cDNA 5530400C23 gene
C12	Insulin-like 6 (INSL6)
D7	Regenerating islet-derived 3 delta (Reg3d)
G4	Chemokine (C-C motif) ligand 7 (Ccl7)

POOL B	
C7	Prolactin family 5, subfamily a, member 1
F8	Pro-opiomelanocortin-alpha (Pomc)
F1	Prolactin family 7, subfamily d, member 1
C8	Prolactin family 7, subfamily b, member 1
G1	Oocyte secreted protein 1 (Oosp1)
C10	Prolactin family 3, subfamily b, member 1
B10	Prolactin family 3, subfamily d, member 1
F9	Neuromedin U
C5	Trophoblast specific protein beta (Tpbpb)
4E1	RIKEN cDNA 5430402E10 gene

POOL C	
G8	Natriuretic peptide precursor type C
E4	Chemokine (C-C motif) ligand 11 (Ccl11)
D5	Intelectin b (Itlnb)
G12	Interleukin 17A
G2	Interleukin 20
H2	Chemokine (C-X-C motif) ligand 9 (Cxcl9)
G7	RIKEN cDNA D730048I06 gene
E3	Ephrin A1
G5	Vasoactive intestinal polypeptide (Vip)
H12	Vitronectin (Vtn)

POOL D	
3G5	RIKEN cDNA 1700029I15 gene
4A1	Defensin, alpha, 20
4A11	Trefoil factor 1 (Tff1)
4B2	Phospholipase A2, group IB
4A10	Pre-B lymphocyte gene 3 (Vpreb3)
4F12	Cystatin 11 (Cst11)
4F9	Seminal vesicle antigen-like 1 (Sval1)
4F11	Defensin beta 22
3H10	Peptidoglycan recognition protein 1
4E6	Odorant binding protein Ia (Obp1a)

POOL E	
2D12	Chemokine (C motif) ligand 1 (Xcl1)
3G1	Salivary protein 1 (Spt1)
3H8	Gastric inhibitory polypeptide (Gip)
3G4	Cystatin 9 (Cst9)
3F11	RIKEN cDNA 1700016D06 gene
1B9	Interleukin 27 (Il27)
3F6	Cystatin 13 (Cst13)
4F7	Family with sequence similarity 3, member B
3E6	Anterior gradient homolog 3 (Agr3)
4A2	Chemokine (C-C motif) ligand 6 (Ccl6)

POOL F	
3G2	RIKEN cDNA 1600029D21 gene
3E11	Carcinoembryonic adhesion molecule 13
3F5	Prolactin family 8, subfamily a, member 81
3G7	RIKEN cDNA 1700040I03 gene
3G10	Phosphatidylethanolamine binding protein 4
3F9	Testis expressed gene 101
4B3	RIKEN cDNA 2210415F13 gene
3F7	Acrosomal vesicle protein 1 (Acrv1)
3H4	CD48 antigen
F3	Chemokine (C-X-C motif) ligand 13 (Cxcl13)

POOL G	
3C5	Proacrosin binding protein (Acrbp)
3D1	RIKEN cDNA 4930568D16 gene
2B4	Cathepsin R (Ctsr)
E7	Thyrotropin releasing hormone (Trh)
4B1	Progastricsin (pepsinogen C)
3B7	Hypothetical protein (Gm10344)
1E2	Renin 1
3A6	Napsin A aspartic peptidase (Napsa)
2B11	Follicle stimulating hormone beta (Fshb)
4C4	Wingless related MMTV integration site 2b

POOL H	
4C10	Spondin 2
1D3	Complement component 8, beta polypeptide
1E8	Asporin (Aspn)
1D6	Nephronectin (Npnt)
H3	Apelin (Apln)
2C11	Carboxylesterase 2E
1D12	Transforming growth factor, beta induced
3C2	Arylsulfatase A (Arsa)
4F1	Fibromodulin (Fmod)
3D2	Matrilin 3 (Matn3)

POOL I	
1C10	Glucosidase, beta, acid (Gba)
4E8	Nephrocan (Nepn)
2F8	Coagulation factor VII (F7)
3H9	RIKEN cDNA 2010109I03 gene
1F6	Biotinidase (Btd)
3E4	Keratocan (Kera)
2C12	Carboxylesterase 2A
3D6	Matrix metallopeptidase 1a
F2	Alpha fetoprotein (Afp)
3D11	Family with sequence similarity 198, memberA

POOL L	
4A4	Regenerating islet-derived 3 gamma (Reg3g)
4D10	Neurotensin (Nts)
1C6	Amelogenin X chromosome (Amelx)
4G2	Lipocalin 9 (Lcn9)
3G6	Lysozyme-like 1 (Lyzl1)
H9	Kallikrein 1 (Klk1)
4A5	Chymotrypsinogen B1 (Ctrb1)
3F10	GLI pathogenesis-related 1 like 1 (Glipr1l1)
1F4	Prolactin family8, subfamily a, member 9
B7	RIKEN cDNA 4930597L12 gene

Figure 4.22 AAV-Pools for the *in vivo* functional selection

The collection of 100 cDNAs coding for secreted factors was organized in 10 AAV pools (A-L) expressing 10 different genes. Each pool was composed by AAV constructs having inserts in the same size range.

4.4 *IN VIVO* FUNCTIONAL SELECTION OF NOVEL SECRETED MOLECULES CONFERRING SKELETAL MUSCLE AND CARDIAC PROTECTION

As already mentioned, the main purpose of this Thesis work was the development of an innovative strategy for the *in vivo*, functional selection of secreted factors providing therapeutic benefit in conditions of tissue degeneration, after gene transfer of an arrayed cDNA collection using AAV vectors. All the results described so far clearly supported the feasibility of this approach and gave us important information on the key points to take into account during each step of this project.

Based on the extensive similarities between the biology and the functional regulation of cardiomyocytes and muscle cells, and considering that several molecules protecting the skeletal muscle also exert a similar beneficial effect on cardiac muscle, **FunSel** was applied to different murine models of tissue damage, one in the skeletal muscle (hind limb ischemia) and the other in the heart (isoproterenol-induced myocardial damage).

4.4.1 *In vivo* functional selection in a model of hind limb ischemia

The first model we exploited for the *in vivo* selection was based on hind limb ischemia induction by femoral artery ligation, a surgical procedure that causes massive skeletal muscle degeneration. **FunSel** was performed using 30 random AAV2 clones, which were injected into the tibialis anterior muscle of mice, which were then subjected to femoral artery ligation, according to the outline reported in **Figure 4.23.**

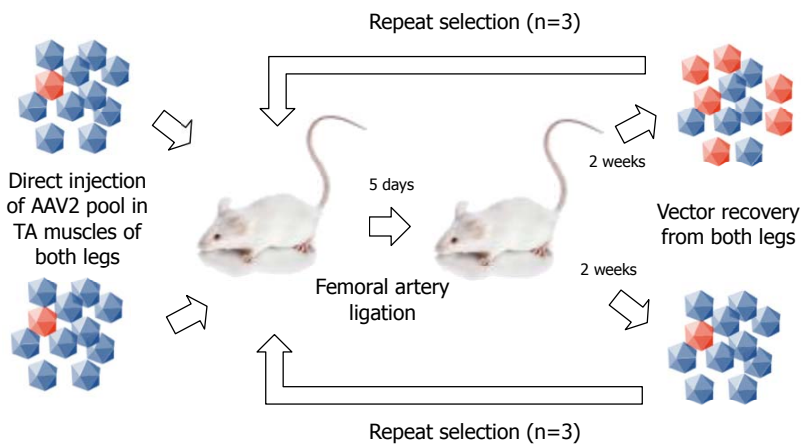

Figure 4.23 Outline of the experimental procedure for AAV vectors selection after induction of skeletal muscle ischemia
Mice were injected with AAV vector pools in the tibialis anterior (TA) muscles of both legs and, after 5 days, an ischemic damage was induced by femoral artery ligation only in the right limb, in order to trigger the selection in one muscle and to use the controlateral one as a control. After 2 weeks viral genomes still present in surviving tissues were recovered, the vector cDNAs from each of the two DNA pools were amplified by PCR using common primers, cloned again into the vector backbone, and the new viral preparations obtained were resubmitted to further cycles of selection up to the identification of a candidate gene (In red, vector coding for a putative beneficial factor, which becomes enriched during selection).

Three AAV2 pools (pools A, B and C), each one containing 10 different clones, were obtained transfecting HEK 293T cells with mixtures of 10

plasmids per pool. As previously mentioned, in order to avoid possible bias in packaging efficiency due to extensive different in insert length, plasmids were grouped into three pools according to their cDNA size. Pool A, B and C were afterwards mixed to obtain a single AAV pool composed of 30 clones, whose inserts ranged from 580 to 1600 bp (named "Tot" in **Figure 4.24**). The PCR pattern generated by amplifying DNA from each pool (A, B, C and Tot) using primers positioned in the common AAV backbone in regions flanking the inserts is shown in **Figure 4.24**.

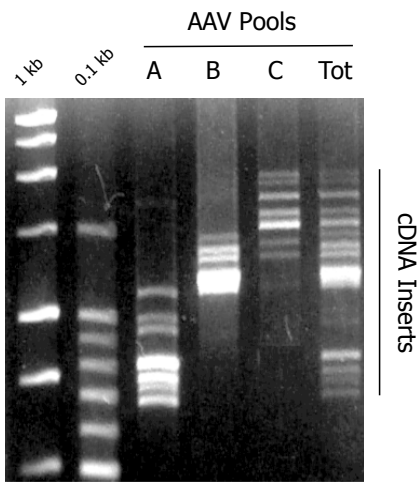

Figure 4.24 PCR amplification of AAV2-cDNA pools before *in vivo* injection. PCR primers spanning the cDNA inserts were used for amplification of three pools of AAV2 vectors (pools A, B and C); grouping of constructs in the pools was according to insert length. The last line shows PCR amplification of the total (Tot), pooled group (A+B+C) of the 30 vectors before *in vivo* injection. First two lines: molecular weight markers.

The obtained AAV2-cDNA pool, expressing 30 different factors, was injected into the tibialis anterior muscles of both legs of CD1 mice (n=10; 30 µl; $3x10^{10}$ AAV2-cDNA vector particles per muscle). After 5 days, uni-lateral hind-limb ischemia was induced in the right limb by ligating the right femoral artery, according to experimental conditions established in the laboratory (Arsic et al., 2004). This treatment is known to induce marked muscle fiber degeneration, followed by adipose tissue substitution, as shown in **Figure 4.25**; muscle fiber regeneration then starts, and becomes complete, in the absence of treatment, in ~40 days.

Tibialis anterior, 3 d after ischemia

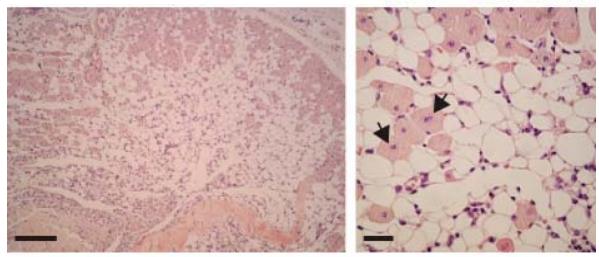

Hematoxylin-Eosin

Figure 4.25 Effects of femoral artery ligation on muscle fiber survival
The picture shows the histology of tibialis anterior muscle sections at two magnifications after 3 days from femoral artery ligation. Extensive loss of muscle fibers and the initial presence of regenerating new fibers, characterized by the presence of a central nucleus (two of which are indicated by arrows), are evident.

Animals were sacrificed 15 days after femoral artery ligation and total DNA from both the ischemic and the non-ischemic muscles was recovered. The DNA samples from different animals were pooled, maintaining the separation between ischemic and non-ischemic muscles.

The vector cDNAs from each of the two pools were then amplified by PCR using primers common to all constructs, checked on a gel to identify possibly enriched vectors among the viral genome recovered from the ischemic muscles and then pooled-cloned again into the pZac2.1 vector backbone, to obtain two new viral preparations. The tibialis anterior of the right leg of additional mice (n=10) were afterwards injected with the AAV2-cDNA vectors generated from the ischemic DNA pool, while the corresponding muscles of the left leg with the vectors from the non-ischemic DNA pool. As we did for the first round of selection, after five days, the right leg was subjected to ischemia according to the same experimental procedure outlined above. The cycle of selection of AAV-cDNAs separately from the ischemic and non-ischemic limbs was repeated

for a total of 3 times.

At the end of the procedure, the representation of the original 30 different cDNA clones after each cycle of selection was analyzed by PCR amplification of the inserts, in order to assess whether one or more vectors were enriched upon selection. As shown in **Figure 4.26** for two representative mice, the PCR pattern of the DNA extracted from the muscles not subject to ischemia resembled that obtained by amplification of vector inserts before the beginning of the selection procedure, thus indicating that *in vivo* injection and recovery of vectors did not introduce any essential bias. After the first cycle of selection, moreover, we did not notice any difference in the pattern of viral genomes rescued from the ischemic muscles. In contrast, an individual band was enriched in the DNA pools recovered from the ischemic legs after the second, and more sharply, after the third round of selection. Sequencing of this enriched band revealed that it corresponded to the cDNA of clone E2 coding, quite unexpectedly, for the secreted hormone with peculiar endocrine functions, **ghrelin**.

Of course after the identification of candidate genes we needed to validate their effective protective role *in vivo*. The beneficial properties of ghrelin in conditions of ischemic damage were therefore extensively characterized. The results of these experiments are described in Chapter 4.5.

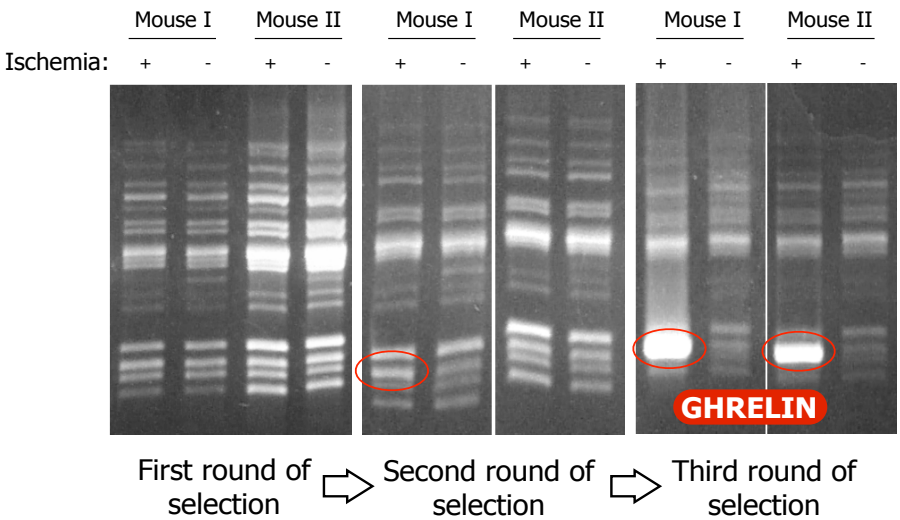

Figure 4.26 PCR amplification of AAV2-cDNA pools after each of three rounds of *in vivo* selection in the muscle
The cDNA inserts of the AAVs recovered from the tibialis anterior muscles after each of three rounds of selection *in vivo* were amplified with PCR primers spanning the inserts. In the picture the pattern of bands referred to two representative mice for each selection cycle; the two lanes show amplification of vectors recovered from the ischemic and non-ischemic legs. The band highly enriched after the third round of selection induced by ischemia corresponds to the cDNA of ghrelin.

4.4.2 *In vivo* functional selection in a model of cardiac damage induced by isoproterenol treatment

The second model of degenerative disease we exploited for the *in vivo* selection of the AAV collection was a model of cardiac damage induced by an acute treatment with a toxic drug. In particular the chemical compound isoproterenol (Iso), a synthetic β-adrenergic receptors agonist structurally similar to adrenaline and having a strong chronotropic/inotropic effect on the heart, when administered at high dosage, induces a very well described infarct-like myocardial lesion including myocytes degeneration, necrosis and subsequent interstitial and perivascular fibrosis (Grimm et al., 1998a). These damages usually result in gradual LV-enlargement and progression towards mild heart failure.

The model is characterized by technical simplicity and excellent reproducibility.

In this model, **FunSel** was performed using the entire collection of secreted molecules, namely all the 100 AAV clones, organized in 10 separated pools expressing 10 factors each (Pools A-L). These were screened *in vivo*, according to the outline reported in **Figure 4.27.**

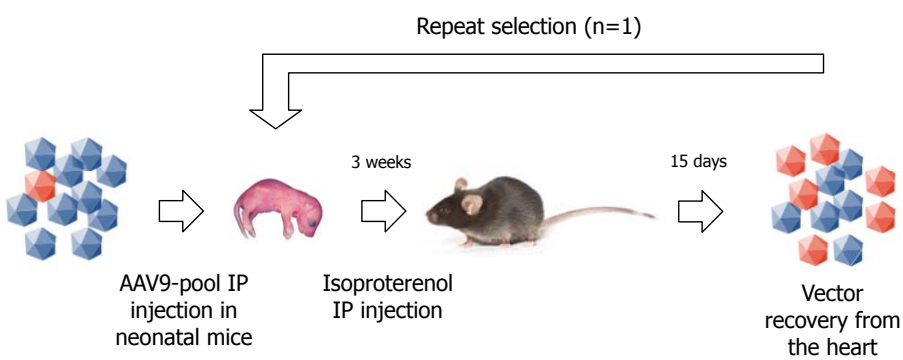

Figure 4.27 Outline of the experimental procedure used to select clones after induction of myocardial damage using isoproterenol
Neonatal mice (n=12) were injected, 3 days after birth, with AAV9 pools intraperitoneally (IP) to reach high levels of heart transduction and 3 weeks later myocardial damage was induced by IP administration of isoproterenol (Iso). After 2 weeks, viral genomes still present in the surviving tissue were recovered, the vector cDNAs amplified by PCR using common primers and compared with the vectors recovered from the hearts of control mice, transduced with the AAV pools, but not submitted to functional selection. As in the previous model, the recovered cDNAs were cloned again into the vector backbone, to generate new viral preparations to resubmit to further cycles of selection up to the identification of a candidate gene (In red, vectors coding for the putative beneficial factor).

For the functional selection in the heart, we generated AAV vectors with serotype 9, which shows, as already described, preferential cardiac transduction (Bish et al., 2008; Pacak et al., 2006).

Before starting the actual selection procedure, we first wanted to understand which was the most suitable route of vector administration. For this purpose, we generated a viral preparation expressing the previously identified ghrelin transgene, administered it *in vivo* ($3x10^{10}$ viral particles) using three different routes and then evaluated the levels of expression of the transgene in the heart at day 15 after transduction. The three delivery routes were: intraperitoneal (IP) injection in neonatal mice (day 3 after birth), intravenous (IV) and IP injection in adult mice (1 month old).

Figure 4.28 shows the intracardiac levels of the transgene as a ratio to the corresponding endogenous gene after the three administration modalities. The results indicate that IP injection in pups was the most effective way to reach a satisfactory myocardial transduction.

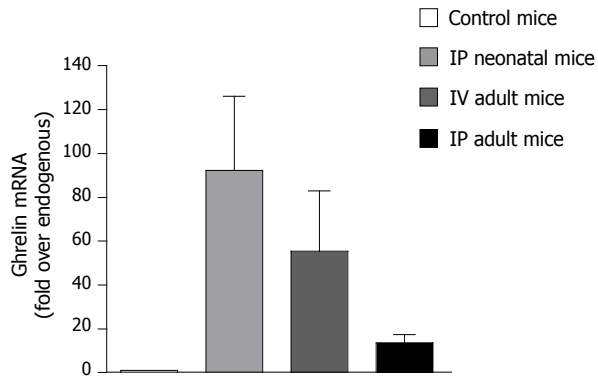

Figure 4.28 Comparison of ghrelin cardiac expression levels upon delivery of AAV9-Ghrelin according to different routes.
Levels of ghrelin cardiac expression (expressed over normal expression of the corresponding cellular gene) 15 days after administration of $3x10^{10}$ viral particles by 3 different routes: IP injection in neonatal mice 3 days after birth, IV and IP injection in adult mice (1 month old). The most efficient level of heart transduction was reached by IP delivery of the vectors in pups.

Next we wanted to determine the optimal isoproterenol dosage that elicited marked damage to the myocardium (necessary to trigger the selection) without inducing significant lethality in the treated mice. In particular, three isoproterenol concentrations (100, 200 and 300 mg/kg) were tested (**Figure 4.29**). Histological analysis at 1 week revealed widespread necrotic areas in the myocardium of all the treated animals but, for the 200 and 300 mg/kg concentrations, the myocyte loss was more evident and a fibrotic scar largely replaced cardiac tissue. The survival rates were respectively 100%, 90% and 50%, therefore the isoproterenol dose of 200 mg/kg, that better balanced heart toxic insult and animal survival, was selected for the subsequent studies.

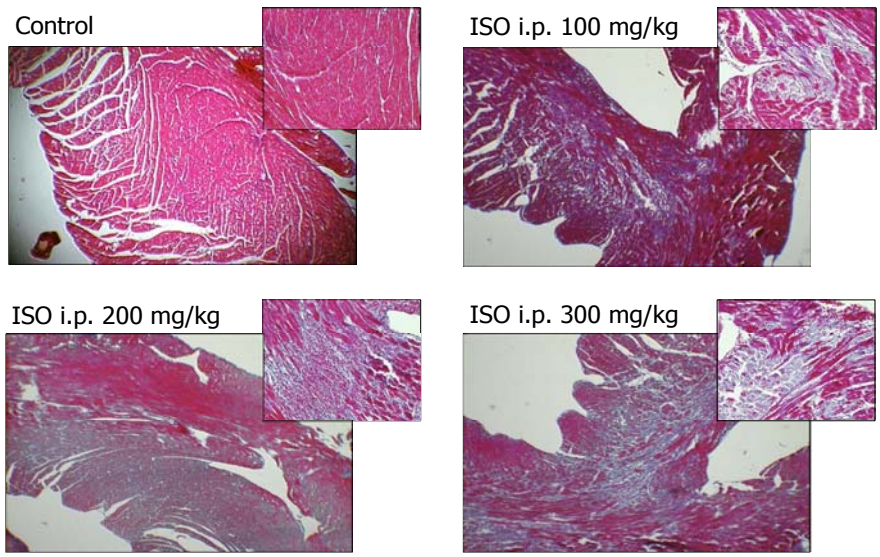

Figure 4.29 Toxic cardiac effects induced by different dosages of isoproterenol
Histological cardiac sections after intraperitoneal injection of different dosages of isoproterenol (100, 200 and 300 mg/kg) in 3 weeks old mice. In the Azan's trichromic stained heart sections at day 7 after damage is evident the extent of myocytes loss and initial fibrotic substitution. The insets show high-magnifications (200X) of the injured area.

Based on these preliminary results, the actual selection experiment was initiated. AAV pools were obtained as previously described and each pool, expressing 10 different factors, was tested individually by intraperitoneal (IP) injection in C57/Bl6 neonatal mice (n=12; 30 µl; $3x10^{10}$ AAV9-cDNA vector particles) 3 days after birth. Three weeks after AAV9 pool delivery, functional selection for cardiac protective factors was triggered by a single treatment with a toxic dose of isoproterenol (200 mg/kg) in half of the animals.

For all the ten analyzed AAV pools, animals were sacrificed 2 weeks after toxic damage and total DNA was recovered from the surviving cardiac

tissue. The vector cDNAs were then amplified by PCR using primers common to all constructs and the pattern of amplified inserts in animals submitted and non-submitted to isoproterenol treatment was compared.
Quite surprisingly, in the AAV-Pool A, a specific cDNA appeared distinctly enriched already after a single cycle of selection (**Figure 4.30A**). Sequencing of this enriched band revealed that it corresponded to the cDNA of clone C12, coding for insulin-like peptide 6 (**INSL6**), a still poorly described growth factor, which is a member of the known anti-fibrotic family of relaxin proteins.
The identification of a candidate that belongs to this class of genes perfectly fitted with the selection model we exploited in this experiment, since this was based, as already mentioned, on the action of a pro-fibrotic drug.

None of the remaining nine analyzed pools (B-L) showed factors that were appreciably enriched after selection (as shown for the representative AAV-PoolE in **Figure 4.30B**). Thus, these pools might either not contain any pro-surviving molecule or necessitate of subsequent rounds of selection to lead to enrichment for a beneficial factor.
Preliminary results on the beneficial properties of INSL6, in conditions of cardiac ischemic damage, are described in Chapter 4.6 of this Thesis work.

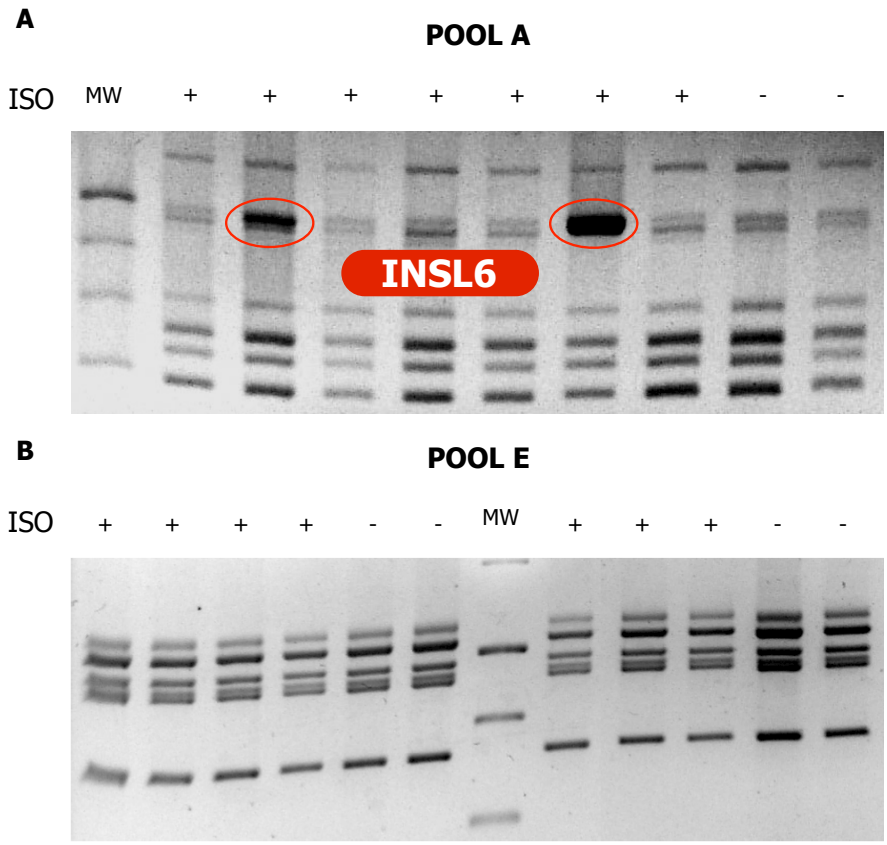

Figure 4.30 PCR amplification of AAV9-cDNA pools after a single round of *in vivo* functional selection in the heart
The cDNA of the AAVs recovered from the hearts after a single round of *in vivo* selection were amplified with PCR primers spanning the inserts. The picture shows a band ladder corresponding to Pool A and Pool E. Each lane corresponds to the viral genome content in the myocardium of each analyzed animal, treated or not with isoproterenol (Iso +/-).
In the upper panel (**A**), AAV Pool-A, showed, in some of the treated animals, the enrichment of a viral genome corresponding to the insulin-like peptide 6 (INSL6). No enrichment for any band was instead evident for AAV-Pool E (**B**), similar to all the other 8 pools.

4.5 CHARACTERIZATION OF THERAPEUTIC EFFECTS OF THE *IN VIVO* SELECTED CANDIDATE GENE GHRELIN

Next we wanted to assess the actual individual protective potential of the two selected clones (Ghrelin and INSL6) *in vivo*, in order to validate the obtained results.

4.5.1 AAV9-Ghrelin prevents isoproterenol and doxorubicin-induced cell death in neonatal rat cardiomyocytes

First we wanted to assess whether the beneficial effects of ghrelin might also be extended to primary cardiomyocytes. For this purpose, neonatal rat cardiomyocyte cultures were established according to conditions already set up in the laboratory (Collesi et al., 2008). Immediately after plating, cells were transduced with either AAV9-LacZ or AAV9-Ghrelin (multiplicity of infection (MOI)=$1x10^4$). After 24 h, cardiomyocytes were treated with the β- adrenoreceptor agonist isoproterenol (10 μM) or the antiblastic drug doxorubicin (1 μM), showing exquisite cardiotoxicity, for 48 and 24 hours respectively. Since these two conditions are known to induce massive cell apoptosis, cell viability was analysed by a live/dead cell viability assay.

In both experimental settings, AAV9-Ghrelin transduction was shown to exert an impressive protective effect, as shown in **Figure 4.31.** Quantification of these experiments indicated that >70% and >50% cardiomyocytes survived after AAV9-Ghrelin transduction compared to <10% in the control, after isoproterenol and doxorubicin treatment respectively.

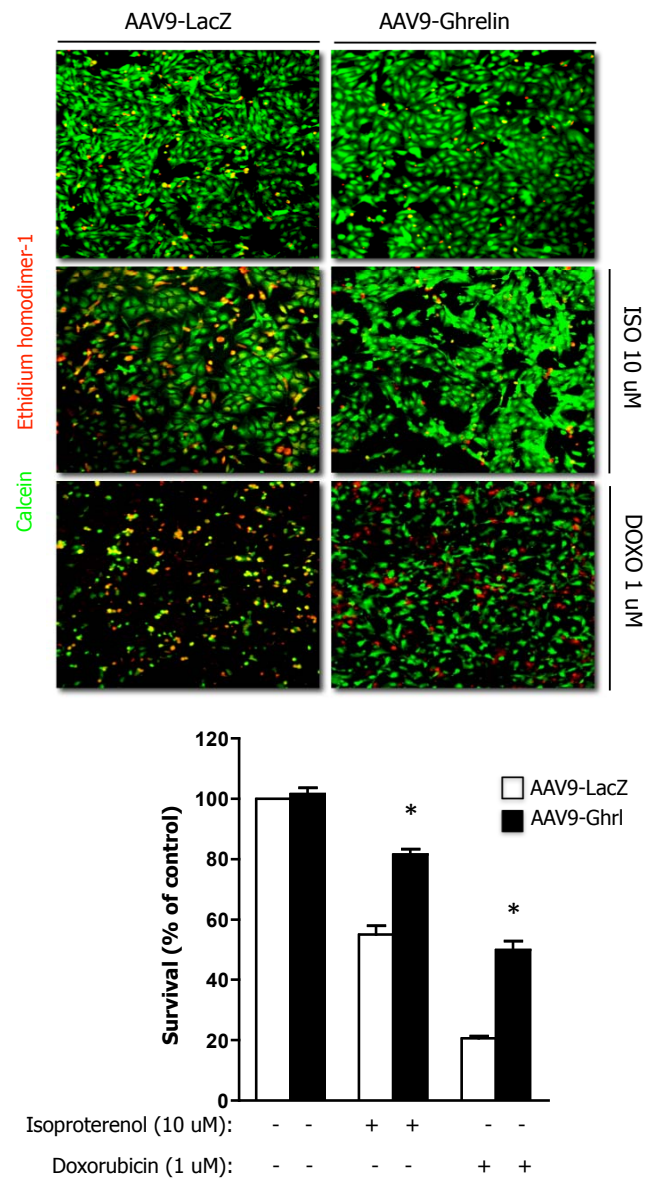

Figure 4.31 Protective effect of ghrelin on cardiomyocytes survival
Rat neonatal cardiomyocytes, transduced with AAV9-LacZ or AAV9-Ghrl (transduction efficiency >40%) were either left untreated or treated with isoproterenol 10 μM (Iso) or doxorubicin 1 μM (Doxo). Upper panel: representative experiment. Nuclei of dead cardiomyocytes are shown in red, living cells in green. Lower panel: quantification of the results. Values are expressed as mean ± SEM of three experiments; * $P< 0.05$.

4.5.2 Long-lasting ghrelin expression in mouse heart preserves cardiac function after myocardial infarction (MI)

The outstanding protection observed by AAV9-Ghrelin transduction in cultured, primary cardiomyocytes prompted us to investigate whether the same vector might also be effective *in vivo*, thus providing a rationale why it was originally selected.

We choose myocardial infarction (MI) as a model to evaluate the cardiac protective properties of ghrelin and the experiment was conducted according to the outline shown in **Figure 4.32**.

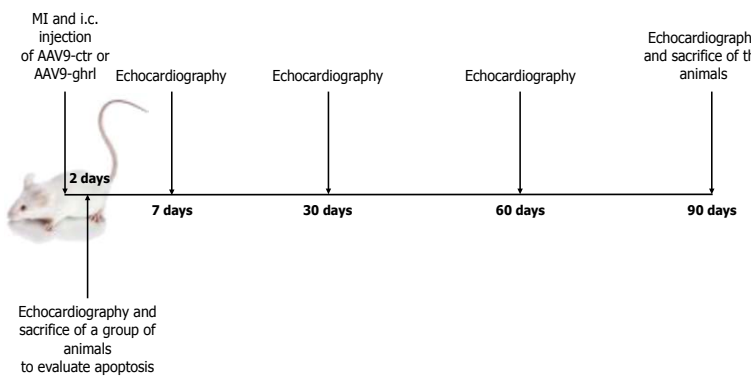

Figure 4.32 AAV9-Ghrelin in a model of myocardial infarction (MI): experimental outline
CD1 mice were submitted to myocardial infarction (MI) and immediately treated by intracardiac (IC) injection of either AAV9-Ghrelin or AAV9-Control. Cardiac function was analysed by echocardiography at 2, 7, 30, 60 and 90 days after MI. For each treatment, a group of mice (n=5) was sacrificed 2 days after infarction to evaluate apoptotic rate, 4 animals were sacrificed at day 7 post-infarction to analyze inflammation markers induction, while the other animals were sacrificed after 3 months.

CD1 mice (n=20 per group) underwent permanent left descendent coronary artery ligation and were immediately injected into the LV peri-infarcted area with $5x10^{10}$ viral particles of AAV9-Ghrelin or a control AAV9 vector containing the empty poly-linker (AAV9-Control). Analysis of the ghrelin mRNA levels at day 90 after the procedure by real-time PCR

indicated robust ghrelin mRNA expression up to this time point (**Figure 4.33A**). In a consistent manner, quantification of acyl- and des-acyl ghrelin protein levels by ELISA also confirmed increased cardiac presence of both peptides at this time point (**Figure 4.33B**). Of notice, the former assay only detects ghrelin expressed in the heart, while the latter both cardiac and circulating ghrelin.

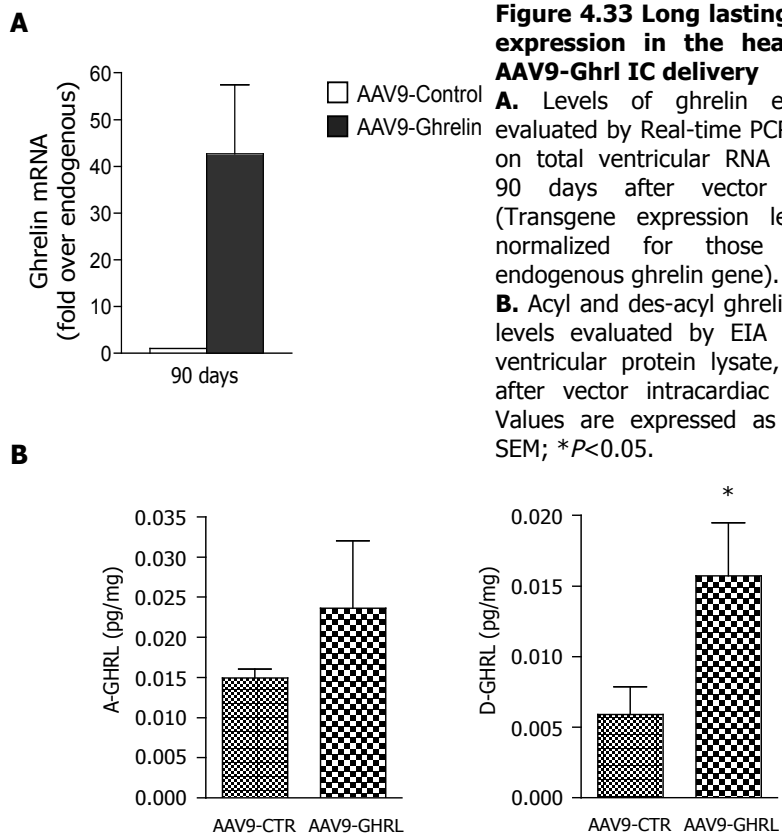

Figure 4.33 Long lasting ghrelin expression in the heart upon AAV9-Ghrl IC delivery
A. Levels of ghrelin expression evaluated by Real-time PCR analysis on total ventricular RNA extracted 90 days after vector injection (Transgene expression levels are normalized for those of the endogenous ghrelin gene).
B. Acyl and des-acyl ghrelin peptide levels evaluated by EIA assay on ventricular protein lysate, 90 days after vector intracardiac injection. Values are expressed as mean ± SEM; **P*<0.05.

A group of animals (n=5) was sacrificed at day 2 and another group (n=4) at day 7 after MI to measure apoptotic rate in the peri-infarcted area and upregulation of inflammatory gene markers, respectively. Cardiac function of the remaining mice was monitored up to three months.

To evaluate global and regional LV function, transthoracic echocardiography was performed at 2, 7, 30 60 and 90 days after myocardial infarction and transduction in sedated mice using the Vevo echocardiography system. As shown in **Figure 4.34**, the LV ejection fraction (LVEF) and fractional shortening (LVFS) were significantly preserved in infarcted mice injected with AAV9-Ghrelin, compared to controls. Of notice, the effect persisted at long times after infarction (90 days), while cardiac performance was progressively deteriorated in control animals (LVEF: 33±5% *vs.* 53±3%; LVFS: 17±4% *vs.* 28±4% in control and ghrelin-transduced animals respectively at day 90 after infarction, $P<0.05$ at all time points).

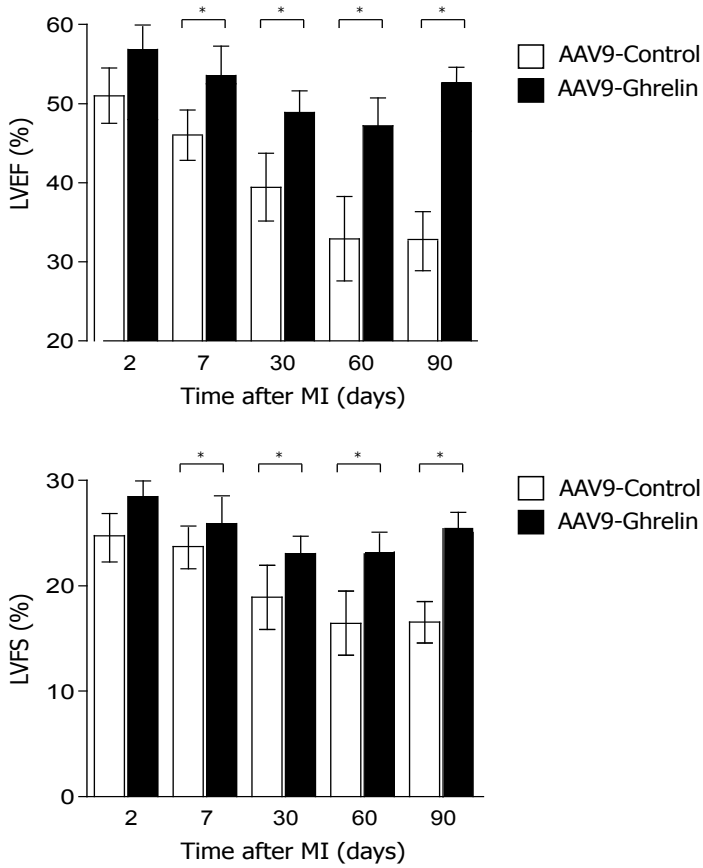

Figure 4.34 AAV9-Ghrelin preserves cardiac function for a prolonged time after myocardial infarction
Left Ventricular Ejection Fraction (LVEF) and Left Ventricular Fractional Shortening (LVFS) of infarcted mice treated with AAV9-Ghrelin or AAV9-Control were measured by echocardiography. Values are expressed as mean ± SEM; **P*<0.05.

4.5.3 Maintenance of myocardial thickening and reduction of infarct size in AAV9-Ghrelin transduced mice

Other important functional parameters, indicating changes of regional cardiac contractility, were significantly different between ghrelin treated and untreated animals, again also at longer time points after myocardial infarction (**Figure 4.35**). At both 1 and 3 months after cardiac gene transfer, the LV end-systolic wall thickening (AWTK) in the border zone of the infarcted hearts injected with AAV9-Ghrelin was markedly improved compared to control mice (24±5% vs. 34±4 and 19±4% vs. 31±3% in control and ghrelin-transduced animals, respectively at day 30 and 90 after infarction, P <0.05 at all time points).

Moreover the LV internal diameter was clearly more enlarged in the control animals, confirming a better progression of cardiac performances after infarction in ghrelin treated mice.

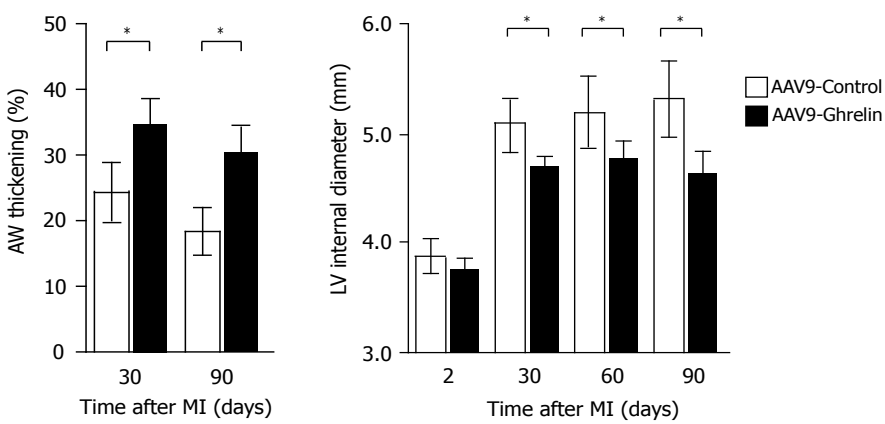

Figure 4.35 Ghrelin improves cardiac contractility after MI
Anterior Wall Thickening (AWTK) and LV internal diameter of infarcted mice treated either with AAV9-Ghrelin or AAV9-Control were measured by echocardiography. Values are expressed as mean ± SEM; *P<0.05.

In the representative transthoracic echocardiographic images shown in **Figure 4.36,** taken 90 days after myocardial infarction, the LV dilatation of AAV9-Control treated mice is evident.

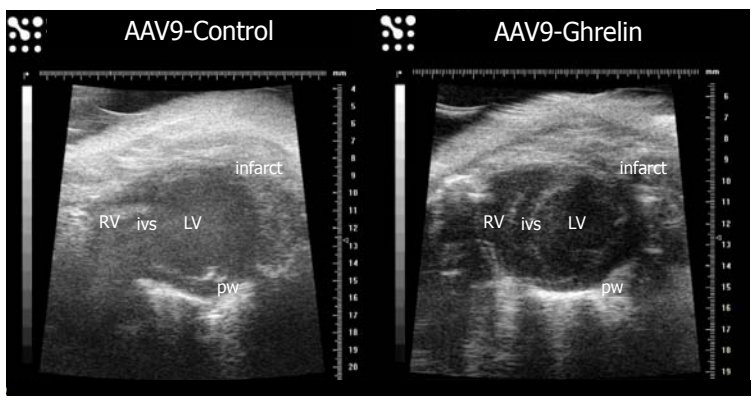

Figure 4.36 Echocardiographic analysis of infarcted hearts
Echocardiographic analysis of AAV9-Ghrelin and AAV9-Control treated mice 3 months after MI. Representative transthoracic parasternal short axis echocardiographic profiles.

At the end of the echocardiography study, animals were sacrificed, hearts were collected and the left ventricle, including the interventricular septum, was carefully dissected and examined for post-infarction fibrosis and chamber remodeling. After washing in PBS, each specimen was cut into 5 pieces of equal thickness from base to apex, fixed in 4% paraformaldeyde and embedded in paraffin for histological analysis.

Morphometric analysis of trichromic-stained LV sections showed that the anterior wall of infarcted, control animals underwent considerable thinning, consistent with the echocardiographic results. In contrast, the AAV9-

Ghrelin-treated hearts showed significant preservation of contractile tissue and reduction of the fibrotic area; representative images are shown in **Figure 4.37A**.

Infarct size was measured on 5 µm thick sections as the percentage of (endocardial + epicardial circumference of infarct area) / (endocardial + epicardial circumference of LV). **Figure 4.37B** reports the quantification of infarct size (47±6% vs. 23±3% in control and ghrelin-transduced animals, respectively at day 90 after infarction, P <0.05).

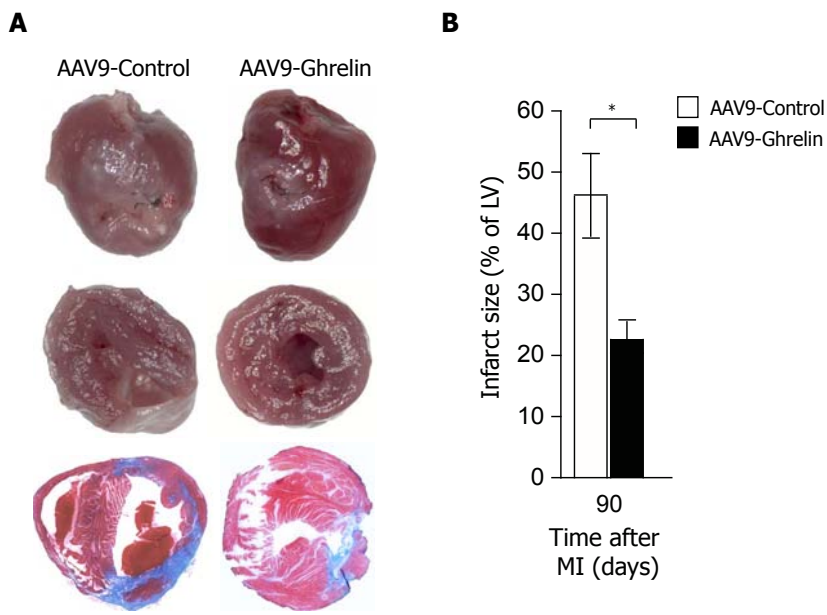

Figure 4.37 Reduction of infarct size in AAV9-Ghrelin transduced hearts
A. Representative AAV9-Control and AAV9-Ghrelin-injected hearts, their LV transverse sections and Azan trichromic staining of the tissue. Fibrotic areas are stained in blue.
B. Quantification of infarct size expressed as percentage of LV. Values are expressed as mean ± SEM; *P<0.05.

4.5.4 Marked decrease of myocardial apoptosis and inflammatory infiltrate after ghrelin transduction in infarcted mice

Given the massive preservation of myocardial tissue after infarction, and considering the protective effect observed in the *in vitro* experiments shown above, in a set of animals (n=5 per group) we assessed the extent of apoptosis in the infarcted hearts treated with the control and ghrelin-expressing vectors.

Infarcted hearts were collected and snap frozen 2 days after MI and vector transduction. As shown in **Figure 4.38**, at this time point ghrelin transgene already started to be expressed in the LV of mice injected with AAV9-Ghrelin, in agreement with the rapid onset exhibited by AAV serotype 9.

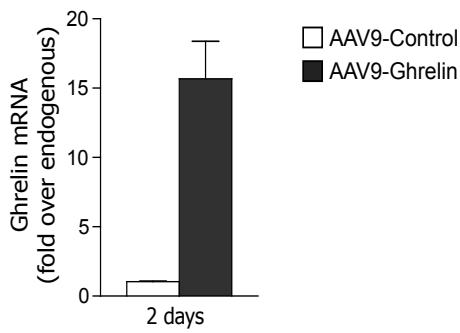

Figure 4.38 Rapid onset of ghrelin expression in the LV upon AAV9-Ghrl IC delivery
Levels of ghrelin expression evaluated by Real-time PCR analysis on total ventricular RNA extracted 2 days after vector injection (Transgene expression levels are normalized for those of the endogenous ghrelin gene).

To evaluate apoptosis, frozen sections were fixed in 4% PFA and treated for immunostaining and TUNEL assay. As shown in **Figure 4.39A** a marked reduction in the number of apoptotic nuclei in the animals treated with AAV9-Ghrelin was clearly noticed. **Figure 4.39B** reports the quantification of TUNEL-positive nuclei (27±4% vs. 7±2% in control and ghrelin-transduced animals respectively).

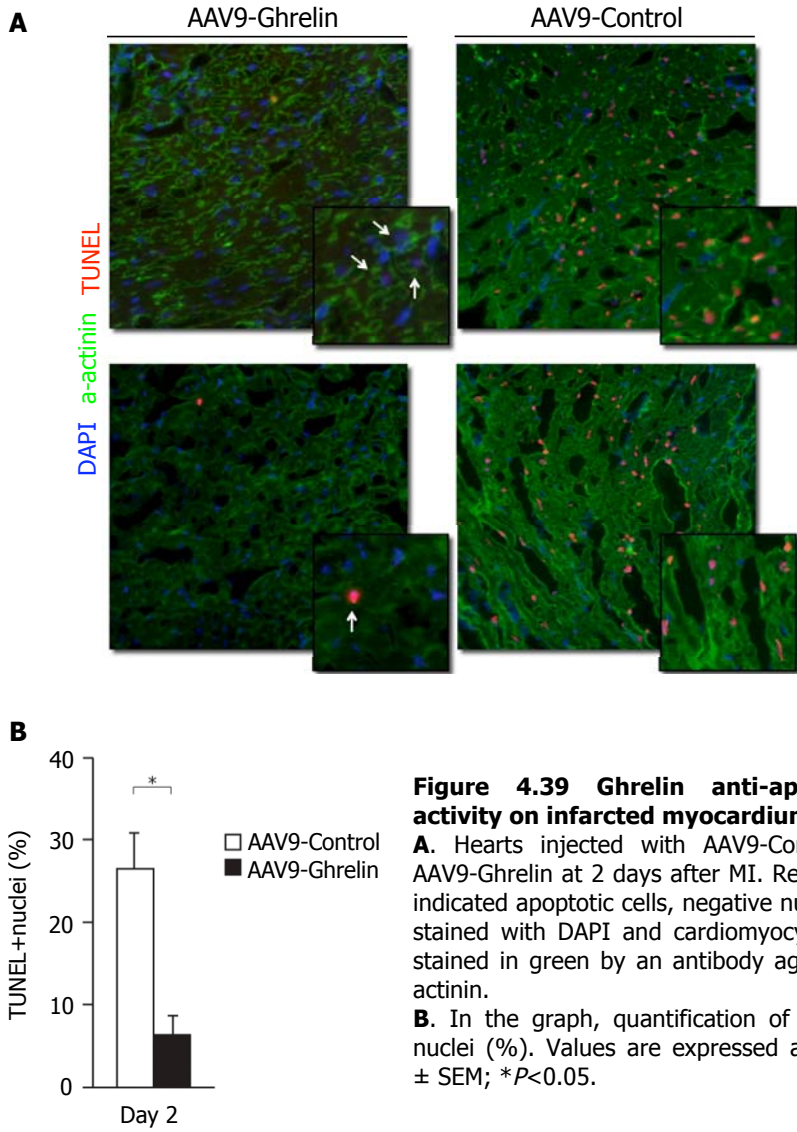

Figure 4.39 Ghrelin anti-apoptotic activity on infarcted myocardium
A. Hearts injected with AAV9-Control or AAV9-Ghrelin at 2 days after MI. Red nuclei indicated apoptotic cells, negative nuclei are stained with DAPI and cardiomyocytes are stained in green by an antibody against α-actinin.
B. In the graph, quantification of positive nuclei (%). Values are expressed as mean ± SEM; **P*<0.05.

Ghrelin has also been recently described as a molecule able to reduce the inflammatory response upon damage (Huang et al., 2009). Therefore, we also stained with hematoxylin and eosin (H&E stain) paraffin embedded sections of infarcted hearts collected 2 days after MI and AAV transduction,

in order to analyze the inflammatory cell infiltration.

As shown in **Figure 4.40A,** a massive inflammatory cells infiltration was evident in the peri-infarctual region of control mice, which was significantly blunted in the ghrelin-expressing hearts. **Figure 4.40B** reports the quantification (22±3% vs. 7±4% in control and ghrelin-transduced animals respectively).

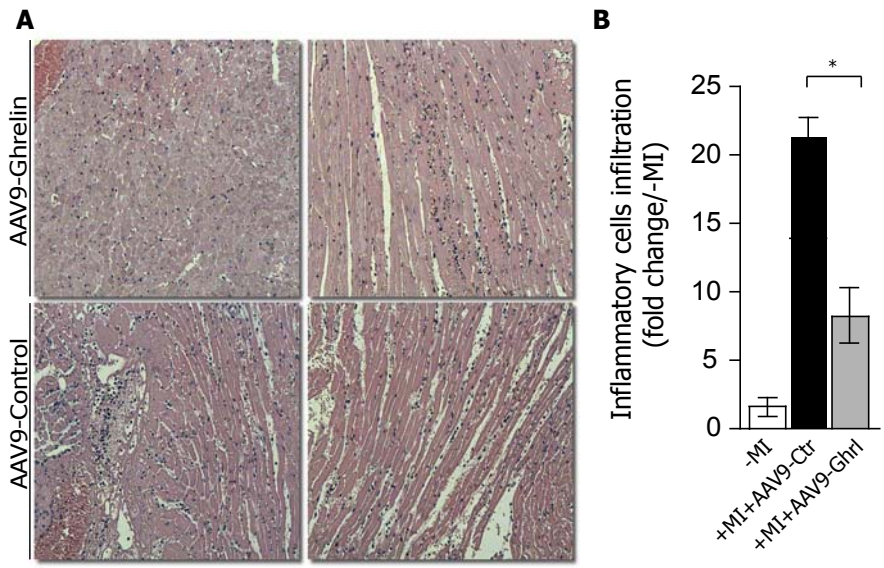

Figure 4.40 Ghrelin reduces inflammatory cell infiltration in the peri-infarctual region
A. Hematoxylin and eosin (H&E) staining (200x magnification) of heart sections two days after MI and intracardiac delivery of either AAV9-Ghrelin or AAV9-Control.
B. In the graph, quantification of inflammatory cells infiltration, calculated as relative increase over normal conditions (-MI). Values are expressed as mean ± SEM; *P<0.05.

Further evidence of an anti-inflammatory effect of ghrelin was obtained by measuring the levels of IL1-β, IL6 and TNFα, which are known to be overexpressed under inflammatory conditions. At day 7 after infarction, the hearts of a group of ghrelin-expressing and control animals (n=4 per

group) were recovered, RNA was extracted form the LV, and expression of the above mentioned genes was analyzed by Real-time PCR. We observed a massive induction of the analyzed factors in AAV9-Control hearts, while their level of activation in ghrelin-expressing samples was similar to normal mice or significantly reduced (**Figure 4.41**).

These results reinforced the idea that the functional beneficial effects we previously described for mice transduced with AAV9-Ghrelin upon cardiac ischemia, could be partially explained by a direct anti-apoptotic and anti-inflammatory action of this molecule in the infarcted myocardium.

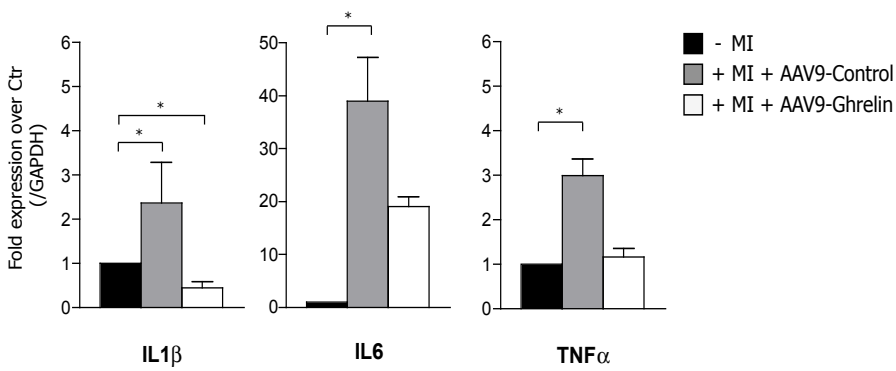

Figure 4.41 Ghrelin reduces the induction of genes upregulated by inflammation

Control and AAV9-Ghrelin treated animals (n=4 per group) were sacrificed 7 days after MI and the expression of the indicated genes was analyzed by Real-time PCR. Values are expressed as mean ± SEM of the levels of expression of the factors vs. uninfarcted control hearts (- MI), after normalization for GAPDH. **P*<0.05.

Recent work has demonstrated that miR-21 deregulated expression contributes to myocardial disease. Upon cardiac damage, this miRNA is upregulated in fibroblast contributing to fibrosis and pathological cardiac hypertrophy (Thum et al., 2008), also acting as a regulator of the matrix metalloprotease-2 (MMP-2) in these cells (Roy et al., 2009).

We therefore compared the levels expression of these miR-21 and MMP-2 in RNA samples of control and ghrelin-expressing animals at day 7 after

infarction. We noticed that the up-regulation of both factors observed after MI was markedly blunted in the ghrelin-expressing hearts (**Figure 4.42**). These results were absolutely in accordance with the previous reported histological observations about a reduced fibrotic tissue deposition and the consequent decrement of infarct size in ghrelin-transduced hearts.

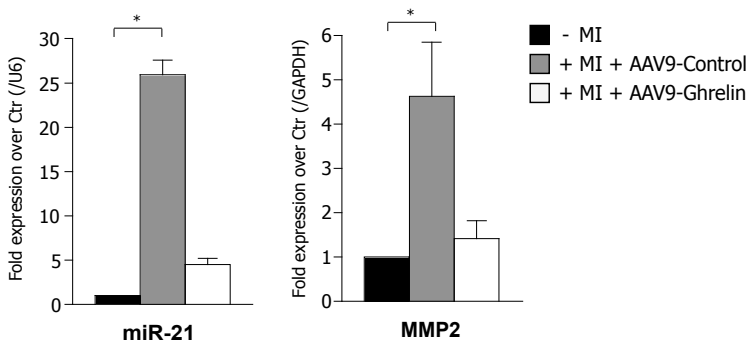

Figure 4.42 Ghrelin impedes the cardiac damage induced overexpression of miR-21 and MMP-2 in fibroblasts
Levels of expression of miR-21 and MMP-2 were analyzed in control and AAV9-Ghrelin treated hearts, 7 days after MI. Values are expressed as mean ± SEM of the levels of expression of the indicated factors vs. uninfarcted control hearts (- MI), after normalization (U6 for miR-21 and GAPDH for MMP-2). *P<0.05.

4.5.5 Ghrelin overexpression counteracts the induction of genes involved in pathological LV remodeling after myocardial infarction

To further confirm the effects of ghrelin on the heart, we analyzed, by Real-time PCR, the genes expression profiles of LV tissue from the infarcted animals (n=8 per group) sacrificed at 3 months after MI.

In agreement with the echocardiographic observations, AAV9-Control treated animals showed a characteristic pattern of gene expression typically associated with pathological LV remodeling, with significant over-expression of β-MHC and cardiac natriuretic peptides (BNP and ANP), and a decrease in the levels of α-MHC, Serca2a, RYR2, and Pgc1α compared to

normal mice (P<0.05 for all the analysed genes).

As shown in **Figure 4.43** these modifications were all significantly counteracted by ghrelin overexpression.

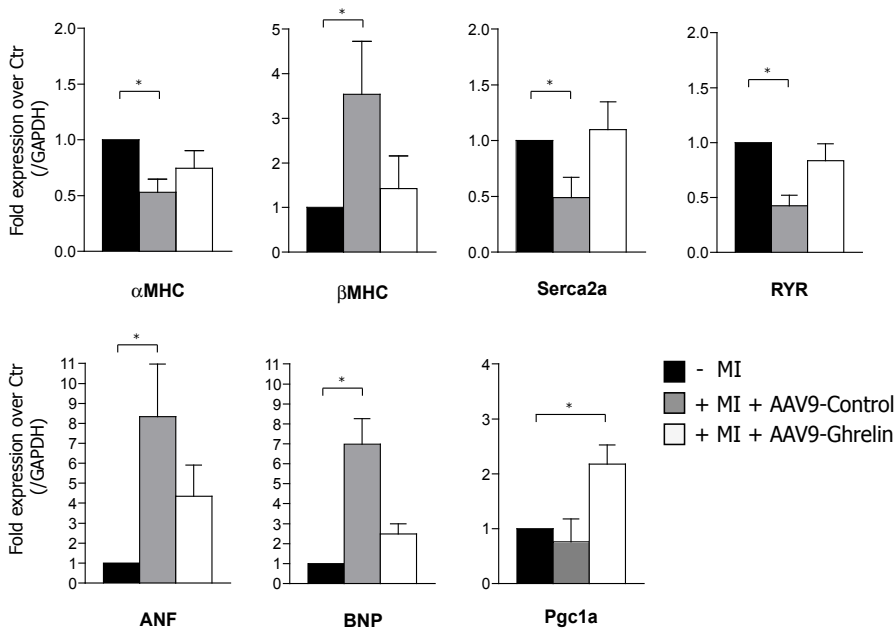

Figure 4.43 Ghrelin prevents gene expression of markers of pathological remodeling in the myocardium of infarcted mice

The expression levels of the indicated genes are analyzed in control and AAV9-Ghrelin treated hearts, 3 months after MI. Values are expressed as mean ± SEM of the levels of expression of the indicated factors vs. uninfarcted control hearts (-MI), after normalization for GAPDH. *P<0.05.

4.6 CHARACTERIZATION OF THERAPEUTIC EFFECTS OF THE *IN VIVO* SELECTED GENE INSULIN-LIKE PEPTIDE 6 (INSL6): PRELIMINARY RESULTS

We also wanted to assess whether insulin-like peptide 6-precursor (INSL6), which was originally selected after isoproterenol-induced myocardial damage, might exert a beneficial effect after myocardial infarction.

4.6.1 AAV9 mediated INSL6 expression in mouse heart preserves cardiac function and reduces infarct size after myocardial infarction

To assess the role of INSL6 in condition of cardiac damage we exploited the models of myocardial infarction already described for the *in vivo* validation of ghrelin.

As in the previous experiment, CD1 mice (n=18 per group) underwent permanent left descendent coronary artery ligation and immediately injected into the LV peri-infarcted area with $5x10^{10}$ viral particles of AAV9-INSL6 or an AAV9-Control vector. Also for this AAV vector, we measured the level of INSL6 transgene expression in the heart, 90 days after viral vector delivery. We observed efficient transduction and long lasting expression of the vector in the cardiac tissue (**Figure 4.44**).

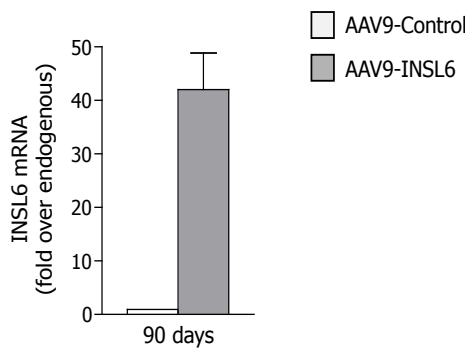

Figure 4.44 Long lasting INSL6 expression in the heart upon viral vector delivery
Levels of INSL6 transcripts evaluated by Real-time PCR analysis on total ventricular RNA extracted 90 days after vector injection.
(Transgene expression levels are normalized for those of the endogenous INSL6 gene).

To evaluate LV function, transthoracic echocardiography was performed at 2, 7, 30 60 and 90 days after myocardial infarction and transduction in sedated mice. LVEF and LVFS were significantly preserved in infarcted mice injected with AAV9-INSL6, compared to control animals. The effect persisted at long times after infarction (90 days), while cardiac performance was progressively deteriorated in control mice (LVEF: 33±5% *vs.* 47±4%; LVFS: 17±4% *vs.* 24±3% in control and INSL6-transduced animals respectively at day 90 after infarction; P <0.05 at all time points) (**Figure 4.45**).

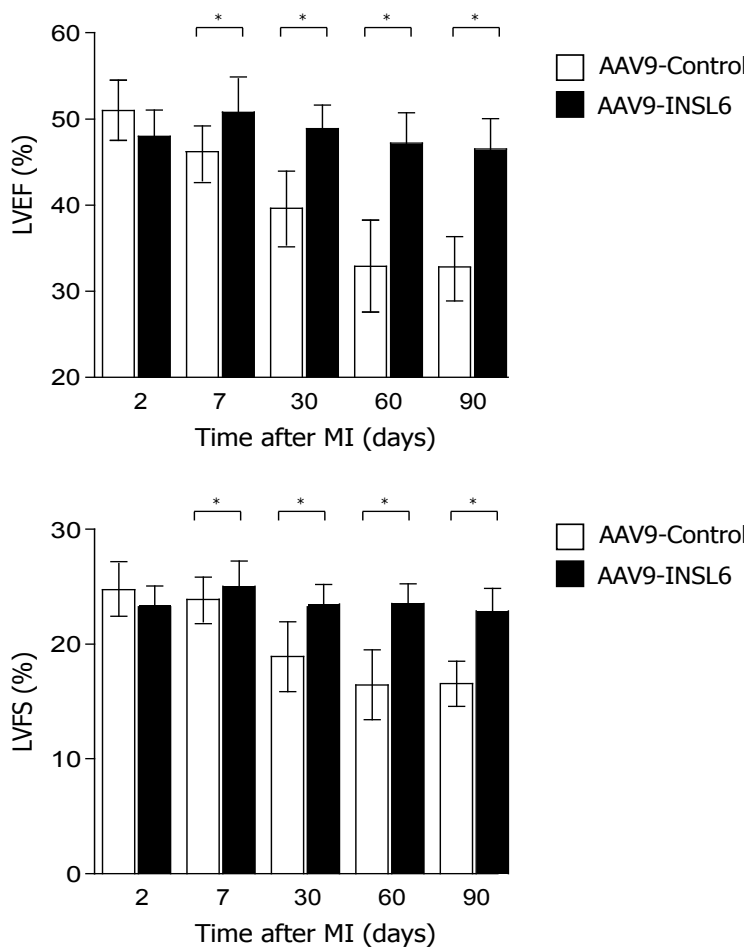

Figure 4.45 INSL6 AAV vector-mediated expression preserves cardiac function for long time after MI
Left Ventricular Ejection Fraction (LVEF) and Left Ventricular Fractional Shortening (LVFS) of infarcted mice treated with AAV9-INSL6 or AAV9-Control were measured by echocardiography. Values are expressed as mean ± SEM; **P*<0.05.

Another main difference between the two groups of animals was the size of the infarct scar, as assessed by echocardiographic analysis. The AAV9-Control-treated mice showed a significant worsening of the ischemic scar evolution; on the contrary the infarct size was preserved and eventually slightly reduced over time in the INSL6 expressing hearts (42.2±4.4% *vs.* 24.5±3.7% and 43.4±6.8% *vs.* 23.6±3.3% in control and INSL6-transduced animals respectively at day 30 and day 90 after infarction; *P* <0.05 at both time points) (**Figure 4.46**).

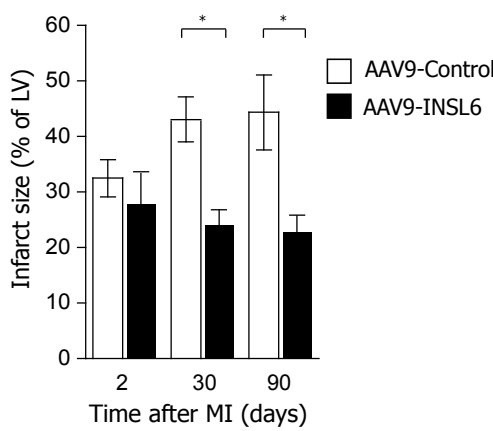

Figure 4.46 Reduction of infarct size in AAV9-INSL6 transduced hearts
Quantification of infarct size expressed as percentage of LV. Values are expressed as mean ± SEM; **P*<0.05.

4.6.2 INSL6 expression in infarcted hearts induces a marked decrease of myocardial apoptosis

At day 2 after myocardial infarction and AAV vectors delivery a set of 6 mice for group (Control vs AAV9-INSL6-transduced) was sacrificed and the hearts collected. Frozen sections of LV cardiac tissue were fixed in 4% PFA and TUNEL staining for apoptosis analysis was performed.

As it appears from the pictures in **Figure 4.47A,** the INSL6-expressing infarcted hearts exhibited a significant decrease in the number of apoptotic nuclei. **Figure 4.47B** reports a quantification of this result. In the animals treated with the control AAV vector, the percentage of apoptotic nuclei detected in the infarcted region at day 2 after infarction approached 30%, while this percentage was>5 times lower in the INSL6-expressing hearts (*P*<0.05).

This result strongly supported the hypothesis that also this gene, like the more extensively described secreted factor ghrelin, could immediately exert its beneficial properties on the damaged hearts, by reducing the cell death of myocytes located in the peri-infarctual region.

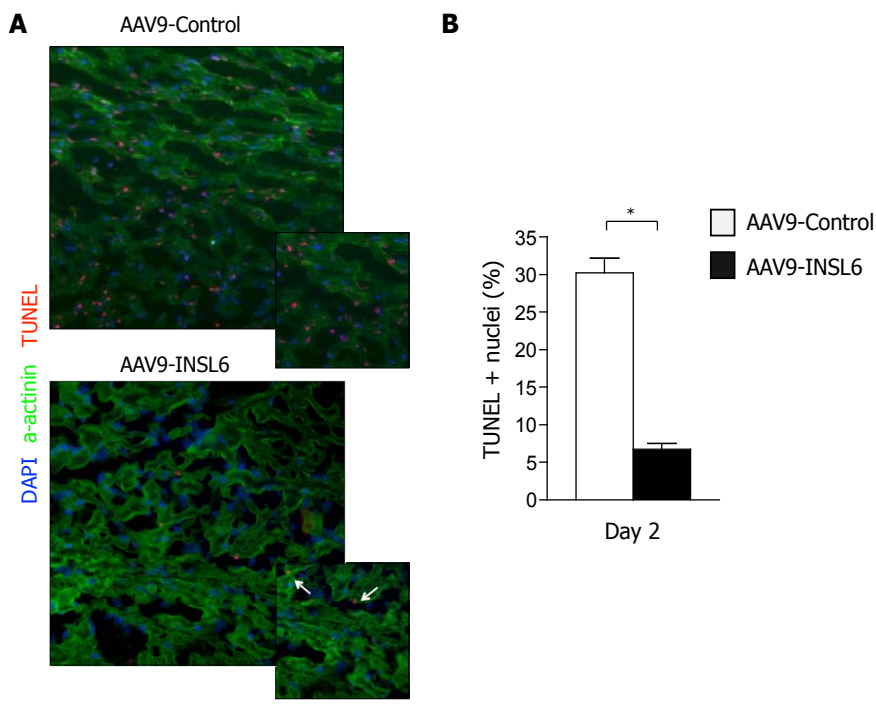

Figure 4.47 INSL6 anti-apoptotic effect on infarcted myocardium
A. Hearts injected with AAV9-Control or AAV9-INSL6 at 2 days after MI were stained to reveal apoptotic nuclei by TUNEL (red), cardiomyocytes using an antibody against α-actinin (green) and total nuclei with DAPI (blue).
B. Graph reporting quantification of positive nuclei (%). Values are expressed as mean ± SEM; **P*<0.05

The molecular mechanism by which INSL6 exerts its beneficial effects in the infarcted hearts clearly needs to be further elucidated. However, the promising preliminary data shown in this Thesis can be considered as convincing indications of the intrinsic validity of the **FunSel** strategy we designed.

5. DISCUSSION

5.1 DEVELOPMENT OF AN INNOVATIVE STRATEGY FOR THE *IN VIVO* FUNCTIONAL SELECTION OF AAV VECTORS EXPRESSING THERAPEUTIC GENES

Degenerative disorders include a broad category of pathologies, among which cardiovascular diseases, and represent a foremost health problem all over the world, essentially linked to the aging of the human population and to the inability of post-mitotic tissues to efficiently regenerate. The notably progresses recently achieved in understanding the cellular and molecular mechanisms driving tissue degeneration have increased the effort towards the development of novel biotherapeutics able to either prevent tissue damage or enhance tissue regeneration.

This Thesis' project stems exactly from these perspectives, since its final purpose was the identification and characterization of novel genes that could be exploited therapeutically for their beneficial properties towards cardiovascular disorders. The novelty resides in the innovative strategy we developed to identify candidate therapeutic factors, based on the possibility, given by AAV vectors, to screen nucleic acids libraries for a given function directly *in vivo*.

Following the birth of genetic engineering, the screening of genetic libraries has provided a powerful means for the rapid identification of therapeutic molecules. Many screenings of genetic libraries have been attempted in the recent past (Kitamura, 1998; Mahon and Whitehead, 2001). Collectively, these strategies have generated powerful biological information, with important repercussions for drug discovery. Unfortunately, however, in only a small percentage of cases the molecules emerging from *in vitro* studies

have advanced to clinical experimentation and entered medical therapy. On the contrary, the majority of the biological therapeutics currently in the clinics is either the result of serendipitous discovery or stem from the outcome of molecule identification based on pre-existing biological or biochemical information. For this reason, the possibility of screening nucleic acid libraries for a particular function directly *in vivo* appears to represent an outstanding tool to identify novel factors, selected by their own relevance in the target tissue.

So far, cDNA libraries have been generated in retroviral (Passioura et al., 2005) or adenoviral vectors (Hillgenberg et al., 2006; Michiels et al., 2002). The former vectors, however, only transduce replicating and not resting cells, while the latter induce a potent immunogenic response that leads to the elimination of the transduced cells in a relatively short time, thus preventing evaluation of the long term effects (Muruve, 2004). The development of our strategy was rendered possible by the availability of a vector system based on AAV, which is produced at very high titers, infects post-mitotic cells *in vivo* very efficiently, can be targeted to a specific tissue/organ and persists in the target cells for prolonged periods of time without transgene silencing (Schnepp et al., 2005). In addition, here we demonstrated the possibility to simultaneously generate pools of AAV vectors composed by a variable numbers of transgenes and use them to transduce cells *in vivo* very efficiently. Since AAV are able to infect cells at a relatively high multiplicity of infection, the strategy we devised entails an iterative procedure of *in vivo* selection, based on the progressive enrichment for one or more factors exerting a beneficial function and therefore favouring, round after round, the survival of the expressing cells.

In particular, in this Thesis we focused our attention on the functional selection, in different degenerative models, of a collection of murine secreted molecules. Once identified a potential beneficial effect of one or

more of these factors in the cardiovascular system, these might be clinically administered not only by gene therapy, but also as recombinant proteins.

5.1.1 Theoretical confirmation of the feasibility of the AAV-mediated *in vivo* functional selection

To validate the possibility to functionally select AAV transgenes *in vivo* through an iterative transduction procedure, we took into account all the variables possibly involved in this process and, by a series of mathematical considerations, we confirmed its theoretical feasibility.

Abundant and rare transcripts are similarly represented in the arrayed library and each clone has the same chance to be enriched during the iterative process of selection. Therefore, if at the beginning of the procedure, the abundance of an AAV coding for a specific transgene is one out of the total number of vectors in the pool (1/POOL), at the end of the experiment this ratio will be modified according to the influence of the different variables, and eventually will correspond to one out of the total number of selected vectors. In particular, six variables that affect the selection experiment have been considered: multiplicity of infection (MOI), transduction efficiency (ET), co-selection effect (COSEL), efficiency of selection (ES), complexity of vectors pools (POOL) and number of selection cycles (CYCLE).

Under ideal conditions, the multiplicity of infection is one (a single viral particle enters a cell, MOI=1), the selection is effective (no cells other than those containing the desired transgene are selected, ES=1) and there is no co-selection of cells not expressing the transgene (COSEL=0). In this case a single round of selection is potentially sufficient to completely select the transgene-expressing cells, independently from the efficiency of transduction (ET), the complexity of the pool (POOL) and the number of performed cycles (CYCLE).

However, during a real selection procedure, most probably ideal conditions will not be met, and therefore a mathematical equation was derived to take into account all the parameters that could affect the procedure. We noticed that, in the case we could efficiently recover all the cells containing the desired transgene (ES=1), the MOI has a very important effect on the selection efficiency, and should anyhow be lower than 10 to permit effective selection. We also observed that the COSEL and ET parameters are strictly correlated; of course, the first becomes less relevant as the second decreases. As mentioned before, when ES=1, performing subsequent cycles of selection does not improve transgene enrichment because it is assumed that only cells containing the transgene are still alive after the selection. Similarly, the vector pool complexity also has no influence.

In the most probable case *in vivo*, ES is less than 1, hence a certain number of cells not containing the desired transgene survive the selection. In this condition, the complexity of the initial pool of vectors (POOL) becomes very important and an increase in the AAV pool complexity or a decrease in the ES are paralleled by a dramatic decrease in the probability of selecting the desired transgene. Whether ES<1, the performance of the process is substantially increased by performing iterative rounds of selection. The strategy we established indeed entails the recovery, by PCR, of all transgenes from the tissues surviving the selection procedure and the re-cloning of these inserts into the vector plasmid to obtain a novel vector pool, which is resubmitted to the selection process. At every cycle, we expect that the ratio between the desired transgene and all the other clones progressively increases. Indeed, this was fully confirmed by the mathematical model analysis, considering many possible values for the ET, MOI, COSEL, ES and POOL variables.

Taken together, the theoretical considerations illustrated by the mathematical analysis clearly supported the feasibility of the functional selection (**FunSel**) approach.

5.1.2 Recombinant AAV vectors can be generated in pools

Once demonstrated the theoretical feasibility of the *in vivo* selection strategy, we started generating an arrayed library of clones to be tested by the described approach. This library derived from the mouse secretome collection, a subset of cDNAs from the RIKEN mouse genes encyclopedia (Grimmond et al., 2003). In particular, we selected 100 full-length cDNAs mainly coding for hormones and growth factors, and cloned them individually into an AAV backbone plasmid for AAV vectors production.

For the first time, we confirmed that recombinant AAV vectors can be generated in pools. In practical terms, we obtained single viral preparations expressing 10 (or more) different genes, just mixing proportional amounts of each AAV plasmid with the desired packaging plasmid and transfecting this mixture into HEK 293T cells for viral production. An accurate, PCR-based analysis on the viral genomes obtained after pooled AAV vectors production demonstrated that all the transgenes composing the pool were represented in the viral preparation.

5.1.3 Definition of critical requirements influencing packaging, *in vivo* transduction and expression of pooled AAV genomes

Based on the results obtained by AAV vector pooled production we investigated the critical elements influencing essential steps of this process, such as viral genomes packaging, *in vivo* transduction efficiency and level of transgene overexpression.

Comparable size of vector transgenes guarantees faithful maintenance of individual gene representation during pooled production

In the devised *in vivo* selection procedure, pools of AAV vectors are simultaneously generated in HEK 293T cells and then used for *in vivo* transduction. An essential requisite of the procedure, therefore, is that packaging of multiple AAV vectors occurs simultaneously in the producing cells and that no significant biased is introduced at this step. In order to confer to all the vectors the same chance to be effective in the target tissue and to be selected after damage only for their functional properties, a balanced representation of all the transgenes in each vector pool must be guaranteed.

The relevance of genome size on AAV packaging has been extensively described by many groups (Allocca et al., 2008; Grieger and Samulski, 2005; Wu et al., 2010). In particular, it is known that smaller DNAs are packaged more efficiently. So far, however, there have been not systematic studies on the mutual influence of genomes of similar or different sizes, pooled together to generate a single viral preparation. For this reason we investigated whether differences in genome size between the different vectors composing a pool, or the total number of vectors in a pool, could affect the packaging properties of each individual AAV.

First of all, we generated a pool composed of 25 vectors of different size and quantified the relative amount of 10 randomly chosen clones in the AAV plasmids preparation, prepared mixing equimolar amount of each plasmid, and in the corresponding viral lysate obtained after pooled AAV vector production. As expected, the representation of the constructs in the viral preparations remained substantially similar to that in the pool of plasmids. Despite a clear trend of decreased packaging efficiency for longer genomes, for 9 out of 10 clones these differences were within a narrow

window of ±2 fold of variation from the expected value, which appears to be an acceptable range in the context of pooled AAV production. The results obtained by analyzing clones with large size (>1500 bp) in the context of pools of heterogeneous size vs. pools of similar large size clearly indicated that the homogeneity of vector insert length was a major parameter to be taken into account during pooled AAV production.

In summary, the results obtained: i) confirmed the relevance of mutual influence among the genomes composing a pool during the viral packaging process, ii) were against the possibility that the packaging limits of the longer genomes observed in the non-homogeneous pool might be due to their specific sequences and iii) highlighted that the generation of AAV pools homogeneous for size is an essential requirement, which is particularly relevant for constructs carrying inserts >1500-2000 bp, which may be disfavored in competitive packaging.

Pool complexity does not influence viral packaging efficiency

To evaluate the influence that an increasing number of clones in a pool could have on their own packaging ability into the corresponding viral particles, we compared the packaging capacity of the genes analyzed in AAV2-Pool25, when included in a pool of 50 or 100 different vectors. As in the previous experiment, an excellent conservation of the investigated, individual clones representation in AAV2-Pool50 and AAV2-Pool100 was observed (variations still in the range of ±2 fold from the expected value), with the exception of the two longer genes, which were packaged less efficiently, similarly to the results obtained with the AAV2-Pool25. Also in this case, we established that the comparable size of the pooled genomes represents an important requirement for equimolar packaging of viral particles. In contrast, the total number of different vectors composing the pool does not seem to significantly influence packaging, indicating that the number of genomes is not limiting for the packaging process itself.

In conclusion, when considered collectively, these results confirmed the possibility to simultaneously package into viral particles several AAV constructs (at least 100) carrying different transgenes. In addition, the individual representation of each construct in the vectors pool fairly reproduced its original proportion in the mix of plasmids, as long as the genomes included in the pool carried inserts of comparable size.

Multiple AAV vectors equally transduce skeletal muscle and persist in the tissue for a long time

An additional major question we investigated was whether individual AAV vectors maintain their infectivity *in vivo* when present in a pool. To address this issue, we quantified the relative abundance of the same 10 previously investigated clones before and 3 days after *in vivo* transduction of the original AAV2-Pool25 into murine tibialis anterior skeletal muscle. We observed that all the viral particles transduced the tissue, that the ratio between their abundance in the original vector preparation and *in vivo* was maintained, and that no major bias in infectivity occurred.

Subsequently, we checked whether the relative vector abundance was maintained over time in the transduced tissue. Of course, answer to this question was not only a matter of AAV vector biology but also strictly correlated with the biology of each single transgene.

As expected, we confirmed the already described decrease of almost one order of magnitude in the global levels of AAV genomes one month after skeletal muscle transduction (Tafuro et al., 2009). Despite this drop, viral DNAs were still clearly detectable in the tissue at this time, thus supporting the *in vivo* persistence of the vector genomes. After quantification, we noticed that the relative abundance of single clones in the muscle was maintained in the same proportion as in the initial viral preparation for 8 out of 10 genes, while two clones resulted enriched after 1 month.

A similar result might be explained speculating that, over this time period, genes exerting a toxic effect would be progressively more depleted from the pool than neutral transgenes while, on the other side, transgenes with beneficial properties on the muscle would be preferentially maintained. In particular, the enrichment of the E2 transgene, which encodes for the endocrine factor ghrelin, at a first examination might appear surprising, however if we consider the results obtained by analyzing the functions of ghrelin in the cardiac and muscle systems, it can be reasonably speculated that its relative enrichment is most likely due to the powerful protective effect exerted by this gene on muscle fibers. As far as the second enriched transgene, instead, it encodes for gastrin, a peptide able to promote contraction on antral smooth muscle cells (Jarrousse et al., 2004), but never associated with a specific function on skeletal muscle so far.

Taking into account these results, we can certainly state that we need to carefully define the timing for viral DNA rescue after *in vivo* functional selection, in order to guarantee enrichment of pro-surviving genes triggered by damage. For this reason, in the following experiments we fixed two weeks after selection induction as the timing for vector genomes recovery.

Proportional maintenance of individual AAV vector expression in vivo according to pool complexity

A final question we wanted to answer was whether expression from the same vector was maintained proportionally to its abundance in the pool upon injection *in vivo*. To address this issue, we quantified the level of expression of two transgenes when transduced into the skeletal muscle as individual vectors or in pools of 25, 50 of 100 AAVs, 15 days after transduction. The experimental results indicated that each individual plasmid was still transcribed when present in the context of a complex pool of vectors (i.e., there was no appreciable saturation of CMV promoter-

driven transcription, and that there was a fair proportionality between the individual clone representation in the AAV mix and the levels of expression of its individual transgene). Despite the considerable dilution of each clone included in the AAV2-Pool100, we still observed a level of expression that exceeded 5-fold that of the endogenous transcript. From this consideration we can conclude that even if AAV pool complexity does not affect viral packaging, it certainly influences the levels of individual transgene overexpression and therefore the generation of pools of vectors composed by a limited number of different clones represents an essential requirement for the implementation of the strategy. Obviously, it is impossible to determine what would be the optimal levels of expression of an individual transgene endowed with potential protective function on the myocardium. In the subsequent experiments, therefore, to guarantee effectiveness of the *in vivo* selection strategy, vectors pools had a complexity of 10 clones, in order to guarantee expression of individual transgenes at levels at least 50-fold higher than their endogenous counterparts.

To summarize, the results shown in this Thesis' section indicate that:

i) Almost 85% of secreted factor cDNAs can be cloned into AAV plasmids and used to obtain infectious AAV vectors.

ii) Multiple AAV vectors can be packaged simultaneously; competition for packaging is more prominent for clones with insert size >1500 bp and this problem can be overcome by packaging clones with insert having similar size.

iii) AAV vector preparations consisting of multiple clones are infectious *in vivo*, where representation of each vector is maintained.

iv) Expression of individual vectors from vector pools is fairly proportional to their relative representation.

5.2 THE SECRETED FACTORS GHRELIN AND INSL6 RESULTED ENRICHED AFTER *IN VIVO* FUNCTIONAL SELECTION IN TWO MODELS OF ISCHEMIC DAMAGE

Collectively, the experiments of validation and setting of the **FunSel** strategy appear to fully support the feasibility of the *in vivo* screening project based on transduction with multiple AAV vector pools. Starting from this evidence, we organized the collection of 100 AAV plasmids coding for secreted molecules in pools composed of 10 different clones with comparable genome size.

In order to identify novel pro-surviving factors that could potentially be exploited therapeutically, we took advantage of two murine models of ischemic disorders, a model of skeletal muscle hind limb ischemia and a model of isoproterenol-induced acute cardiac damage. These models guarantee a diffuse damage in the target tissue and thus perfectly fit with the requirement of **FunSel** principles, which entail the functional selection of vectors expressing pro-surviving or pro-regenerating genes. It has extensively been shown that several molecules protecting skeletal muscle, such as IGF-I and VEGF-A, also exert a comparable beneficial effect on cardiomyocytes (Arsic et al., 2004; Barton et al., 2002; Ferrarini et al., 2006; Jacquier et al., 2007; Rissanen et al., 2005; Su et al., 2003).

5.2.1 Ghrelin as a protective gene selected after skeletal muscle damage

For the functional selection in the skeletal muscle, we pooled three AAV serotype 2 group of vectors, each one containing 10 constructs of comparable genome size, obtaining a final viral preparation of 30 vectors that we injected into the tibialis anterior muscle of both legs of CD1 mice.

Afterwards, hind-limb ischemia was induced only in the right limb to trigger the functional selection of the viral genomes.

Three successive rounds of *in vivo* injection of the AAV pools, uni-lateral induction of ischemia, recovery of viral DNA from both the ischemic and the non-ischemic muscles and production of novel viral preparations generated from the pooled re-cloning of the rescued genomes, were required to detect enrichment of a candidate gene among the genomes recovered from the ischemic legs.

The enriched vector, progressively selected for its own function *in vivo,* codes for the secreted hormone Ghrelin, a peptide mainly produced by the stomach (Kojima et al., 1999) and involved in neuroendocrine and metabolic metabolism. However, a growing body of literature about this gene recently profiled a complex range of functions for this peptide, which involve many different tissues, among which also the heart. Also relevant to the results presented here, it was shown that ghrelin induce differentiation of C2C12 myoblasts by inhibiting their proliferation and favoring their differentiation (Filigheddu et al., 2007).

All these findings suggest that the identification of ghrelin as candidate gene in this experimental model is fully consistent with the principle of **FunSel**, and supports its efficacy.

5.2.2 Implementation of the selection strategy in a model of isoproterenol-induced cardiac damage identified INSL6 as a candidate protective gene

We also exploited a model of isoproterenol-induced acute cardiac damage to test selection of our AAV clone collection. A single intraperitoneal administration of high dosage of isoproterenol causes cardiomyocyte necrosis and interstitial fibrosis (Benjamin et al., 1989; Grimm et al.,

1998a), and the induced ischemic-like lesion is widespread in all the myocardium, thus representing an efficient selection driver.

For this second selection approach, we screened the full AAV collection of 100 secreted factors, again organized in pool composed by 10 vectors each. We generated 10 pools of AAV vectors with capsid 9 (this serotype transduces cardiomyocytes very efficiently), and in this case we selected them individually *in vivo*. The AAV pools were delivered by intraperitoneal (IP) injection in newborn mice, since this represents a very effective route of administration to obtain whole heart transduction), followed by a single acute IP administration of a toxic dose of isoproterenol.

While for 9 out of 10 pools after the first round of selection we could not observe any difference in the genome composition of the vector pools rescued from the heart of mice submitted to isoproterenol treatment compared to control animals, very unexpectedly one pool revealed the clear enrichment of a single clone, corresponding to the insulin-like peptide 6 (INSL6) cDNA.

INSL6 is a poorly characterized growth factor belonging to the well-known insulin/relaxin superfamily. Its identification in the screening appears very interesting, because this factor represents really a novel secreted molecule, never associated with the cardiovascular system.

The anti-fibrotic properties of relaxin have been extensively described in the past. The local production of this peptide by cardiomyocytes was related to a possible beneficial role of this molecule in cardiac disease conditions (Teichman et al., 2010). On the contrary, INSL6 has mainly been associated with germ cell development so far (Burnicka-Turek et al., 2009) and its identification as a candidate protective gene in a model of cardiac fibrosis makes it a very attractive factor to be further investigated. It is important to notice that we focused our attention on INSL6 because of its surprising enrichment already after a single cycle of selection in the heart,

and thus we stopped the screening; it is possible that subsequent rounds of selection would have brought to light other interesting secreted factors, including ghrelin, however maybe less effective than INSL6 in this experimental model.

5.3 AAV9-MEDIATED GHRELIN EXPRESSION IN THE MOUSE HEART IMPROVES CARDIAC FUNCTION AFTER INFARCTION

The molecules identified by the *in vivo* functional selection were afterwards characterized for their protective potential against myocardial infarction.

5.3.1 AAV9-Ghrelin prevents neonatal rat cardiomyocytes cell death *in vitro*

With reference to ghrelin we initially tested its effects *in vitro*. Neonatal rat cardiomyocyte cultures were established according to conditions already set up by the laboratory (Collesi et al., 2008), transduced with an AAV9 vector expressing ghrelin and then treated with two toxic drugs inducing cell death, namely isoproterenol and doxorubicin. In both cases ghrelin exerted a potent pro-surviving effect on cardiomyocytes, confirming the anti-apoptotic properties of this peptide, already described in other cell systems (Kim et al., 2004; Kim et al., 2005).

As mentioned in the Results section, the AAV vector we generated codes for the ghrelin precursor, which is then cleaved to give rise to the mature peptide. Since the GOAT enzyme is expressed at very low levels in cardiomyocytes, compared to the gut (Lim et al., 2011; Lin et al., 2011), it is expected that the prevalent form of the peptide in the cells will be des-acylated. It is thus des-acyl ghrelin that exerts most of the observed pro-

surviving effect in cardiomyocytes, confirming the findings of other groups in other cell models (Baldanzi et al., 2002; Granata et al., 2007).

5.3.2 Cardiac gene transfer of ghrelin exerts beneficial effects after myocardial infarction in mice

Following the results obtained *in vitro*, we investigated the effectiveness of AAV9-Ghrelin in a model of murine cardiac infarction, induced by left descendent coronary artery ligation, as previously described (Gao et al., 2000).

After 3 months of follow-up, LV ejection fraction and fractional shortening of infarcted mice transduced with ghrelin were significantly preserved, while cardiac performance progressively deteriorated in control mice. In addition, LV wall thickness and both global and regional contractile function were not significantly changed compared to baseline in AAV9-Ghrelin transduced hearts. The fibrotic area was consistently smaller in these animals, which exhibited reduced infarct size and no LV dilation. A very interesting observation is that these parameters were still improving after 90 days.

The protection from apoptosis observed in cultured cardiomyocytes was clearly evident also *in vivo*, 2 days after intracardiac AAV9-Ghrelin vector delivery and MI induction, thus explaining the consistent decreased loss of cardiac mass exhibited by ghrelin overexpressing mice.

In addition, a prominent reduction in the massive inflammatory cells infiltration usually occurring soon after damage in the peri-infarctual region was also observed in the ghrelin-treated animals, thus confirming the anti-inflammatory properties of this peptide (Huang et al., 2009; Li et al., 2004). Moreover, the levels of induction of genes generally overexpressed under inflammatory conditions, such as IL1-β, IL6 and TNFα were significantly decreased.

Recently, it was demonstrated that, after cardiac damage, miR-21 is strongly upregulated in fibroblasts (Thum et al., 2008). This overexpression contributes to fibrotic tissue deposition and cardiac hypertrophy, also through a direct action of the miR-21 on MMP-2 expression (Roy et al., 2009). Our data are fully consistent with these findings. Indeed, after myocardial infarction, we observed a massive induction of miR-21 and MMP-2 transcription in control animals, while the ghrelin-treated mice exhibited a normalization of the levels of activation of these genes.

In agreement with the echocardiographic observations, we also noticed that AAV9-Ghrelin transduced mice did not exhibit the typical pattern of deregulated gene expression usually associated with pathological LV remodeling (Gidh-Jain et al., 1998). Ghrelin overexpression indeed significantly counteracted the increase in transcriptional levels of genes such as β-MHC and the cardiac natriuretic peptides (ANF and BNP), which we instead observed in control animals, and also normalized the expression of markers like α-MHC, Serca2a, RYR2 and PGC1α, typically downregulated in pathological hypertrophy conditions.

The major conclusion that can be drown from these results is that a persistent expression of Ghrelin after myocardial infarction exerts prolonged beneficial effects in terms of contractility, preservation of viable cardiac tissue and prevention of pathological LV remodeling. The anti-apoptotic and anti-inflammatory actions of this gene soon after infarction certainly contributed to the preservation of cardiac function, impeding a massive loss of myocardial tissue and therefore maintaining contractility and wall thickening after damage.

The definition of the relative contribution of acylated and des-acylated ghrelin in protecting the infarcted myocardium still needs to be clearly defined, in order to clarify and eventually definitively demonstrate the presence, in the cardiac tissue, of a receptor alternative to the acyl- specific

GHSR-1a, and thus able to also bind des-acyl ghrelin (Lear et al., 2010; Li et al., 2006). Different groups have hypothesized the existence of this putative receptor, showing the effectiveness of both acyl and des-acyl ghrelin in different cell types, not expressing GHSR-1a (Gauna et al., 2006; Muccioli et al., 2004; Thompson et al., 2004). The potential observation of the AAV9-Ghrelin beneficial effects in GHSR null mice (Sun et al., 2004) submitted to myocardial infarction could represent a final demonstration of the outstanding role of this alternative receptor in supporting the cardioprotective functions of this molecule.

5.4 CARDIAC GENE TRANSFER OF INSL6 EXERTS BENEFICIAL EFFECTS AFTER MYOCARDIAL INFARCTION IN MICE

As we did for Ghrelin, the other secreted factor identified by the *in vivo* functional selection, namely INSL6, was also afterwards characterized for its protective potential against myocardial infarction.

AAV9-mediated INSL6 expression in infarcted mouse hearts improved cardiac performance preserving LV ejection fraction and LV fractional shortening and reducing the ischemic scar evolution after three months. Unexpectedly, a reduction in infarct size was observed in these animals already at day 2 after damage, and infarcts remained smaller than in the controls over time. As we described for ghrelin-transduced animals also INSL6 overexpressing hearts exhibited a marked decrease in myocardial apoptosis soon after infarction.

In this Thesis we report only preliminary data related to the INSL6 cardioprotective effects. A more extensive characterization of the functions of this molecule in the ischemic heart will certainly be required, especially

should this molecule be further considered potential therapeutic applications. Of notice, our results are consistent with the recent evidence that INSL6 acts as a pro-regenerative factor in conditions of muscular injury induced by cardiotoxin (Zeng et al., 2010), thus confirming the concept that several molecules protecting skeletal muscle often also exert a comparable beneficial effect on cardiomyocytes.

CONCLUSIONS

In conclusion, in this Thesis work we propose for the first time the development of **FunSel**, an innovative functional selection procedure, based on *in vivo* gene transfer of an arrayed library cloned into AAV vectors, for the identification of novel secreted factors sustaining cardiac function. Collectively, the obtained results support both the theoretical and technical feasibility of this strategy and fully validate the possibility to generate and transduce *in vivo* multiple AAV vector pools and to screen them for their functional effect under degenerative conditions. The detected cardioprotective effect of Ghrelin and INSL-6 not only represent a proof-of-principle of the efficacy of the **FunSel** procedure, but also represent a potentially interesting result by itself. The dissection of the molecular pathways through which the two factors exert their beneficial activity will represent an important experimental goal for the near future.

6. BIBLIOGRAPHY

Abrescia, P., and Golino, P. (2005). Free radicals and antioxidants in cardiovascular diseases. Expert Rev Cardiovasc Ther *3*, 159-171.

Agata, J., Chao, L., and Chao, J. (2002). Kallikrein gene delivery improves cardiac reserve and attenuates remodeling after myocardial infarction. Hypertension *40*, 653-659.

Agrawal, R.S., Muangman, S., Layne, M.D., Melo, L., Perrella, M.A., Lee, R.T., Zhang, L., Lopez-Ilasaca, M., and Dzau, V.J. (2004). Pre-emptive gene therapy using recombinant adeno-associated virus delivery of extracellular superoxide dismutase protects heart against ischemic reperfusion injury, improves ventricular function and prolongs survival. Gene Ther *11*, 962-969.

Ahmet, I., Sawa, Y., Iwata, K., and Matsuda, H. (2002). Gene transfection of hepatocyte growth factor attenuates cardiac remodeling in the canine heart: A novel gene therapy for cardiomyopathy. J Thorac Cardiovasc Surg *124*, 957-963.

Ait-Oufella, H., Taleb, S., Mallat, Z., and Tedgui, A. (2011). Recent advances on the role of cytokines in atherosclerosis. Arterioscler Thromb Vasc Biol *31*, 969-979.

Akache, B., Grimm, D., Pandey, K., Yant, S.R., Xu, H., and Kay, M.A. (2006). The 37/67-kilodalton laminin receptor is a receptor for adeno-associated virus serotypes 8, 2, 3, and 9. J Virol *80*, 9831-9836.

Alexander, I.E., Russell, D.W., and Miller, A.D. (1994). DNA-damaging agents greatly increase the transduction of nondividing cells by adeno-associated virus vectors. J Virol *68*, 8282-8287.

Alloatti, G., Arnoletti, E., Bassino, E., Penna, C., Perrelli, M.G., Ghe, C., and Muccioli, G. (2010). Obestatin affords cardioprotection to the ischemic-reperfused isolated rat heart and inhibits apoptosis in cultures of similarly stressed cardiomyocytes. Am J Physiol Heart Circ Physiol *299*, H470-481.

Allocca, M., Doria, M., Petrillo, M., Colella, P., Garcia-Hoyos, M., Gibbs, D., Kim, S.R., Maguire, A., Rex, T.S., Di Vicino, U.*, et al.* (2008). Serotype-dependent packaging of large genes in adeno-associated viral vectors results in effective gene delivery in mice. J Clin Invest *118*, 1955-1964.

Andersen, D.C., Andersen, P., Schneider, M., Jensen, H.B., and Sheikh, S.P. (2009). Murine "cardiospheres" are not a source of stem cells with cardiomyogenic potential. Stem Cells *27*, 1571-1581.

Anderson, J.L., Adams, C.D., Antman, E.M., Bridges, C.R., Califf, R.M., Casey, D.E., Jr., Chavey, W.E., 2nd, Fesmire, F.M., Hochman, J.S., Levin, T.N.*, et al.* (2007). ACC/AHA 2007 guidelines for the management of patients with unstable angina/non-ST-Elevation myocardial infarction: a report of the American College of Cardiology/American Heart Association Task Force on Practice Guidelines (Writing Committee to Revise the 2002 Guidelines for the Management of Patients With

Unstable Angina/Non-ST-Elevation Myocardial Infarction) developed in collaboration with the American College of Emergency Physicians, the Society for Cardiovascular Angiography and Interventions, and the Society of Thoracic Surgeons endorsed by the American Association of Cardiovascular and Pulmonary Rehabilitation and the Society for Academic Emergency Medicine. J Am Coll Cardiol *50*, e1-e157.

Anderson, L.L., Jeftinija, S., and Scanes, C.G. (2004). Growth hormone secretion: molecular and cellular mechanisms and in vivo approaches. Exp Biol Med (Maywood) *229*, 291-302.

Aoki, M., Morishita, R., Taniyama, Y., Kida, I., Moriguchi, A., Matsumoto, K., Nakamura, T., Kaneda, Y., Higaki, J., and Ogihara, T. (2000). Angiogenesis induced by hepatocyte growth factor in non-infarcted myocardium and infarcted myocardium: up-regulation of essential transcription factor for angiogenesis, ets. Gene Ther *7*, 417-427.

Ariyasu, H., Takaya, K., Tagami, T., Ogawa, Y., Hosoda, K., Akamizu, T., Suda, M., Koh, T., Natsui, K., Toyooka, S.*, et al.* (2001). Stomach is a major source of circulating ghrelin, and feeding state determines plasma ghrelin-like immunoreactivity levels in humans. J Clin Endocrinol Metab *86*, 4753-4758.

Arsic, N., Zacchigna, S., Zentilin, L., Ramirez-Correa, G., Pattarini, L., Salvi, A., Sinagra, G., and Giacca, M. (2004). Vascular endothelial growth factor stimulates skeletal muscle regeneration in vivo. Mol Ther *10*, 844-854.

Arsic, N., Zentilin, L., Zacchigna, S., Santoro, D., Stanta, G., Salvi, A., Sinagra, G., and Giacca, M. (2003). Induction of functional neovascularization by combined VEGF and angiopoietin-1 gene transfer using AAV vectors. Mol Ther *7*, 450-459.

Asokan, A., Hamra, J.B., Govindasamy, L., Agbandje-McKenna, M., and Samulski, R.J. (2006). Adeno-associated virus type 2 contains an integrin alpha5beta1 binding domain essential for viral cell entry. J Virol *80*, 8961-8969.

Atchison, R.W., Casto, B.C., and Hammon, W.M. (1965). Adenovirus-Associated Defective Virus Particles. Science *149*, 754-756.

Atluri, P., and Woo, Y.J. (2008). Pro-angiogenic cytokines as cardiovascular therapeutics: assessing the potential. BioDrugs *22*, 209-222.

Auricchio, A., O'Connor, E., Weiner, D., Gao, G.P., Hildinger, M., Wang, L., Calcedo, R., and Wilson, J.M. (2002). Noninvasive gene transfer to the lung for systemic delivery of therapeutic proteins. J Clin Invest *110*, 499-504.

Baker, J.G., Hill, S.J., and Summers, R.J. (2011). Evolution of beta-blockers: from anti-anginal drugs to ligand-directed signalling. Trends Pharmacol Sci *32*, 227-234.

Baldanzi, G., Filigheddu, N., Cutrupi, S., Catapano, F., Bonissoni, S., Fubini, A., Malan, D., Baj, G., Granata, R., Broglio, F.*, et al.* (2002). Ghrelin and des-acyl ghrelin inhibit cell death in cardiomyocytes and endothelial cells through ERK1/2 and PI 3-kinase/AKT. J Cell Biol *159*, 1029-1037.

Balsam, L.B., Wagers, A.J., Christensen, J.L., Kofidis, T., Weissman, I.L., and Robbins, R.C. (2004). Haematopoietic stem cells adopt mature haematopoietic fates in ischaemic myocardium. Nature *428*, 668-673.

Bani, D., Masini, E., Bello, M.G., Bigazzi, M., and Sacchi, T.B. (1998). Relaxin protects against myocardial injury caused by ischemia and reperfusion in rat heart. Am J Pathol *152*, 1367-1376.

Bantel-Schaal, U., Braspenning-Wesch, I., and Kartenbeck, J. (2009). Adeno-associated virus type 5 exploits two different entry pathways in human embryo fibroblasts. J Gen Virol *90*, 317-322.

Barazzoni, R., Bosutti, A., Stebel, M., Cattin, M.R., Roder, E., Visintin, L., Cattin, L., Biolo, G., Zanetti, M., and Guarnieri, G. (2005). Ghrelin regulates mitochondrial-lipid metabolism gene expression and tissue fat distribution in liver and skeletal muscle. Am J Physiol Endocrinol Metab *288*, E228-235.

Barile, L., Messina, E., Giacomello, A., and Marban, E. (2007). Endogenous cardiac stem cells. Prog Cardiovasc Dis *50*, 31-48.

Barreras, A., and Gurk-Turner, C. (2003). Angiotensin II receptor blockers. Proc (Bayl Univ Med Cent) *16*, 123-126.

Bartlett, J.S., Kleinschmidt, J., Boucher, R.C., and Samulski, R.J. (1999). Targeted adeno-associated virus vector transduction of nonpermissive cells mediated by a bispecific F(ab'gamma)2 antibody. Nat Biotechnol *17*, 181-186.

Bartlett, J.S., Wilcher, R., and Samulski, R.J. (2000). Infectious entry pathway of adeno-associated virus and adeno-associated virus vectors. J Virol *74*, 2777-2785.

Barton, E.R., Morris, L., Musaro, A., Rosenthal, N., and Sweeney, H.L. (2002). Muscle-specific expression of insulin-like growth factor I counters muscle decline in mdx mice. J Cell Biol *157*, 137-148.

Bathgate, R.A., Ivell, R., Sanborn, B.M., Sherwood, O.D., and Summers, R.J. (2006). International Union of Pharmacology LVII: recommendations for the nomenclature of receptors for relaxin family peptides. Pharmacol Rev *58*, 7-31.

Bathgate, R.A., Samuel, C.S., Burazin, T.C., Layfield, S., Claasz, A.A., Reytomas, I.G., Dawson, N.F., Zhao, C., Bond, C., Summers, R.J.*, et al.* (2002). Human relaxin gene 3 (H3) and the equivalent mouse relaxin (M3) gene. Novel members of the relaxin peptide family. J Biol Chem *277*, 1148-1157.

Baumgartner, I., Pieczek, A., Manor, O., Blair, R., Kearney, M., Walsh, K., and Isner, J.M. (1998). Constitutive expression of phVEGF165 after intramuscular gene transfer promotes collateral vessel development in patients with critical limb ischemia. Circulation *97*, 1114-1123.

Bearzi, C., Rota, M., Hosoda, T., Tillmanns, J., Nascimbene, A., De Angelis, A., Yasuzawa-Amano, S., Trofimova, I., Siggins, R.W., Lecapitaine, N.*, et al.* (2007). Human cardiac stem cells. Proc Natl Acad Sci U S A *104*, 14068-14073.

Bedendi, I., Alloatti, G., Marcantoni, A., Malan, D., Catapano, F., Ghe, C., Deghenghi, R., Ghigo, E., and Muccioli, G. (2003). Cardiac effects of ghrelin and its endogenous derivatives des-octanoyl ghrelin and des-Gln14-ghrelin. Eur J Pharmacol *476*, 87-95.

Bednarek, M.A., Feighner, S.D., Pong, S.S., McKee, K.K., Hreniuk, D.L., Silva, M.V., Warren, V.A., Howard, A.D., Van Der Ploeg, L.H., and Heck, J.V. (2000). Structure-function studies on the new growth hormone-releasing peptide, ghrelin: minimal sequence of ghrelin necessary for activation of growth hormone secretagogue receptor 1a. J Med Chem *43*, 4370-4376.

Beitnes, J.O., Hopp, E., Lunde, K., Solheim, S., Arnesen, H., Brinchmann, J.E., Forfang, K., and Aakhus, S. (2009). Long-term results after intracoronary injection of autologous mononuclear bone marrow cells in acute myocardial infarction: the ASTAMI randomised, controlled study. Heart *95*, 1983-1989.

Beltrami, A.P., Barlucchi, L., Torella, D., Baker, M., Limana, F., Chimenti, S., Kasahara, H., Rota, M., Musso, E., Urbanek, K.*, et al.* (2003). Adult cardiac stem cells are multipotent and support myocardial regeneration. Cell *114*, 763-776.

Benjamin, I.J., Jalil, J.E., Tan, L.B., Cho, K., Weber, K.T., and Clark, W.A. (1989). Isoproterenol-induced myocardial fibrosis in relation to myocyte necrosis. Circ Res *65*, 657-670.

Bergmann, O., Bhardwaj, R.D., Bernard, S., Zdunek, S., Barnabe-Heider, F., Walsh, S., Zupicich, J., Alkass, K., Buchholz, B.A., Druid, H.*, et al.* (2009). Evidence for cardiomyocyte renewal in humans. Science *324*, 98-102.

Bernardo, B.C., Weeks, K.L., Pretorius, L., and McMullen, J.R. (2010). Molecular distinction between physiological and pathological cardiac hypertrophy: experimental findings and therapeutic strategies. Pharmacol Ther *128*, 191-227.

Berns, K.I. (1990). Parvovirus replication. Microbiol Rev *54*, 316-329.

Berry, M.F., Pirolli, T.J., Jayasankar, V., Morine, K.J., Moise, M.A., Fisher, O., Gardner, T.J., Patterson, P.H., and Woo, Y.J. (2004). Targeted overexpression of leukemia inhibitory factor to preserve myocardium in a rat model of postinfarction heart failure. J Thorac Cardiovasc Surg *128*, 866-875.

Bers, D.M. (2008). Calcium cycling and signaling in cardiac myocytes. Annu Rev Physiol *70*, 23-49.

Bish, L.T., Morine, K., Sleeper, M.M., Sanmiguel, J., Wu, D., Gao, G., Wilson, J.M., and Sweeney, H.L. (2008). Adeno-associated virus (AAV) serotype 9 provides global cardiac gene transfer superior to AAV1, AAV6, AAV7, and AAV8 in the mouse and rat. Hum Gene Ther *19*, 1359-1368.

Blankinship, M.J., Gregorevic, P., Allen, J.M., Harper, S.Q., Harper, H., Halbert, C.L., Miller, A.D., and Chamberlain, J.S. (2004). Efficient transduction of skeletal muscle using vectors based on adeno-associated virus serotype 6. Mol Ther *10*, 671-678.

Blinderman, C.D., Homel, P., Billings, J.A., Portenoy, R.K., and Tennstedt, S.L. (2008). Symptom distress and quality of life in patients with advanced congestive heart failure. J Pain Symptom Manage *35*, 594-603.

Bohenzky, R.A., LeFebvre, R.B., and Berns, K.I. (1988). Sequence and symmetry requirements within the internal palindromic sequences of the adeno-associated virus terminal repeat. Virology *166*, 316-327.

Bolli, R., Chugh, A.R., D'Amario, D., Loughran, J.H., Stoddard, M.F., Ikram, S., Beache, G.M., Wagner, S.G., Leri, A., Hosoda, T.*, et al.* (2011). Cardiac stem cells in patients with ischaemic cardiomyopathy (SCIPIO): initial results of a randomised phase 1 trial. Lancet *378*, 1847-1857.

Bowers, C.Y., Momany, F., Reynolds, G.A., Chang, D., Hong, A., and Chang, K. (1980). Structure-activity relationships of a synthetic pentapeptide that specifically releases growth hormone in vitro. Endocrinology *106*, 663-667.

Bowles, D.E., Rabinowitz, J.E., and Samulski, R.J. (2003). Marker rescue of adeno-associated virus (AAV) capsid mutants: a novel approach for chimeric AAV production. J Virol *77*, 423-432.

Brailoiu, G.C., Dun, S.L., Yin, D., Yang, J., Chang, J.K., and Dun, N.J. (2005). Insulin-like 6 immunoreactivity in the mouse brain and testis. Brain Res *1040*, 187-190.

Broglio, F., Arvat, E., Benso, A., Gottero, C., Muccioli, G., Papotti, M., van der Lely, A.J., Deghenghi, R., and Ghigo, E. (2001). Ghrelin, a natural GH secretagogue produced by the stomach, induces hyperglycemia and reduces insulin secretion in humans. J Clin Endocrinol Metab *86*, 5083-5086.

Broglio, F., Benso, A., Castiglioni, C., Gottero, C., Prodam, F., Destefanis, S., Gauna, C., van der Lely, A.J., Deghenghi, R., Bo, M.*, et al.* (2003). The endocrine response to ghrelin as a function of gender in humans in young and elderly subjects. J Clin Endocrinol Metab *88*, 1537-1542.

Buerke, M., Murohara, T., Skurk, C., Nuss, C., Tomaselli, K., and Lefer, A.M. (1995). Cardioprotective effect of insulin-like growth factor I in myocardial ischemia followed by reperfusion. Proc Natl Acad Sci U S A *92*, 8031-8035.

Bullesbach, E.E., and Schwabe, C. (2000). The relaxin receptor-binding site geometry suggests a novel gripping mode of interaction. J Biol Chem *275*, 35276-35280.

Burger, C., Gorbatyuk, O.S., Velardo, M.J., Peden, C.S., Williams, P., Zolotukhin, S., Reier, P.J., Mandel, R.J., and Muzyczka, N. (2004). Recombinant AAV viral vectors pseudotyped with viral capsids from serotypes 1, 2, and 5 display differential efficiency and cell tropism after delivery to different regions of the central nervous system. Mol Ther *10*, 302-317.

Burnicka-Turek, O., Shirneshan, K., Paprotta, I., Grzmil, P., Meinhardt, A., Engel, W., and Adham, I.M. (2009). Inactivation of insulin-like factor 6 disrupts the progression of spermatogenesis at late meiotic prophase. Endocrinology *150*, 4348-4357.

Camina, J.P. (2006). Cell biology of the ghrelin receptor. J Neuroendocrinol *18*, 65-76.

Camina, J.P., Carreira, M.C., El Messari, S., Llorens-Cortes, C., Smith, R.G., and Casanueva, F.F. (2004). Desensitization and endocytosis mechanisms of ghrelin-activated growth hormone secretagogue receptor 1a. Endocrinology *145*, 930-940.

Carlini, V.P., Schioth, H.B., and Debarioglio, S.R. (2007). Obestatin improves memory performance and causes anxiolytic effects in rats. Biochem Biophys Res Commun *352*, 907-912.

Carvalho, A.B., and de Carvalho, A.C. (2010). Heart regeneration: Past, present and future. World J Cardiol *2*, 107-111.

Cervelli, T., Palacios, J.A., Zentilin, L., Mano, M., Schwartz, R.A., Weitzman, M.D., and Giacca, M. (2008). Processing of recombinant AAV genomes occurs in specific nuclear structures that overlap with foci of DNA-damage-response proteins. J Cell Sci *121*, 349-357.

Chatterjee, S., Stewart, A.S., Bish, L.T., Jayasankar, V., Kim, E.M., Pirolli, T., Burdick, J., Woo, Y.J., Gardner, T.J., and Sweeney, H.L. (2002). Viral gene transfer of the antiapoptotic factor Bcl-2 protects against chronic postischemic heart failure. Circulation *106*, I212-217.

Chejanovsky, N., and Carter, B.J. (1989). Mutagenesis of an AUG codon in the adeno-associated virus rep gene: effects on viral DNA replication. Virology *173*, 120-128.

Chen, C.Y., Chao, Y., Chang, F.Y., Chien, E.J., Lee, S.D., and Doong, M.L. (2005). Intracisternal des-acyl ghrelin inhibits food intake and non-nutrient gastric emptying in conscious rats. Int J Mol Med *16*, 695-699.

Chen, S.L., Fang, W.W., Ye, F., Liu, Y.H., Qian, J., Shan, S.J., Zhang, J.J., Chunhua, R.Z., Liao, L.M., Lin, S.*, et al.* (2004). Effect on left ventricular function of intracoronary transplantation of autologous bone marrow mesenchymal stem cell in patients with acute myocardial infarction. Am J Cardiol *94*, 92-95.

Chimenti, I., Smith, R.R., Li, T.S., Gerstenblith, G., Messina, E., Giacomello, A., and Marban, E. (2010). Relative roles of direct regeneration versus paracrine effects of human cardiosphere-derived cells transplanted into infarcted mice. Circ Res *106*, 971-980.

Chu, K.M., Chow, K.B., Leung, P.K., Lau, P.N., Chan, C.B., Cheng, C.H., and Wise, H. (2007). Over-expression of the truncated ghrelin receptor polypeptide attenuates the constitutive activation of phosphatidylinositol-specific phospholipase C by ghrelin receptors but has no effect on ghrelin-stimulated extracellular signal-regulated kinase 1/2 activity. Int J Biochem Cell Biol *39*, 752-764.

Chung, H., Seo, S., Moon, M., and Park, S. (2008). Phosphatidylinositol-3-kinase/Akt/glycogen synthase kinase-3 beta and ERK1/2 pathways mediate protective effects of acylated and unacylated ghrelin against oxygen-glucose deprivation-induced apoptosis in primary rat cortical neuronal cells. J Endocrinol *198*, 511-521.

Cittadini, A., Monti, M.G., Iaccarino, G., Di Rella, F., Tsichlis, P.N., Di Gianni, A., Stromer, H., Sorriento, D., Peschle, C., Trimarco, B.*, et al.* (2006). Adenoviral gene transfer of Akt enhances myocardial contractility and intracellular calcium handling. Gene Ther *13*, 8-19.

Cohen, S., Behzad, A.R., Carroll, J.B., and Pante, N. (2006). Parvoviral nuclear import: bypassing the host nuclear-transport machinery. J Gen Virol *87*, 3209-3213.

Cohn, J.N., Ferrari, R., and Sharpe, N. (2000). Cardiac remodeling--concepts and clinical implications: a consensus paper from an international forum on cardiac remodeling. Behalf of an International Forum on Cardiac Remodeling. J Am Coll Cardiol *35*, 569-582.

Collaboration, A.T. (2002). Collaborative meta-analysis of randomised trials of antiplatelet therapy for prevention of death, myocardial infarction, and stroke in high risk patients. BMJ *324*, 71-86.

Collesi, C., Zentilin, L., Sinagra, G., and Giacca, M. (2008). Notch1 signaling stimulates proliferation of immature cardiomyocytes. J Cell Biol *183*, 117-128.

Conti, E., Carrozza, C., Capoluongo, E., Volpe, M., Crea, F., Zuppi, C., and Andreotti, F. (2004). Insulin-like growth factor-1 as a vascular protective factor. Circulation *110*, 2260-2265.

Coura Rdos, S., and Nardi, N.B. (2007). The state of the art of adeno-associated virus-based vectors in gene therapy. Virol J *4*, 99.

Dandapat, A., Hu, C.P., Li, D., Liu, Y., Chen, H., Hermonat, P.L., and Mehta, J.L. (2008). Overexpression of TGFbeta1 by adeno-associated virus type-2 vector protects myocardium from ischemia-reperfusion injury. Gene Ther *15*, 415-423.

Date, Y., Murakami, N., Toshinai, K., Matsukura, S., Niijima, A., Matsuo, H., Kangawa, K., and Nakazato, M. (2002). The role of the gastric afferent vagal nerve in ghrelin-induced feeding and growth hormone secretion in rats. Gastroenterology *123*, 1120-1128.

Davis, R.C., Hobbs, F.D., Kenkre, J.E., Roalfe, A.K., Hare, R., Lancashire, R.J., and Davies, M.K. (2002). Prevalence of left ventricular systolic dysfunction and heart failure in high risk patients: community based epidemiological study. BMJ *325*, 1156.

Daya, S., and Berns, K.I. (2008). Gene therapy using adeno-associated virus vectors. Clin Microbiol Rev *21*, 583-593.

del Monte, F., Williams, E., Lebeche, D., Schmidt, U., Rosenzweig, A., Gwathmey, J.K., Lewandowski, E.D., and Hajjar, R.J. (2001). Improvement in survival and cardiac metabolism after gene transfer of sarcoplasmic reticulum Ca(2+)-ATPase in a rat model of heart failure. Circulation *104*, 1424-1429.

Delaughter, M.C., Taffet, G.E., Fiorotto, M.L., Entman, M.L., and Schwartz, R.J. (1999). Local insulin-like growth factor I expression induces physiologic, then pathologic, cardiac hypertrophy in transgenic mice. FASEB J *13*, 1923-1929.

Delhanty, P.J., van der Eerden, B.C., van der Velde, M., Gauna, C., Pols, H.A., Jahr, H., Chiba, H., van der Lely, A.J., and van Leeuwen, J.P. (2006). Ghrelin and unacylated ghrelin stimulate human osteoblast growth via mitogen-activated protein kinase (MAPK)/phosphoinositide 3-kinase (PI3K) pathways in the absence of GHS-R1a. J Endocrinol *188*, 37-47.

Demers, A., McNicoll, N., Febbraio, M., Servant, M., Marleau, S., Silverstein, R., and Ong, H. (2004). Identification of the growth hormone-releasing peptide binding site in CD36: a photoaffinity cross-linking study. Biochem J *382*, 417-424.

Deng, X.F., Rokosh, D.G., and Simpson, P.C. (2000). Autonomous and growth factor-induced hypertrophy in cultured neonatal mouse cardiac myocytes. Comparison with rat. Circ Res *87*, 781-788.

Di Pasquale, G., and Chiorini, J.A. (2006). AAV transcytosis through barrier epithelia and endothelium. Mol Ther *13*, 506-516.

Di Pasquale, G., Davidson, B.L., Stein, C.S., Martins, I., Scudiero, D., Monks, A., and Chiorini, J.A. (2003). Identification of PDGFR as a receptor for AAV-5 transduction. Nat Med *9*, 1306-1312.

Ding, W., Zhang, L., Yan, Z., and Engelhardt, J.F. (2005). Intracellular trafficking of adeno-associated viral vectors. Gene Ther *12*, 873-880.

Dixit, V.D., Schaffer, E.M., Pyle, R.S., Collins, G.D., Sakthivel, S.K., Palaniappan, R., Lillard, J.W., Jr., and Taub, D.D. (2004). Ghrelin inhibits leptin- and activation-induced proinflammatory cytokine expression by human monocytes and T cells. J Clin Invest *114*, 57-66.

Donath, M.Y., Sutsch, G., Yan, X.W., Piva, B., Brunner, H.P., Glatz, Y., Zapf, J., Follath, F., Froesch, E.R., and Kiowski, W. (1998). Acute cardiovascular effects of insulin-like growth factor I in patients with chronic heart failure. J Clin Endocrinol Metab *83*, 3177-3183.

Douar, A.M., Poulard, K., Stockholm, D., and Danos, O. (2001). Intracellular trafficking of adeno-associated virus vectors: routing to the late endosomal compartment and proteasome degradation. J Virol *75*, 1824-1833.

Dschietzig, T., Richter, C., Bartsch, C., Laule, M., Armbruster, F.P., Baumann, G., and Stangl, K. (2001). The pregnancy hormone relaxin is a player in human heart failure. FASEB J *15*, 2187-2195.

Du, X.J., Samuel, C.S., Gao, X.M., Zhao, L., Parry, L.J., and Tregear, G.W. (2003). Increased myocardial collagen and ventricular diastolic dysfunction in relaxin deficient mice: a gender-specific phenotype. Cardiovasc Res *57*, 395-404.

Du, Y.Y., Zhou, S.H., Zhou, T., Su, H., Pan, H.W., Du, W.H., Liu, B., and Liu, Q.M. (2008). Immuno-inflammatory regulation effect of mesenchymal stem cell transplantation in a rat model of myocardial infarction. Cytotherapy *10*, 469-478.

Duan, D., Li, Q., Kao, A.W., Yue, Y., Pessin, J.E., and Engelhardt, J.F. (1999). Dynamin is required for recombinant adeno-associated virus type 2 infection. J Virol *73*, 10371-10376.

Duerr, R.L., Huang, S., Miraliakbar, H.R., Clark, R., Chien, K.R., and Ross, J., Jr. (1995). Insulin-like growth factor-1 enhances ventricular hypertrophy and function during the onset of experimental cardiac failure. J Clin Invest *95*, 619-627.

Dutheil, N., Shi, F., Dupressoir, T., and Linden, R.M. (2000). Adeno-associated virus site-specifically integrates into a muscle-specific DNA region. Proc Natl Acad Sci U S A *97*, 4862-4866.

Dzimiri, N., Muiya, P., Andres, E., and Al-Halees, Z. (2004). Differential functional expression of human myocardial G protein receptor kinases in left ventricular cardiac diseases. Eur J Pharmacol *489*, 167-177.

Engelhardt, S., Hein, L., Dyachenkow, V., Kranias, E.G., Isenberg, G., and Lohse, M.J. (2004). Altered calcium handling is critically involved in the cardiotoxic effects of chronic beta-adrenergic stimulation. Circulation *109*, 1154-1160.

Enomoto, M., Nagaya, N., Uematsu, M., Okumura, H., Nakagawa, E., Ono, F., Hosoda, H., Oya, H., Kojima, M., Kanmatsuse, K.*, et al.* (2003). Cardiovascular and hormonal effects of subcutaneous administration of ghrelin, a novel growth hormone-releasing peptide, in healthy humans. Clin Sci (Lond) *105*, 431-435.

Failli, P., Nistri, S., Quattrone, S., Mazzetti, L., Bigazzi, M., Sacchi, T.B., and Bani, D. (2002). Relaxin up-regulates inducible nitric oxide synthase expression and nitric oxide generation in rat coronary endothelial cells. FASEB J *16*, 252-254.

Falk, E. (2006). Pathogenesis of atherosclerosis. J Am Coll Cardiol *47*, C7-12.

Fedak, P.W., Verma, S., Weisel, R.D., and Li, R.K. (2005). Cardiac remodeling and failure: from molecules to man (Part I). Cardiovasc Pathol *14*, 1-11.

Feighner, S.D., Howard, A.D., Prendergast, K., Palyha, O.C., Hreniuk, D.L., Nargund, R., Underwood, D., Tata, J.R., Dean, D.C., Tan, C.P.*, et al.* (1998). Structural requirements for the activation of the human growth hormone secretagogue receptor by peptide and nonpeptide secretagogues. Mol Endocrinol *12*, 137-145.

Feng, D., Chen, J., Yue, Y., Zhu, H., Xue, J., and Jia, W.W. (2006). A 16bp Rep binding element is sufficient for mediating Rep-dependent integration into AAVS1. J Mol Biol *358*, 38-45.

Ferrara, N. (1999). Vascular endothelial growth factor: molecular and biological aspects. Curr Top Microbiol Immunol *237*, 1-30.

Ferrara, N., Gerber, H.P., and LeCouter, J. (2003). The biology of VEGF and its receptors. Nat Med *9*, 669-676.

Ferrara, N., and Henzel, W.J. (1989). Pituitary follicular cells secrete a novel heparin-binding growth factor specific for vascular endothelial cells. Biochem Biophys Res Commun *161*, 851-858.

Ferrarini, M., Arsic, N., Recchia, F.A., Zentilin, L., Zacchigna, S., Xu, X., Linke, A., Giacca, M., and Hintze, T.H. (2006). Adeno-associated virus-mediated transduction of VEGF165 improves cardiac tissue viability and functional recovery after permanent coronary occlusion in conscious dogs. Circ Res *98*, 954-961.

Fields, P.A., and Larkin, L.H. (1981). Purification and immunohistochemical localization of relaxin in the human term placenta. J Clin Endocrinol Metab *52*, 79-85.

Filigheddu, N., Gnocchi, V.F., Coscia, M., Cappelli, M., Porporato, P.E., Taulli, R., Traini, S., Baldanzi, G., Chianale, F., Cutrupi, S.*, et al.* (2007). Ghrelin and des-acyl ghrelin promote differentiation and fusion of C2C12 skeletal muscle cells. Mol Biol Cell *18*, 986-994.

Fisher, C., Berry, C., Blue, L., Morton, J.J., and McMurray, J. (2003). N-terminal pro B type natriuretic peptide, but not the new putative cardiac hormone relaxin, predicts prognosis in patients with chronic heart failure. Heart *89*, 879-881.

Fonarow, G.C. (2005). Practical considerations of beta-blockade in the management of the post-myocardial infarction patient. Am Heart J *149*, 984-993.

Francis, G.S. (2001). Pathophysiology of chronic heart failure. Am J Med *110 Suppl 7A*, 37S-46S.

Frishman, W.H., and Saunders, E. (2011). beta-Adrenergic blockers. J Clin Hypertens (Greenwich) *13*, 649-653.

Fromes, Y., Salmon, A., Wang, X., Collin, H., Rouche, A., Hagege, A., Schwartz, K., and Fiszman, M.Y. (1999). Gene delivery to the myocardium by intrapericardial injection. Gene Ther *6*, 683-688.

Gandhi, S., Weinberg, I., Margey, R., and Jaff, M.R. (2011). Comprehensive medical management of peripheral arterial disease. Prog Cardiovasc Dis *54*, 2-13.

Gao, G., Vandenberghe, L.H., and Wilson, J.M. (2005). New recombinant serotypes of AAV vectors. Curr Gene Ther *5*, 285-297.

Gao, X.M., Dart, A.M., Dewar, E., Jennings, G., and Du, X.J. (2000). Serial echocardiographic assessment of left ventricular dimensions and function after myocardial infarction in mice. Cardiovasc Res *45*, 330-338.

Garcia, E.A., and Korbonits, M. (2006). Ghrelin and cardiovascular health. Curr Opin Pharmacol *6*, 142-147.

Garcia, J.M., Garcia-Touza, M., Hijazi, R.A., Taffet, G., Epner, D., Mann, D., Smith, R.G., Cunningham, G.R., and Marcelli, M. (2005). Active ghrelin levels and active to total ghrelin ratio in cancer-induced cachexia. J Clin Endocrinol Metab *90*, 2920-2926.

Gauna, C., Delhanty, P.J., Hofland, L.J., Janssen, J.A., Broglio, F., Ross, R.J., Ghigo, E., and van der Lely, A.J. (2005). Ghrelin stimulates, whereas des-octanoyl ghrelin inhibits, glucose output by primary hepatocytes. J Clin Endocrinol Metab *90*, 1055-1060.

Gauna, C., Delhanty, P.J., van Aken, M.O., Janssen, J.A., Themmen, A.P., Hofland, L.J., Culler, M., Broglio, F., Ghigo, E., and van der Lely, A.J. (2006). Unacylated ghrelin is active on the INS-1E rat insulinoma cell line independently of the growth hormone secretagogue receptor type 1a and the corticotropin releasing factor 2 receptor. Mol Cell Endocrinol *251*, 103-111.

Gersh, B.J., Simari, R.D., Behfar, A., Terzic, C.M., and Terzic, A. (2009). Cardiac cell repair therapy: a clinical perspective. Mayo Clin Proc *84*, 876-892.

Ghosh, A., Yue, Y., Lai, Y., and Duan, D. (2008). A hybrid vector system expands adeno-associated viral vector packaging capacity in a transgene-independent manner. Mol Ther *16*, 124-130.

Ghosh, A., Yue, Y., Long, C., Bostick, B., and Duan, D. (2007). Efficient whole-body transduction with trans-splicing adeno-associated viral vectors. Mol Ther *15*, 750-755.

Giacca, M. (2007). Virus-mediated gene transfer to induce therapeutic angiogenesis: where do we stand? Int J Nanomedicine *2*, 527-540.

Giacca, M. (2010). Non-redundant functions of the protein isoforms arising from alternative splicing of the VEGF-A pre-mRNA. Transcription *1*, 149-153.

Giacca, M., and Zacchigna, S. (2012). VEGF gene therapy: therapeutic angiogenesis in the clinic and beyond. Gene Ther.

Gidh-Jain, M., Huang, B., Jain, P., Gick, G., and El-Sherif, N. (1998). Alterations in cardiac gene expression during ventricular remodeling following experimental myocardial infarction. J Mol Cell Cardiol *30*, 627-637.

Giordano, F.J., Ping, P., McKirnan, M.D., Nozaki, S., DeMaria, A.N., Dillmann, W.H., Mathieu-Costello, O., and Hammond, H.K. (1996). Intracoronary gene transfer of fibroblast growth factor-5 increases blood flow and contractile function in an ischemic region of the heart. Nat Med *2*, 534-539.

Girod, A., Wobus, C.E., Zadori, Z., Ried, M., Leike, K., Tijssen, P., Kleinschmidt, J.A., and Hallek, M. (2002). The VP1 capsid protein of adeno-associated virus type 2 is carrying a phospholipase A2 domain required for virus infectivity. J Gen Virol *83*, 973-978.

Glass, C.K., and Witztum, J.L. (2001). Atherosclerosis. the road ahead. Cell *104*, 503-516.

Gnanapavan, S., Kola, B., Bustin, S.A., Morris, D.G., McGee, P., Fairclough, P., Bhattacharya, S., Carpenter, R., Grossman, A.B., and Korbonits, M. (2002). The tissue distribution of the mRNA of ghrelin and subtypes of its receptor, GHS-R, in humans. J Clin Endocrinol Metab *87*, 2988.

Goldsmith, L.T., Weiss, G., Palejwala, S., Plant, T.M., Wojtczuk, A., Lambert, W.C., Ammur, N., Heller, D., Skurnick, J.H., Edwards, D.*, et al.* (2004). Relaxin regulation of endometrial structure and function in the rhesus monkey. Proc Natl Acad Sci U S A *101*, 4685-4689.

Goncalves, M.A. (2005). Adeno-associated virus: from defective virus to effective vector. Virol J *2*, 43.

Granata, R., Isgaard, J., Alloatti, G., and Ghigo, E. (2011). Cardiovascular actions of the ghrelin gene-derived peptides and growth hormone-releasing hormone. Exp Biol Med (Maywood) *236*, 505-514.

Granata, R., Settanni, F., Biancone, L., Trovato, L., Nano, R., Bertuzzi, F., Destefanis, S., Annunziata, M., Martinetti, M., Catapano, F.*, et al.* (2007). Acylated and unacylated ghrelin promote proliferation and inhibit apoptosis of pancreatic

beta-cells and human islets: involvement of 3',5'-cyclic adenosine monophosphate/protein kinase A, extracellular signal-regulated kinase 1/2, and phosphatidyl inositol 3-Kinase/Akt signaling. Endocrinology *148*, 512-529.

Grieger, J.C., and Samulski, R.J. (2005). Packaging capacity of adeno-associated virus serotypes: impact of larger genomes on infectivity and postentry steps. J Virol *79*, 9933-9944.

Grimm, D., Elsner, D., Schunkert, H., Pfeifer, M., Griese, D., Bruckschlegel, G., Muders, F., Riegger, G.A., and Kromer, E.P. (1998a). Development of heart failure following isoproterenol administration in the rat: role of the renin-angiotensin system. Cardiovasc Res *37*, 91-100.

Grimm, D., Kern, A., Rittner, K., and Kleinschmidt, J.A. (1998b). Novel tools for production and purification of recombinant adenoassociated virus vectors. Hum Gene Ther *9*, 2745-2760.

Grimmond, S.M., Miranda, K.C., Yuan, Z., Davis, M.J., Hume, D.A., Yagi, K., Tominaga, N., Bono, H., Hayashizaki, Y., Okazaki, Y.*, et al.* (2003). The mouse secretome: functional classification of the proteins secreted into the extracellular environment. Genome Res *13*, 1350-1359.

Grines, C.L., Watkins, M.W., Helmer, G., Penny, W., Brinker, J., Marmur, J.D., West, A., Rade, J.J., Marrott, P., Hammond, H.K.*, et al.* (2002). Angiogenic Gene Therapy (AGENT) trial in patients with stable angina pectoris. Circulation *105*, 1291-1297.

Grines, C.L., Watkins, M.W., Mahmarian, J.J., Iskandrian, A.E., Rade, J.J., Marrott, P., Pratt, C., and Kleiman, N. (2003). A randomized, double-blind, placebo-controlled trial of Ad5FGF-4 gene therapy and its effect on myocardial perfusion in patients with stable angina. J Am Coll Cardiol *42*, 1339-1347.

Guo, Z.F., Ren, A.J., Zheng, X., Qin, Y.W., Cheng, F., Zhang, J., Wu, H., Yuan, W.J., and Zou, L. (2008). Different responses of circulating ghrelin, obestatin levels to fasting, re-feeding and different food compositions, and their local expressions in rats. Peptides *29*, 1247-1254.

Gyongyosi, M., Khorsand, A., Zamini, S., Sperker, W., Strehblow, C., Kastrup, J., Jorgensen, E., Hesse, B., Tagil, K., Botker, H.E.*, et al.* (2005). NOGA-guided analysis of regional myocardial perfusion abnormalities treated with intramyocardial injections of plasmid encoding vascular endothelial growth factor A-165 in patients with chronic myocardial ischemia: subanalysis of the EUROINJECT-ONE multicenter double-blind randomized study. Circulation *112*, I157-165.

Hajjar, R.J., Zsebo, K., Deckelbaum, L., Thompson, C., Rudy, J., Yaroshinsky, A., Ly, H., Kawase, Y., Wagner, K., Borow, K.*, et al.* (2008). Design of a phase 1/2 trial of intracoronary administration of AAV1/SERCA2a in patients with heart failure. J Card Fail *14*, 355-367.

Hao, X., Mansson-Broberg, A., Grinnemo, K.H., Siddiqui, A.J., Dellgren, G., Brodin, L.A., and Sylven, C. (2007). Myocardial angiogenesis after plasmid or adenoviral VEGF-A(165) gene transfer in rat myocardial infarction model. Cardiovasc Res *73*, 481-487.

Harbison, C.E., Chiorini, J.A., and Parrish, C.R. (2008). The parvovirus capsid odyssey: from the cell surface to the nucleus. Trends Microbiol *16*, 208-214.

Hare, J.M., Traverse, J.H., Henry, T.D., Dib, N., Strumpf, R.K., Schulman, S.P., Gerstenblith, G., DeMaria, A.N., Denktas, A.E., Gammon, R.S.*, et al.* (2009). A randomized, double-blind, placebo-controlled, dose-escalation study of intravenous adult human mesenchymal stem cells (prochymal) after acute myocardial infarction. J Am Coll Cardiol *54*, 2277-2286.

Hata, J.A., Williams, M.L., and Koch, W.J. (2004). Genetic manipulation of myocardial beta-adrenergic receptor activation and desensitization. J Mol Cell Cardiol *37*, 11-21.

Hauck, B., Xu, R.R., Xie, J., Wu, W., Ding, Q., Sipler, M., Wang, H., Chen, L., Wright, J.F., and Xiao, W. (2006). Efficient AAV1-AAV2 hybrid vector for gene therapy of hemophilia. Hum Gene Ther *17*, 46-54.

Hausenloy, D.J., and Yellon, D.M. (2009). Cardioprotective growth factors. Cardiovasc Res *83*, 179-194.

Hedman, M., Hartikainen, J., Syvanne, M., Stjernvall, J., Hedman, A., Kivela, A., Vanninen, E., Mussalo, H., Kauppila, E., Simula, S.*, et al.* (2003). Safety and feasibility of catheter-based local intracoronary vascular endothelial growth factor gene transfer in the prevention of postangioplasty and in-stent restenosis and in the treatment of chronic myocardial ischemia: phase II results of the Kuopio Angiogenesis Trial (KAT). Circulation *107*, 2677-2683.

Heineke, J., and Molkentin, J.D. (2006). Regulation of cardiac hypertrophy by intracellular signalling pathways. Nat Rev Mol Cell Biol *7*, 589-600.

Hendel, R.C., Henry, T.D., Rocha-Singh, K., Isner, J.M., Kereiakes, D.J., Giordano, F.J., Simons, M., and Bonow, R.O. (2000). Effect of intracoronary recombinant human vascular endothelial growth factor on myocardial perfusion: evidence for a dose-dependent effect. Circulation *101*, 118-121.

Henry, T.D., Annex, B.H., McKendall, G.R., Azrin, M.A., Lopez, J.J., Giordano, F.J., Shah, P.K., Willerson, J.T., Benza, R.L., Berman, D.S.*, et al.* (2003). The VIVA trial: Vascular endothelial growth factor in Ischemia for Vascular Angiogenesis. Circulation *107*, 1359-1365.

Henry, T.D., Grines, C.L., Watkins, M.W., Dib, N., Barbeau, G., Moreadith, R., Andrasfay, T., and Engler, R.L. (2007). Effects of Ad5FGF-4 in patients with angina: an analysis of pooled data from the AGENT-3 and AGENT-4 trials. J Am Coll Cardiol *50*, 1038-1046.

Henry, T.D., Rocha-Singh, K., Isner, J.M., Kereiakes, D.J., Giordano, F.J., Simons, M., Losordo, D.W., Hendel, R.C., Bonow, R.O., Eppler, S.M.*, et al.* (2001). Intracoronary administration of recombinant human vascular endothelial growth factor to patients with coronary artery disease. Am Heart J *142*, 872-880.

Hermonat, P.L., and Muzyczka, N. (1984). Use of adeno-associated virus as a mammalian DNA cloning vector: transduction of neomycin resistance into mammalian tissue culture cells. Proc Natl Acad Sci U S A *81*, 6466-6470.

Hiasa, K., Ishibashi, M., Ohtani, K., Inoue, S., Zhao, Q., Kitamoto, S., Sata, M., Ichiki, T., Takeshita, A., and Egashira, K. (2004). Gene transfer of stromal cell-derived factor-1alpha enhances ischemic vasculogenesis and angiogenesis via vascular endothelial growth factor/endothelial nitric oxide synthase-related pathway: next-generation chemokine therapy for therapeutic neovascularization. Circulation *109*, 2454-2461.

Hillgenberg, M., Hofmann, C., Stadler, H., and Loser, P. (2006). High-efficiency system for the construction of adenovirus vectors and its application to the generation of representative adenovirus-based cDNA expression libraries. J Virol *80*, 5435-5450.

Hochedlinger, K., and Jaenisch, R. (2006). Nuclear reprogramming and pluripotency. Nature *441*, 1061-1067.

Holst, B., Cygankiewicz, A., Jensen, T.H., Ankersen, M., and Schwartz, T.W. (2003). High constitutive signaling of the ghrelin receptor--identification of a potent inverse agonist. Mol Endocrinol *17*, 2201-2210.

Holst, B., Holliday, N.D., Bach, A., Elling, C.E., Cox, H.M., and Schwartz, T.W. (2004). Common structural basis for constitutive activity of the ghrelin receptor family. J Biol Chem *279*, 53806-53817.

Hoshijima, M., Ikeda, Y., Iwanaga, Y., Minamisawa, S., Date, M.O., Gu, Y., Iwatate, M., Li, M., Wang, L., Wilson, J.M.*, et al.* (2002). Chronic suppression of heart-failure progression by a pseudophosphorylated mutant of phospholamban via in vivo cardiac rAAV gene delivery. Nat Med *8*, 864-871.

Hosoda, H., Kojima, M., Matsuo, H., and Kangawa, K. (2000). Purification and characterization of rat des-Gln14-Ghrelin, a second endogenous ligand for the growth hormone secretagogue receptor. J Biol Chem *275*, 21995-22000.

Hosoda, H., Kojima, M., Mizushima, T., Shimizu, S., and Kangawa, K. (2003). Structural divergence of human ghrelin. Identification of multiple ghrelin-derived molecules produced by post-translational processing. J Biol Chem *278*, 64-70.

Howard, A.D., Feighner, S.D., Cully, D.F., Arena, J.P., Liberator, P.A., Rosenblum, C.I., Hamelin, M., Hreniuk, D.L., Palyha, O.C., Anderson, J.*, et al.* (1996). A receptor in pituitary and hypothalamus that functions in growth hormone release. Science *273*, 974-977.

Hsu, S.Y., Nakabayashi, K., Nishi, S., Kumagai, J., Kudo, M., Sherwood, O.D., and Hsueh, A.J. (2002). Activation of orphan receptors by the hormone relaxin. Science *295*, 671-674.

Huang, C.X., Yuan, M.J., Huang, H., Wu, G., Liu, Y., Yu, S.B., Li, H.T., and Wang, T. (2009). Ghrelin inhibits post-infarct myocardial remodeling and improves cardiac function through anti-inflammation effect. Peptides *30*, 2286-2291.

Hudson, P., John, M., Crawford, R., Haralambidis, J., Scanlon, D., Gorman, J., Tregear, G., Shine, J., and Niall, H. (1984). Relaxin gene expression in human ovaries and the predicted structure of a human preprorelaxin by analysis of cDNA clones. EMBO J *3*, 2333-2339.

Hunt, S.A., Abraham, W.T., Chin, M.H., Feldman, A.M., Francis, G.S., Ganiats, T.G., Jessup, M., Konstam, M.A., Mancini, D.M., Michl, K.*, et al.* (2009). 2009 focused update incorporated into the ACC/AHA 2005 Guidelines for the Diagnosis and Management of Heart Failure in Adults: a report of the American College of Cardiology Foundation/American Heart Association Task Force on Practice Guidelines: developed in collaboration with the International Society for Heart and Lung Transplantation. Circulation *119*, e391-479.

Huser, D., Gogol-Doring, A., Lutter, T., Weger, S., Winter, K., Hammer, E.M., Cathomen, T., Reinert, K., and Heilbronn, R. (2010). Integration preferences of wildtype AAV-2 for consensus rep-binding sites at numerous loci in the human genome. PLoS Pathog *6*, e1000985.

Inagaki, K., Fuess, S., Storm, T.A., Gibson, G.A., McTiernan, C.F., Kay, M.A., and Nakai, H. (2006). Robust systemic transduction with AAV9 vectors in mice: efficient global cardiac gene transfer superior to that of AAV8. Mol Ther *14*, 45-53.

Inagaki, K., Lewis, S.M., Wu, X., Ma, C., Munroe, D.J., Fuess, S., Storm, T.A., Kay, M.A., and Nakai, H. (2007). DNA palindromes with a modest arm length of greater, similar 20 base pairs are a significant target for recombinant adeno-associated virus vector integration in the liver, muscles, and heart in mice. J Virol *81*, 11290-11303.

Insull, W., Jr. (2009). The pathology of atherosclerosis: plaque development and plaque responses to medical treatment. Am J Med *122*, S3-S14.

Ion, R., Telvi, L., Chaussain, J.L., Barbet, J.P., Nunes, M., Safar, A., Rethore, M.O., Fellous, M., and McElreavey, K. (1998). Failure of testicular development associated with a rearrangement of 9p24.1 proximal to the SNF2 gene. Hum Genet *102*, 151-156.

Ishii, S., Koyama, H., Miyata, T., Nishikage, S., Hamada, H., Miyatake, S., and Shigematsu, H. (2004). Appropriate control of ex vivo gene therapy delivering basic fibroblast growth factor promotes successful and safe development of collateral vessels in rabbit model of hind limb ischemia. J Vasc Surg *39*, 629-638.

Isner, J.M. (2002). Myocardial gene therapy. Nature *415*, 234-239.

Isner, J.M., Pieczek, A., Schainfeld, R., Blair, R., Haley, L., Asahara, T., Rosenfield, K., Razvi, S., Walsh, K., and Symes, J.F. (1996). Clinical evidence of angiogenesis after arterial gene transfer of phVEGF165 in patient with ischaemic limb. Lancet *348*, 370-374.

Itoh, N., and Ornitz, D.M. (2011). Fibroblast growth factors: from molecular evolution to roles in development, metabolism and disease. J Biochem *149*, 121-130.

Ivell, R., and Grutzner, F. (2009). Evolution and male fertility: lessons from the insulin-like factor 6 gene (Insl6). Endocrinology *150*, 3986-3990.

Iwanaga, Y., Hoshijima, M., Gu, Y., Iwatate, M., Dieterle, T., Ikeda, Y., Date, M.O., Chrast, J., Matsuzaki, M., Peterson, K.L.*, et al.* (2004). Chronic phospholamban inhibition prevents progressive cardiac dysfunction and pathological remodeling after infarction in rats. J Clin Invest *113*, 727-736.

Jacquier, A., Higgins, C.B., Martin, A.J., Do, L., Saloner, D., and Saeed, M. (2007). Injection of adeno-associated viral vector encoding vascular endothelial growth factor gene in infarcted swine myocardium: MR measurements of left ventricular function and strain. Radiology *245*, 196-205.

Jarrousse, C., Lods, N., Michel, F., Bali, J.P., and Magous, R. (2004). Cultured gastrointestinal smooth muscle cells: cell response to contractile agonists depends on their phenotypic state. Cell Tissue Res *316*, 221-232.

Jaski, B.E., Jessup, M.L., Mancini, D.M., Cappola, T.P., Pauly, D.F., Greenberg, B., Borow, K., Dittrich, H., Zsebo, K.M., and Hajjar, R.J. (2009). Calcium upregulation by percutaneous administration of gene therapy in cardiac disease (CUPID Trial), a first-in-human phase 1/2 clinical trial. J Card Fail *15*, 171-181.

Jessup, M., Abraham, W.T., Casey, D.E., Feldman, A.M., Francis, G.S., Ganiats, T.G., Konstam, M.A., Mancini, D.M., Rahko, P.S., Silver, M.A.*, et al.* (2009). 2009 focused update: ACCF/AHA Guidelines for the Diagnosis and Management of Heart Failure in Adults: a report of the American College of Cardiology Foundation/American Heart Association Task Force on Practice Guidelines: developed in collaboration with the International Society for Heart and Lung Transplantation. Circulation *119*, 1977-2016.

Jessup, M., and Brozena, S. (2003). Heart failure. N Engl J Med *348*, 2007-2018.

Jin, H., Wyss, J.M., Yang, R., and Schwall, R. (2004). The therapeutic potential of hepatocyte growth factor for myocardial infarction and heart failure. Curr Pharm Des *10*, 2525-2533.

Johnson, J.S., and Samulski, R.J. (2009). Enhancement of adeno-associated virus infection by mobilizing capsids into and out of the nucleolus. J Virol *83*, 2632-2644.

Kaludov, N., Brown, K.E., Walters, R.W., Zabner, J., and Chiorini, J.A. (2001). Adeno-associated virus serotype 4 (AAV4) and AAV5 both require sialic acid binding for hemagglutination and efficient transduction but differ in sialic acid linkage specificity. J Virol *75*, 6884-6893.

Kano, M.R., Morishita, Y., Iwata, C., Iwasaka, S., Watabe, T., Ouchi, Y., Miyazono, K., and Miyazawa, K. (2005). VEGF-A and FGF-2 synergistically promote neoangiogenesis through enhancement of endogenous PDGF-B-PDGFRbeta signaling. J Cell Sci *118*, 3759-3768.

Kashiwakura, Y., Tamayose, K., Iwabuchi, K., Hirai, Y., Shimada, T., Matsumoto, K., Nakamura, T., Watanabe, M., Oshimi, K., and Daida, H. (2005). Hepatocyte growth factor receptor is a coreceptor for adeno-associated virus type 2 infection. J Virol *79*, 609-614.

Kasik, J., Muglia, L., Stephan, D.A., and Menon, R.K. (2000). Identification, chromosomal mapping, and partial characterization of mouse InsI6: a new member of the insulin family. Endocrinology *141*, 458-461.

Kastrup, J., Jorgensen, E., Ruck, A., Tagil, K., Glogar, D., Ruzyllo, W., Botker, H.E., Dudek, D., Drvota, V., Hesse, B.*, et al.* (2005). Direct intramyocardial plasmid vascular endothelial growth factor-A165 gene therapy in patients with stable severe

angina pectoris A randomized double-blind placebo-controlled study: the Euroinject One trial. J Am Coll Cardiol *45*, 982-988.

Katz, M.G., Swain, J.D., Tomasulo, C.E., Sumaroka, M., Fargnoli, A., and Bridges, C.R. (2011). Current strategies for myocardial gene delivery. J Mol Cell Cardiol *50*, 766-776.

Kawai, J., Shinagawa, A., Shibata, K., Yoshino, M., Itoh, M., Ishii, Y., Arakawa, T., Hara, A., Fukunishi, Y., Konno, H.*, et al.* (2001). Functional annotation of a full-length mouse cDNA collection. Nature *409*, 685-690.

Kawamura, K., Kumagai, J., Sudo, S., Chun, S.Y., Pisarska, M., Morita, H., Toppari, J., Fu, P., Wade, J.D., Bathgate, R.A.*, et al.* (2004). Paracrine regulation of mammalian oocyte maturation and male germ cell survival. Proc Natl Acad Sci U S A *101*, 7323-7328.

Kawase, Y., Ly, H.Q., Prunier, F., Lebeche, D., Shi, Y., Jin, H., Hadri, L., Yoneyama, R., Hoshino, K., Takewa, Y.*, et al.* (2008). Reversal of cardiac dysfunction after long-term expression of SERCA2a by gene transfer in a pre-clinical model of heart failure. J Am Coll Cardiol *51*, 1112-1119.

Kaye, D.M., Preovolos, A., Marshall, T., Byrne, M., Hoshijima, M., Hajjar, R., Mariani, J.A., Pepe, S., Chien, K.R., and Power, J.M. (2007). Percutaneous cardiac recirculation-mediated gene transfer of an inhibitory phospholamban peptide reverses advanced heart failure in large animals. J Am Coll Cardiol *50*, 253-260.

Kehat, I., Kenyagin-Karsenti, D., Snir, M., Segev, H., Amit, M., Gepstein, A., Livne, E., Binah, O., Itskovitz-Eldor, J., and Gepstein, L. (2001). Human embryonic stem cells can differentiate into myocytes with structural and functional properties of cardiomyocytes. J Clin Invest *108*, 407-414.

Kim, J.B., Greber, B., Arauzo-Bravo, M.J., Meyer, J., Park, K.I., Zaehres, H., and Scholer, H.R. (2009). Direct reprogramming of human neural stem cells by OCT4. Nature *461*, 649-643.

Kim, M.S., Yoon, C.Y., Jang, P.G., Park, Y.J., Shin, C.S., Park, H.S., Ryu, J.W., Pak, Y.K., Park, J.Y., Lee, K.U.*, et al.* (2004). The mitogenic and antiapoptotic actions of ghrelin in 3T3-L1 adipocytes. Mol Endocrinol *18*, 2291-2301.

Kim, S.W., Her, S.J., Park, S.J., Kim, D., Park, K.S., Lee, H.K., Han, B.H., Kim, M.S., Shin, C.S., and Kim, S.Y. (2005). Ghrelin stimulates proliferation and differentiation and inhibits apoptosis in osteoblastic MC3T3-E1 cells. Bone *37*, 359-369.

Kitamura, T. (1998). New experimental approaches in retrovirus-mediated expression screening. Int J Hematol *67*, 351-359.

Kocher, A.A., Schuster, M.D., Szabolcs, M.J., Takuma, S., Burkhoff, D., Wang, J., Homma, S., Edwards, N.M., and Itescu, S. (2001). Neovascularization of ischemic myocardium by human bone-marrow-derived angioblasts prevents cardiomyocyte apoptosis, reduces remodeling and improves cardiac function. Nat Med *7*, 430-436.

Kojima, M., Hosoda, H., Date, Y., Nakazato, M., Matsuo, H., and Kangawa, K. (1999). Ghrelin is a growth-hormone-releasing acylated peptide from stomach. Nature *402*, 656-660.

Kojima, M., Hosoda, H., Matsuo, H., and Kangawa, K. (2001). Ghrelin: discovery of the natural endogenous ligand for the growth hormone secretagogue receptor. Trends Endocrinol Metab *12*, 118-122.

Kojima, M., and Kangawa, K. (2005). Ghrelin: structure and function. Physiol Rev *85*, 495-522.

Kondoh, K., Koyama, H., Miyata, T., Takato, T., Hamada, H., and Shigematsu, H. (2004). Conduction performance of collateral vessels induced by vascular endothelial growth factor or basic fibroblast growth factor. Cardiovasc Res *61*, 132-142.

Konstam, M.A., Kramer, D.G., Patel, A.R., Maron, M.S., and Udelson, J.E. (2011). Left ventricular remodeling in heart failure: current concepts in clinical significance and assessment. JACC Cardiovasc Imaging *4*, 98-108.

Korbonits, M., Ciccarelli, E., Ghigo, E., and Grossman, A.B. (1999). The growth hormone secretagogue receptor. Growth Horm IGF Res *9 Suppl A*, 93-99.

Korbonits, M., Goldstone, A.P., Gueorguiev, M., and Grossman, A.B. (2004). Ghrelin--a hormone with multiple functions. Front Neuroendocrinol *25*, 27-68.

Kornowski, R., Fuchs, S., Leon, M.B., and Epstein, S.E. (2000). Delivery strategies to achieve therapeutic myocardial angiogenesis. Circulation *101*, 454-458.

Kotin, R.M., Siniscalco, M., Samulski, R.J., Zhu, X.D., Hunter, L., Laughlin, C.A., McLaughlin, S., Muzyczka, N., Rocchi, M., and Berns, K.I. (1990). Site-specific integration by adeno-associated virus. Proc Natl Acad Sci U S A *87*, 2211-2215.

Kui, L., Weiwei, Z., Ling, L., Daikun, H., Guoming, Z., Linuo, Z., and Renming, H. (2009). Ghrelin inhibits apoptosis induced by high glucose and sodium palmitate in adult rat cardiomyocytes through the PI3K-Akt signaling pathway. Regul Pept *155*, 62-69.

Kumagai, J., Hsu, S.Y., Matsumi, H., Roh, J.S., Fu, P., Wade, J.D., Bathgate, R.A., and Hsueh, A.J. (2002). INSL3/Leydig insulin-like peptide activates the LGR8 receptor important in testis descent. J Biol Chem *277*, 31283-31286.

Kupatt, C., Hinkel, R., Pfosser, A., El-Aouni, C., Wuchrer, A., Fritz, A., Globisch, F., Thormann, M., Horstkotte, J., Lebherz, C.*, et al.* (2010). Cotransfection of vascular endothelial growth factor-A and platelet-derived growth factor-B via recombinant adeno-associated virus resolves chronic ischemic malperfusion role of vessel maturation. J Am Coll Cardiol *56*, 414-422.

Kusano, K.F., Pola, R., Murayama, T., Curry, C., Kawamoto, A., Iwakura, A., Shintani, S., Ii, M., Asai, J., Tkebuchava, T.*, et al.* (2005). Sonic hedgehog myocardial gene therapy: tissue repair through transient reconstitution of embryonic signaling. Nat Med *11*, 1197-1204.

Kwon, I., and Schaffer, D.V. (2008). Designer gene delivery vectors: molecular engineering and evolution of adeno-associated viral vectors for enhanced gene transfer. Pharm Res *25*, 489-499.

Laflamme, M.A., and Murry, C.E. (2011). Heart regeneration. Nature *473*, 326-335.

Laham, R.J., Chronos, N.A., Pike, M., Leimbach, M.E., Udelson, J.E., Pearlman, J.D., Pettigrew, R.I., Whitehouse, M.J., Yoshizawa, C., and Simons, M. (2000). Intracoronary basic fibroblast growth factor (FGF-2) in patients with severe ischemic heart disease: results of a phase I open-label dose escalation study. J Am Coll Cardiol *36*, 2132-2139.

Lau, J.F., Weinberg, M.D., and Olin, J.W. (2011). Peripheral artery disease. Part 1: clinical evaluation and noninvasive diagnosis. Nat Rev Cardiol *8*, 405-418.

Lauwers, E., Landuyt, B., Arckens, L., Schoofs, L., and Luyten, W. (2006). Obestatin does not activate orphan G protein-coupled receptor GPR39. Biochem Biophys Res Commun *351*, 21-25.

Lear, P.V., Iglesias, M.J., Feijoo-Bandin, S., Rodriguez-Penas, D., Mosquera-Leal, A., Garcia-Rua, V., Gualillo, O., Ghe, C., Arnoletti, E., Muccioli, G*., et al.* (2010). Des-acyl ghrelin has specific binding sites and different metabolic effects from ghrelin in cardiomyocytes. Endocrinology *151*, 3286-3298.

Lekgabe, E.D., Kiriazis, H., Zhao, C., Xu, Q., Moore, X.L., Su, Y., Bathgate, R.A., Du, X.J., and Samuel, C.S. (2005). Relaxin reverses cardiac and renal fibrosis in spontaneously hypertensive rats. Hypertension *46*, 412-418.

Leung, P.K., Chow, K.B., Lau, P.N., Chu, K.M., Chan, C.B., Cheng, C.H., and Wise, H. (2007). The truncated ghrelin receptor polypeptide (GHS-R1b) acts as a dominant-negative mutant of the ghrelin receptor. Cell Signal *19*, 1011-1022.

Levonen, A.L., Vahakangas, E., Koponen, J.K., and Yla-Herttuala, S. (2008). Antioxidant gene therapy for cardiovascular disease: current status and future perspectives. Circulation *117*, 2142-2150.

Li, L., Zhang, L.K., Pang, Y.Z., Pan, C.S., Qi, Y.F., Chen, L., Wang, X., Tang, C.S., and Zhang, J. (2006). Cardioprotective effects of ghrelin and des-octanoyl ghrelin on myocardial injury induced by isoproterenol in rats. Acta Pharmacol Sin *27*, 527-535.

Li, Q., Bolli, R., Qiu, Y., Tang, X.L., Guo, Y., and French, B.A. (2001). Gene therapy with extracellular superoxide dismutase protects conscious rabbits against myocardial infarction. Circulation *103*, 1893-1898.

Li, W.G., Gavrila, D., Liu, X., Wang, L., Gunnlaugsson, S., Stoll, L.L., McCormick, M.L., Sigmund, C.D., Tang, C., and Weintraub, N.L. (2004). Ghrelin inhibits proinflammatory responses and nuclear factor-kappaB activation in human endothelial cells. Circulation *109*, 2221-2226.

Lim, C.T., Kola, B., Grossman, A., and Korbonits, M. (2011). The expression of ghrelin O-acyltransferase (GOAT) in human tissues. Endocr J *58*, 707-710.

Lin, T., Meng, Q., Sui, D., Peng, D., Li, Y., Liu, X., Xie, L., and Li, N. (2011). Molecular cloning and expression analysis of porcine ghrelin o-acyltransferase. Biochem Genet *49*, 576-586.

Lin, Y., Matsumura, K., Fukuhara, M., Kagiyama, S., Fujii, K., and Iida, M. (2004). Ghrelin acts at the nucleus of the solitary tract to decrease arterial pressure in rats. Hypertension *43*, 977-982.

Liu, C., Eriste, E., Sutton, S., Chen, J., Roland, B., Kuei, C., Farmer, N., Jornvall, H., Sillard, R., and Lovenberg, T.W. (2003). Identification of relaxin-3/INSL7 as an endogenous ligand for the orphan G-protein-coupled receptor GPCR135. J Biol Chem *278*, 50754-50764.

Liu, C., Kuei, C., Sutton, S., Chen, J., Bonaventure, P., Wu, J., Nepomuceno, D., Kamme, F., Tran, D.T., Zhu, J.*, et al.* (2005). INSL5 is a high affinity specific agonist for GPCR142 (GPR100). J Biol Chem *280*, 292-300.

Liu, X., Simpson, J.A., Brunt, K.R., Ward, C.A., Hall, S.R., Kinobe, R.T., Barrette, V., Tse, M.Y., Pang, S.C., Pachori, A.S.*, et al.* (2007). Preemptive heme oxygenase-1 gene delivery reveals reduced mortality and preservation of left ventricular function 1 yr after acute myocardial infarction. Am J Physiol Heart Circ Physiol *293*, H48-59.

Liu, X., Voulgaropoulou, F., Chen, R., Johnson, P.R., and Clark, K.R. (2000). Selective Rep-Cap gene amplification as a mechanism for high-titer recombinant AAV production from stable cell lines. Mol Ther *2*, 394-403.

Lobov, I.B., Brooks, P.C., and Lang, R.A. (2002). Angiopoietin-2 displays VEGF-dependent modulation of capillary structure and endothelial cell survival in vivo. Proc Natl Acad Sci U S A *99*, 11205-11210.

Lok, S., Johnston, D.S., Conklin, D., Lofton-Day, C.E., Adams, R.L., Jelmberg, A.C., Whitmore, T.E., Schrader, S., Griswold, M.D., and Jaspers, S.R. (2000). Identification of INSL6, a new member of the insulin family that is expressed in the testis of the human and rat. Biol Reprod *62*, 1593-1599.

Lopaschuk, G.D., Ussher, J.R., Folmes, C.D., Jaswal, J.S., and Stanley, W.C. (2010). Myocardial fatty acid metabolism in health and disease. Physiol Rev *90*, 207-258.

Lopez, J.J., Laham, R.J., Stamler, A., Pearlman, J.D., Bunting, S., Kaplan, A., Carrozza, J.P., Sellke, F.W., and Simons, M. (1998). VEGF administration in chronic myocardial ischemia in pigs. Cardiovasc Res *40*, 272-281.

Losordo, D.W., and Dimmeler, S. (2004). Therapeutic angiogenesis and vasculogenesis for ischemic disease. Part I: angiogenic cytokines. Circulation *109*, 2487-2491.

Losordo, D.W., Vale, P.R., Symes, J.F., Dunnington, C.H., Esakof, D.D., Maysky, M., Ashare, A.B., Lathi, K., and Isner, J.M. (1998). Gene therapy for myocardial angiogenesis: initial clinical results with direct myocardial injection of phVEGF165 as sole therapy for myocardial ischemia. Circulation *98*, 2800-2804.

Louboutin, J.P., Wang, L., and Wilson, J.M. (2005). Gene transfer into skeletal muscle using novel AAV serotypes. J Gene Med *7*, 442-451.

Lu, C., Walker, W.H., Sun, J., Weisz, O.A., Gibbs, R.B., Witchel, S.F., Sperling, M.A., and Menon, R.K. (2006). Insulin-like peptide 6: characterization of secretory status and posttranslational modifications. Endocrinology *147*, 5611-5623.

Lu, H., Xu, X., Zhang, M., Cao, R., Brakenhielm, E., Li, C., Lin, H., Yao, G., Sun, H., Qi, L.*, et al.* (2007). Combinatorial protein therapy of angiogenic and arteriogenic factors remarkably improves collaterogenesis and cardiac function in pigs. Proc Natl Acad Sci U S A *104*, 12140-12145.

Luo, Z., Diaco, M., Murohara, T., Ferrara, N., Isner, J.M., and Symes, J.F. (1997). Vascular endothelial growth factor attenuates myocardial ischemia-reperfusion injury. Ann Thorac Surg *64*, 993-998.

Lusis, A.J. (2000). Atherosclerosis. Nature *407*, 233-241.

Lux, K., Goerlitz, N., Schlemminger, S., Perabo, L., Goldnau, D., Endell, J., Leike, K., Kofler, D.M., Finke, S., Hallek, M.*, et al.* (2005). Green fluorescent protein-tagged adeno-associated virus particles allow the study of cytosolic and nuclear trafficking. J Virol *79*, 11776-11787.

Ly, H., Kawase, Y., Yoneyama, R., and Hajjar, R.J. (2007). Gene therapy in the treatment of heart failure. Physiology (Bethesda) *22*, 81-96.

Mahon, G.M., and Whitehead, I.P. (2001). Retrovirus cDNA expression library screening for oncogenes. Methods Enzymol *332*, 211-221.

Makinen, K., Manninen, H., Hedman, M., Matsi, P., Mussalo, H., Alhava, E., and Yla-Herttuala, S. (2002). Increased vascularity detected by digital subtraction angiography after VEGF gene transfer to human lower limb artery: a randomized, placebo-controlled, double-blinded phase II study. Mol Ther *6*, 127-133.

Makkar, R.R., Smith, R.R., Cheng, K., Malliaras, K., Thomson, L.E., Berman, D., Czer, L.S., Marban, L., Mendizabal, A., Johnston, P.V.*, et al.* (2012). Intracoronary cardiosphere-derived cells for heart regeneration after myocardial infarction (CADUCEUS): a prospective, randomised phase 1 trial. Lancet *379*, 895-904.

Masini, E., Nistri, S., Vannacci, A., Bani Sacchi, T., Novelli, A., and Bani, D. (2004). Relaxin inhibits the activation of human neutrophils: involvement of the nitric oxide pathway. Endocrinology *145*, 1106-1112.

Masuda, Y., Tanaka, T., Inomata, N., Ohnuma, N., Tanaka, S., Itoh, Z., Hosoda, H., Kojima, M., and Kangawa, K. (2000). Ghrelin stimulates gastric acid secretion and motility in rats. Biochem Biophys Res Commun *276*, 905-908.

Matsumoto, T., and Claesson-Welsh, L. (2001). VEGF receptor signal transduction. Sci STKE *2001*, re21.

Matsuura, K., Nagai, T., Nishigaki, N., Oyama, T., Nishi, J., Wada, H., Sano, M., Toko, H., Akazawa, H., Sato, T.*, et al.* (2004). Adult cardiac Sca-1-positive cells differentiate into beating cardiomyocytes. J Biol Chem *279*, 11384-11391.

Maudsley, S., Martin, B., and Luttrell, L.M. (2005). The origins of diversity and specificity in g protein-coupled receptor signaling. J Pharmacol Exp Ther *314*, 485-494.

Maurice, J.P., Hata, J.A., Shah, A.S., White, D.C., McDonald, P.H., Dolber, P.C., Wilson, K.H., Lefkowitz, R.J., Glower, D.D., and Koch, W.J. (1999). Enhancement of cardiac function after adenoviral-mediated in vivo intracoronary beta2-adrenergic receptor gene delivery. J Clin Invest *104*, 21-29.

Mauritz, C., Schwanke, K., Reppel, M., Neef, S., Katsirntaki, K., Maier, L.S., Nguemo, F., Menke, S., Haustein, M., Hescheler, J.*, et al.* (2008). Generation of

functional murine cardiac myocytes from induced pluripotent stem cells. Circulation *118*, 507-517.

McCarty, D.M., Fu, H., Monahan, P.E., Toulson, C.E., Naik, P., and Samulski, R.J. (2003). Adeno-associated virus terminal repeat (TR) mutant generates self-complementary vectors to overcome the rate-limiting step to transduction in vivo. Gene Ther *10*, 2112-2118.

McGowan, B.M., Stanley, S.A., Ghatei, M.A., and Bloom, S.R. (2009). Relaxin-3 and its role in neuroendocrine function. Ann N Y Acad Sci *1160*, 250-255.

McGuane, J.T., Debrah, J.E., Sautina, L., Jarajapu, Y.P., Novak, J., Rubin, J.P., Grant, M.B., Segal, M., and Conrad, K.P. (2011). Relaxin induces rapid dilation of rodent small renal and human subcutaneous arteries via PI3 kinase and nitric oxide. Endocrinology *152*, 2786-2796.

Melo, L.G., Agrawal, R., Zhang, L., Rezvani, M., Mangi, A.A., Ehsan, A., Griese, D.P., Dell'Acqua, G., Mann, M.J., Oyama, J.*, et al.* (2002). Gene therapy strategy for long-term myocardial protection using adeno-associated virus-mediated delivery of heme oxygenase gene. Circulation *105*, 602-607.

Melo, L.G., Pachori, A.S., Kong, D., Gnecchi, M., Wang, K., Pratt, R.E., and Dzau, V.J. (2004). Gene and cell-based therapies for heart disease. FASEB J *18*, 648-663.

Merten, O.W., Geny-Fiamma, C., and Douar, A.M. (2005). Current issues in adeno-associated viral vector production. Gene Ther *12 Suppl 1*, S51-61.

Messina, E., De Angelis, L., Frati, G., Morrone, S., Chimenti, S., Fiordaliso, F., Salio, M., Battaglia, M., Latronico, M.V., Coletta, M.*, et al.* (2004). Isolation and expansion of adult cardiac stem cells from human and murine heart. Circ Res *95*, 911-921.

Meyer, G.P., Wollert, K.C., Lotz, J., Pirr, J., Rager, U., Lippolt, P., Hahn, A., Fichtner, S., Schaefer, A., Arseniev, L.*, et al.* (2009). Intracoronary bone marrow cell transfer after myocardial infarction: 5-year follow-up from the randomized-controlled BOOST trial. Eur Heart J *30*, 2978-2984.

Michael, L.H., Ballantyne, C.M., Zachariah, J.P., Gould, K.E., Pocius, J.S., Taffet, G.E., Hartley, C.J., Pham, T.T., Daniel, S.L., Funk, E.*, et al.* (1999). Myocardial infarction and remodeling in mice: effect of reperfusion. Am J Physiol *277*, H660-668.

Michiels, F., van Es, H., van Rompaey, L., Merchiers, P., Francken, B., Pittois, K., van der Schueren, J., Brys, R., Vandersmissen, J., Beirinckx, F.*, et al.* (2002). Arrayed adenoviral expression libraries for functional screening. Nat Biotechnol *20*, 1154-1157.

Milei, J., Nunez, R.G., and Rapaport, M. (1978). Pathogenesis of isoproterenol-induced myocardial lesions: its reation to human 'coagulative myocytolysis'. Cardiology *63*, 139-151.

Miller, D.G., Trobridge, G.D., Petek, L.M., Jacobs, M.A., Kaul, R., and Russell, D.W. (2005). Large-scale analysis of adeno-associated virus vector integration sites in normal human cells. J Virol *79*, 11434-11442.

Moelker, A.D., Baks, T., Wever, K.M., Spitskovsky, D., Wielopolski, P.A., van Beusekom, H.M., van Geuns, R.J., Wnendt, S., Duncker, D.J., and van der Giessen, W.J. (2007). Intracoronary delivery of umbilical cord blood derived unrestricted somatic stem cells is not suitable to improve LV function after myocardial infarction in swine. J Mol Cell Cardiol *42*, 735-745.

Molina, E.J., Palma, J., Gupta, D., Torres, D., Gaughan, J.P., Houser, S., and Macha, M. (2009). Reverse remodeling is associated with changes in extracellular matrix proteases and tissue inhibitors after mesenchymal stem cell (MSC) treatment of pressure overload hypertrophy. J Tissue Eng Regen Med *3*, 85-91.

Mookerjee, I., Solly, N.R., Royce, S.G., Tregear, G.W., Samuel, C.S., and Tang, M.L. (2006). Endogenous relaxin regulates collagen deposition in an animal model of allergic airway disease. Endocrinology *147*, 754-761.

Moore, X.L., Tan, S.L., Lo, C.Y., Fang, L., Su, Y.D., Gao, X.M., Woodcock, E.A., Summers, R.J., Tregear, G.W., Bathgate, R.A*., et al.* (2007). Relaxin antagonizes hypertrophy and apoptosis in neonatal rat cardiomyocytes. Endocrinology *148*, 1582-1589.

Mori, S., Wang, L., Takeuchi, T., and Kanda, T. (2004). Two novel adeno-associated viruses from cynomolgus monkey: pseudotyping characterization of capsid protein. Virology *330*, 375-383.

Morishita, R., Nakamura, S., Hayashi, S., Taniyama, Y., Moriguchi, A., Nagano, T., Taiji, M., Noguchi, H., Takeshita, S., Matsumoto, K*., et al.* (1999). Therapeutic angiogenesis induced by human recombinant hepatocyte growth factor in rabbit hind limb ischemia model as cytokine supplement therapy. Hypertension *33*, 1379-1384.

Morishita, R., Sugimoto, T., Aoki, M., Kida, I., Tomita, N., Moriguchi, A., Maeda, K., Sawa, Y., Kaneda, Y., Higaki, J*., et al.* (1997). In vivo transfection of cis element "decoy" against nuclear factor-kappaB binding site prevents myocardial infarction. Nat Med *3*, 894-899.

Morton, G.J., and Schwartz, M.W. (2001). The NPY/AgRP neuron and energy homeostasis. Int J Obes Relat Metab Disord *25 Suppl 5*, S56-62.

Muccioli, G., Pons, N., Ghe, C., Catapano, F., Granata, R., and Ghigo, E. (2004). Ghrelin and des-acyl ghrelin both inhibit isoproterenol-induced lipolysis in rat adipocytes via a non-type 1a growth hormone secretagogue receptor. Eur J Pharmacol *498*, 27-35.

Muhlhauser, J., Pili, R., Merrill, M.J., Maeda, H., Passaniti, A., Crystal, R.G., and Capogrossi, M.C. (1995). In vivo angiogenesis induced by recombinant adenovirus vectors coding either for secreted or nonsecreted forms of acidic fibroblast growth factor. Hum Gene Ther *6*, 1457-1465.

Muller, O.J., Katus, H.A., and Bekeredjian, R. (2007). Targeting the heart with gene therapy-optimized gene delivery methods. Cardiovasc Res *73*, 453-462.

Murry, C.E., Field, L.J., and Menasche, P. (2005). Cell-based cardiac repair: reflections at the 10-year point. Circulation *112*, 3174-3183.

Murry, C.E., Soonpaa, M.H., Reinecke, H., Nakajima, H., Nakajima, H.O., Rubart, M., Pasumarthi, K.B., Virag, J.I., Bartelmez, S.H., Poppa, V.*, et al.* (2004). Haematopoietic stem cells do not transdifferentiate into cardiac myocytes in myocardial infarcts. Nature *428*, 664-668.

Muruve, D.A. (2004). The innate immune response to adenovirus vectors. Hum Gene Ther *15*, 1157-1166.

Nagaya, N., and Kangawa, K. (2003). Ghrelin improves left ventricular dysfunction and cardiac cachexia in heart failure. Curr Opin Pharmacol *3*, 146-151.

Nagaya, N., Kojima, M., Uematsu, M., Yamagishi, M., Hosoda, H., Oya, H., Hayashi, Y., and Kangawa, K. (2001a). Hemodynamic and hormonal effects of human ghrelin in healthy volunteers. Am J Physiol Regul Integr Comp Physiol *280*, R1483-1487.

Nagaya, N., Moriya, J., Yasumura, Y., Uematsu, M., Ono, F., Shimizu, W., Ueno, K., Kitakaze, M., Miyatake, K., and Kangawa, K. (2004). Effects of ghrelin administration on left ventricular function, exercise capacity, and muscle wasting in patients with chronic heart failure. Circulation *110*, 3674-3679.

Nagaya, N., Uematsu, M., Kojima, M., Ikeda, Y., Yoshihara, F., Shimizu, W., Hosoda, H., Hirota, Y., Ishida, H., Mori, H.*, et al.* (2001b). Chronic administration of ghrelin improves left ventricular dysfunction and attenuates development of cardiac cachexia in rats with heart failure. Circulation *104*, 1430-1435.

Nakai, H., Storm, T.A., and Kay, M.A. (2000). Recruitment of single-stranded recombinant adeno-associated virus vector genomes and intermolecular recombination are responsible for stable transduction of liver in vivo. J Virol *74*, 9451-9463.

Nakai, H., Wu, X., Fuess, S., Storm, T.A., Munroe, D., Montini, E., Burgess, S.M., Grompe, M., and Kay, M.A. (2005). Large-scale molecular characterization of adeno-associated virus vector integration in mouse liver. J Virol *79*, 3606-3614.

Nakai, H., Yant, S.R., Storm, T.A., Fuess, S., Meuse, L., and Kay, M.A. (2001). Extrachromosomal recombinant adeno-associated virus vector genomes are primarily responsible for stable liver transduction in vivo. J Virol *75*, 6969-6976.

Nakazato, M., Murakami, N., Date, Y., Kojima, M., Matsuo, H., Kangawa, K., and Matsukura, S. (2001). A role for ghrelin in the central regulation of feeding. Nature *409*, 194-198.

Namba, T., Koike, H., Murakami, K., Aoki, M., Makino, H., Hashiya, N., Ogihara, T., Kaneda, Y., Kohno, M., and Morishita, R. (2003). Angiogenesis induced by endothelial nitric oxide synthase gene through vascular endothelial growth factor expression in a rat hindlimb ischemia model. Circulation *108*, 2250-2257.

Nappi, J.M., and Sieg, A. (2011). Aldosterone and aldosterone receptor antagonists in patients with chronic heart failure. Vasc Health Risk Manag *7*, 353-363.

Natalucci, G., Riedl, S., Gleiss, A., Zidek, T., and Frisch, H. (2005). Spontaneous 24-h ghrelin secretion pattern in fasting subjects: maintenance of a meal-related pattern. Eur J Endocrinol *152*, 845-850.

Nelson, T.J., Martinez-Fernandez, A., Yamada, S., Perez-Terzic, C., Ikeda, Y., and Terzic, A. (2009). Repair of acute myocardial infarction by human stemness factors induced pluripotent stem cells. Circulation *120*, 408-416.

Ni, T.H., McDonald, W.F., Zolotukhin, I., Melendy, T., Waga, S., Stillman, B., and Muzyczka, N. (1998). Cellular proteins required for adeno-associated virus DNA replication in the absence of adenovirus coinfection. J Virol *72*, 2777-2787.

Nikol, S., Baumgartner, I., Van Belle, E., Diehm, C., Visona, A., Capogrossi, M.C., Ferreira-Maldent, N., Gallino, A., Wyatt, M.G., Wijesinghe, L.D.*, et al.* (2008). Therapeutic angiogenesis with intramuscular NV1FGF improves amputation-free survival in patients with critical limb ischemia. Mol Ther *16*, 972-978.

Nogueiras, R., Tschop, M.H., and Zigman, J.M. (2008). Central nervous system regulation of energy metabolism: ghrelin versus leptin. Ann N Y Acad Sci *1126*, 14-19.

Noma, T., Lemaire, A., Naga Prasad, S.V., Barki-Harrington, L., Tilley, D.G., Chen, J., Le Corvoisier, P., Violin, J.D., Wei, H., Lefkowitz, R.J.*, et al.* (2007). Beta-arrestin-mediated beta1-adrenergic receptor transactivation of the EGFR confers cardioprotection. J Clin Invest *117*, 2445-2458.

Nussbaum, J., Minami, E., Laflamme, M.A., Virag, J.A., Ware, C.B., Masino, A., Muskheli, V., Pabon, L., Reinecke, H., and Murry, C.E. (2007). Transplantation of undifferentiated murine embryonic stem cells in the heart: teratoma formation and immune response. FASEB J *21*, 1345-1357.

O'Riordan, C.R., Lachapelle, A.L., Vincent, K.A., and Wadsworth, S.C. (2000). Scaleable chromatographic purification process for recombinant adeno-associated virus (rAAV). J Gene Med *2*, 444-454.

Oh, H., Bradfute, S.B., Gallardo, T.D., Nakamura, T., Gaussin, V., Mishina, Y., Pocius, J., Michael, L.H., Behringer, R.R., Garry, D.J.*, et al.* (2003). Cardiac progenitor cells from adult myocardium: homing, differentiation, and fusion after infarction. Proc Natl Acad Sci U S A *100*, 12313-12318.

Okazaki, Y., Furuno, M., Kasukawa, T., Adachi, J., Bono, H., Kondo, S., Nikaido, I., Osato, N., Saito, R., Suzuki, H.*, et al.* (2002). Analysis of the mouse transcriptome based on functional annotation of 60,770 full-length cDNAs. Nature *420*, 563-573.

Okita, K., Nakagawa, M., Hyenjong, H., Ichisaka, T., and Yamanaka, S. (2008). Generation of mouse induced pluripotent stem cells without viral vectors. Science *322*, 949-953.

Okubo, S., Wildner, O., Shah, M.R., Chelliah, J.C., Hess, M.L., and Kukreja, R.C. (2001). Gene transfer of heat-shock protein 70 reduces infarct size in vivo after ischemia/reperfusion in the rabbit heart. Circulation *103*, 877-881.

Olin, J.W., Allie, D.E., Belkin, M., Bonow, R.O., Casey, D.E., Jr., Creager, M.A., Gerber, T.C., Hirsch, A.T., Jaff, M.R., Kaufman, J.A.*, et al.* (2011). ACCF/AHA/ACR/SCAI/SIR/SVM/SVN/SVS 2010 performance measures for adults with peripheral artery disease: a report of the American College of Cardiology Foundation/American Heart Association Task Force on Performance Measures, the

American College of Radiology, the Society for Cardiac Angiography and Interventions, the Society for Interventional Radiology, the Society for Vascular Medicine, the Society for Vascular Nursing, and the Society for Vascular Surgery (Writing Committee to Develop Clinical Performance Measures for Peripheral Artery Disease). J Vasc Nurs *29*, 23-60.

Orlic, D., Kajstura, J., Chimenti, S., Jakoniuk, I., Anderson, S.M., Li, B., Pickel, J., McKay, R., Nadal-Ginard, B., Bodine, D.M.*, et al.* (2001). Bone marrow cells regenerate infarcted myocardium. Nature *410*, 701-705.

Otto, B., Cuntz, U., Fruehauf, E., Wawarta, R., Folwaczny, C., Riepl, R.L., Heiman, M.L., Lehnert, P., Fichter, M., and Tschop, M. (2001). Weight gain decreases elevated plasma ghrelin concentrations of patients with anorexia nervosa. Eur J Endocrinol *145*, 669-673.

Pacak, C.A., Mah, C.S., Thattaliyath, B.D., Conlon, T.J., Lewis, M.A., Cloutier, D.E., Zolotukhin, I., Tarantal, A.F., and Byrne, B.J. (2006). Recombinant adeno-associated virus serotype 9 leads to preferential cardiac transduction in vivo. Circ Res *99*, e3-9.

Parry, L.J., and Vodstrcil, L.A. (2007). Relaxin physiology in the female reproductive tract during pregnancy. Adv Exp Med Biol *612*, 34-48.

Passioura, T., Shen, S., Symonds, G., and Dolnikov, A. (2005). A retroviral library genetic screen identifies IRF-2 as an inhibitor of N-ras-induced growth suppression in leukemic cells. Oncogene *24*, 7327-7336.

Patel, T.H., Kimura, H., Weiss, C.R., Semenza, G.L., and Hofmann, L.V. (2005). Constitutively active HIF-1alpha improves perfusion and arterial remodeling in an endovascular model of limb ischemia. Cardiovasc Res *68*, 144-154.

Pathak, A., Baldwin, B., and Kranias, E.G. (2007). Key protein alterations associated with hyperdynamic cardiac function: insights based on proteomic analysis of the protein phosphatase 1 inhibitor-1 overexpressing hearts. Hellenic J Cardiol *48*, 30-36.

Pathak, A., del Monte, F., Zhao, W., Schultz, J.E., Lorenz, J.N., Bodi, I., Weiser, D., Hahn, H., Carr, A.N., Syed, F.*, et al.* (2005). Enhancement of cardiac function and suppression of heart failure progression by inhibition of protein phosphatase 1. Circ Res *96*, 756-766.

Pavlou, A.K., and Reichert, J.M. (2004). Recombinant protein therapeutics--success rates, market trends and values to 2010. Nat Biotechnol *22*, 1513-1519.

Pearlman, J.D., Hibberd, M.G., Chuang, M.L., Harada, K., Lopez, J.J., Gladstone, S.R., Friedman, M., Sellke, F.W., and Simons, M. (1995). Magnetic resonance mapping demonstrates benefits of VEGF-induced myocardial angiogenesis. Nat Med *1*, 1085-1089.

Pedretti, A., Villa, M., Pallavicini, M., Valoti, E., and Vistoli, G. (2006). Construction of human ghrelin receptor (hGHS-R1a) model using a fragmental prediction approach and validation through docking analysis. J Med Chem *49*, 3077-3085.

Penela, P., Murga, C., Ribas, C., Lafarga, V., and Mayor, F., Jr. (2010). The complex G protein-coupled receptor kinase 2 (GRK2) interactome unveils new physiopathological targets. Br J Pharmacol *160*, 821-832.

Pennock, G.D., Yun, D.D., Agarwal, P.G., Spooner, P.H., and Goldman, S. (1997). Echocardiographic changes after myocardial infarction in a model of left ventricular diastolic dysfunction. Am J Physiol *273*, H2018-2029.

Pepe, M., Mamdani, M., Zentilin, L., Csiszar, A., Qanud, K., Zacchigna, S., Ungvari, Z., Puligadda, U., Moimas, S., Xu, X.*, et al.* (2010). Intramyocardial VEGF-B167 gene delivery delays the progression towards congestive failure in dogs with pacing-induced dilated cardiomyopathy. Circ Res *106*, 1893-1903.

Perabo, L., Buning, H., Kofler, D.M., Ried, M.U., Girod, A., Wendtner, C.M., Enssle, J., and Hallek, M. (2003). In vitro selection of viral vectors with modified tropism: the adeno-associated virus display. Mol Ther *8*, 151-157.

Perin, E.C., Dohmann, H.F., Borojevic, R., Silva, S.A., Sousa, A.L., Mesquita, C.T., Rossi, M.I., Carvalho, A.C., Dutra, H.S., Dohmann, H.J.*, et al.* (2003). Transendocardial, autologous bone marrow cell transplantation for severe, chronic ischemic heart failure. Circulation *107*, 2294-2302.

Phan, H.M., Gao, M.H., Lai, N.C., Tang, T., and Hammond, H.K. (2007). New signaling pathways associated with increased cardiac adenylyl cyclase 6 expression: implications for possible congestive heart failure therapy. Trends Cardiovasc Med *17*, 215-221.

Philpott, N.J., Gomos, J., Berns, K.I., and Falck-Pedersen, E. (2002). A p5 integration efficiency element mediates Rep-dependent integration into AAVS1 at chromosome 19. Proc Natl Acad Sci U S A *99*, 12381-12385.

Planat-Benard, V., Silvestre, J.S., Cousin, B., Andre, M., Nibbelink, M., Tamarat, R., Clergue, M., Manneville, C., Saillan-Barreau, C., Duriez, M.*, et al.* (2004). Plasticity of human adipose lineage cells toward endothelial cells: physiological and therapeutic perspectives. Circulation *109*, 656-663.

Ponikowski, P., Metra, M., Teerlink, J.R., Unemori, E., Felker, G.M., Voors, A.A., Filippatos, G., Greenberg, B., Teichman, S.L., Severin, T.*, et al.* (2012). Design of the RELAXin in acute heart failure study. Am Heart J *163*, 149-155 e141.

Ponnazhagan, S., Mahendra, G., Kumar, S., Thompson, J.A., and Castillas, M., Jr. (2002). Conjugate-based targeting of recombinant adeno-associated virus type 2 vectors by using avidin-linked ligands. J Virol *76*, 12900-12907.

Popovic, V., Miljic, D., Micic, D., Damjanovic, S., Arvat, E., Ghigo, E., Dieguez, C., and Casanueva, F.F. (2003). Ghrelin main action on the regulation of growth hormone release is exerted at hypothalamic level. J Clin Endocrinol Metab *88*, 3450-3453.

Powell, R.J., Simons, M., Mendelsohn, F.O., Daniel, G., Henry, T.D., Koga, M., Morishita, R., and Annex, B.H. (2008). Results of a double-blind, placebo-controlled study to assess the safety of intramuscular injection of hepatocyte growth factor

plasmid to improve limb perfusion in patients with critical limb ischemia. Circulation *118*, 58-65.

Prasad, K.M., Xu, Y., Yang, Z., Acton, S.T., and French, B.A. (2011). Robust cardiomyocyte-specific gene expression following systemic injection of AAV: in vivo gene delivery follows a Poisson distribution. Gene Ther *18*, 43-52.

Qing, K., Mah, C., Hansen, J., Zhou, S., Dwarki, V., and Srivastava, A. (1999). Human fibroblast growth factor receptor 1 is a co-receptor for infection by adeno-associated virus 2. Nat Med *5*, 71-77.

Quinn, K., Quirion, M.R., Lo, C.Y., Misplon, J.A., Epstein, S.L., and Chiorini, J.A. (2011). Intranasal administration of adeno-associated virus type 12 (AAV12) leads to transduction of the nasal epithelia and can initiate transgene-specific immune response. Mol Ther *19*, 1990-1998.

Raake, P., von Degenfeld, G., Hinkel, R., Vachenauer, R., Sandner, T., Beller, S., Andrees, M., Kupatt, C., Schuler, G., and Boekstegers, P. (2004). Myocardial gene transfer by selective pressure-regulated retroinfusion of coronary veins: comparison with surgical and percutaneous intramyocardial gene delivery. J Am Coll Cardiol *44*, 1124-1129.

Rabinowitz, J.E., Bowles, D.E., Faust, S.M., Ledford, J.G., Cunningham, S.E., and Samulski, R.J. (2004). Cross-dressing the virion: the transcapsidation of adeno-associated virus serotypes functionally defines subgroups. J Virol *78*, 4421-4432.

Rabinowitz, J.E., Rolling, F., Li, C., Conrath, H., Xiao, W., Xiao, X., and Samulski, R.J. (2002). Cross-packaging of a single adeno-associated virus (AAV) type 2 vector genome into multiple AAV serotypes enables transduction with broad specificity. J Virol *76*, 791-801.

Rader, R.A. (2008). (Re)defining biopharmaceutical. Nat Biotechnol *26*, 743-751.

Rajagopalan, S., Olin, J.W., Young, S., Erikson, M., Grossman, P.M., Mendelsohn, F.O., Regensteiner, J.G., Hiatt, W.R., and Annex, B.H. (2004). Design of the Del-1 for therapeutic angiogenesis trial (DELTA-1), a phase II multicenter, double-blind, placebo-controlled trial of VLTS-589 in subjects with intermittent claudication secondary to peripheral arterial disease. Hum Gene Ther *15*, 619-624.

Rebolledo, B., Lai, N.C., Gao, M.H., Takahashi, T., Roth, D.M., Baird, S.M., and Hammond, H.K. (2006). Adenylylcyclase gene transfer increases function of the failing heart. Hum Gene Ther *17*, 1043-1048.

Reich, S.J., Auricchio, A., Hildinger, M., Glover, E., Maguire, A.M., Wilson, J.M., and Bennett, J. (2003). Efficient trans-splicing in the retina expands the utility of adeno-associated virus as a vector for gene therapy. Hum Gene Ther *14*, 37-44.

Ren, J. (2002). Short-term administration of insulin-like growth factor I (IGF-1) does not induce myocardial IGF-1 resistance. Growth Horm IGF Res *12*, 162-168.

Risau, W. (1997). Mechanisms of angiogenesis. Nature *386*, 671-674.

Rissanen, T.T., Korpisalo, P., Markkanen, J.E., Liimatainen, T., Orden, M.R., Kholova, I., de Goede, A., Heikura, T., Grohn, O.H., and Yla-Herttuala, S. (2005).

Blood flow remodels growing vasculature during vascular endothelial growth factor gene therapy and determines between capillary arterialization and sprouting angiogenesis. Circulation *112*, 3937-3946.

Rissanen, T.T., Markkanen, J.E., Arve, K., Rutanen, J., Kettunen, M.I., Vajanto, I., Jauhiainen, S., Cashion, L., Gruchala, M., Narvanen, O.*, et al.* (2003). Fibroblast growth factor 4 induces vascular permeability, angiogenesis and arteriogenesis in a rabbit hindlimb ischemia model. FASEB J *17*, 100-102.

Rissanen, T.T., and Yla-Herttuala, S. (2007). Current status of cardiovascular gene therapy. Mol Ther *15*, 1233-1247.

Roger, V.L., Go, A.S., Lloyd-Jones, D.M., Adams, R.J., Berry, J.D., Brown, T.M., Carnethon, M.R., Dai, S., de Simone, G., Ford, E.S.*, et al.* (2011). Heart disease and stroke statistics--2011 update: a report from the American Heart Association. Circulation *123*, e18-e209.

Rosengart, T.K., Lee, L.Y., Patel, S.R., Kligfield, P.D., Okin, P.M., Hackett, N.R., Isom, O.W., and Crystal, R.G. (1999). Six-month assessment of a phase I trial of angiogenic gene therapy for the treatment of coronary artery disease using direct intramyocardial administration of an adenovirus vector expressing the VEGF121 cDNA. Ann Surg *230*, 466-470; discussion 470-462.

Ross, R. (1999). Atherosclerosis--an inflammatory disease. N Engl J Med *340*, 115-126.

Roy, S., Khanna, S., Hussain, S.R., Biswas, S., Azad, A., Rink, C., Gnyawali, S., Shilo, S., Nuovo, G.J., and Sen, C.K. (2009). MicroRNA expression in response to murine myocardial infarction: miR-21 regulates fibroblast metalloprotease-2 via phosphatase and tensin homologue. Cardiovasc Res *82*, 21-29.

Ruixing, Y., Jinzhen, W., Dezhai, Y., and Jiaquan, L. (2007). Cardioprotective role of cardiotrophin-1 gene transfer in a murine model of myocardial infarction. Growth Factors *25*, 286-294.

Rutledge, E.A., and Russell, D.W. (1997). Adeno-associated virus vector integration junctions. J Virol *71*, 8429-8436.

Sami, S., and Willerson, J.T. (2010). Contemporary treatment of unstable angina and non-ST-segment-elevation myocardial infarction (part 2). Tex Heart Inst J *37*, 262-275.

Samuel, C.S., and Hewitson, T.D. (2006). Relaxin in cardiovascular and renal disease. Kidney Int *69*, 1498-1502.

Samuel, C.S., Tian, H., Zhao, L., and Amento, E.P. (2003). Relaxin is a key mediator of prostate growth and male reproductive tract development. Lab Invest *83*, 1055-1067.

Samuel, C.S., Unemori, E.N., Mookerjee, I., Bathgate, R.A., Layfield, S.L., Mak, J., Tregear, G.W., and Du, X.J. (2004a). Relaxin modulates cardiac fibroblast proliferation, differentiation, and collagen production and reverses cardiac fibrosis in vivo. Endocrinology *145*, 4125-4133.

Samuel, C.S., Zhao, C., Bond, C.P., Hewitson, T.D., Amento, E.P., and Summers, R.J. (2004b). Relaxin-1-deficient mice develop an age-related progression of renal fibrosis. Kidney Int *65*, 2054-2064.

Samuel, C.S., Zhao, C., Yang, Q., Wang, H., Tian, H., Tregear, G.W., and Amento, E.P. (2005). The relaxin gene knockout mouse: a model of progressive scleroderma. J Invest Dermatol *125*, 692-699.

Samulski, R.J., Zhu, X., Xiao, X., Brook, J.D., Housman, D.E., Epstein, N., and Hunter, L.A. (1991). Targeted integration of adeno-associated virus (AAV) into human chromosome 19. EMBO J *10*, 3941-3950.

Sands, M.S. (2011). AAV-mediated liver-directed gene therapy. Methods Mol Biol *807*, 141-157.

Sanlioglu, S., Benson, P.K., Yang, J., Atkinson, E.M., Reynolds, T., and Engelhardt, J.F. (2000). Endocytosis and nuclear trafficking of adeno-associated virus type 2 are controlled by rac1 and phosphatidylinositol-3 kinase activation. J Virol *74*, 9184-9196.

Saric, T., Frenzel, L.P., and Hescheler, J. (2008). Immunological barriers to embryonic stem cell-derived therapies. Cells Tissues Organs *188*, 78-90.

Sarkar, N., Ruck, A., Kallner, G., S, Y.H., Blomberg, P., Islam, K.B., van der Linden, J., Lindblom, D., Nygren, A.T., Lind, B.*, et al.* (2001). Effects of intramyocardial injection of phVEGF-A165 as sole therapy in patients with refractory coronary artery disease--12-month follow-up: angiogenic gene therapy. J Intern Med *250*, 373-381.

Sato, M., Nakahara, K., Goto, S., Kaiya, H., Miyazato, M., Date, Y., Nakazato, M., Kangawa, K., and Murakami, N. (2006). Effects of ghrelin and des-acyl ghrelin on neurogenesis of the rat fetal spinal cord. Biochem Biophys Res Commun *350*, 598-603.

Saudan, P., Vlach, J., and Beard, P. (2000). Inhibition of S-phase progression by adeno-associated virus Rep78 protein is mediated by hypophosphorylated pRb. EMBO J *19*, 4351-4361.

Schachinger, V., Assmus, B., Britten, M.B., Honold, J., Lehmann, R., Teupe, C., Abolmaali, N.D., Vogl, T.J., Hofmann, W.K., Martin, H.*, et al.* (2004). Transplantation of progenitor cells and regeneration enhancement in acute myocardial infarction: final one-year results of the TOPCARE-AMI Trial. J Am Coll Cardiol *44*, 1690-1699.

Schachinger, V., Erbs, S., Elsasser, A., Haberbosch, W., Hambrecht, R., Holschermann, H., Yu, J., Corti, R., Mathey, D.G., Hamm, C.W.*, et al.* (2006). Improved clinical outcome after intracoronary administration of bone-marrow-derived progenitor cells in acute myocardial infarction: final 1-year results of the REPAIR-AMI trial. Eur Heart J *27*, 2775-2783.

Schmidt, M., Voutetakis, A., Afione, S., Zheng, C., Mandikian, D., and Chiorini, J.A. (2008). Adeno-associated virus type 12 (AAV12): a novel AAV serotype with sialic acid- and heparan sulfate proteoglycan-independent transduction activity. J Virol *82*, 1399-1406.

Schnepp, B.C., Jensen, R.L., Chen, C.L., Johnson, P.R., and Clark, K.R. (2005). Characterization of adeno-associated virus genomes isolated from human tissues. J Virol *79*, 14793-14803.

Schultz, B.R., and Chamberlain, J.S. (2008). Recombinant adeno-associated virus transduction and integration. Mol Ther *16*, 1189-1199.

Schumacher, B., Pecher, P., von Specht, B.U., and Stegmann, T. (1998). Induction of neoangiogenesis in ischemic myocardium by human growth factors: first clinical results of a new treatment of coronary heart disease. Circulation *97*, 645-650.

Schwarz, E.R., Speakman, M.T., Patterson, M., Hale, S.S., Isner, J.M., Kedes, L.H., and Kloner, R.A. (2000). Evaluation of the effects of intramyocardial injection of DNA expressing vascular endothelial growth factor (VEGF) in a myocardial infarction model in the rat--angiogenesis and angioma formation. J Am Coll Cardiol *35*, 1323-1330.

Schwenke, D.O., Tokudome, T., Kishimoto, I., Horio, T., Shirai, M., Cragg, P.A., and Kangawa, K. (2008). Early ghrelin treatment after myocardial infarction prevents an increase in cardiac sympathetic tone and reduces mortality. Endocrinology *149*, 5172-5176.

Seim, I., Walpole, C., Amorim, L., Josh, P., Herington, A., and Chopin, L. (2011). The expanding roles of the ghrelin-gene derived peptide obestatin in health and disease. Mol Cell Endocrinol *340*, 111-117.

Seisenberger, G., Ried, M.U., Endress, T., Buning, H., Hallek, M., and Brauchle, C. (2001). Real-time single-molecule imaging of the infection pathway of an adeno-associated virus. Science *294*, 1929-1932.

Selvin, E., and Erlinger, T.P. (2004). Prevalence of and risk factors for peripheral arterial disease in the United States: results from the National Health and Nutrition Examination Survey, 1999-2000. Circulation *110*, 738-743.

Senter, S., and Francis, G.S. (2009). A new, precise definition of acute myocardial infarction. Cleve Clin J Med *76*, 159-166.

Shah, A.M., and Mann, D.L. (2011). In search of new therapeutic targets and strategies for heart failure: recent advances in basic science. Lancet *378*, 704-712.

Shah, A.S., Lilly, R.E., Kypson, A.P., Tai, O., Hata, J.A., Pippen, A., Silvestry, S.C., Lefkowitz, R.J., Glower, D.D., and Koch, W.J. (2000). Intracoronary adenovirus-mediated delivery and overexpression of the beta(2)-adrenergic receptor in the heart : prospects for molecular ventricular assistance. Circulation *101*, 408-414.

Shanes, J.G., Minadeo, K.N., Moret, A., Groner, M., and Tabaie, S.A. (2007). Statin therapy in heart failure: prognostic effects and potential mechanisms. Am Heart J *154*, 617-623.

Shen, S., Bryant, K.D., Brown, S.M., Randell, S.H., and Asokan, A. (2011). Terminal N-linked galactose is the primary receptor for adeno-associated virus 9. J Biol Chem *286*, 13532-13540.

Sherwood, O.D. (2004). Relaxin's physiological roles and other diverse actions. Endocr Rev *25*, 205-234.

Shi, R.Z., and Li, Q.P. (2008). Improving outcome of transplanted mesenchymal stem cells for ischemic heart disease. Biochem Biophys Res Commun *376*, 247-250.

Shiomi, T., Tsutsui, H., Matsusaka, H., Murakami, K., Hayashidani, S., Ikeuchi, M., Wen, J., Kubota, T., Utsumi, H., and Takeshita, A. (2004). Overexpression of glutathione peroxidase prevents left ventricular remodeling and failure after myocardial infarction in mice. Circulation *109*, 544-549.

Simons, M., Annex, B.H., Laham, R.J., Kleiman, N., Henry, T., Dauerman, H., Udelson, J.E., Gervino, E.V., Pike, M., Whitehouse, M.J.*, et al.* (2002). Pharmacological treatment of coronary artery disease with recombinant fibroblast growth factor-2: double-blind, randomized, controlled clinical trial. Circulation *105*, 788-793.

Sipo, I., Fechner, H., Pinkert, S., Suckau, L., Wang, X., Weger, S., and Poller, W. (2007). Differential internalization and nuclear uncoating of self-complementary adeno-associated virus pseudotype vectors as determinants of cardiac cell transduction. Gene Ther *14*, 1319-1329.

Smith, C.M., Shen, P.J., Banerjee, A., Bonaventure, P., Ma, S., Bathgate, R.A., Sutton, S.W., and Gundlach, A.L. (2010). Distribution of relaxin-3 and RXFP3 within arousal, stress, affective, and cognitive circuits of mouse brain. J Comp Neurol *518*, 4016-4045.

Soares, J.B., Rocha-Sousa, A., Castro-Chaves, P., Henriques-Coelho, T., and Leite-Moreira, A.F. (2006). Inotropic and lusitropic effects of ghrelin and their modulation by the endocardial endothelium, NO, prostaglandins, GHS-R1a and KCa channels. Peptides *27*, 1616-1623.

Soeki, T., Kishimoto, I., Schwenke, D.O., Tokudome, T., Horio, T., Yoshida, M., Hosoda, H., and Kangawa, K. (2008). Ghrelin suppresses cardiac sympathetic activity and prevents early left ventricular remodeling in rats with myocardial infarction. Am J Physiol Heart Circ Physiol *294*, H426-432.

Sonntag, F., Bleker, S., Leuchs, B., Fischer, R., and Kleinschmidt, J.A. (2006). Adeno-associated virus type 2 capsids with externalized VP1/VP2 trafficking domains are generated prior to passage through the cytoplasm and are maintained until uncoating occurs in the nucleus. J Virol *80*, 11040-11054.

Sonntag, F., Schmidt, K., and Kleinschmidt, J.A. (2010). A viral assembly factor promotes AAV2 capsid formation in the nucleolus. Proc Natl Acad Sci U S A *107*, 10220-10225.

Squadrito, F., Deodato, B., Squadrito, G., Seminara, P., Passaniti, M., Venuti, F.S., Giacca, M., Minutoli, L., Adamo, E.B., Bellomo, M.*, et al.* (2003). Gene transfer of IkappaBalpha limits infarct size in a mouse model of myocardial ischemia-reperfusion injury. Lab Invest *83*, 1097-1104.

Srivastava, A., Lusby, E.W., and Berns, K.I. (1983). Nucleotide sequence and organization of the adeno-associated virus 2 genome. J Virol *45*, 555-564.

Stahnke, S., Lux, K., Uhrig, S., Kreppel, F., Hosel, M., Coutelle, O., Ogris, M., Hallek, M., and Buning, H. (2011). Intrinsic phospholipase A2 activity of adeno-associated virus is involved in endosomal escape of incoming particles. Virology *409*, 77-83.

Stanley, W.C., Recchia, F.A., and Lopaschuk, G.D. (2005). Myocardial substrate metabolism in the normal and failing heart. Physiol Rev *85*, 1093-1129.

Steiger, A., Dresler, M., Schussler, P., and Kluge, M. (2011). Ghrelin in mental health, sleep, memory. Mol Cell Endocrinol *340*, 88-96.

Stewart, D.J., Hilton, J.D., Arnold, J.M., Gregoire, J., Rivard, A., Archer, S.L., Charbonneau, F., Cohen, E., Curtis, M., Buller, C.E.*, et al.* (2006). Angiogenic gene therapy in patients with nonrevascularizable ischemic heart disease: a phase 2 randomized, controlled trial of AdVEGF(121) (AdVEGF121) versus maximum medical treatment. Gene Ther *13*, 1503-1511.

Stewart, D.J., Kutryk, M.J., Fitchett, D., Freeman, M., Camack, N., Su, Y., Della Siega, A., Bilodeau, L., Burton, J.R., Proulx, G.*, et al.* (2009). VEGF gene therapy fails to improve perfusion of ischemic myocardium in patients with advanced coronary disease: results of the NORTHERN trial. Mol Ther *17*, 1109-1115.

Stewart, S., MacIntyre, K., Hole, D.J., Capewell, S., and McMurray, J.J. (2001). More 'malignant' than cancer? Five-year survival following a first admission for heart failure. Eur J Heart Fail *3*, 315-322.

Strauer, B.E., Brehm, M., Zeus, T., Kostering, M., Hernandez, A., Sorg, R.V., Kogler, G., and Wernet, P. (2002). Repair of infarcted myocardium by autologous intracoronary mononuclear bone marrow cell transplantation in humans. Circulation *106*, 1913-1918.

Strauer, B.E., Yousef, M., and Schannwell, C.M. (2010). The acute and long-term effects of intracoronary Stem cell Transplantation in 191 patients with chronic heARt failure: the STAR-heart study. Eur J Heart Fail *12*, 721-729.

Su, E.J., Cioffi, C.L., Stefansson, S., Mittereder, N., Garay, M., Hreniuk, D., and Liau, G. (2003). Gene therapy vector-mediated expression of insulin-like growth factors protects cardiomyocytes from apoptosis and enhances neovascularization. Am J Physiol Heart Circ Physiol *284*, H1429-1440.

Suckau, L., Fechner, H., Chemaly, E., Krohn, S., Hadri, L., Kockskamper, J., Westermann, D., Bisping, E., Ly, H., Wang, X.*, et al.* (2009). Long-term cardiac-targeted RNA interference for the treatment of heart failure restores cardiac function and reduces pathological hypertrophy. Circulation *119*, 1241-1252.

Sugano, M., Tsuchida, K., Hata, T., and Makino, N. (2004). In vivo transfer of soluble TNF-alpha receptor 1 gene improves cardiac function and reduces infarct size after myocardial infarction in rats. FASEB J *18*, 911-913.

Summerford, C., Bartlett, J.S., and Samulski, R.J. (1999). AlphaVbeta5 integrin: a co-receptor for adeno-associated virus type 2 infection. Nat Med *5*, 78-82.

Summerford, C., and Samulski, R.J. (1998). Membrane-associated heparan sulfate proteoglycan is a receptor for adeno-associated virus type 2 virions. J Virol *72*, 1438-1445.

Sun, Y., Ahmed, S., and Smith, R.G. (2003). Deletion of ghrelin impairs neither growth nor appetite. Mol Cell Biol *23*, 7973-7981.

Sun, Y., Wang, P., Zheng, H., and Smith, R.G. (2004). Ghrelin stimulation of growth hormone release and appetite is mediated through the growth hormone secretagogue receptor. Proc Natl Acad Sci U S A *101*, 4679-4684.

Sutton, M.G., and Sharpe, N. (2000). Left ventricular remodeling after myocardial infarction: pathophysiology and therapy. Circulation *101*, 2981-2988.

Swynghedauw, B. (1999). Molecular mechanisms of myocardial remodeling. Physiol Rev *79*, 215-262.

Sylven, C., Sarkar, N., Insulander, P., Kenneback, G., Blomberg, P., Islam, K., and Drvota, V. (2002). Catheter-based transendocardial myocardial gene transfer. J Interv Cardiol *15*, 7-13.

Tafuro, S., Ayuso, E., Zacchigna, S., Zentilin, L., Moimas, S., Dore, F., and Giacca, M. (2009). Inducible adeno-associated virus vectors promote functional angiogenesis in adult organisms via regulated vascular endothelial growth factor expression. Cardiovasc Res *83*, 663-671.

Takahashi, K., and Yamanaka, S. (2006). Induction of pluripotent stem cells from mouse embryonic and adult fibroblast cultures by defined factors. Cell *126*, 663-676.

Takaya, K., Ariyasu, H., Kanamoto, N., Iwakura, H., Yoshimoto, A., Harada, M., Mori, K., Komatsu, Y., Usui, T., Shimatsu, A.*, et al.* (2000). Ghrelin strongly stimulates growth hormone release in humans. J Clin Endocrinol Metab *85*, 4908-4911.

Takemura, G., and Fujiwara, H. (2004). Role of apoptosis in remodeling after myocardial infarction. Pharmacol Ther *104*, 1-16.

Takeshita, S., Weir, L., Chen, D., Zheng, L.P., Riessen, R., Bauters, C., Symes, J.F., Ferrara, N., and Isner, J.M. (1996). Therapeutic angiogenesis following arterial gene transfer of vascular endothelial growth factor in a rabbit model of hindlimb ischemia. Biochem Biophys Res Commun *227*, 628-635.

Tang, M.L., Samuel, C.S., and Royce, S.G. (2009). Role of relaxin in regulation of fibrosis in the lung. Ann N Y Acad Sci *1160*, 342-347.

Tang, X.L., Rokosh, G., Sanganalmath, S.K., Yuan, F., Sato, H., Mu, J., Dai, S., Li, C., Chen, N., Peng, Y.*, et al.* (2010). Intracoronary administration of cardiac progenitor cells alleviates left ventricular dysfunction in rats with a 30-day-old infarction. Circulation *121*, 293-305.

Taymans, J.M., Vandenberghe, L.H., Haute, C.V., Thiry, I., Deroose, C.M., Mortelmans, L., Wilson, J.M., Debyser, Z., and Baekelandt, V. (2007). Comparative

analysis of adeno-associated viral vector serotypes 1, 2, 5, 7, and 8 in mouse brain. Hum Gene Ther *18*, 195-206.

Teichman, S.L., Unemori, E., Teerlink, J.R., Cotter, G., and Metra, M. (2010). Relaxin: review of biology and potential role in treating heart failure. Curr Heart Fail Rep *7*, 75-82.

Tendera, M., Aboyans, V., Bartelink, M.L., Baumgartner, I., Clement, D., Collet, J.P., Cremonesi, A., De Carlo, M., Erbel, R., Fowkes, F.G.*, et al.* (2011). ESC Guidelines on the diagnosis and treatment of peripheral artery diseases: Document covering atherosclerotic disease of extracranial carotid and vertebral, mesenteric, renal, upper and lower extremity arteries * The Task Force on the Diagnosis and Treatment of Peripheral Artery Diseases of the European Society of Cardiology (ESC). Eur Heart J *32*, 2851-2906.

Thompson, N.M., Gill, D.A., Davies, R., Loveridge, N., Houston, P.A., Robinson, I.C., and Wells, T. (2004). Ghrelin and des-octanoyl ghrelin promote adipogenesis directly in vivo by a mechanism independent of the type 1a growth hormone secretagogue receptor. Endocrinology *145*, 234-242.

Thum, T., Gross, C., Fiedler, J., Fischer, T., Kissler, S., Bussen, M., Galuppo, P., Just, S., Rottbauer, W., Frantz, S.*, et al.* (2008). MicroRNA-21 contributes to myocardial disease by stimulating MAP kinase signalling in fibroblasts. Nature *456*, 980-984.

Thurston, G., Rudge, J.S., Ioffe, E., Zhou, H., Ross, L., Croll, S.D., Glazer, N., Holash, J., McDonald, D.M., and Yancopoulos, G.D. (2000). Angiopoietin-1 protects the adult vasculature against plasma leakage. Nat Med *6*, 460-463.

Thygesen, K., Alpert, J.S., and White, H.D. (2007). Universal definition of myocardial infarction. Eur Heart J *28*, 2525-2538.

Toma, C., Pittenger, M.F., Cahill, K.S., Byrne, B.J., and Kessler, P.D. (2002). Human mesenchymal stem cells differentiate to a cardiomyocyte phenotype in the adult murine heart. Circulation *105*, 93-98.

Toshinai, K., Yamaguchi, H., Sun, Y., Smith, R.G., Yamanaka, A., Sakurai, T., Date, Y., Mondal, M.S., Shimbara, T., Kawagoe, T.*, et al.* (2006). Des-acyl ghrelin induces food intake by a mechanism independent of the growth hormone secretagogue receptor. Endocrinology *147*, 2306-2314.

Towbin, J.A., and Bowles, N.E. (2002). The failing heart. Nature *415*, 227-233.

Tratschin, J.D., Miller, I.L., and Carter, B.J. (1984). Genetic analysis of adeno-associated virus: properties of deletion mutants constructed in vitro and evidence for an adeno-associated virus replication function. J Virol *51*, 611-619.

Tschop, M., Smiley, D.L., and Heiman, M.L. (2000). Ghrelin induces adiposity in rodents. Nature *407*, 908-913.

Tse, H.F., Thambar, S., Kwong, Y.L., Rowlings, P., Bellamy, G., McCrohon, J., Thomas, P., Bastian, B., Chan, J.K., Lo, G.*, et al.* (2007). Prospective randomized trial of direct endomyocardial implantation of bone marrow cells for treatment of severe coronary artery diseases (PROTECT-CAD trial). Eur Heart J *28*, 2998-3005.

Tsubota, Y., Owada-Makabe, K., Yukawa, K., and Maeda, M. (2005). Hypotensive effect of des-acyl ghrelin at nucleus tractus solitarii of rat. Neuroreport *16*, 163-166.

Tsurumi, Y., Takeshita, S., Chen, D., Kearney, M., Rossow, S.T., Passeri, J., Horowitz, J.R., Symes, J.F., and Isner, J.M. (1996). Direct intramuscular gene transfer of naked DNA encoding vascular endothelial growth factor augments collateral development and tissue perfusion. Circulation *94*, 3281-3290.

Udelson, J.E., Dilsizian, V., Laham, R.J., Chronos, N., Vansant, J., Blais, M., Galt, J.R., Pike, M., Yoshizawa, C., and Simons, M. (2000). Therapeutic angiogenesis with recombinant fibroblast growth factor-2 improves stress and rest myocardial perfusion abnormalities in patients with severe symptomatic chronic coronary artery disease. Circulation *102*, 1605-1610.

Unemori, E.N., Lewis, M., Constant, J., Arnold, G., Grove, B.H., Normand, J., Deshpande, U., Salles, A., Pickford, L.B., Erikson, M.E.*, et al.* (2000). Relaxin induces vascular endothelial growth factor expression and angiogenesis selectively at wound sites. Wound Repair Regen *8*, 361-370.

Vale, P.R., Losordo, D.W., Milliken, C.E., McDonald, M.C., Gravelin, L.M., Curry, C.M., Esakof, D.D., Maysky, M., Symes, J.F., and Isner, J.M. (2001). Randomized, single-blind, placebo-controlled pilot study of catheter-based myocardial gene transfer for therapeutic angiogenesis using left ventricular electromechanical mapping in patients with chronic myocardial ischemia. Circulation *103*, 2138-2143.

Van de Werf, F., Bax, J., Betriu, A., Blomstrom-Lundqvist, C., Crea, F., Falk, V., Filippatos, G., Fox, K., Huber, K., Kastrati, A.*, et al.* (2008). Management of acute myocardial infarction in patients presenting with persistent ST-segment elevation: the Task Force on the Management of ST-Segment Elevation Acute Myocardial Infarction of the European Society of Cardiology. Eur Heart J *29*, 2909-2945.

van der Laan, A., Hirsch, A., Nijveldt, R., van der Vleuten, P.A., van der Giessen, W.J., Doevendans, P.A., Waltenberger, J., Ten Berg, J.M., Aengevaeren, W.R., Zwaginga, J.J.*, et al.* (2008). Bone marrow cell therapy after acute myocardial infarction: the HEBE trial in perspective, first results. Neth Heart J *16*, 436-439.

Van Der Westhuizen, E.T., Summers, R.J., Halls, M.L., Bathgate, R.A., and Sexton, P.M. (2007). Relaxin receptors--new drug targets for multiple disease states. Curr Drug Targets *8*, 91-104.

van Ramshorst, J., Bax, J.J., Beeres, S.L., Dibbets-Schneider, P., Roes, S.D., Stokkel, M.P., de Roos, A., Fibbe, W.E., Zwaginga, J.J., Boersma, E.*, et al.* (2009). Intramyocardial bone marrow cell injection for chronic myocardial ischemia: a randomized controlled trial. JAMA *301*, 1997-2004.

Walsh, G. (2006). Biopharmaceutical benchmarks 2006. Nat Biotechnol *24*, 769-776.

Walters, R.W., Yi, S.M., Keshavjee, S., Brown, K.E., Welsh, M.J., Chiorini, J.A., and Zabner, J. (2001). Binding of adeno-associated virus type 5 to 2,3-linked sialic acid is required for gene transfer. J Biol Chem *276*, 20610-20616.

Wang, W., Yang, Z.J., Ma, D.C., Wang, L.S., Xu, S.L., Zhang, Y.R., Cao, K.J., Zhang, F.M., and Ma, W.Z. (2006). Induction of collateral artery growth and improvement of post-infarct heart function by hepatocyte growth factor gene transfer. Acta Pharmacol Sin *27*, 555-560.

Watson, K., Watson, B.D., and Pater, K.S. (2006). Peripheral arterial disease: a review of disease awareness and management. Am J Geriatr Pharmacother *4*, 365-379.

Weber, M., Rabinowitz, J., Provost, N., Conrath, H., Folliot, S., Briot, D., Cherel, Y., Chenuaud, P., Samulski, J., Moullier, P*., et al.* (2003). Recombinant adeno-associated virus serotype 4 mediates unique and exclusive long-term transduction of retinal pigmented epithelium in rat, dog, and nonhuman primate after subretinal delivery. Mol Ther *7*, 774-781.

White, H.D., and Chew, D.P. (2008). Acute myocardial infarction. Lancet *372*, 570-584.

White, J.D., Thesier, D.M., Swain, J.B., Katz, M.G., Tomasulo, C., Henderson, A., Wang, L., Yarnall, C., Fargnoli, A., Sumaroka, M*., et al.* (2011). Myocardial gene delivery using molecular cardiac surgery with recombinant adeno-associated virus vectors in vivo. Gene Ther *18*, 546-552.

Wiley, K.E., and Davenport, A.P. (2002). Comparison of vasodilators in human internal mammary artery: ghrelin is a potent physiological antagonist of endothelin-1. Br J Pharmacol *136*, 1146-1152.

Wilkinson, T.N., Speed, T.P., Tregear, G.W., and Bathgate, R.A. (2005). Evolution of the relaxin-like peptide family. BMC Evol Biol *5*, 14.

Williams, M.L., Hata, J.A., Schroder, J., Rampersaud, E., Petrofski, J., Jakoi, A., Milano, C.A., and Koch, W.J. (2004). Targeted beta-adrenergic receptor kinase (betaARK1) inhibition by gene transfer in failing human hearts. Circulation *109*, 1590-1593.

Wilson, B.D., Ii, M., Park, K.W., Suli, A., Sorensen, L.K., Larrieu-Lahargue, F., Urness, L.D., Suh, W., Asai, J., Kock, G.A*., et al.* (2006). Netrins promote developmental and therapeutic angiogenesis. Science *313*, 640-644.

Woo, Y.J., Zhang, J.C., Vijayasarathy, C., Zwacka, R.M., Englehardt, J.F., Gardner, T.J., and Sweeney, H.L. (1998). Recombinant adenovirus-mediated cardiac gene transfer of superoxide dismutase and catalase attenuates postischemic contractile dysfunction. Circulation *98*, II255-260; discussion II260-251.

Work, L.M., Buning, H., Hunt, E., Nicklin, S.A., Denby, L., Britton, N., Leike, K., Odenthal, M., Drebber, U., Hallek, M*., et al.* (2006). Vascular bed-targeted in vivo gene delivery using tropism-modified adeno-associated viruses. Mol Ther *13*, 683-693.

Wu, J., Hecker, J.G., and Chiamvimonvat, N. (2009). Antioxidant enzyme gene transfer for ischemic diseases. Adv Drug Deliv Rev *61*, 351-363.

Wu, J., Zhao, W., Zhong, L., Han, Z., Li, B., Ma, W., Weigel-Kelley, K.A., Warrington, K.H., and Srivastava, A. (2007). Self-complementary recombinant

adeno-associated viral vectors: packaging capacity and the role of rep proteins in vector purity. Hum Gene Ther *18*, 171-182.

Wu, P., Xiao, W., Conlon, T., Hughes, J., Agbandje-McKenna, M., Ferkol, T., Flotte, T., and Muzyczka, N. (2000). Mutational analysis of the adeno-associated virus type 2 (AAV2) capsid gene and construction of AAV2 vectors with altered tropism. J Virol *74*, 8635-8647.

Wu, Z., Miller, E., Agbandje-McKenna, M., and Samulski, R.J. (2006). Alpha2,3 and alpha2,6 N-linked sialic acids facilitate efficient binding and transduction by adeno-associated virus types 1 and 6. J Virol *80*, 9093-9103.

Wu, Z., Yang, H., and Colosi, P. (2010). Effect of genome size on AAV vector packaging. Mol Ther *18*, 80-86.

Xiao, X., Li, J., and Samulski, R.J. (1998). Production of high-titer recombinant adeno-associated virus vectors in the absence of helper adenovirus. J Virol *72*, 2224-2232.

Xu, Z., Lin, S., Wu, W., Tan, H., Wang, Z., Cheng, C., Lu, L., and Zhang, X. (2008). Ghrelin prevents doxorubicin-induced cardiotoxicity through TNF-alpha/NF-kappaB pathways and mitochondrial protective mechanisms. Toxicology *247*, 133-138.

Yalkinoglu, A.O., Heilbronn, R., Burkle, A., Schlehofer, J.R., and zur Hausen, H. (1988). DNA amplification of adeno-associated virus as a response to cellular genotoxic stress. Cancer Res *48*, 3123-3129.

Yamamoto, C., Fukuda, N., Matsumoto, T., Higuchi, T., Ueno, T., and Matsumoto, K. (2010). Zinc-finger transcriptional factor Sall1 induces angiogenesis by activation of the gene for VEGF-A. Hypertens Res *33*, 143-148.

Yan, L., Vatner, D.E., Kim, S.J., Ge, H., Masurekar, M., Massover, W.H., Yang, G., Matsui, Y., Sadoshima, J., and Vatner, S.F. (2005). Autophagy in chronically ischemic myocardium. Proc Natl Acad Sci U S A *102*, 13807-13812.

Yan, Z., Ritchie, T.C., Duan, D., and Engelhardt, J.F. (2002). Recombinant AAV-mediated gene delivery using dual vector heterodimerization. Methods Enzymol *346*, 334-357.

Yan, Z., Zak, R., Zhang, Y., Ding, W., Godwin, S., Munson, K., Peluso, R., and Engelhardt, J.F. (2004). Distinct classes of proteasome-modulating agents cooperatively augment recombinant adeno-associated virus type 2 and type 5-mediated transduction from the apical surfaces of human airway epithelia. J Virol *78*, 2863-2874.

Yan, Z., Zhang, Y., Duan, D., and Engelhardt, J.F. (2000). Trans-splicing vectors expand the utility of adeno-associated virus for gene therapy. Proc Natl Acad Sci U S A *97*, 6716-6721.

Yang, J., Brown, M.S., Liang, G., Grishin, N.V., and Goldstein, J.L. (2008). Identification of the acyltransferase that octanoylates ghrelin, an appetite-stimulating peptide hormone. Cell *132*, 387-396.

Yang, Z., Zhang, F., Ma, W., Chen, B., Zhou, F., Xu, Z., Zhang, Y., Zhang, D., Zhu, T., Wang, L.*, et al.* (2010). A novel approach to transplanting bone marrow stem cells to repair human myocardial infarction: delivery via a noninfarct-relative artery. Cardiovasc Ther *28*, 380-385.

Yla-Herttuala, S., and Alitalo, K. (2003). Gene transfer as a tool to induce therapeutic vascular growth. Nat Med *9*, 694-701.

Yoshimoto, A., Mori, K., Sugawara, A., Mukoyama, M., Yahata, K., Suganami, T., Takaya, K., Hosoda, H., Kojima, M., Kangawa, K.*, et al.* (2002). Plasma ghrelin and desacyl ghrelin concentrations in renal failure. J Am Soc Nephrol *13*, 2748-2752.

Yu, J., Vodyanik, M.A., Smuga-Otto, K., Antosiewicz-Bourget, J., Frane, J.L., Tian, S., Nie, J., Jonsdottir, G.A., Ruotti, V., Stewart, R.*, et al.* (2007). Induced pluripotent stem cell lines derived from human somatic cells. Science *318*, 1917-1920.

Yusuf, S., Teo, K.K., Pogue, J., Dyal, L., Copland, I., Schumacher, H., Dagenais, G., Sleight, P., and Anderson, C. (2008). Telmisartan, ramipril, or both in patients at high risk for vascular events. N Engl J Med *358*, 1547-1559.

Zacchigna, S., Pattarini, L., Zentilin, L., Moimas, S., Carrer, A., Sinigaglia, M., Arsic, N., Tafuro, S., Sinagra, G., and Giacca, M. (2008). Bone marrow cells recruited through the neuropilin-1 receptor promote arterial formation at the sites of adult neoangiogenesis in mice. J Clin Invest *118*, 2062-2075.

Zachary, I., and Gliki, G. (2001). Signaling transduction mechanisms mediating biological actions of the vascular endothelial growth factor family. Cardiovasc Res *49*, 568-581.

Zachary, I., and Morgan, R.D. (2011). Therapeutic angiogenesis for cardiovascular disease: biological context, challenges, prospects. Heart *97*, 181-189.

Zadori, Z., Szelei, J., Lacoste, M.C., Li, Y., Gariepy, S., Raymond, P., Allaire, M., Nabi, I.R., and Tijssen, P. (2001). A viral phospholipase A2 is required for parvovirus infectivity. Dev Cell *1*, 291-302.

Zeng, L., Akasaki, Y., Sato, K., Ouchi, N., Izumiya, Y., and Walsh, K. (2010). Insulin-like 6 is induced by muscle injury and functions as a regenerative factor. J Biol Chem *285*, 36060-36069.

Zentilin, L., Marcello, A., and Giacca, M. (2001). Involvement of cellular double-stranded DNA break binding proteins in processing of the recombinant adeno-associated virus genome. J Virol *75*, 12279-12287.

Zentilin, L., Puligadda, U., Lionetti, V., Zacchigna, S., Collesi, C., Pattarini, L., Ruozi, G., Camporesi, S., Sinagra, G., Pepe, M.*, et al.* (2010). Cardiomyocyte VEGFR-1 activation by VEGF-B induces compensatory hypertrophy and preserves cardiac function after myocardial infarction. FASEB J *24*, 1467-1478.

Zhang, G.G., Teng, X., Liu, Y., Cai, Y., Zhou, Y.B., Duan, X.H., Song, J.Q., Shi, Y., Tang, C.S., Yin, X.H.*, et al.* (2009). Inhibition of endoplasm reticulum stress by ghrelin protects against ischemia/reperfusion injury in rat heart. Peptides *30*, 1109-1116.

Zhang, J.V., Ren, P.G., Avsian-Kretchmer, O., Luo, C.W., Rauch, R., Klein, C., and Hsueh, A.J. (2005). Obestatin, a peptide encoded by the ghrelin gene, opposes ghrelin's effects on food intake. Science *310*, 996-999.

Zhong, J., Eliceiri, B., Stupack, D., Penta, K., Sakamoto, G., Quertermous, T., Coleman, M., Boudreau, N., and Varner, J.A. (2003). Neovascularization of ischemic tissues by gene delivery of the extracellular matrix protein Del-1. J Clin Invest *112*, 30-41.

Zhong, L., Zhou, X., Li, Y., Qing, K., Xiao, X., Samulski, R.J., and Srivastava, A. (2008). Single-polarity recombinant adeno-associated virus 2 vector-mediated transgene expression in vitro and in vivo: mechanism of transduction. Mol Ther *16*, 290-295.

Zhou, X., Zeng, X., Fan, Z., Li, C., McCown, T., Samulski, R.J., and Xiao, X. (2008). Adeno-associated virus of a single-polarity DNA genome is capable of transduction in vivo. Mol Ther *16*, 494-499.

Zhu, X., Cao, Y., Voogd, K., and Steiner, D.F. (2006). On the processing of proghrelin to ghrelin. J Biol Chem *281*, 38867-38870.

Zhu, Y.H., Ma, T.M., and Wang, X. (2005). Gene transfer of heat-shock protein 20 protects against ischemia/reperfusion injury in rat hearts. Acta Pharmacol Sin *26*, 1193-1200.

Zolotukhin, S., Byrne, B.J., Mason, E., Zolotukhin, I., Potter, M., Chesnut, K., Summerford, C., Samulski, R.J., and Muzyczka, N. (1999). Recombinant adeno-associated virus purification using novel methods improves infectious titer and yield. Gene Ther *6*, 973-985.

Zornoff, L.A., Paiva, S.A., Duarte, D.R., and Spadaro, J. (2009). Ventricular remodeling after myocardial infarction: concepts and clinical implications. Arq Bras Cardiol *92*, 150-164.

7. APPENDIX

Zentilin L., Puligadda U., Lionetti V., Zacchigna S., Collesi C., Pattarini L., Ruozi G., Camporesi S., Sinagra G., Pepe M., Recchia F.A., and Giacca M. Cardiomyocyte VEGFR-1 activation by VEGF-B induces compensatory hypertrophy and preserves cardiac function after myocardial infarction. *FASEB J.* 2010; 24(5):1467-78.
PAPER ATTACHED

Carrer A., Moimas S., Zacchigna S., Pattarini L., Zentilin L., Ruozi G., Mano M., Sinigaglia M., Maione F., Serini G., Giraudo E., Bussolino F., and Giacca M. Neuropilin-1 identifies a subset of GR1-monocytes that induce tumor vessel normalization and inhibit tumor growth. *Cancer Research - In press.*

The FASEB Journal • Research Communication

Cardiomyocyte VEGFR-1 activation by VEGF-B induces compensatory hypertrophy and preserves cardiac function after myocardial infarction

Lorena Zentilin,*[,1] Uday Puligadda,*[,1] Vincenzo Lionetti,†[,1] Serena Zacchigna,* Chiara Collesi,* Lucia Pattarini,* Giulia Ruozi,* Silvia Camporesi,* Gianfranco Sinagra,‡ Martino Pepe,§ Fabio A. Recchia,†[,§] and Mauro Giacca*[,‖,2]

*Molecular Medicine Laboratory, International Centre for Genetic Engineering and Biotechnology (ICGEB), Trieste, Italy; †Scuola Superiore Sant'Anna, Sector of Medicine, Pisa, Italy; ‡SC Cardiologia, Azienda Ospedaliera-Universitaria "Ospedali Riuniti di Trieste," Ospedale di Cattinara, Trieste, Italy; §New York Medical College, Valhalla, New York, USA; and ‖Department of Biomedicine, Faculty of Medicine, University of Trieste, Trieste, Italy

ABSTRACT **Mounting evidence indicates that the function of members of the vascular endothelial growth factor (VEGF) family extends beyond blood vessel formation. Here, we show that the prolonged intramyocardial expression of VEGF-A_{165} and VEGF-B_{167} on adeno-associated virus-mediated gene delivery determined a marked improvement in cardiac function after myocardial infarction in rats, by promoting cardiac contractility, preserving viable cardiac tissue, and preventing remodeling of the left ventricle (LV) over time. Consistent with this functional outcome, animals treated with both factors showed diminished fibrosis and increased contractile myocardium, which were more pronounced after expression of the selective VEGF receptor-1 (VEGFR-1) ligand VEGF-B, in the absence of significant induction of angiogenesis. We found that cardiomyocytes expressed VEGFR-1, VEGFR-2, and neuropilin-1 and that, in particular, VEGFR-1 was specifically up-regulated in hypoxia and on exposure to oxidative stress. VEGF-B exerted powerful antiapoptotic effect in both cultured cardiomyocytes and after myocardial infarction *in vivo*. Finally, VEGFR-1 activation by VEGF-B was found to elicit a peculiar gene expression profile proper of the compensatory, hypertrophic response, consisting in activation of αMHC and repression of βMHC and skeletal α-actin, and an increase in SERCA2a, RYR, PGC1α, and cardiac natriuretic peptide transcripts, both in cultured cardiomyocytes and in infarcted hearts. The finding that VEGFR-1 activation by VEGF-B prevents loss of cardiac mass and promotes maintenance of cardiac contractility over time has obvious therapeutic implications.—Zentilin, L., Puligadda, U., Lionetti, V., Zacchigna, S., Collesi, C., Pattarini, L., Ruozi, G., Camporesi, S., Sinagra, G., Pepe, M., Recchia, F. A., Giacca, M. Cardiomyocyte VEGFR-1 activation by VEGF-B induces compensatory hypertrophy and preserves cardiac function after myocardial infarction. *FASEB J.* 24, 1467–1478 (2010). www.fasebj.org**

Key Words: apoptosis · adeno-associated virus, angiogenesis · gene therapy · gene expression

MEMBERS OF THE VASCULAR ENDOTHELIAL growth factor (VEGF) family and their receptors are essential regulators of vasculogenesis, angiogenesis, and vessel maintenance in both embryo and adults (for reviews, see refs. 1–4). In particular, the 165-aa isoform of VEGF-A (VEGF-A herein for brevity) possesses full angiogenic and arteriogenic activity, mainly through binding to VEGFR-2, which stimulates pathways important for mitogenesis, migration, and survival of endothelial cells (4, 5).

VEGF-A also binds VEGFR-1 with an affinity that is ≥10 times higher than that of VEGFR-2 (6); however, the significance of this interaction remains elusive, especially since this receptor appears unable to transduce an angiogenic signal in endothelial cells (7). Multiple evidence suggests that VEGF-B, a VEGFR-1-exclusive ligand that is produced in a heparin-binding isoform of 167 aa (VEGF-B_{167}) and a diffusible isoform of 186 aa (VEGF-B_{186}) (7, 8) might selectively be active in the myocardium. Indeed, the VEGF-B gene, shows prominent expression in the heart during embryonic development (9), and mice with knockouts for this factor display a mild cardiac phenotype, characterized, at least in one strain, by decreased heart size (10). In addition, recent evidence indicates that transgenic mice specifically expressing VEGF-B_{167} in the myocardium undergo massive myocardial hypertrophy, in the absence of a significant increase of cardiac angiogenesis (11).

A few studies have also explored the effects of VEGF-A and VEGF-B in the heart after myocardial infarction. In particular, VEGF-B_{167} was described to significantly increase revascularization of the infarcted myocardium; however, it failed to enhance vascular growth in the skin or ischemic limb (12). The reasons

[1] These authors contributed equally to this work.

[2] Correspondence: CGEB Trieste, Molecular Medicine Laboratory, Padriciano, 99, 34012 Trieste (Italy). E-mail: giacca@icgeb.org

doi: 10.1096/fj.09-143180

for the selective cardiac benefit of VEGF-B delivery remained unexplained. Another recent study, entailing the delivery of VEGF-B_{186} after infarction in pigs and rabbits using adenoviral vectors, indicated that the factor induced myocardial-specific angiogenesis and arteriogenesis and, most notably, improved myocardial function a few days after vector injection (13). As far as VEGF-A is concerned, in a previous study of acute myocardial infarction in dogs, we observed that the sustained expression of this factor, delivered to the heart using an adeno-associated virus (AAV)-based vector determined remarkable recovery of the regional myocardial contractility, up to 4 wk after injury (14). Surprisingly, the improvement in myocardial function started to be significant as early as 48 h after vector injection, a temporal frame not compatible with the formation of new blood vessels and suggestive of a direct effect of VEGF on resident cardiomyocytes, additional to angiogenesis (14).

Taken together, this variegated information leaves a series of essential questions outstanding, including to what extent the cardiac effects of the VEGFs are secondary to the induction of angiogenesis or directly exerted onto myocardial cells, which is the receptor involved, and how long the beneficial effect exerted by the factors lasts after cardiac injury. To provide answers to these questions, we took advantage of the possibility of delivering *in vivo* VEGF-A and VEGF-B_{167} (herein VEGF-B for brevity) to the heart using vectors based on the AAV, and to assess their effects for prolonged periods of time both in normal conditions and after myocardial infarction. Over the past few years, these vectors have gained increasing popularity due to several favorable characteristics, in particular, their ability to transduce postmitotic cells, including cardiomyocytes, at high efficiency and to drive gene expression for very prolonged periods of time in the absence of noticeable inflammation (15, 16).

Here, we show that the AAV-mediated, intramyocardial expression of VEGF-A and, most notably, of VEGF-B determines a marked improvement in cardiac function after permanent coronary artery occlusion in rats, ensuing from the direct protection of cardiomyocytes from apoptosis and up-regulation of genes driving compensatory, hypertrophic response. These results clearly indicate that the role of VEGFs in the heart extends beyond their angiogenic properties, and point toward VEGFR-1 signaling as an important mediator of cardiomyocyte function, with clear therapeutic implications.

MATERIALS AND METHODS

Production, purification, and characterization of rAAV vectors

rAAV vectors were prepared by the AAV Vector Unit at ICGEB Trieste (http://www.icgeb.org/avu-core-facility.html), as described previously (17, 18). AAV titers were in the range of 1×10^{12} to 1×10^{13} genome copies (gc)/ml.

Animal studies and echocardiography

Animal care and treatment were conducted in conformity with institutional guidelines in compliance with national and international laws and policies (European Economic Community Council Directive 86/609, OJL 358, December 12, 1987), after institutional review board approval. Myocardial infarction (MI) was produced in male Wistar rats at 2 mo of age, by permanent left anterior descending coronary artery ligation, as described previously (19). After ligation, they were immediately injected into the LV with 10 μl of recombinant AAV vectors, corresponding to 5×10^{10} gc, with 3 separate injections into the viable myocardium bordering the infarct using a tubercoline syringe with a 30-gauge needle. Four groups of animals were studied (n=10/group), receiving AAV2-VEGF-A, AAV2-VEGF-B, AAV2-LacZ, or saline.

To evaluate global and regional LV function, transthoracic echocardiography was performed before thoracotomy, 28 d and 3 mo after MI in sedated rats with a commercially available echocardiography system (MyLab 30; Esaote, Genoa, Italy) equipped with a 12-MHz linear transducer, as described previously (20). Analysis was as recommended by the American Society of Echocardiography (21); all measurements were performed by an experienced cardiologist and an echocardiography expert blinded to treatment groups.

At the end of the echocardiography study, hearts were collected, and the LV, including the interventricular septum, was carefully dissected. After washing in PBS, each specimen was cut into 4 or 5 pieces of equal thickness from base to apex, fixed in 4% paraformaldeyde, and embedded in paraffin for histological analysis. Infarct size was measured on 5-μm-thick sections as the percentage of (endocardial+epicardial circumference of infarct area)/(endocardial+epicardial circumference of LV).

For the detection of apoptosis *in vivo*, infarcted hearts were collected and snap-frozen 3 d after MI. Frozen sections from each sample were fixed in 4% buffered paraformaldehyde (PFA) and then treated as described above for immunostaining and TUNEL.

Isolation and treatment of neonatal rat ventricular cardiomyocytes

Ventricular myocytes from 1- to 2-d-old rats were prepared according to a previously detailed protocol, yielding ≥90% purity (22). Cells were collected and plated at a density of 500 cells/mm^2 into 100-mm dishes (for RNA and protein analysis), or multiwell slides coated with 0.2% gelatin (for immunofluorescence staining). When indicated, cells were treated with rhVEGF-A (100 ng/ml; R&D Systems, Minneapolis, MN, USA), rhVEGF-B (100 ng/ml; R&D Systems), thyroid hormone (100 nM; Sigma, St. Louis, MO, USA) and phenylephrine (20 μM; Sigma). For the detection of VEGF receptors, growth-factor stimulation was performed at 37°C for 7 min in serum-free medium containing 4.5 g/L glucose, 0.1% w/v BSA, 4 μg/ml B12, 10 μg/ml insulin, and 10 μg/ml transferrin.

Apoptosis was induced by culturing serum-starved cells for 48 h at 37°C in a 5% O_2-95% N_2 atmosphere using a hypoxia incubator chamber (Billups-Rothenberg, San Diego, CA, USA) and then switching to 20% O_2 for an additional 24 h. Cells were then fixed in 3% PFA and 2% sucrose in PBS. Apoptotic cells were visualized by the TUNEL (TdT-mediated dUTP nick-end labeling) assay, using the *in situ* cell death detection kit, TMR red (Roche Diagnostics, Mannheim, Germany), according to the manufacturer's instructions. At least 10 high-magnification fields were counted for each experimental condition. Analysis of cardiomyocyte survival was

performed using the Live&Dead assay (Molecular Probes, Eugene, OR, USA) after treatment with 200 nM epirubicin for 90 m in serum free medium.

Quantification of nucleic acids by real-time PCR

Total RNA from isolated cardiomyocytes or dissected LV heart tissue samples was extracted using TRIzol reagent (Invitrogen, Carlsbad, CA, USA) according to the manufacturer's instructions, and reverse-transcribed using hexameric random primers.

Quantification of gene expression was performed by real-time PCR, using predeveloped and custom-designed assays (Applied Biosystems, Foster City, CA, USA) or SYBRGreen (Bio-Rad Laboratories, Hercules, CA, USA). Total RNA from isolated cardiomyocytes or dissected LV heart tissue samples was extracted using TRIzol reagent (Invitrogen) according to manufacturer's instructions and reverse transcribed using hexameric random primers. The cDNA was used as a template for real-time PCR amplification to detect the expression levels of the rat VEGF receptors (*VEGFR-1*, *VEGFR-2*, *NP-1*), as well as of α-*MHC*, β-*MHC*, *sk* α-*actin*, *ANF*, *BNP*, *SERCA2a*, *RYR2*, and *PGC1*α. The housekeeping genes *GAPDH* and *HPRT* were used to normalize the results.

For the detection of vector specific DNA in heart samples, total DNA, purified by Proteinase K/phenol-chloroform extraction method, was subjected to real-time PCR amplification using a TaqMan probe and primers that specifically match sequences in the CMV promoter, common to all AAV vectors used in this study.

Sequences of primers and probes used

Primers

Rat *PGC-1* F 5′-TGCAGCCAAGACTCTGTATGG-3′, R 5′-GGCAAAGAGGCTGGTCCTC-3′; rat *BNP*: F 5′-CAGCTCTCAAAGGACCAAGG-3′, R 5′-GCCCAAAGCAGCTTGAACTA-3′; rat *HPRT*: F 5′-GCCCTTGACTATAATGAGCACTCAG-3′, R 5′-GTAGATTCAACTTGCCGCTGTTT-3′; mouse *iVEGF-B*: F 5′-TTGCACTGCTGCAGCTGGCTC-3′, R 5′-GCTGGGCACTAGTTGTTTGA-3′; CMV promoter: F 5′-TGGGCGGTAGGCGTGTA-3′, R 5′-CGATCTGACGGTTCACTAAACG-3′.

Taqman probes (assay)

Rat β-*MHC*: (FAM)-Rn00568328_m1; rat α-*MHC*: (FAM)-Rn00568304_m1; rat *RYR2*: (FAM)-Rn01470303_m1; rat *SERCA2a*: (FAM)-Rn00568762_m1; rat *ANP*: (FAM)-Rn00561661_n1; rat *sk* α-*actin*: (FAM)-Rn00570060_g1; rat *Flk1*: (FAM)-Rn 00564986_m1; rat *Flt1*: (FAM)-Rn 01409523_g1; rat *NP1*: (FAM)-Rn 00435380_m1; human *VEGF-*A_{165}: (FAM)-Hs00173626_m1; rat *GAPDH*: (VIC)-TaqMan Endogenous control (4352338E); CMV: (FAM)-TGGGAGGTCTATATAAGC.

Histology and immunofluorescence

Vasculature staining was performed on paraffin-embedded sections, blocked for 1 h with 2% BSA in PBS; endothelial cells were detected using FITC-conjugated *Lycopersicum esculentum* lectin (Vector Laboratories) and vascular smooth muscle cells (VSMCs) using a Cy3-conjugated anti-α-SMA mouse monoclonal antibody (clone 1A4, Sigma). Pericytes were detected using a rabbit polyclonal anti-NG2 antibody (Chemicon, Temecula, CA, USA) on 4% paraformaldehyde-fixed frozen sections after overnight blocking with 5% horse serum. The detection of VEGF receptors by immunofluorescence was performed on frozen sections (5 μm thick), fixed in IHC Zinc Fixative (Pharmingen, BD Biosciences, San Jose, CA, USA), and blocked for 30 m with 5% goat or 5% horse serum in PBS, depending on the secondary antibody.

The following primary antibodies were used for immunofluorescence studies in cardiomyocytes: goat anti-mouse Flk-1 (AF644; R&D Systems), 1:100; goat polyclonal anti-mouse Flt-1 (AF471; R&D Systems), 1:20; goat polyclonal anti-rat neuropilin-1 (AF566; R&D Systems), 1:50; and mouse anti-α-sarcomeric actinin monoclonal antibody (EA-53; Abcam, Cambridge MA, USA), 1:100. Alexa Fluor 594 donkey anti-goat, Alexa Fluor 594 donkey anti-rabbit, and Alexa Fluor 488 donkey anti-mouse were used as secondary antibodies (Molecular Probes). Nuclei were counterstained with DAPI.

Images were acquired at room temperature with a DMLB upright fluorescence microscope (Leica Microsystems, Wetzlar, Germany) equipped with a charge-coupled device camera (CoolSNAP CF; Roper Scientific, Trenton, NJ, USA) using MetaView 4.6 quantitative analysis software (MDS Analytical Technologies, Toronto, ON, Canada).

Immunoprecipitation and Western blot analysis

For the detection of VEGF receptors, freshly isolated cardiomyocytes were allowed to attach in 100-mm dishes and then left overnight in serum-free medium. Stimulation was performed by incubating the cell cultures at 37°C for 7 min in 2 ml of serum or 2 ml of serum-free medium containing 50 ng/ml recombinant huVEGF-A_{165} and 100 ng/ml huVEGF-B. After washing with PBS on ice, samples were lysed in RIPA buffer (20 mM Tris-HCl, pH 7.4; 150 mM NaCl; 5 mM EDTA; 1% NaDoc; 1% Triton X-100; and 0.1% SDS) containing 90 μg/ml PMSF, 100 μM $NaVO_4$, 50 mM NaF, 20 μg/ml aprotinin, and 20 μg/ml leupeptin (Sigma-Aldrich). Protein concentration was determined by the Bradford method (Bio-Rad Laboratories); 200 μg of proteins was resolved on 6% SDS-PAGE and transferred to nitrocellulose membranes (GE Healthcare, New York, NY, USA). Immunoblots were blocked in 5% bovine serum albumin in TBS-Tween (50 mM Tris-HCl, pH 7.4; 200 mM NaCl; and 0.1% Tween 20). Membranes were incubated with the following primary antibodies (dilution 1:1000) overnight at 4°C: rabbit polyclonal anti-Flk-1 (C-1158; Santa Cruz Biotechnology, Santa Cruz, CA, USA), rabbit polyclonal anti-Flt-1 (C-17; Santa Cruz Biotechnology), mouse monoclonal anti-phospho-Tyrosine (PY20; Biolegend, San Diego, CA, USA), goat polyclonal anti-rat neuropilin-1 (AF566; R&D Systems), and mouse monoclonal tubulin (B-5–1-2; Sigma). Membranes were then washed in Tris-buffered saline and 0.1% Tween 20 in blocking buffer and incubated with the appropriate HPR-conjugated secondary antibodies for 45 m at room temperature. Proteins were detected by enhanced chemiluminescence (GE Healthcare).

In vivo VEGF receptor tyrosine phosphorylation was evaluated by Western blot analysis with anti-phosphotyrosine antibodies on immunoprecipitates. Two milligrams of cell lysates was incubated with either rabbit polyclonal anti-Flk-1 (C-1158; Santa Cruz Biotechnology) or rabbit polyclonal anti-Flt-1 (C-17; Santa Cruz Biotechnology) antisera coupled to Sepharose-Protein A (20 ml packed beads/ml lysate) overnight at 4°C with agitation. Sepharose-protein A-bound proteins were washed 4 times with RIPA buffer and separated on 6% SDS–polyacrylamide gels, followed by immunoblotting with either mouse monoclonal anti-phosphotyrosine antibodies (PY20; Biolegend) or with anti-Flk-1 specific phosphotyrosine antibodies (VEGF-Receptor2-Y1175; Cell Signaling, Beverly, MA, USA).

Statistical analysis

One-way ANOVA and Bonferroni/Dunn's *post hoc* test were used to compare multiple groups. Pairwise comparison between groups was performed using the Student's t test. Dose-response effect was assessed by regression analysis. $P < 0.05$ was set as a threshold for statistical significance.

RESULTS

Long-term effects of AAV-mediated VEGF-B and VEGF-A expression in normal rat myocardium

To comparatively assess the effects of VEGF-A and VEGF-B, we generated two AAV vectors, based on AAV serotype 2 (AAV2), expressing the respective cDNAs in a constitutive manner from the CMV IE gene promoter. The efficiency of transduction and expression of these vectors were first assessed by injecting 5×10^{10} AAV particles into the LV free wall of normal rats; control animals were injected with either saline or AAV2-LacZ (n=6/group). As detected by real-time PCR quantification, the levels of expression of the two transgenes was persistent at both 30 d (not shown) and 90 d postinjection (**Fig. 1*A, B***). Consistent with our previous observations (14, 17, 23), no inflammatory response was detected in the animals injected with either saline or AAV2-LacZ at either time point (data not shown). No differences were detected between AAV2-LacZ- or saline-injected animals in none of the parameters considered throughout this work, neither in normal nor in infarcted animals. The results obtained in the two groups were therefore pooled and collectively labeled as control in all figures.

Representative images of the vasculature in the AAV-injected and control hearts at 30 d after injection are shown in Fig. 1*C* after staining with anti-CD31 and anti-αSMA antibodies to detect endothelial and smooth muscle cells (SMCs), respectively. Consistent with our previous findings in the normoperfused skeletal muscle (17, 18), we observed that the prolonged expression of VEGF-A in the heart determined a marked angiogenic response, characterized by a significant increase in the number of capillaries (Fig. 1D) and, most notably, of small arteries in the 20- to 250-μm-diameter range (Fig. 1*E*), with a consequent increase in the arteriole/capillary ratio (Fig. 1*F*). In contrast, AAV2-VEGF-B had a very modest angiogenic effect, with the exception of the sporadic formation of enlarged vascular structures, connected to the circulation, apparently devoid of αSMA- and NG2-positive mural cells (arrows in Fig. 1*C* and Supplemental Fig. 1).

VEGF-B, a specific VEGFR-1 ligand, preserves myocardial function after infarction

Next, we assessed the effects of the two vectors on cardiac function after myocardial infarction. Rats (n=10/group) underwent permanent left descendent coronary artery ligation and immediate injection into the LV peri-infarcted area of 5×10^{10} viral particles of AAV2-VEGFA, AAV2-VEGFB, AAV2-LacZ, or saline (pooled control group). Global and regional LV function was analyzed by echocardiography at 1 and 3 mo after infarction; representative M-mode echocardiograms at the latter time point are shown in **Fig. 2*A***. The LV ejection fraction (LVEF) and LV fractional shortening (LVFS) were significantly preserved in infarcted rats injected with both AAV2-VEGF-B and AAV-VEGF-A, compared to untreated animals, in the absence of significant changes in heart rate (P<0.05 for both treatments at either time point; Fig. 2*B, C*, respectively). Preservation of LV performance was significantly more pronounced in the infarcted hearts treated with

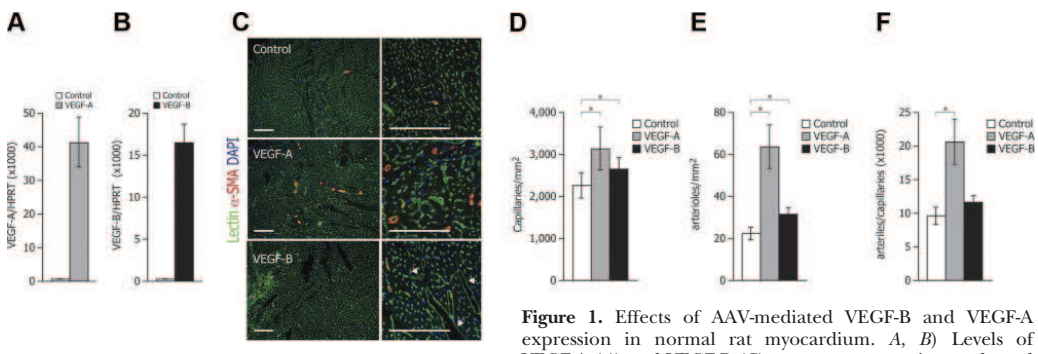

Figure 1. Effects of AAV-mediated VEGF-B and VEGF-A expression in normal rat myocardium. *A, B*) Levels of VEGF-A (*A*) and VEGF-B (*B*) transgene transcripts evaluated by real-time PCR analysis on total ventricular RNA extracted 90 d after vector injection. Transgene expression levels (n=8) are normalized for those of the endogenous HPRT gene. *C*) Left panels: representative immunostainings of the vasculature in rat myocardium injected with AAV-LacZ (control), AAV-VEGF-A, and AAV-VEGF-B, as indicated. Right panels: enlarged views. Capillaries were detected using FITC-conjugated *L. esculentum* lectin (Vector Laboratories), staining endothelial cells, and VSMCs using a Cy3-conjugated anti-αSMA mouse monoclonal antibody; nuclei were stained in blue with DAPI. Scale bars = 500 μm. *D, E*) Quantification of capillary and arteriole density. *F*) Ratio between number of arteries and capillaries. Values are expressed as means ± SE. *$P < 0.05$.

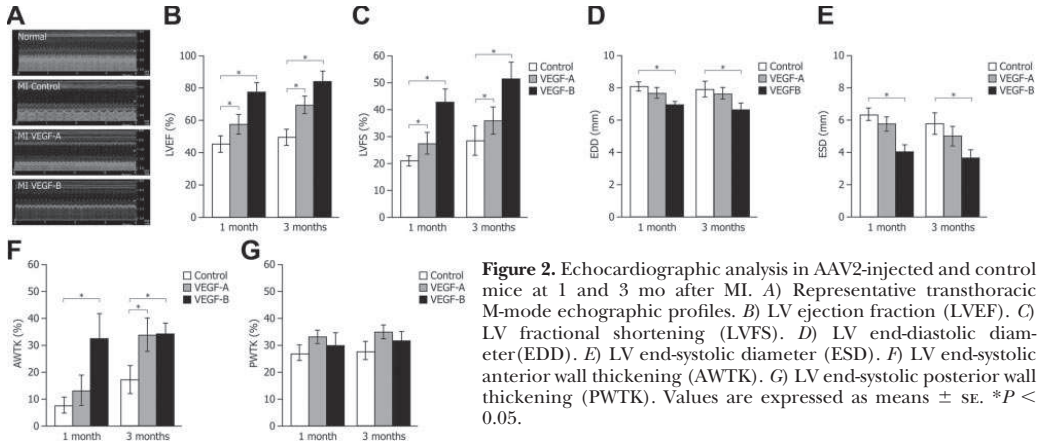

Figure 2. Echocardiographic analysis in AAV2-injected and control mice at 1 and 3 mo after MI. *A*) Representative transthoracic M-mode echographic profiles. *B*) LV ejection fraction (LVEF). *C*) LV fractional shortening (LVFS). *D*) LV end-diastolic diameter(EDD). *E*) LV end-systolic diameter (ESD). *F*) LV end-systolic anterior wall thickening (AWTK). *G*) LV end-systolic posterior wall thickening (PWTK). Values are expressed as means ± SE. $*P <$ 0.05.

VEGF-B at 1 mo and, in particular, at 3 mo of treatment (LVEF: 48±8 *vs.* 85±9%; LVFS: 29±8 *vs.* 52±7% in control and VEGF-B animals, respectively; $P<0.05$ in all cases). At both time points, the LV end-diastolic diameter (EDD) and LV end-systolic diameter (ESD) were also significantly reduced in rats that had received AAV2-VEGF-B (EDD: 7.9±1.2 and 6.8±0.8 mm; ESD: 5.9±0.7 and 3.8±0.9 mm in control and VEGF-B animals at 3 mo of treatment; $P<0.05$ in all cases; Figs. 2*D, E,* respectively).

The changes of regional cardiac contractility are shown in Fig. 2*F, G*. At both 1 and 3 mo after cardiac gene transfer, the LV end-systolic wall thickening (AWTK) in the border zone of the infarcted hearts injected with AAV2-VEGF-B was markedly improved compared to control rats (18.5±3.0 *vs.* 32.2±2.9% for control and VEGF-B at 3 mo; $P<0.05$). Similarly, the LV anterior wall end-diastolic and end-systolic thickness (AWTd and AWTs, respectively) of the border zone, two indexes of regional mass, were selectively preserved in the infarcted hearts expressing VEGF-B ($P<0.05$ in both cases; Supplemental Fig. 2*A, C*). No changes in the function and structure of the LV remote regions of the infarcted hearts were observed in any experimental group.

With the caveat that echocardiography in small animals might not provide sufficient sensitivity to detect differences in thickening of the border zone of a small MI, these data unanimously indicated that the prolonged expression of both VEGF-A and VEGF-B markedly improved recovery of LV performance after infarction.

Animals were sacrificed at 3 mo by induction of ischemia, and the hearts were examined for postinfarction fibrosis and chamber remodeling. Morphometric analysis of trichromic-stained LV sections showed that the anterior wall of infarcted control animals underwent considerable thinning, consistent with the echocardiographic results. In contrast, the AAV2-VEGFA- and, more remarkably, the AAV2-VEGFB-treated hearts showed significant preservation of contractile tissue and reduction of the fibrotic area (see **Fig. 3*A*** for representative cross-sections and Fig. 3*C* for high-magnification view of the extent of fibrotic substitution); the infarct size was determined as 36.2 ± 6.0% of the LV in control animals *vs.* 21.5 ± 2.5 and 17.2 ± 3.5% in the VEGF-A- and VEGF-B-expressing animals, respectively ($P<0.05$ in both cases; Fig. 3*B*).

Molecular characterization of heart samples on animal sacrifice confirmed the persistence of the vector genomes in the injected myocardium (Supplemental Fig. 3*A*). Consistently, AAV-mediated expression of both VEGF-A and VEGF-B was detected by real-time PCR using transgene specific primers (Supplemental Fig. 3*B*). The local expression of the transgenes did not induce significant variation of the levels of VEGF receptors mRNA (Supplemental Fig. 3*C*).

Similar to noninfarcted hearts (Fig. 1), the animals treated with VEGF-A showed a significant increment in the number of capillaries and arterioles, which was not evident in those injected with AAV2-VEGF-B (see Fig. 3*D* for representative images and Fig. 3*E, F* for quantification of the number of capillaries and arterioles, respectively).

Thus, the marked recovery of LV ventricular performance after myocardial infarction, in particular, observed on VEGF-B gene delivery occurred in the absence of significant induction of angiogenesis.

Cardiomyocytes express functional VEGF receptors *in vitro* and *in vivo*

To explore whether VEGF exerted a direct effect on cardiomyocytes, we first assessed the levels of expression of the VEGF receptors in these cells. A first set of experiments was performed using total RNA extracted from primary cultures highly enriched in α-actinin-positive cardiomyocytes by three subsequent subplating steps (>90% purity; see Materials and Methods and ref. 22); these cultures were established along complementary cultures of α-actinin-negative stromal cells (<1% α-actinin positivity). Both cultures were maintained for

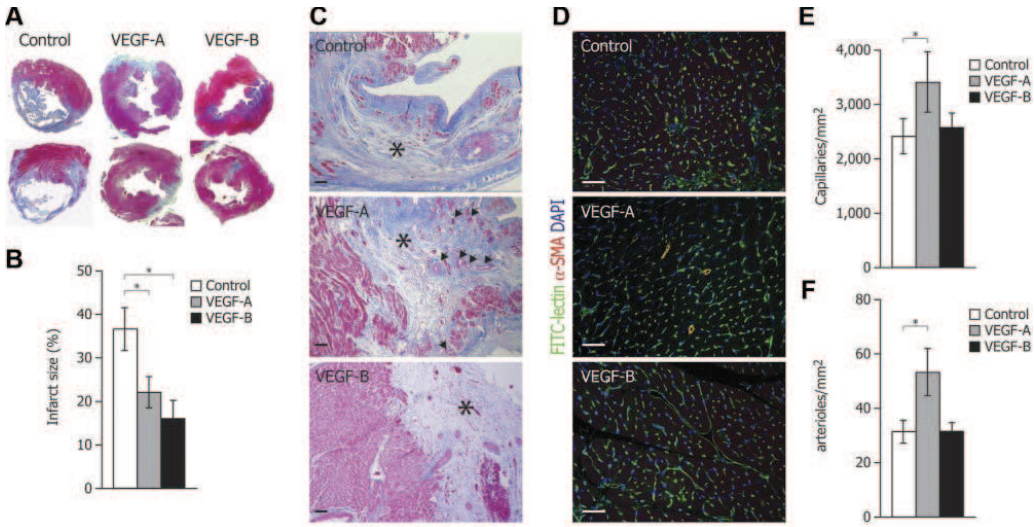

Figure 3. Morphometric and histological analysis of infarcted hearts 3 mo after gene transfer. *A*) Representative Azan trichrome stainings of LV transverse sections of control and AAV2-VEGF-A- and AAV2-VEGF-B-injected hearts. *B*) Quantification of infarct size (% of LV). *C*) High-magnification (×200) microphotographs of trichrome-stained sections showing the extent of fibrotic substitution of the infarcted scars (asterisks); arrows indicate new vessels in the VEGF-A expressing hearts. *D*) Visualization of vessels by immunofluorescence in the peri-infarcted area (green, endothelial cells; red, α-SMA$^+$ cells; blue, cell nuclei). *E*) Quantification of capillary density (FITC-lectin$^+$ vessels). *F*) Quantification of α-SMA$^+$ arterioles. Values are expressed as means ± SE. *$P < 0.05$. Scale bars = 200 μm.

7–14 d. We found that *VEGFR-1*, *VEGFR-2*, and *Np1* were all expressed in neonatal rat cardiomyocytes, albeit at levels that were 3 orders of magnitude lower than those of human umbilical vein endothelial cells (HUVECs); stromal cells only expressed *VEGFR-1* and *Np1*, not *VEGFR-2* (**Fig. 4*A***). Of potential interest, expression of *VEGFR-1* selectively increased when cardiomyocytes were placed in a hypoxic environment (2% O_2) or exposed to oxidative stress (H_2O_2 100 μM); >5 fold and ~3-fold induction, respectively; Fig. 4*B*).

Expression of VEGFR-1, VEGFR-2, and Np1 was also detected by Western blot analysis in neonatal cardiomyocyte cell lysates (Fig. 4*C*, top panel). Most notably, these receptors appeared to be functional, since immmunoprecipitation using specific anti-VEGFR-1 and anti-VEGFR-2 antibodies followed by Western blot analysis with anti-phosphotyrosine antibodies revealed specific phosphorylation of both VEGFR-1 and VEGFR-2 in response to recombinant VEGF-A and of VEGFR-1 in response to recombinant VEGF-B (Fig. 4*C*, bottom panel).

Finally, expression of VEGF receptors was also detected by immunofluorescence on histological sections of frozen adult rat heart tissue (Fig. 4*D*). Of interest, while the localization of VEGFR-2 and Np1 fluorescence was consistent with the prominent expression of these receptors on vascular endothelial cells, VEGFR-1 appeared to cluster at the intercalated disks between cardiomyocytes.

VEGF-A and VEGF-B inhibit cardiomyocyte apoptosis

The reduction in infarct size and preservation of muscle mass in animals treated with VEGF-A and VEGF-B suggested that these factors either stimulated the limited cardiomyocyte proliferation that is normally observed in the infarct border zone (24) or prevented delayed cardiomyocyte loss after infarction. The former possibility was tested by evaluating the effects of the two factors on cardiomyocyte proliferation. Under standard culture conditions (22), ~0.2% of neonatal cardiomyocytes incorporate BrdU at d 1 after isolation; this percentage was unchanged on addition of either recombinant VEGF-A or VEGF-B (**Fig. 5*A***). We also explored the possibility that the expression of the two factors after AAV-mediated gene delivery in the infarcted hearts *in vivo* might promote regeneration of the damaged cardiac tissue through stimulation of cardiomyocyte replication or cardiac stem cell recruitment. However, we failed to detect any increase in the number of BrdU-positive, proliferating cells in infarct border zone in any of the treated animals compared to controls (data not shown).

An alternative possibility is that the VEGFs might induce protection of cardiomyocytes against ischemic death. To test this hypothesis, we exposed cardiomyocytes to hypoxia for 48 h followed by 24 h reoxygenation either in the absence, or presence, of recombinant VEGF-B or VEGF-A. As revealed by a TUNEL assay, the percentage of apoptotic cells dropped from

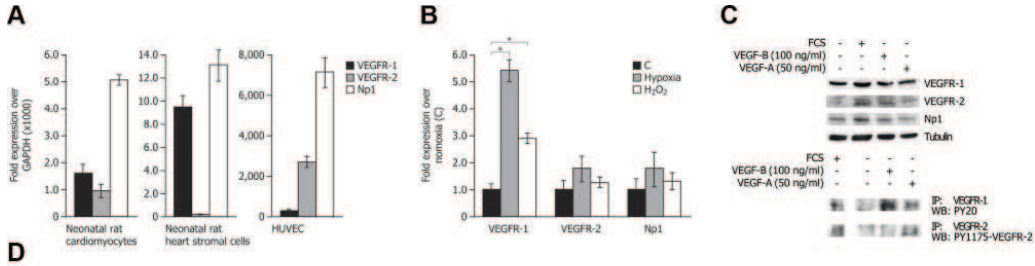

Figure 4. Cardiomyocytes express functional VEGF receptors. *A*) Levels of expression of *VEGFR-1*, *VEGFR-2*, and *Np1* by real-time PCR in rat α-actinin-positive neonatal cardiomyocytes, α-actinin-negative cardiac stromal cells, and HUVECs. *B*) Levels of expression of VEGF receptors in cardiomyocytes in response to hypoxic (2% O_2) or oxidative stress (H_2O_2 100 μM). *C*) Top panel: Western blotting showing specific detection of VEGFR-1, VEGFR-2, and Np1 in cell lysates of neonatal cardiomyocytes, with or without stimulation with fetal calf serum (FCS), recombinant VEGF-A, or VEGF-B, as indicated. Bottom panel: immunodetection of VEGF receptor phosphorylation on stimulation. VEGFR-1- or VEGF-2-specific immunocomplexes were probed with the indicated anti-phosphotyrosine-specific antibodies. *D*) Immunofluorescence staining of VEGFR-1, VEGFR-2, and Np1 on histological sections of frozen adult rat heart tissue. Larger pictures at left and magnifications at right show fluorescence in all three channels (red, receptors; green, sarcomeric α-actinin; blue, cell nuclei); smaller pictures show 2-channel fluorescence (top: blue/red; bottom: blue/green). Arrows indicate VEGFR-1 clusters at the intercalated disks between cardiomyocytes. Scale bars = 200 μm. Values are expressed as means ± SE. $^*P < 0.05$.

~17.2 ± 3.3% of controls to 7.6 ± 1.2 and 8.0 ± 1.0% in the VEGF-A and VEGF-B-treated cultures, respectively ($P<0.05$ in both cases; Fig. 5*B*). The protection from death was also evident when cardiomyocytes were exposed for 90 min to the cardiotoxic drug epirubicin. Under these conditions, the number of dead cells in the cultures added with either recombinant VEGF decreased from 61.8 ± 8.5% in controls to 13.8 ± 6.0 and 11.2 ± 4.2% in the VEGF-A and VEGF-B-treated cultures, respectively ($P<0.05$ in both cases; Fig. 5*C*).

Consistent with the conclusion that VEGF exerts an antiapoptotic effect, we also observed that the number of TUNEL-positive cells in the infarct border zone at 48 h after infarction was significantly lower in the animals injected with either AAV2-VEGF-A or AAV2-VEGF-B compared to controls (from 17.2±8.0 to 4.5±1.4 and 5.5±1.5%, respectively; $n=4$/group; $P < 0.05$ *vs.* control in both cases; Fig. 5*D*).

VEGF-A and VEGF-B activate expression of genes involved in the regulation of myocardial contractility and metabolism

Besides protection from apoptosis, the changes in regional contractility observed in the infarcted animals treated with VEGF-A and VEGF-B also suggested that these factors might directly affect cardiomyocyte activity. To further explore this issue, we analyzed the levels of expression of a series of genes involved in cardiomyocyte function in cells treated for 24 h with recombinant VEGF-A or VEGF-B. In particular, we evaluated the expression profile of genes specifically involved in cardiac contractility (α*MHC*, β*MHC*), intracellular calcium handling (*SERCA2a*, *RYR2*), mitochondrial energetics (*PGC1*α), and of some typical genetic markers of hypertrophy, such as skeletal α-actin (sk α-act) and cardiac natriuretic peptides (*ANF* and *BNP*). The modifications in the levels of expression of these genes were compared to those found in response to the α-adrenergic agonist phenylephrine (PE) or to the thyroid hormone triiodo-L-thyronine (T3). These compounds are known to induce characteristic myocyte hypertrophy responses, consisting in the up-regulation of fetal genes of pathological hypertrophy (including β*MHC*, *sk α-act*, *ANF*, and *BNP*) in the case of PE (25, 26), while reproducing physiological hypertrophy (increase of α*MHC* and *SERCA2a*, and repression of β*MHC* transcripts) in the case of T3 (27, 28).

Both VEGFs were found to increase expression of α*MHC* (which is the predominant contractile protein in adult rodents; ref. 29) and repress that of β*MHC*, similar to T3, and different from PE ($P<0.05$ between VEGF-treated and control cardiomyocytes). VEGF-B also inhibited expression of *sk α-act*. Both factors promoted elevation of the *ANF* and *BNP* transcripts and, most notably, they also determined elevation of the *SERCA2a*, *RYR*, and *PGC1*α mRNAs, similar to T3 ($P<0.05$) (**Fig. 6**).

Taken together, these data indicate that both VEGF-A and VEGF-B evoke, in isolated cardiomyocytes, a gene expression program proper of compensatory hypertrophy similar to that induced by the thyroid hormone. Of note, this response can be initiated by the sole treatment with VEGF-B, a selective VEGFR-1 ligand.

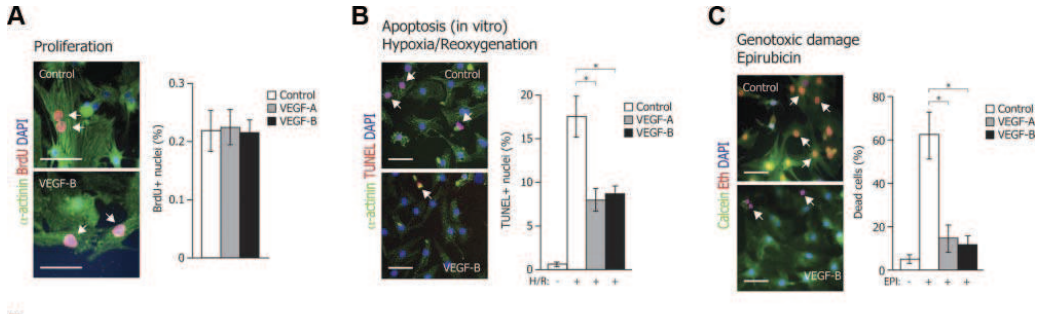

Figure 5. VEGFs protect cardiomyocytes from apoptosis *in vitro* and *in vivo*. *A*) Recombinant VEGFs do not induce neonatal rat cardiomyocyte proliferation. Left panels: representative images of α-actinin-positive cardiac myocytes showing positivity to BrdU immunostaining (red; arrows) with or without exposure to recombinant VEGF-B. Right panel: quantification of BrdU-positive nuclei. *B*) VEGFs protect cardiomyocytes from apoptosis *in vitro*. Left panels: representative images of TUNEL$^+$ cardiomyocytes (arrows) exposed to hypoxia for 48 h followed by 24 h with or without VEGF-B. Right panel: quantification of TUNEL$^+$ nuclei. *C*) Left panels: representative images of a cell viability assay based on the simultaneous determination of live (green, calcein) and dead (red, ethidium homodimer-1, Eth; arrow) cardiomyocytes after *in vitro* exposure to epirubicin in the presence or absence VEGF-B. Right panel: quantification of dead cells. *D*) Detection of apoptotic nuclei *in vivo* at d 3 after MI. Right panels: representative images of TUNEL$^+$ nuclei (arrows) in infarcted hearts from a control and a VEGF-B-injected mouse; cardiomyocytes are stained by positivity to α-actinin (green). Right: quantification of TUNEL$^+$ nuclei. Values are expressed as means ± SE. $^*P < 0.05$. Scale bars = 20 μm (*A*, *D*); 50 μm (*B*, *C*).

VEGF-B overexpression counteracts the induction of genes involved in pathological LV remodeling after myocardial infarction

To further explore the effects of VEGF receptor stimulation *in vivo*, we also analyzed the expression profile of LV tissue from a subset of AAV-transduced, infarcted animals (n=6/group) by real-time PCR. Consistent with the echocardiography results, control animals at 3 mo after infarction showed the characteristic pattern of gene expression commonly associated with pathological LV remodeling, involving significant (P<0.05) overexpression of βMHC and sk α-act contractile proteins, an increase in the cardiac natriuretic peptides, and a decrease in the levels of *SERCA2a*, *RYR*, and *PGC1α* mRNAs as compared to normal rats (**Fig. 7**). Remarkably, these modifications were all significantly counteracted by both VEGF-A and, most notably, VEGF-B overexpression. In the VEGF-A and VEGF-B-treated hearts, the levels of β*MHC*, *ANF*, *BNP*, *SERCA2a*, and *RYR* were unchanged compared to normal animals; those of α*MHC* and *PGC1α* were even significantly

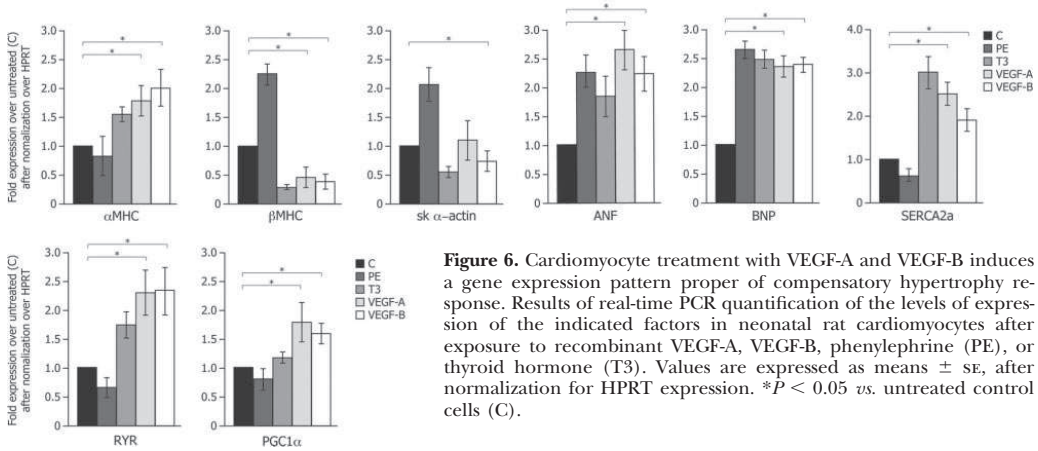

Figure 6. Cardiomyocyte treatment with VEGF-A and VEGF-B induces a gene expression pattern proper of compensatory hypertrophy response. Results of real-time PCR quantification of the levels of expression of the indicated factors in neonatal rat cardiomyocytes after exposure to recombinant VEGF-A, VEGF-B, phenylephrine (PE), or thyroid hormone (T3). Values are expressed as means ± SE, after normalization for HPRT expression. $^*P < 0.05$ *vs.* untreated control cells (C).

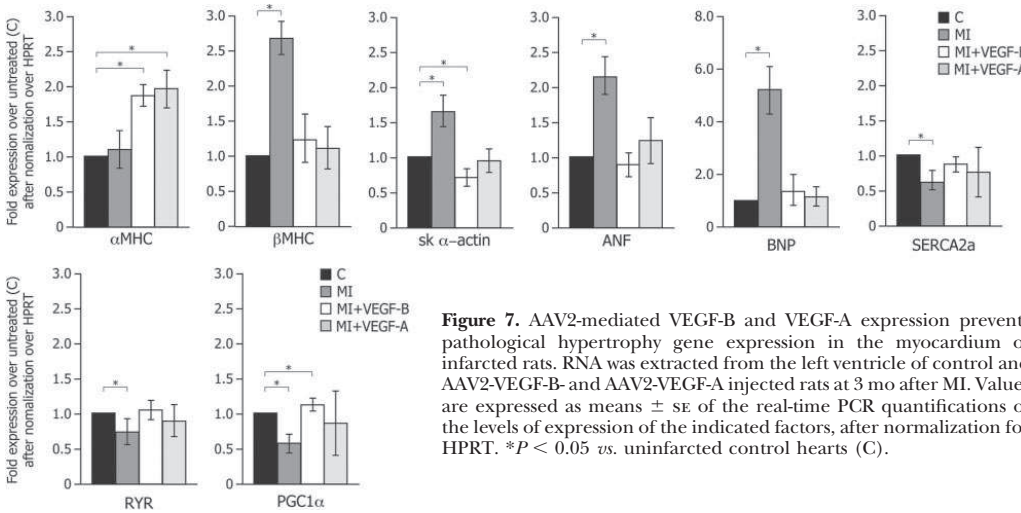

Figure 7. AAV2-mediated VEGF-B and VEGF-A expression prevents pathological hypertrophy gene expression in the myocardium of infarcted rats. RNA was extracted from the left ventricle of control and AAV2-VEGF-B- and AAV2-VEGF-A injected rats at 3 mo after MI. Values are expressed as means ± SE of the real-time PCR quantifications of the levels of expression of the indicated factors, after normalization for HPRT. $*P < 0.05$ *vs.* uninfarcted control hearts (C).

increased, and that of sk α-act was decreased ($P<0.05$ in all cases).

Collectively, these observations further support the conclusion that VEGFR-1 stimulation by specific ligands exerts a beneficial effect on the myocardial tissue.

DISCUSSION

A relevant conclusion of this study is that the continuous expression of VEGF after myocardial infarction exerts prolonged beneficial effects in terms of increase in contractility, prevention of pathological LV remodeling, and preservation of viable cardiac tissue. All our findings are consistent with the notion that VEGF exerts these effects through the activation of VEGFR-1 expressed in cardiomyocytes: *1*) isolated rat cardiomyocytes express VEGFR-1; *2*) VEGFR tyrosine kinases becomes activated on binding to the recombinant VEGFR-1 ligands PlGF and VEGF-B; *3*) the levels of expression VEGFR-1 are selectively up-regulated in hypoxia and on oxidative stress; and *4*) most notably, cardiomyocyte treatment with VEGF-B activates a peculiar gene expression program, reminiscent of that observed during compensatory hypertrophy. In this context, the localization of VEGFR-1 in the intercalated disks between cardiomyocytes appears intriguing, since these structures also act as mechanical stress sensors during muscle contraction, besides supporting synchronized cardiomyocyte contraction (30). Further studies are clearly required to understand the functional significance of VEGFR-1 localization at these structures. In this respect, it might be worth noting that, both in zebrafish and in cultured rat cardiomyocytes, VEGF-A has been reported to exert a positive inotropic effect by increasing calcium transients through its interaction with VEGFR-1 and downstream PLCγ-1 activation (31).

The observation that VEGFs exert a direct activity on cardiomyocytes is indeed not surprising. A large body of evidence now indicates that expression of the VEGF receptors is not restricted to endothelial cells and that their ligands exert a variety of fundamental functions in other cell types. These nonangiogenic functions of VEGFs include, among others, the potential to prevent neuronal cell death from ischemia and promote neurogenesis (32, 33), the capacity to stimulate hepatocyte regeneration after liver damage (34), and the ability to promote osteoblast migration and differentiation (35, 36). In the skeletal muscle, we showed that VEGF-A exerts a powerful regenerative effect after ischemic and nonischemic muscle damage by promoting satellite cell differentiation (23, 37). Finally, several groups have described an effect of VEGF-A on various cells of hematopoietic origin, showing that this factor is able to mediate monocyte chemotaxis (38), hematopoietic stem cell survival (39), mobilization of endothelial progenitor cells (40), and the selective recruitment of a population of bone marrow-derived, $CD11b^+$ mononuclear cells, which are essential for vessel maturation at the sites of adult neoangiogenesis (18).

The different VEGF receptors appear variably involved in mediating these nonangiogenic functions of their ligands. For example, skeletal muscle regeneration appears to selectively require VEGFR-2, since PlGF is ineffective at stimulating this process compared to VEGF-A (23); in contrast, the effects on monocytes require VEGFR-1 (38), those on hematopoietic progenitors are mediated by both VEGFR-1 and VEGFR-2 (39–41), and those determining the recruitment of bone marrow-derived $CD11b^+$ cells require the presence of Np1 (18).

The prolonged expression of VEGF-B in the heart elicits only a modest angiogenic response compared to VEGF-A, essentially consisting in the generation of enlarged vessels devoid of α-SMA-positive cells. A lack

of angiogenesis and presence of abnormally enlarged capillaries was also recently reported in a VEGF-B-transgenic mouse (11). An apparent controversy exists concerning the possible angiogenic role of VEGF-B exogenously delivered *in vivo*, ranging from promotion of unrestricted angiogenesis (42), ability to potentiate, rather than induce, angiogenesis when transgenically expressed in endothelial cells (43), induction of selective revascularization of the ischemic myocardium but not of other organs (12), or no angiogenic effect at all in several tissues after adenoviral gene delivery (44, 45). Recent work has also indicated that the delivery VEGF-B to the infarcted myocardium in rabbits and pigs using an adenoviral vector promoted angiogenesis and arteriogenesis by acting on endothelial cells (13). All these apparent discrepancies might be attributable to differences in genetic background, phenotyping methodology, use of different VEGF-B isoforms, or, most important, use of different strategies for VEGF-B overproduction (recombinant proteins, naked plasmid DNA, or adenoviral vectors). In this respect, AAV vectors currently represent the only available system to deliver genes to the adult myocardium and allow their prolonged expression over time. Other vector systems, such as the first generation adenoviruses used in other studies, are fraught with the induction of a potent inflammatory and immune reaction (46), which, besides blurring the biological response, restricts observation to a few days after vector inoculation.

Besides the possible direct modulation of cardiac contractility, the main consequences of VEGF expression are, on one hand, the protection of cardiomyocytes from apoptosis while, on the other hand, the induction of a gene expression program of compensatory hypertrophy. Cardiomyocytes thus join the list of the numerous cell types in which different VEGF family members exert a powerful antiapoptotic effect, including endothelial cells (5), neurons (47), embryonic stem cells, (48) and skeletal muscle cells (23, 49). Protection from apoptosis was clearly evident when VEGF-B was administered, in both cultured cardiomyocytes and after myocardial infarction *in vivo*, again suggesting that a relevant receptor mediating the antiapoptotic effect was VEGFR-1. The recent observations that VEGF-B rescues retinal and motor neurons from apoptosis (50, 51) and inhibits the expression of a number of proapoptotic genes in noncardiomyocyte cells (50) is fully consistent with this conclusion.

In addition to protection from apoptosis, VEGF-B transduction in the heart elicited a peculiar gene expression profile, consisting of the activation of αMHC and the repression of βMHC and skeletal α-actin, and the increase in SERCA2a, RYR, and PGC1α gene expression, together with the increase in the levels of the cardiac natriuretic peptide mRNAs. This pattern of gene expression resembles that induced by the thyroid hormone T3, which is usually considered a marker of benign, compensatory hypertropic response to cardiac stimulation (52, 53). These findings appear to be in full agreement with the recent observation that a transgenic mouse overexpressing VEGF-B showed clear signs of cardiac hypertrophy, but without compromising cardiac function (11); with the report that VEGF-B-knockout mice have smaller hearts (10); and with the observation that the injection of the VEGF-B protein after infarction leads to myocardial hypertrophy (54). Our results extend these findings further, and show that these effects of VEGF-B are exerted through direct activity on cardiomyocytes. Of note, in our experiments, VEGF-A and VEGF-B equally protected cardiomyocytes from apoptosis and induced a beneficial gene expression profile; however, VEGF-B scored superior to VEGF-A in preserving LV function after myocardial infarction. This observation might either indicate that the two factors activate VEGFR-1 differently, for example, exploiting different coreceptors, or that the prolonged activation of VEGFR-2 by VEGF-A might be somehow detrimental for the infarcted myocardium, for example, by inducing a leaky vasculature. Further experiments will obviously be required to distinguish between these possibilities.

In conclusion, the finding that VEGF-B exerts a marked beneficial effect on the infarcted myocardium by preventing loss of cardiac mass and promoting cardiac contractility has obvious therapeutic implications, in terms of both direct utilization of VEGF-B (or PlGF) for therapeutic purposes and the identification of alternative, synthetic activators of VEGFR-1. FJ

The authors are grateful to Marina Dapas and Michela Zotti for superb technical support in AAV production, to Mauro Sturnega for help in animal experimentation, and to Suzanne Kerbavcic for editorial assistance. This work was supported by a grant from the Fondazione CR Trieste, Trieste, Italy; by grants from the Regione Friuli Venezia Giulia, Italy; and by a grant from the World Anti-Doping Agency (WADA), Montreal, Canada. F.A.R. is an Established Investigator of the American Heart Association.

REFERENCES

1. Ferrara, N., Gerber, H. P., and LeCouter, J. (2003) The biology of VEGF and its receptors. *Nat. Med.* **9,** 669–676
2. Carmeliet, P. (2005) Angiogenesis in life, disease and medicine. *Nature* **438,** 932–936
3. Adams, R. H., and Alitalo, K. (2007) Molecular regulation of angiogenesis and lymphangiogenesis. *Nat. Rev. Mol. Cell. Biol.* **8,** 464–478
4. Olsson, A. K., Dimberg, A., Kreuger, J., and Claesson-Welsh, L. (2006) VEGF receptor signalling - in control of vascular function. *Nat. Rev. Mol. Cell. Biol.* **7,** 359–371
5. Neufeld, G., Cohen, T., Gengrinovitch, S., and Poltorak, Z. (1999) Vascular endothelial growth factor (VEGF) and its receptors. *FASEB J.* **13,** 9–22
6. Sawano, A., Iwai, S., Sakurai, Y., Ito, M., Shitara, K., Nakahata, T., and Shibuya, M. (2001) Flt-1, vascular endothelial growth factor receptor 1, is a novel cell surface marker for the lineage of monocyte-macrophages in humans. *Blood* **97,** 785–791
7. Park, J. E., Chen, H. H., Winer, J., Houck, K. A., and Ferrara, N. (1994) Placenta growth factor. Potentiation of vascular endothelial growth factor bioactivity, in vitro and in vivo, and high affinity binding to Flt-1 but not to Flk-1/KDR. *J. Biol. Chem.* **269,** 25646–25654
8. Olofsson, B., Pajusola, K., Kaipainen, A., von Euler, G., Joukov, V., Saksela, O., Orpana, A., Pettersson, R. F., Alitalo, K., and Eriksson, U. (1996) Vascular endothelial growth factor B, a

novel growth factor for endothelial cells. *Proc. Natl. Acad. Sci. U. S. A.* **93,** 2576–2581
9. Lagercrantz, J., Farnebo, F., Larsson, C., Tvrdik, T., Weber, G., and Piehl, F. (1998) A comparative study of the expression patterns for vegf, vegf-b/vrf and vegf-c in the developing and adult mouse. *Biochim. Biophys. Acta* **1398,** 157–163
10. Bellomo, D., Headrick, J. P., Silins, G. U., Paterson, C. A., Thomas, P. S., Gartside, M., Mould, A., Cahill, M. M., Tonks, I. D., Grimmond, S. M., Townson, S., Wells, C., Little, M., Cummings, M. C., Hayward, N. K., and Kay, G. F. (2000) Mice lacking the vascular endothelial growth factor-B gene (VEGFB) have smaller hearts, dysfunctional coronary vasculature, and impaired recovery from cardiac ischemia. *Circ. Res.* **86,** E29–E35
11. Karpanen, T., Bry, M., Ollila, H. M., Seppanen-Laakso, T., Liimatta, E., Leskinen, H., Kivela, R., Helkamaa, T., Merentie, M., Jeltsch, M., Paavonen, K., Andersson, L. C., Mervaala, E., Hassinen, I. E., Yla-Herttuala, S., Oresic, M., and Alitalo, K. (2008) Overexpression of vascular endothelial growth factor-B in mouse heart alters cardiac lipid metabolism and induces myocardial hypertrophy. *Circ. Res.* **103,** 1018–1026
12. Li, X., Tjwa, M., Van Hove, I., Enholm, B., Neven, E., Paavonen, K., Jeltsch, M., Juan, T. D., Sievers, R. E., Chorianopoulos, E., Wada, H., Vanwildemeersch, M., Noel, A., Foidart, J. M., Springer, M. L., von Degenfeld, G., Dewerchin, M., Blau, H. M., Alitalo, K., Eriksson, U., Carmeliet, P., and Moons, L. (2008) Reevaluation of the role of VEGF-B suggests a restricted role in the revascularization of the ischemic myocardium. *Arterioscler. Thromb. Vasc. Biol.* **28,** 1614–1620
13. Lahteenvuo, J. E., Lahteenvuo, M. T., Kivela, A., Rosenlew, C., Falkevall, A., Klar, J., Heikura, T., Rissanen, T. T., Vahakangas, E., Korpisalo, P., Enholm, B., Carmeliet, P., Alitalo, K., Eriksson, U., and Yla-Herttuala, S. (2009) Vascular endothelial growth factor-B induces myocardium-specific angiogenesis and arteriogenesis via vascular endothelial growth factor receptor-1- and neuropilin receptor-1-dependent mechanisms. *Circulation* **119,** 845–856
14. Ferrarini, M., Arsic, N., Recchia, F. A., Zentilin, L., Zacchigna, S., Xu, X., Linke, A., Giacca, M., and Hintze, T. H. (2006) Adeno-Associated Virus-mediated transduction of VEGF165 improves cardiac tissue viability and functional recovery after permanent coronary occlusion in conscious dogs. *Circ. Res.* **98,** 954–961
15. Favre, D., Provost, N., Blouin, V., Blancho, G., Cherel, Y., Salvetti, A., and Moullier, P. (2001) Immediate and long-term safety of recombinant adeno-associated virus injection into the nonhuman primate muscle. *Mol. Ther.* **4,** 559–566
16. Mueller, C., and Flotte, T. R. (2008) Clinical gene therapy using recombinant adeno-associated virus vectors. *Gene Ther.* **15,** 858–863
17. Arsic, N., Zentilin, L., Zacchigna, S., Santoro, D., Stanta, G., Salvi, S., Sinagra, G., and Giacca, M. (2003) Induction of functional neovascularization by combined VEGF and angiopoietin-1 gene transfer using AAV vectors. *Mol. Ther.* **7,** 450–459
18. Zacchigna, S., Pattarini, L., Zentilin, L., Moimas, S., Carrer, A., Sinigaglia, M., Arsic, N., Tafuro, S., Sinagra, G., and Giacca, M. (2008) Bone marrow cells recruited through the Neuropilin-1 receptor promote arterial formation at the sites of adult neoangiogenesis. *J. Clin. Invest.* **118,** 2062–2075
19. Pfeffer, M. A., Pfeffer, J. M., Fishbein, M. C., Fletcher, P. J., Spadaro, J., Kloner, R. A., and Braunwald, E. (1979) Myocardial infarct size and ventricular function in rats. *Circ. Res.* **44,** 503–512
20. Ventura, C., Cantoni, S., Bianchi, F., Lionetti, V., Cavallini, C., Scarlata, I., Foroni, L., Maioli, M., Bonsi, L., Alviano, F., Fossati, V., Bagnara, G. P., Pasquinelli, G., Recchia, F. A., and Perbellini, A. (2007) Hyaluronan mixed esters of butyric and retinoic acid drive cardiac and endothelial fate in term placenta human mesenchymal stem cells and enhance cardiac repair in infarcted rat hearts. *J. Biol. Chem.* **282,** 14243–14252
21. Sahn, D. J., DeMaria, A., Kisslo, J., and Weyman, A. (1978) Recommendations regarding quantitation in M-mode echocardiography: results of a survey of echocardiographic measurements. *Circulation* **58,** 1072–1083
22. Collesi, C., Zentilin, L., Sinagra, G., and Giacca, M. (2008) Notch1 signaling stimulates proliferation of immature cardiomyocytes. *J. Cell Biol.* **183,** 117–128
23. Arsic, N., Zacchigna, S., Zentilin, L., Ramirez-Correa, G., Pattarini, L., Salvi, A., Sinagra, G., and Giacca, M. (2004) Vascular endothelial growth factor stimulates skeletal muscle regeneration in vivo. *Mol. Ther.* **10,** 844–854
24. Beltrami, A. P., Urbanek, K., Kajstura, J., Yan, S. M., Finato, N., Bussani, R., Nadal-Ginard, B., Silvestri, F., Leri, A., Beltrami, C. A., and Anversa, P. (2001) Evidence that human cardiac myocytes divide after myocardial infarction. *N. Engl. J. Med.* **344,** 1750–1757
25. Eble, D. M., Qi, M., Waldschmidt, S., Lucchesi, P. A., Byron, K. L., and Samarel, A. M. (1998) Contractile activity is required for sarcomeric assembly in phenylephrine-induced cardiac myocyte hypertrophy. *Am. J. Physiol.* **274,** C1226–C1237
26. Simpson, P. C., Kariya, K., Karns, L. R., Long, C. S., and Karliner, J. S. (1991) Adrenergic hormones and control of cardiac myocyte growth. *Mol. Cell. Biochem.* **104,** 35–43
27. Brent, G. A. (1994) The molecular basis of thyroid hormone action. *N. Engl. J. Med.* **331,** 847–853
28. Dillmann, W. (2009) Cardiac hypertrophy and thyroid hormone signaling. [E-pub ahead of print] *Heart Fail. Rev.* PMID: 19125327
29. Tardiff, J. C., Hewett, T. E., Factor, S. M., Vikstrom, K. L., Robbins, J., and Leinwand, L. A. (2000) Expression of the beta (slow)-isoform of MHC in the adult mouse heart causes dominant-negative functional effects. *Am. J. Physiol. Heart. Circ. Physiol.* **278,** H412–H419
30. Hoshijima, M. (2006) Mechanical stress-strain sensors embedded in cardiac cytoskeleton: Z disk, titin, and associated structures. *Am. J. Physiol. Heart. Circ. Physiol.* **290,** H1313–H1325
31. Rottbauer, W., Just, S., Wessels, G., Trano, N., Most, P., Katus, H. A., and Fishman, M. C. (2005) VEGF-PLCγ1 pathway controls cardiac contractility in the embryonic heart. *Genes Dev.* **19,** 1624–1634
32. Jin, K., Zhu, Y., Sun, Y., Mao, X. O., Xie, L., and Greenberg, D. A. (2002) Vascular endothelial growth factor (VEGF) stimulates neurogenesis in vitro and in vivo. *Proc. Natl. Acad. Sci. U. S. A.* **99,** 11946–11950
33. Lambrechts, D., Storkebaum, E., Morimoto, M., Del-Favero, J., Desmet, F., Marklund, S. L., Wyns, S., Thijs, V., Andersson, J., van Marion, I., Al-Chalabi, A., Bornes, S., Musson, R., Hansen, V., Beckman, L., Adolfsson, R., Pall, H. S., Prats, H., Vermeire, S., Rutgeerts, P., Katayama, S., Awata, T., Leigh, N., Lang-Lazdunski, L., Dewerchin, M., Shaw, C., Moons, L., Vlietinck, R., Morrison, K. E., Robberecht, W., Van Broeckhoven, C., Collen, D., Andersen, P. M., and Carmeliet, P. (2003) VEGF is a modifier of amyotrophic lateral sclerosis in mice and humans and protects motoneurons against ischemic death. *Nat. Genet.* **34,** 383–394
34. LeCouter, J., Moritz, D. R., Li, B., Phillips, G. L., Liang, X. H., Gerber, H. P., Hillan, K. J., and Ferrara, N. (2003) Angiogenesis-independent endothelial protection of liver: role of VEGFR-1. *Science* **299,** 890–893
35. Deckers, M. M., Karperien, M., van der Bent, C., Yamashita, T., Papapoulos, S. E., and Lowik, C. W. (2000) Expression of vascular endothelial growth factors and their receptors during osteoblast differentiation. *Endocrinology* **141,** 1667–1674
36. Mayr-Wohlfart, U., Waltenberger, J., Hausser, H., Kessler, S., Gunther, K. P., Dehio, C., Puhl, W., and Brenner, R. E. (2002) Vascular endothelial growth factor stimulates chemotactic migration of primary human osteoblasts. *Bone* **30,** 472–477
37. Messina, S., Mazzeo, A., Bitto, A., Aguennouz, M., Migliorato, A., De Pasquale, M. G., Minutoli, L., Altavilla, D., Zentilin, L., Giacca, M., Squadrito, F., and Vita, G. (2007) VEGF overexpression via adeno-associated virus gene transfer promotes skeletal muscle regeneration and enhances muscle function in mdx mice. *FASEB J.* **21,** 3737–3746
38. Barleon, B., Sozzani, S., Zhou, D., Weich, H. A., Mantovani, A., and Marme, D. (1996) Migration of human monocytes in response to vascular endothelial growth factor (VEGF) is mediated via the VEGF receptor flt-1. *Blood* **87,** 3336–33343
39. Gerber, H. P., Malik, A. K., Solar, G. P., Sherman, D., Liang, X. H., Meng, G., Hong, K., Marsters, J. C., and Ferrara, N. (2002) VEGF regulates haematopoietic stem cell survival by an internal autocrine loop mechanism. *Nature* **417,** 954–958
40. Lyden, D., Hattori, K., Dias, S., Costa, C., Blaikie, P., Butros, L., Chadburn, A., Heissig, B., Marks, W., Witte, L., Wu, Y., Hicklin, D., Zhu, Z., Hackett, N. R., Crystal, R. G., Moore, M. A., Hajjar,

K. A., Manova, K., Benezra, R., and Rafii, S. (2001) Impaired recruitment of bone-marrow-derived endothelial and hematopoietic precursor cells blocks tumor angiogenesis and growth. *Nat. Med.* **7,** 1194–1201
41. Ziegler, B. L., Valtieri, M., Porada, G. A., De Maria, R., Muller, R., Masella, B., Gabbianelli, M., Casella, I., Pelosi, E., Bock, T., Zanjani, E. D., and Peschle, C. (1999) KDR receptor: a key marker defining hematopoietic stem cells. *Science* **285,** 1553–1558
42. Silvestre, J. S., Tamarat, R., Ebrahimian, T. G., Le-Roux, A., Clergue, M., Emmanuel, F., Duriez, M., Schwartz, B., Branellec, D., and Levy, B. I. (2003) Vascular endothelial growth factor-B promotes in vivo angiogenesis. *Circ. Res.* **93,** 114–123
43. Mould, A. W., Greco, S. A., Cahill, M. M., Tonks, I. D., Bellomo, D., Patterson, C., Zournazi, A., Nash, A., Scotney, P., Hayward, N. K., and Kay, G. F. (2005) Transgenic overexpression of vascular endothelial growth factor-B isoforms by endothelial cells potentiates postnatal vessel growth in vivo and in vitro. *Circ. Res.* **97,** e60–70
44. Rissanen, T. T., Markkanen, J. E., Gruchala, M., Heikura, T., Puranen, A., Kettunen, M. I., Kholova, I., Kauppinen, R. A., Achen, M. G., Stacker, S. A., Alitalo, K., and Yla-Herttuala, S. (2003) VEGF-D is the strongest angiogenic and lymphangiogenic effector among VEGFs delivered into skeletal muscle via adenoviruses. *Circ. Res.* **92,** 1098–1106
45. Bhardwaj, S., Roy, H., Gruchala, M., Viita, H., Kholova, I., Kokina, I., Achen, M. G., Stacker, S. A., Hedman, M., Alitalo, K., and Yla-Herttuala, S. (2003) Angiogenic responses of vascular endothelial growth factors in periadventitial tissue. *Hum. Gene Ther.* **14,** 1451–1462
46. Liu, Q., and Muruve, D. A. (2003) Molecular basis of the inflammatory response to adenovirus vectors. *Gene Ther.* **10,** 935–940
47. Storkebaum, E., and Carmeliet, P. (2004) VEGF: a critical player in neurodegeneration. *J. Clin. Invest.* **113,** 14–18
48. Brusselmans, K., Bono, F., Collen, D., Herbert, J. M., Carmeliet, P., and Dewerchin, M. (2005) A novel role for vascular endothelial growth factor as an autocrine survival factor for embryonic stem cells during hypoxia. *J. Biol. Chem.* **280,** 3493–3499
49. Germani, A., Di Carlo, A., Mangoni, A., Straino, S., Giacinti, C., Turrini, P., Biglioli, P., and Capogrossi, M. C. (2003) Vascular endothelial growth factor modulates skeletal myoblast function. *Am. J. Pathol.* **163,** 1417–1428
50. Li, Y., Zhang, F., Nagai, N., Tang, Z., Zhang, S., Scotney, P., Lennartsson, J., Zhu, C., Qu, Y., Fang, C., Hua, J., Matsuo, O., Fong, G. H., Ding, H., Cao, Y., Becker, K. G., Nash, A., Heldin, C. H., and Li, X. (2008) VEGF-B inhibits apoptosis via VEGFR-1-mediated suppression of the expression of BH3-only protein genes in mice and rats. *J. Clin. Invest.* **118,** 913–923
51. Poesen, K., Lambrechts, D., Van Damme, P., Dhondt, J., Bender, F., Frank, N., Bogaert, E., Claes, B., Heylen, L., Verheyen, A., Raes, K., Tjwa, M., Eriksson, U., Shibuya, M., Nuydens, R., Van Den Bosch, L., Meert, T., D'Hooge, R., Sendtner, M., Robberecht, W., and Carmeliet, P. (2008) Novel role for vascular endothelial growth factor (VEGF) receptor-1 and its ligand VEGF-B in motor neuron degeneration. *J. Neurosci.* **28,** 10451–10459
52. Trivieri, M. G., Oudit, G. Y., Sah, R., Kerfant, B. G., Sun, H., Gramolini, A. O., Pan, Y., Wickenden, A. D., Croteau, W., Morreale de Escobar, G., Pekhletski, R., St Germain, D., Maclennan, D. H., and Backx, P. H. (2006) Cardiac-specific elevations in thyroid hormone enhance contractility and prevent pressure overload-induced cardiac dysfunction. *Proc. Natl. Acad. Sci. U. S. A.* **103,** 6043–6048
53. Schaub, M. C., Hefti, M. A., Harder, B. A., and Eppenberger, H. M. (1997) Various hypertrophic stimuli induce distinct phenotypes in cardiomyocytes. *J. Mol. Med.* **75,** 901–920
54. Tirziu, D., Chorianopoulos, E., Moodie, K. L., Palac, R. T., Zhuang, Z. W., Tjwa, M., Roncal, C., Eriksson, U., Fu, Q., Elfenbein, A., Hall, A. E., Carmeliet, P., Moons, L., and Simons, M. (2007) Myocardial hypertrophy in the absence of external stimuli is induced by angiogenesis in mice. *J. Clin. Invest.* **117,** 3188–3197

Received for publication August 10, 2009.
Accepted for publication November 25, 2009.